VIEWPOINT AGGREGATION VIA RELATIONAL MODELING AND ANALYSIS: A NEW APPROACH TO SYSTEMS PHYSIOLOGY

A Dissertation
Presented to
The Academic Faculty

by

Cassie S. Mitchell

In Partial Fulfillment
of the Requirements for the Degree
Doctor of Philosophy in the
School of Biomedical Engineering

Georgia Institute of Technology
May 2009

VIEWPOINT AGGREGATION VIA RELATIONAL MODELING AND ANALYSIS: A NEW APPROACH TO SYSTEMS PHYSIOLOGY

Approved by:

Dr. Robert H. Lee, Advisor
School of Biomedical Engineering
Georgia Institute of Technology and Emory University

Dr. Melissa Kemp
School of Biomedical Engineering
Georgia Institute of Technology and Emory University

Dr. Dr. Lena Ting
School of Biodmedical Engineering
Georgia Institute of Technology and Emory University

Dr. Kurt Wiesenfeld
School of Physics
Georgia Institute of Technology

Dr. Astrid Prinz
School of Biomedical Engineering
Georgia Institute of Technology and Emory University

Date Approved: March 23, 2009

ACKNOWLEDGEMENTS

First, I would like to thank God for His many blessings, through triumphs but especially through life's tough challenges. It is an honor to research the amazing physiologic systems that He has created. I also want to give my utmost thanks, appreciation, and respect to Dr. Robert H. Lee, who I am privileged and honored to call advisor, mentor, colleague, and friend. I could not have asked for a more exciting, collaborative, helpful or supportive research environment. More importantly, Dr. Lee's significant positive impact has shaped far more than just my research aspirations and abilities, and for that I am eternally grateful. Next, I would like to thank my dissertation committee members (Dr. Lena Ting, Dr. Astrid Prinz, Dr. Melissa Kemp, and Dr. Kurt Wiesenfeld) for their time, input, advice, comments, and support in my project. Next, I would like to thank the faculty, staff, my classmates, friends, and church members for their encouragement, support, and prayers. Last but certainly not least, I would like to especially thank my family and specifically my parents, Randy and Clara Mitchell, for the unconditional love, support, determination, and perseverance they have provided. I would not be here without them. Finally, I would like to give a special thanks to my mother, Clara, for being both my hero and my earthly enabler and for never giving up on me.

Financial Support: I would like to thank the National Science Foundation for their financial support via a Graduate Research Fellowship and Integrative Graduate Education and Research Traineeship and the Oklahoma Department of Rehabilitation Services for their financial support of necessary disability-related services and technology.

TABLE OF CONTENTS

LIST OF TABLES

LIST OF FIGURES

LIST OF SYMBOLS AND ABBREVIATIONS

ALS	Amyotrophic Lateral Sclerosis
NMDA	N-methyl-D-aspartate
R3	review-relate-refine
S3	search-survey-and summarize
SA	sensitivity analysis
SCI	Spinal Cord Injury

* Note that mathematical symbols (such as variables, parameters, and model outputs) are specifically defined within the chapter that they are used.

SUMMARY

The key to understanding any system, including physiologic and pathologic systems, is to obtain a truly comprehensive view of the system. The purpose of this dissertation was to develop foundational analytical and modeling tools, which would enable such a comprehensive view to be obtained of any physiological or pathological system by combining experimental, clinical, and theoretical viewpoints. Specifically, we focus on the development of analytical and modeling techniques capable of predicting and prioritizing the mechanisms, emergent dynamics, and underlying principles necessary in order to obtain a comprehensive system understanding. Since physiologic systems are inherently complex systems, our approach was to translate the philosophy of complex systems into a set of applied and quantitative methods, which focused on the relationships within the system that result in the system's emergent properties and behavior. The result was a set of developed techniques, referred to as *relational modeling and analysis* that utilize relationships as either a placeholder or bridging structure from which unknown aspects of the system can be effectively explored. These techniques were subsequently tested via the construction and analysis of models of five very different systems: synaptic neurotransmitter spillover, secondary spinal cord injury, physiological and pathological axonal transport, and amyotrophic lateral sclerosis and to analyze neurophysiological data of in vivo cat spinal motoneurons. Our relationship-based methodologies provide an equivalent means by which the different perspectives can be compared, contrasted, and aggregated into a truly comprehensive viewpoint that can drive research forward.

CHAPTER 1

INTRODUCTION

Ask any biomedical engineer, myself included, and they will say that one of the reasons they entered the field was to 'make a difference' or to 'help others' through the application of their skills to either prevent or treat human illness and disease or to positively impact the lives of patients with health or physical ailments. As in any engineering endeavor, whether it is designing an oil refinery, a river dam, an electric power plant, or yes, even a treatment for a medical pathology, the key to success is to truly understand the problem or process that constitutes intervention. In fact, the actual task of comprehensively understanding and conceptualizing a problem, process, or system is a significant part of engineering. It is the primary task emphasized in engineering education, and it is the first and arguably the most important task of any engineering project, regardless of discipline. However, a major challenge for biomedical engineers is that our 'systems', the physiologies and pathologies in which we wish to intervene or apply treatment, are amazingly complex. This high degree of biological complexity has hampered our ability to comprehend and understand how these processes work. In many devastating conditions such as secondary spinal cord injury and amyotrophic lateral sclerosis to name two specific examples, this inability has and continues to result in a host of failed clinical trials by treatments that initially, that is without our full understanding of the pathology, seemed promising. Thus, irrespective of the specific type of physiology, pathology, ailment or condition being investigated, there

is a significant and fundamental need to obtain a comprehensive view of its inner workings in order to most effectively and efficiently identify, design, and apply interventions, which positively affect the lives of patients. My over-arching research goal is to provide foundational research that enables comprehensive views of complex physiological and pathological systems to be obtained, and thus facilitates biomedical engineers in our ultimate goal, to help others—the patients that can benefit from the fruits of their collectively applied skills.

A truly comprehensive view of any physiologic or pathologic system necessitates multiple perspectives, including clinical, experimental and theoretical viewpoints, which respectively address the questions of 'what', 'how', and 'why'. Yet, the traditional approach to physiologic systems has rather single-handedly relied upon hypothesis-driven experimentation, both in vitro and in vivo. Clinical viewpoints, in which actual human data is collected, is less common, with most studies focusing on pathologies and therapeutics. However, the use of system-level theory, such as quantitative meta-analysis or computational models is infrequent, with only a few small niches of research pursuing such views, particularly at the system level.

While not as common in the study of physiologic systems, the tool that engineers have often employed in an attempt to obtain a comprehensive understanding of the inner workings or mechanisms of any number of studied systems is, in fact, the computational model. The purpose of the computational model is no different than any other kind of model or prototype used as a simplified representation or visualization. A computational

model allows researchers to ‘conceptualize’ highly complex systems in a manageable, quantitative manner by translating the language of biology to the language of math. Perhaps a more applied analogy is to think of a computational model as a map. The model has inputs, which signify the initial ‘starting point’ of the system, mathematical equations that represent the actual process path, parameters that represent the coordinates of that path, and outputs, which reveal the ‘final destination’ or process products or outcomes. The system map represented by the computational model thus provides a means for engineers and scientists to explore the ‘landscape’ or inner workings of their systems.

Using computational models to obtain an overall or system-level understanding of a physiological or pathological system has many potential advantages. In contrast to experiments alone, which due to the inherent nature of their methodology are forced to focus on either a single or at most a couple of physiological or pathological factors at a time, models can simultaneously simulate the effects of multiple factors and their interactions. Furthermore, preclinical experimentation and especially a clinical trial can take years and hundreds of thousands if not millions of dollars to screen a single therapy. Given the speed and efficiency at which a model can simulate (as quickly as seconds to minutes for a single treatment), models have the promise to be used as a financially inexpensive high-throughput test bed to screen thousands of possible mechanistic hypotheses and therapeutics, prior to committing to expensive and lengthy preclinical and clinical trials. Thus, the computational model has the potential to not only provide the much needed comprehensive view and high level of understanding of the physiologies

and pathologies of the very patients that we wish to treat, but also to use that view to prioritize, predict, and speed the process from therapeutic identification through preclinical development to clinical success.

Despite the many potential benefits of computational models, they are infrequently used as an exploratory or predictive biomedical research tool, and they are even more rarely used in the study of diseased states or pathologies. Instead, models have lagged far behind their experimental counterparts, reserved as a confirmatory tool utilized mostly to look at the biophysics and function of normal non-diseased state physiologies. Given the many advantages of models and their great promise, it leads one to ask the obvious question: Why aren't computational models currently employed to obtain the comprehensive and predictive views that are essential to biomedical engineers and biomedical scientists to explore, understand, an treat the complex pathologies that plague a multitude of patients?

Two main obstacles have prevented the use of models as a means of early comprehensive system exploration and prediction, especially in the research of pathologies. First and foremost, traditional techniques of model analysis are often unable to explain the emergent and robust complex and often adaptive behavior of the biological systems they are intended to represent. This inability is largely due to the models being inherently reductionistic in nature, whereas the biological systems they are intended to convey are inherently complex. Complex biological systems exhibit complicated patterns of emergence, behaviors that are irreducible to the system's constituent parts. Yet, how we,

as humans, go about conceptualizing and subsequently modeling such systems is precisely on a reductionistic, component-by-component basis, stringing together any number of conceptualized parts until the model exhibits one or more desired outcomes or properties. Because the whole is greater than the sum of its parts, it is unrealistic to assume that any model, regardless of its level of detail and number of parts or components, can fully represent the actual system, particularly when viewed solely at the component level. While models will always be reductionistic in that they will only consist of the conceptualized components that we as humans manage, our analytical techniques that we use to characterize models do not need to be restricted to such reductionism. We contend that a primary problem with current model analytical techniques is that they do not fully consider, identify or address the complex nature, properties, and dynamics of the biological systems that they characterize. Thus, what is needed to overcome this obstacle are techniques able to look through the model's reductionism to unveil the complex system-level properties that lie beneath. In essence, we need a technique that 'raises the hood' of the model to see how the set of components, as a whole, relate and interact to produce dynamics and properties that characterize the physiologies and pathologies that we wish to understand.

Secondly, in addition to the short falls of model analysis, the approach utilized by traditional modeling methodology has prevented the construction of models early in the research process. While traditional modeling methodology has been successfully used to develop models that confirm theories and hypotheses regarding biological systems in which we already have some level of understanding, these model construction techniques

have not been amenable to the study of systems in which we do not have a great deal of information or pre-existing conceptualizations, particularly regarding system-level behavior. This inability is largely due to the fact that the traditional approach to many biological models has been to model 'deep' instead of 'wide'. That is, biological models are often constructed by piling as much detail as possible into the individual components of a model until the model exhibits the desired properties. Again, this reductionistic approach, which emphasizes the detailed properties of individual components rather then the holistic behavior and interactions of those components, which produce the system's emergent behavior, requires too much upfront knowledge of a system. This knowledge barrier prevents the development of a full-fledged system model on the front end of the research process, and limits the utilization of the model as an exploratory tool that complements and refines the experimental process rather than trailing and confirming it. It is for this reason that pathologies, for which there is even less understanding and fewer details known than in normal, non-diseased state physiologies, are highly under-modeled.

Goal

The goal of this dissertation is to lower these two aforementioned barriers by laying the necessary foundation to move models forward in the research process—from a confirmatory tool to an exploratory tool, which helps to direct and prioritize experimental and clinical research by providing the comprehensive, system level view of physiologies and pathologies that is needed in order to identify, develop, and evaluate effective therapeutic strategies.

Specific Objectives

The specific objectives of this dissertation individually address each of the two aforementioned obstacles, which correspond to the short falls of current model analytical and development techniques to produce comprehensive system-level views of complex physiological and pathological systems:

1) Develop and evaluate analytical tool(s) to tease out and explain the underlying mechanisms, organizing principles, and/or dynamics of emergent, complex adaptive behavior within computational models.
2) Develop and evaluate methodology that enables initial, system-level "scaffolding" models to be quickly built and assessed based on available literature or experimental data without the need for unknown detailed component properties.

Approach

It is our ***assertion*** that the philosophy of complexity theory, the study of complex systems, can be utilized to develop methods capable of identifying, characterizing and even predicting the inner workings, dynamics, and emergent behavior of complex physiologies and pathologies. Thus, the ***approach*** utilized to accomplish these objectives consists of using complex systems theory and philosophy to develop applied methodological and analytical modeling tools. The developed modeling tools are referred to as *relational modeling* and the analysis tools are referred to as *relational analysis*. These complex systems-based tools are developed and tested within five very different physiological and pathological systems whose only commonality is they are neural in

nature: synaptic neurotransmitter spillover, axonal transport, spinal cord injury (SCI), amyotrophic lateral sclerosis (ALS), and motoneurons. To insure the robustness of the developed analytical tools of relational analysis in examining complex system dynamics in all types of models, these systems were modeled using both a variety of traditional techniques, including mechanistic and conceptual modeling, in addition to the newly developed relational modeling technique. In addition to testing on computational models, the usability and effectiveness of the relational analysis technique is also evaluated on experimental data using neurophysiological recordings from cat spinal motoneurons. The relational modeling methodologies are used to construct comprehensive views of two highly clinically significant, yet lesser understood neuropathologies: secondary SCI and ALS.

Dissertation Organization

The overall organization of this dissertation is by system test case study since the primary intent is to illustrate the use, applicability and efficacy of the developed methods within different physiological and pathological systems. Chapters 2-3 lay the foundation of this dissertation by providing a literature review and the philosophy of approach. Chapters 3-6 focus on the developed relational modeling and analysis tools. Chapters 7-10 are physiological and pathological test cases in which we develop and test our relational modeling and/or relational analysis tools. Chapter 11 provides the conclusions of this work.

Outline of Chapters

Chapter 2: **Literature Review** provides an overview and history of computational modeling and the theoretical fields that primarily use it, computational neuroscience and systems biology. The field of complex systems is also reviewed.

Chapter 3: Philosophy of Approach explains the complex systems based philosophy, which was used to develop the methodological tools, and how this philosophy was synthesized into an analytical approach. Additionally it provides an overview of our generalized modeling process.

Chapter 4: Relational Analysis discusses relational analysis in detail including why, when, and how to use it. It also serves as a user's guide for the relational analysis technique of search-survey-and-summarize (S3).

Chapter 5: Component Analysis discusses component analysis, including the detailed steps. It also illustrates an experimental test case in which neurophysiological data from in vivo cat spinal cord motoneurons is analyzed using component analysis.

Chapter 6: **Relational Modeling** discusses relational modeling in detail. It also serves as a user's guide for the relational modeling technique of review-relate-refine (R3).

Chapter 7: Synaptic Neurotransmitter Spillover encompasses the test case of neurotransmitter spillover. It includes two publications. The first develops and analyzes the primary spillover model using traditional methods (Mitchell et al 2007) and the second develops and uses relational analysis to differentiate between two different model implementations (Mitchell and Lee 2007).

Chapter 8: Secondary Spinal Cord Injury includes the published spinal cord injury model (Mitchell and Lee 2008), the first relational model using our developed R3 technique.

Chapter 9: Axonal Transport includes the physiologic portion of the axonal transport test case. It includes the published cooperative axonal transport model (Mitchell and Lee 2009).

Chapter 10: Amyotrophic Lateral Sclerosis is aggregation of our work in ALS using our developed relational analysis and modeling methodologies. It includes a submitted publication of a computational model of ALS-disrupted axonal transport (Mitchell and Lee, in revision) and a preliminary relational model of the comprehensive ALS pathology (Mitchell and Lee, in preparation).

Chapter 11: Conclusions summarizes our conclusions on the developed methodologies, viewpoints, and a new approach to systems physiology.

CHAPTER 2

LITERATURE REVIEW

This chapter lays the background required to understand the philosophy of our approach (Chapter 3) by discussing the current research techniques and applications of computational modeling in the analysis of biological systems. Within this chapter, the history of the field(s) which utilize computational modeling are discussed, as well as their current techniques, and the pros and cons of those techniques in regards to their ability to produce, analyze, and predict the emergent properties and dynamics of physiologic and pathologic systems.

The field of computational modeling is, in and of itself, not a single field. Rather, computational modeling exists among theoretical fields, which use it as a tool to investigate their respective systems. Of fields that have extensively used computational models to study physiological systems, the theoretical fields of computational neuroscience and systems biology have used computational modeling and associated quantitative techniques the most. While both systems biologists and computational neuroscientists have the same overall goal—the desire to better understand their respective systems, including mechanisms, dynamics, and organizing principles--- as a whole, each field has undertaken different means and methods to pursue their equivalent goals. This chapter describes the history of computational neuroscience and systems biology, focusing on the advantages and disadvantages of their techniques and the traits

of their systems, which necessitate a certain technique. Finally, the chapter concludes with some necessary background on complex systems.

Computational Neuroscience

Computational neuroscience is a field that uses mathematics and theory in order to describe, examine and analyze the behavior, function, and dynamics of individual neurons, neural networks, and the brain and spinal cord, which comprise the central nervous system. Computational neuroscience has made provided enormous contributions to computational modeling through the addition, application, and implementation of important quantitative techniques, particularly techniques such as the 'black box' model, large and complex mechanistic models, information theory, and parameter searches (which are all discussed in this section). While computational neuroscientists have been quite successful in producing the emergent properties of the neurons in which they study, the field in general often falls short in explaining why and how these properties are produced, a key requirement for studying neural physiologies and especially pathologies.

Though the term "computational neuroscience" did not appear until the mid-1980's (Sejnowski et al. 1988), most consider the birth of the field to be in 1952 with the publication of the classic Hodgkin-Huxley neuron model, a quantitative description of neuronal membrane current and excitation using parameters obtained from the giant squid axon, developed by Alan L. Hodgkin and Andrew F. Huxley (Hodgkin and Huxley 1952). However, some argue that the true starting point of computational neuroscience was in 1907 when Louis Lapicque first introduced the integrate-and-fire neuron model

(Brunel and van Rossum 2007; Lapicque 1907). These original models were more or less "black box" models that describe the neuron model using an input-output transform. They assumed that neurons were isopotential, and they ignored the contributions of dendrites.

The next significant advance in computational neuroscience was by Wilfrid Rall who used the mathematics of the cable theory to show that the dendrites and their numerous arborizations largely affect the processing of synaptic input by the soma (Rall 1959; Rall 1964; Rall 1962). The neuronal models of today often incorporate hundreds of neuronal "compartments" (e.g. individual pieces of a neuron which are computationally modeled as a single unit), mainly to account for the strong impact of these large dendrites (Rose and Cushing 2004; Shapiro and Lee 2007). In addition to getting "larger", recent neuron models have become increasingly more complex. For example, some include numerous sodium channel subtypes rather than modeling sodium as a single influx (Naundorf et al. 2006) or include detailed channel kinetics such as a 12-state Markov model for a single sodium channel (Kuo and Bean 1994), and active transporters and pumps (Lopreore et al. 2008).

While some of the newer, complex additions to neuronal models are mechanistic in nature, based off first-principles kinetics, diffusion, and electrotonics, much of neuronal modeling and computational neuroscience still remains largely "black box" intermixed with some degree of mechanistic modeling. This is particularly true of large neuronal network models. Other than alleviating computational requirements, a feat that has been

greatly helped by the advent of new simulator technologies (Bower and Beeman 1998; Carnevale and Hines 2005; Graas et al. 2004; Weinstein and Lee 2006), the need for the black box approach largely remains for two reasons. First, much is still unknown in regards to neuronal mechanisms and especially as to connectivity. Secondly, computational neuroscience lacks the extensive databases that the systems biologists have at their disposal. Thus, traditional data-driven techniques, which require very large, complete data sets, such as those used by systems biologists to explore the enormous genomics and proteomics databases, are not amenable to most of computational and experimental neuroscience. Therefore, the current analytical approaches that best lend themselves to computational neuroscience include information theoretic approaches such as infomax learning (Okajima 2004) and Bayesian methods (Pearl and Russell 2003) and other traditional input-output transformation techniques; for a review of computational neuroscience techniques see (Dayan and Abbott 2001; Rieke et al. 1997). Another common technique set includes monte-carlo or random analysis in which random parameter sets (i.e. parameter searches) and/or connectivities are simulated to aid in the investigation of dynamics(Goldman et al. 2001; Mitchell and Lee 2007; Prinz et al. 2004; Van Geit et al. 2008). However, the pitfalls of such methods is that, though they allow us to recapitulate experimental outputs, they do not give us insight as to how or why we have reached them. Thus, mechanistic deduction from such methods alone becomes very difficult.

Systems Biology

Systems biology is a field that attempts to take a 'systems' or 'top down' approach to the analysis of biological systems. Instead of focusing on the individual components within a system, the goal of systems biology is to look at multi-scale interactions, functions and dynamics across different physiological levels, such as cellular, tissue, and body systems. However, while most in the field would agree with this overall goal, much of what is currently considered 'systems biology' typically does not work at the true systems level nor does it focus on system-level interactions. Instead, most research focuses on one or two scalar levels and looks only at the implications of those levels on the system. Many researchers reside in the areas of metabolics, genomics, and proteomics where high-throughput arrays, analyses and databases can be used to quantify how specific individual changes affect all of metabolism, the genome or proteome. Thus, systems biologists often focus on the relationships within their studied systems. In fact, much can be learned from systems biology given that it has pioneered the application of multi-variate statistics to extract important system relationships from large datasets. However, systems biology has been unable to 'drill' through a system and utilize the relationships to look at how the components of a system interact to produce the emergent properties, dynamics, and organizing principles which encompass the physiologies and pathologies that we wish to explore. In this section, the history of systems biology is highlighted along with currents relationship-extracting techniques currently utilized by the field.

Similarly to computational neuroscience, systems biology was also rediscovered and defined far after its origin. Ludwig von Bertalanffy is often considered the father of the

field for his work in general systems theory applied to biological systems, work that first appeared around 1950 but was not recognized until the mid-1960's (von Bertalanffy 1968; von Bertalanffy 1950). After Bertanlanffy, some of the earliest contributions to the field came in the 1970's from the very independent and isolated efforts of a variety of fields, including metabolism (Savageau 1969), cardiophysiology (Heppner and Plonsey 1970; Melbin and Patterson 1970), and developmental biology (Meinhardt and Gierer 1974), to name a few.

However, "systems biology" as we currently know it did not become popularized until the late-1990's. Its rebirth was largely due to the advent of high-throughput experimental technologies such as the gene chip and microarray (Lashkari et al. 1997), which revolutionized the study of genomics (Collins et al. 1998), proteomics (Anderson and Anderson 1998), and other 'omic' fields by providing large compilations and databases of quantitative metrics and output that could describe a system in its entirety, such as the Human Genome Project (Collins et al. 1998). In sharp contrast to computational neuroscience, the chief issue of systems biology is an overwhelming availability of extremely complex experimental data. Since theses large experimental databases serve as the primary source of data, systems biology became data-driven resulting in the need for interpretative data analysis and manipulation techniques.

Because the data pool is so overwhelmingly large, systems biologists spend a good deal of time determining the "importance" of various metrics by looking at their correlations using multi-variate statistics (Hair et al. 2006). In addition, graph theory is used to unveil

the topology of detailed genetic and molecular networks in an effort to determine their underlying organizing principles and dynamics (Strogatz 2001; Wouters et al. 2003). Thus, the tools of systems biologists lean towards systems theory in order to describe how the numerous components in their databases result in a functional "system".

Complex Systems

While systems biology and complex systems are presently distinct fields, they share underlying principles and foundational mathematic origins, as well as many mathematical research contributors, including Ludwig von Bertalanffy. However, the two fields diverged not long after their birth when early system biologists turned to "reductionist" approaches, which attempt to study the global properties of a system by the independent study and combining of its simpler, sub-system components (Ricard, 2006).

However, real systems, including biological systems, have properties that cannot be seen when viewed solely from the independent component perspective. For example, say that a real system, XY, can be defined by a mathematical function $H(X,Y) = H(X) + H(Y)$ that describes its properties or degrees of freedom using two independent subsystems, H(X) and H(Y). The result of H(X,Y) produces integrated properties that cannot be seen when the two subsystems are considered independently. These integrated properties are referred to as *emergent* and the system is said to be *complex* (Ricard, 2006). Neurons are a perfect example of how combining different subsystems (channel kinetics) can result in an action potential, an emergent property of the neural system.

Typically, complex systems are very robust. They possess the ability to undergo radical qualitative change while maintaining systemic integrity. Complex systems theorists attribute such innate ability to undergo change to the fact that complex systems show a domain between deterministic order and randomness (Cilliers 1998), which is complex and often referred to as "the edge of chaos" (Bak 1996). Unlike chaotic systems, complex systems develop far from equilibrium at the edge of chaos and are history-dependent (Buchanan 2000). Complex systems evolve at a critical state built up by a history of irreversible and unexpected events. These additional defining attributes of complex systems add to the balance of adaptability and predictability of their functionality (Buchanan 2000).

In fact, it is this very lack of robustness that results in the inability of reductionistic computational models to either fully produce or uncover the rich emergent features of many physiological systems. From a modeler's standpoint, some of the larger pitfalls with reductionism, listed in no particular order, include the following:

- Failure to produce any or all of the emergent properties
- Failure to be as robust as the real system
- "Breaking" of fundamental system component relationships (i.e. wrong correlation sign or magnitude) in order to produce desired features
- Inability to explain how or why an emergent feature appears
- Inability to characterize the dynamics of emergent features

Not surprisingly, it has become increasingly obvious to modelers and non-modelers alike, that the global properties of a system cannot always be predicted from the independent study of corresponding sub-systems (Ricard, 2006). In a series of articles published in Science entitled "Beyond Reductionism", scientists from several fields including neuroscientists, chemists, physicists, biologists, and social scientists reached the same conclusion that the study of emergent global properties of a system of interactions between local subsystems is essential to understand their physical nature in quantitative scientific terms (Gallagher and Appenzeller, 1999). To date, despite the common agreement that the study of emergent properties is one of the keys to understanding physical mechanisms of models, there is little to no consensus as to how to go about quantitatively and methodically studying them. Instead, the field still remains largely philosophical.

The methods that do exist to study complexity are centered on quantifying the flow of information, often referred to as information theory. The methods of information theory are based on probability theory and statistics. The most important metrics used are entropy, the information in a random variable, and mutual information, the amount of information in common between two random variables. While information theory has been used to model and characterize some aspects of physiological systems, such as quantifying the complexity of the brain to determine the segregation of areas of function (Tononi 1994), this technique is not amenable or applicable as a general modeling tool for constructing and analyzing most physiological and pathological systems.

Table 2.1. Summary of methods used by computational neuroscientists, systems biologists, and complex systems theorists, including their advantages and disadvantages.

Field	Methods	Advantages	Disadvantages
Computational Neuroscience	• Information Theory • Bayesian networks • Random analysis • Parameter searches	• Able to achieve output goals • Requires no knowledge of mechanisms • Requires less data	• Difficult to infer mechanisms from non-unique solutions • Do not know "why" outputs are achieved
Systems Biology	• Graphical theory • Cluster analysis • PCA	• Able to handle large data sets	• Overly restrictive assumptions • Inability to look at all "layers" of the system
Complex Systems	• Information theory	• Uses simple relationships to explain complex behavior • Does not require that mechanisms be known	• Largely philosophical • Currently no applications-based methods • Information theory is not amenable to all biological questions

CHAPTER 3

PHILOSOPHY BEHIND THE APPROACH

The disconnect between the computational models of the physiological systems that we wish to explore and the actual systems, themselves, is the gulf that lies between reductionism and complexity. It is a requirement that our models be reductionistic in nature, yet, the physiologies and pathologies that we wish to study are quite obviously complex. To date, this inescapable fact has left biomedical engineers in a quandary since, as noted in the background, most of what has been proposed to analyze complex systems has fallen into the category of 'descriptive philosophy'. Unfortunately, this philosophy alone does not solve the biomedical engineers' quandary. This fact is perhaps best exemplified by a quote of a very famous scientist, which has served as a source of inspiration for this entire project:

> "The love of complexity without reductionism makes art; the love of complexity with reductionism makes science." --Edward O. Wilson, *Consilience*

The above quote eloquently states our methodological goal: to make science by developing an analytical approach that would allow the complex properties and dynamics of physiologic and pathologic systems to be explored through what are unavoidably reductionistic computational models. To do this, we translated the philosophical art,

which describes the rich features, properties, and characteristics of complex systems into a set of applied quantitative techniques.

This chapter describes the perspective and philosophy from which our methodologies are derived. The first section of this chapter describes our over-arching view of physiologic systems, as complex biological systems, and discusses their conserved fundamental properties. The second section of this chapter describes how we utilize the aforementioned complex systems philosophy as an analytical approach to develop methods capable of exploring complex biological systems. In the third and final section in this chapter our generalized modeling process is outlined.

Physiologic systems described as complex systems

Real physiologic systems are inherently complex in that a huge number of inputs, governed under an extremely dynamic set of relationships, are used to generate a large set of robust yet predictable behavioral patterns which are said to be "emergent". This fundamental feature of biological systems was first described by Csete and Doyle (Csete and Doyle 2004) as the "bowtie" effect. A critical principle of the bowtie is dimensional restriction. That is, a large number of inputs (i.e. multi-dimensional system input) are transformed or dimensionally restricted through mechanisms governed by underlying relationships to produce emergent, complex adaptive behavior (i.e. multi-dimensional system output) as shown in **Figure 1**. The system utilizes positive and negative feedback to alter or "tune" these relationships to respond to changing input or environmental conditions or to initiate a change in behavioral output.

As shown in Figure 1, it is the inner relationships and emergence, which form the "knot" or "pinch point" of the bowtie. It is at this pinch point where the driving mechanics of a system reside. Therefore, it is our ability to 'see' what happens inside the pinch point, which holds the key to unlocking the mechanisms, dynamics, and organizing principles that are central to bioscientific and clinical research. Thus, we focus our methodological development on the relationships that specify the dimensional restriction and emergence, which, together, encompass the pinch point.

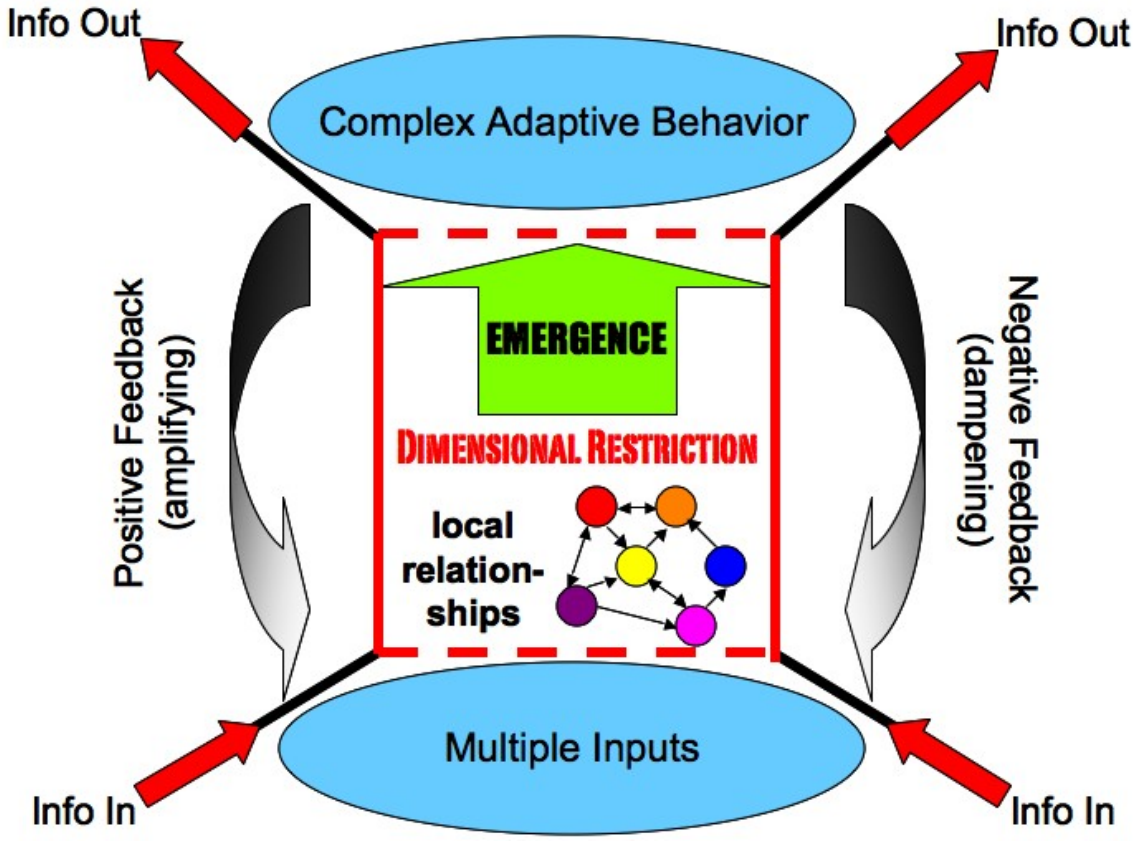

Figure 3.1. The bowtie effect of complex biological systems. Multi-dimensional input is dimensionally restricted via local relationships that govern system mechanisms to produce multi-dimensional complex adaptive behavior. The system uses positive and negative feedback in order to "tune" the behavioral response.

There are two critical aspects or properties of complex biological systems that influence the relationships and resulting dimensional restriction and emergence seen at the pinch point--redundancy and degeneracy. *Redundancy* is defined as identical structural units or subsystems which perform the same function, whereas *degeneracy* is defined as structurally different units or subsystems which can perform the same function (Tononi et al. 1999). These properties can affect the magnitude, probability or certainty of an emergent property or response. For example, a neuronal cell contains numerous identical or redundant sodium channels that can affect the magnitude and certainty of its fundamental emergent property, the action potential. Simultaneously, sodium channels can be degenerate in that there are different types of sodium channels (e.g. Nav 1.6 vs Nav 1.3), which are structurally different but perform the same function of controlling sodium influx into the cell. However, the best example of degeneracy is the brain. The brain has multiple activation pathways that can be used in order to accomplish a task. Such degenerate paths become apparent particularly in brain-injured patients such as those who have incurred a traumatic brain injury, had brain surgery, or experienced a stroke. These patients often have damage, which initially limits certain motor tasks or skills such as speech or language. However, with time, these patients adapt by activating degenerate networks, which enable them to "regain" lost functions. Such adaptability makes complex biological systems extremely robust.

While complex biological systems are extremely robust over long periods of time, they also have the ability to undergo radical qualitative change while maintaining systemic integrity. For example, consider a patient with a prosthetic arm/hand who has undergone

the relatively new procedure to redirect cutaneous sensation from the hand to the chest skin of human amputees with targeted reinnervation (Kuiken et al. 2007). Such patients learn to activate their prosthetic hand using the chest muscles and "feel" the sensation from objects touching their prosthetic hand as if is was their real hand except this sensation is mapped to the chest. The sensory map is transformed such that literally touching the area where the prosthesis is reinnervated is as if the physiological hand were being touched. This adaptability is so superb that such a patient can even distinguish sensations as being felt from individual fingers.

Complex systems philosophy utilized as an analytical approach

We assert that the redundancy and degeneracy within complex systems directly results in the flexibility and robustness that is seen in complex biological systems. The remainder of this chapter discusses how these fundamental properties of complex systems, particularly the formation of pinch points, can be used to model complex biological systems, including physiologies and pathologies.

In the Introduction, a model was described as a system map in which the inputs signify the initial starting point, equations represent the system path(s), parameters specify the coordinates of the path(s), and outputs specify the final destination or system outcome. Typically most modelers will fixate on the final destination (the outputs). However, as is shown in the bowtie effect, it is in the path where the complex relationships between inputs and outputs are created which result in the emergent properties and behavior that characterize a particular system. Thus, it is this path, the pinch point that contains critical

information about the underlying physiological mechanisms involved in a biological process. Models, just like maps, can include varying levels of details and complexity, which illustrate the system paths. For example, a simple model may only show major highways similar to a road map, whereas a more complex model may include additional features, similar to the mountains, rivers, and elevations shown on a more detailed physical or topological map. The level of complexity included in a model may or may not affect the measured outputs. However, it can definitely influence the model dynamics, what happens between the starting point and final destination, and it is these dynamics, which are a measure of the relationships within a system.

Thus, using traditional output-value based analytical techniques, there is no way of knowing whether the model implemented, whether a detailed mechanistic model or a high-level 'black box' model, correctly illustrates the dynamics that occur at the pinch point. Furthermore, because there is little to aid in the determination of the input-output function, typical output value based techniques of modeling and analysis are highly reliant upon knowing or understanding a considerable amount about a system—either bottom-level detailed, mechanisms or top-level, higher conceptual understanding.

In contrast, our general approach to modeling methodology and analysis is to shift the attention back to the 'pinch point', where the mechanisms and organizing principles that we wish to reveal are actually contained, by focusing on the relationships within a system rather than purely its quantitative output values. We use these system relationships as either a placeholder or bridging structure from which unknown aspects of a system can be

effectively explored. For example, our data analysis technique, relational analysis, utilizes the intrinsic relationships among the system outputs in order to deduce the mechanisms and dynamics, which are occurring inside the pinch point. Similarly, relational modeling, utilizes the measured intrinsic experimental relationships within the system in order to reproduce the dynamics, which specify the outputs.

Our generalized bridging framework for biological and neural complex systems, termed *Heuristic Emergence via Dimensional Restriction* (HEDR), is the philosophical basis from which relational modeling and relational analysis are derived. HEDR has become our (the Lee lab's) 'manifesto' for the exploration and analysis of complex biological systems, and has been formally written as the following:

> We believe that the structural similarities we observe reflect a fundamental feature of biological systems at all levels. We refer to this common feature as a "pinch point" –a dimensional reduction producing the emergence of functional behaviors. Furthermore, we believe that the overabundance of dimensions, due to redundancy/degeneracy, provides the key building material from which these pinch points are formed. By warping, squeezing and folding, the nonlinear dynamics of specific mechanisms within the underlying system transform these dimensions. The redundancies/degeneracies in the system are critical for robustness, allowing adaptation and reconfigurability that would be impossible in an actual, low-dimensional system. Finally, we believe that each pinch point implements what can be considered a heuristic solution for producing a behavior,

with the "degree" of pinch being tied to the degree of emergence and to the "certainty" of the heuristic.

The development of our relational analysis and relational modeling methodologies using HEDR principles is discussed in the methodology chapters: Chapters 4 for relational analysis, Chapter 5 for the close relative of relational analysis, component analysis, and Chapter 6 for relational modeling. Furthermore, it is in these aforementioned chapters where the detailed steps of these methodologies are specifically laid out. However, the application of these methodologies is discussed within the specific system test case chapters, 7-10 for relational analysis, and 8 and 10 for relational modeling. Examples of component analysis, including its use to analyze experimental data, are given both specifically within the component analysis (Chapter 5) and within the relational analysis test cases.

Generalized Modeling Process

In this section, our generalized modeling process is outlined. Figure 2 illustrates our generalized modeling workflow. The overall process is an iterative approach that incorporates experimental, clinical, and theoretical data/input into a 'working model' that is evaluated and refined with the techniques developed in this dissertation, namely relational and component analysis.

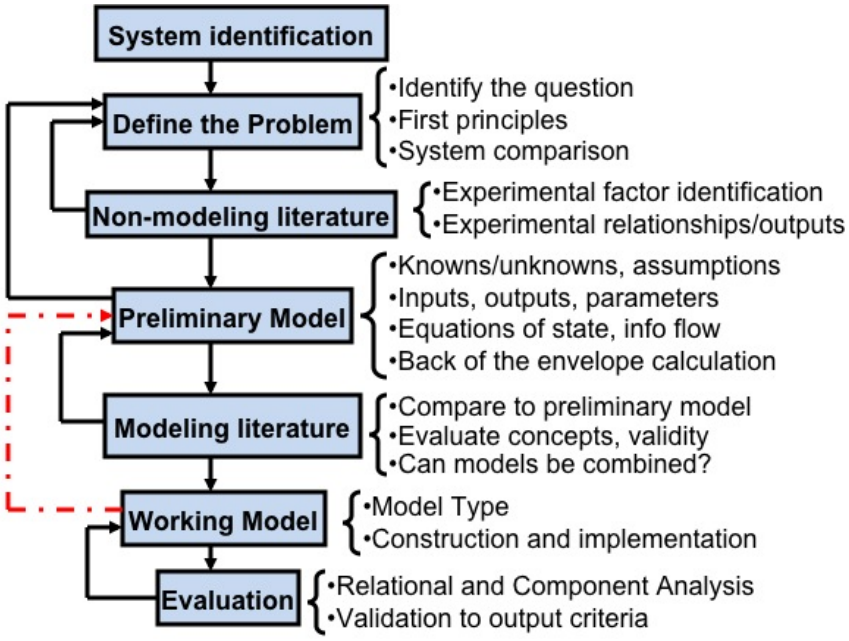

Figure 3.2. Modeling Process Workflow. The diagram illustrates the major steps of our modeling process. The overall process is an iterative approach that includes experimental, clinical, and theoretical input into the construction of a 'working model' that is evaluated and refined using our complex systems based approaches of relational and component analysis.

The process begins with identification of the system to be studied. In general, system identification is based on the interests of the researcher and the type of question the researcher wishes to investigate. In this work, our scientific/research interest in particular systems did influence the types of systems that we chose to model. For example, our particular research interests favor neural systems, both physiological and pathological. As such, that is the one commonality between all of the test case systems. However, specific system selection for the test cases was also influenced by the properties of the system. We wanted to insure our developed methods were robust enough to handle a wide range of systems modeled using a variety of model construction techniques. Thus, we desired to have a diverse range of systems—systems that varied in their properties,

the level to which they had been experimentally investigated, and our level of a priori knowledge.

The next stage of the process works towards developing a 'preliminary model', a 'back of the envelope' calculation or general estimate of the primary system behavior/emergent property(ies). It is at this point when the translation from the 'language of biology to the language of mathematics' first occurs. This initial translation is usually quite crude, consisting of a few simple relationships or generalized mathematical functions to estimate one or more aspects of system behavior. In fact, this initial or preliminary model may or may not be an actual computational model in the traditional sense of a formally coded computer program; it could be as simple as a theoretical conceptualization within a spreadsheet. This 'back of the envelope' calculation is the starting point from which the model is first synthesized from multiple influencing perspectives, including the experimental/clinical literature (labeled as 'non-modeling literature' in Figure 2) and theoretical literature stemming from existing theories or computational models within the field (labeled as 'modeling literature' in Figure 2).

After a few iterations with a preliminary model based on input from multiple sources and perspectives, a working model is developed. This working model is the traditional computer model, but the label of 'working model' is used instead to signify that the model evolves through an iterative process of evaluation and refinement. It is during this stage when the model strategy (bottom-up/top-down/middle-out) and type are chosen based on the properties of the system, the type of data available and the status of the field

(i.e. the level to which either detailed mechanisms and/or comprehensive theories have been developed). With each iteration, the model is re-evaluated not just at the quantitative level (i.e. parameters, etc), but also at the conceptual level to insure that the model is not forcing the modeler's assumptions inappropriately onto the modeled system, a common issue particularly in black-box or higher level mechanistic models. Thus, even the model strategy and type can continue to change or evolve very late in the process.

The iterative process of evaluation and refinement (see Figure 3) is accomplished using our repertoire of analytical techniques, namely relational and component analysis. The process begins with an initial 'base case' simulation from which output values are extracted using system-specific metrics that characterize the model's behavior or emergent property(ies). Next, data is collected that represents multiple or different system responses or 'model operating points'. Once data is collected, relational and component analysis are used to evaluate both system and component level properties, respectively. As previously mentioned, these techniques focus on the relationships within the system, which result in the emergence and dimensional restriction that occurs at the pinch point. Specifically, the quantitative output relationships are qualitatively visualized on a map referred to as a 'landscape'. This detailed map provides critical system insight that can be used to predict and prioritize mechanisms and dynamics and to identify areas of the model that need improved and refined.

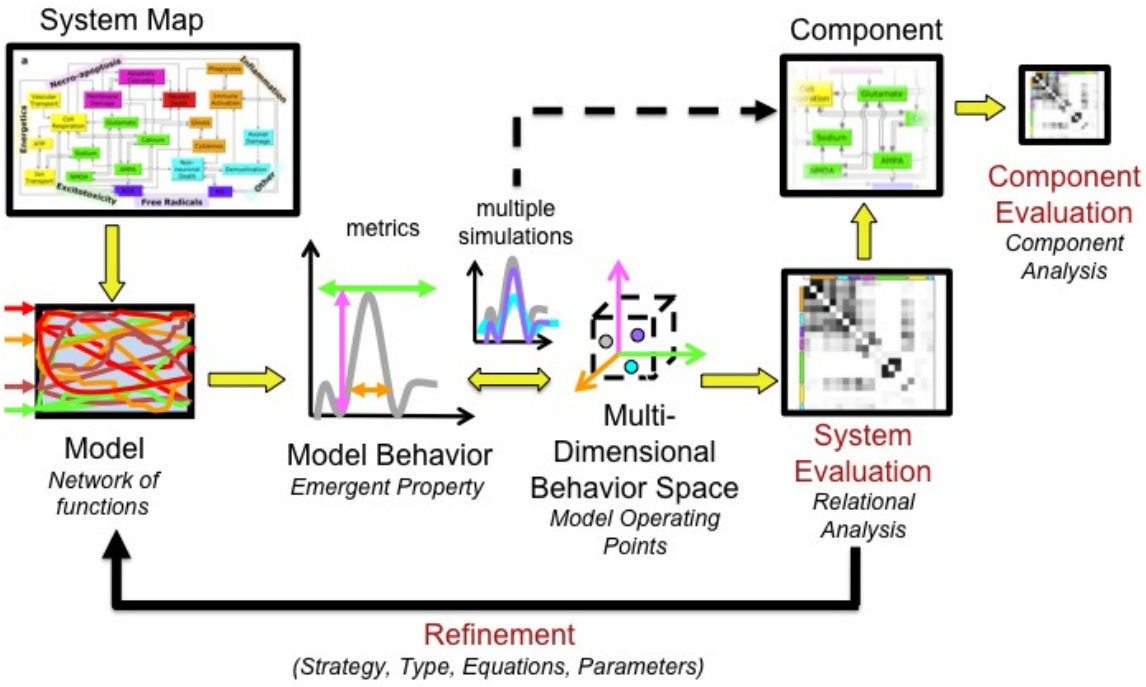

Figure 3.3. Model Evaluation and Refinement. This diagram shows the basic process beginning with the initial simulation, extraction of output metrics characterizing the model's behavior or emergent property(ies), accumulation of data representing multiple model operating points and/or behaviors, and model evaluation via relational and component analysis. The product of relational and component analysis, the system landscape, is used to refine the model.

Different Viewpoints

We recognize three basic modeling viewpoints, each which uses a different general approach in the model development and construction process: bottom-up, top-down, and middle-out. Each type of model can offer a very different and unique perspective into a system. However, despite the benefits of multiple viewpoints, typically modelers' tend to use only a single viewpoint, the viewpoint that most assists with the efficient construction and implementation of their system model. In some cases, depending on the amount and

type of a priori knowledge of a system, there may be no initial choice in which viewpoint to utilize. These viewpoints include:

1. *Bottom-up.* The bottom up viewpoint is a detailed-oriented perspective that is used to lay the foundation of the model. It typically utilizes individual mechanisms and first principles, customary to the typical mechanistic model with which scientists are most familiar.
2. *Top-down.* The top down viewpoint is less focused on structurally recapitulating the detail of individual mechanisms, but rather, it instead utilizes higher level theories from which the components of the model are conceptualized. Thus, top down models are often referred to as 'conceptual models'.
3. *Middle*-out. The term 'middle-out' is not one that is likely to be seen in the standard computational modeling literature. Rather, it is a term that we have coined to refer to models, which are data-centric. This viewpoint is thus dependent upon experimental data, not only for validation, but also for its structural foundation, construction, and implementation. The 'middle-out' viewpoint is best described by our newly developed approach of relational modeling using the R3 technique.

CHAPTER 4

RELATIONAL ANALYSIS

As bioscientists and bioengineers, the goal of our models is to identify, understand, and predict the mechanisms, dynamics, and organizing principles that are central to our respective physiological and pathological systems and their respective emergent property(ies). Using complex systems theory as a methodological guide, the bowtie effect states that the inner workings that we wish to reveal occur at the dimensionally restrictive "pinch point". Therefore, what is needed is an analytical method to view the inner workings of pinch points. The set of analytical tool(s) we have developed for this exact purpose we refer to as "relational analysis". Relational analysis allows us to "pop the hood" on the model and to see what happens beneath the surface, inside the pinch point. With this inside view, we can assess, characterize, and predict system dynamics, behavior and emergent properties in ways not possible with traditional methods used alone.

The philosophical basis of relational analysis is rooted in complex systems theory in that it uses the system's underlying relationships and emergence. The relational analysis methods that we developed can be thought of as a camera that can see through a low-dimensional pinch point, revealing the warping, squeezing and folding of the underlying, high-dimensional, redundant/degenerate mechanisms. This relational analysis camera can be used to assess origin and degree of pinch, thereby helping us to assess the implications of the pinch point on model behavior. Thus, relational analysis is simply an

analytical technique that allows us quantify the relationships within the model or system, which are a result of the pinch point. The main product of relational analysis is the model or system landscape, which reveals the "shape" or topology of the system under a certain set of specified model conditions. This landscape, composed of a cross-correlation matrix of the system's or model's outputs, reveals the relationships or interactions which comprise the system's dynamics and describe the system's emergent property(ies). By revealing the topology of the system, a series of landscapes of the system and/or of its components can unveil dynamics, which can be used to pose hypotheses regarding system mechanisms and behavior.

Search-survey-and-summarize (S^3)

While relational analysis is composed of several techniques or subsets of techniques, our overall strategy or technique is referred to as "search-survey-and-summarize", or S^3 for short. As the name implies, the standard S^3 method contains three basic parts: *search* for a set of parameter values that give rise to the selected target output values (we define each set as a homologue), *survey* the model output landscape by cross-correlating sensitivity analyses for each homologue and *summarize* by statistical analysis of the population of homologue landscapes. Essentially S^3 looks to assess the model at various operating points of interest, collect data regarding the sensitivity and robustness of those operating points, evaluate and visualize the output relationships which are created at the specified operating point(s) within a model landscape, and to compare and contrast the dynamics illustrated within a landscape or set of landscapes to explore or formulate hypotheses regarding both mechanistic and system-level behavior. The basics of

relational analysis and specifically the technique of S^3 are published (Mitchell and Lee, 2007), but this chapter expounds on those basics and focuses on the what, when, where, how and why of the process.

Before beginning S^3…

Before relational analysis can be performed, a model must be up and running. Different ways to construct a model are discussed in the General Modeling Methodology section of Chapter 3. However, beyond the model construction, the next step is specifying the outputs that are to be included as part of the relational analysis. This section briefly outlines model output selection.

Output types. The first step to relational analysis is defining the relationships that are to be analyzed. The analyzed relationships of relational analysis are typically the model output relationships. Although not a requirement, the output metrics and their relationships usually describe or quantify one or more emergent properties of the system. Relational analysis does not discriminate the types of model outputs. That is, any metric that is a single, quantifiable entity can be used as an output, and these output metrics need not be of the same type or units. However, if a model utilizes graphical output or "traces" to represent an emergent property or other characterizing feature, then such a graphical output will need to be decomposed into a set of metrics which describe or characterize the graph or trace. An example of such a graphical trace is the emergent property and output of a neuron model, the action potential. Thus, typical outputs for relational analysis of a neuron model might include spike height, spike width, time of

onset, half-activation and time constants, etc. Other possibilities for outputs, particularly in models that include kinetics or pathways, include concentrations (such as measures of glutamate), degrees of activation (such as receptor or enzyme activation) or percent or fractional compositions. Whether measurements are electrical, physical, chemical, statistical, and/or combination thereof, or even something else not mentioned here in this text makes no difference since all of the output metrics will be analyzed relative to one another.

Minimum outputs. While the type(s) of outputs do not matter for relational analysis, the number of outputs does influence the outcome and particularly the efficacy of relational analysis. In general, more outputs are better. In fact, it is helpful if some outputs are 'degenerate' in that they are different methods that ultimately measure the same thing or 'redundant' in that they are the same metrics measured at different time points or different conditions. More outputs equate to more insight into the system and give more discriminatory power to differentiate, compare, and contrast models, properties and/or systems. Based on the test cases in this dissertation in which relational analysis was applied to models of varying complexity and size and at various stages within model development, the loose 'minimum' number of outputs is about 8-10.

Maximum outputs. Also, since the general method of relational analysis arises from statistical techniques adapted to larger data sets, relational analysis itself is also best suited for visualizing and analyzing multiple outputs. While there is no set maximum, analyzing or visualizing more than 30 outputs at a time and particularly in a single

landscape, can be a little difficult to intuit in one setting. However, despite this difficulty, much information can be honed from the system-wide landscape. To aid in visualization and analysis in a case where there are large numbers of outputs that make the overall landscape difficult to singly intuit, component analysis is especially helpful to dissect the system into smaller sub-systems and smaller landscapes, which parse the total number of outputs (see Chapter 5 for a discussion and user guide on Component Analysis).

Other metric types. Relational analysis can potentially be applied to any set of metrics that describe the system, not just the final model output metrics. Other examples include experimental metrics, intermediate metrics within a model or sub-model, state variable metrics, or possibly model parameter metrics within an automated search. While these "others" do not strictly fit within the main technique of relational analysis, the search-survey-and-summarize, they often fit modified forms of it, "survey and summarize", or fit within the relational analysis technique of component analysis.

Search

The first step of relational analysis is to gather output data from various model operating points, typically through either a series of manual or automated searches using one or more optimization techniques. As defined in the background, a search seeks to find one or more parameter value sets that result in a specified set of quantitative model outputs call the target output values or simply the 'target'. We define such multiple, non-unique parameter value sets, which are capable of producing the same quantitative target output values as 'homologues'.

There are three common reasons that engineers typically perform a search: 1) To find parameter value sets that produce the target output values of a characterized behavior in a mechanistic model in which experimental parameter values are either unknown or questionable. 2) To 'fit' output data in which mechanisms are not clearly known as in a black box model. 3) To analyze different structures or 'circuitry' of a system as in computational neuroscience neural networks. While we also believe the search to be useful in the above three purposes, our main purpose of the search is to exploit parameter non-uniqueness to gain additional 'views' of the system as explained in the 'Why Search' section below.

Why Search? Although this step is not required and it may not even be possible with every model, it definitely adds to the versatility and robustness of the analysis by giving as many 'views' through the pinch point as possible. These views can later be used to compare and contrast the underlying relationships and dynamics of different sets of unique model operating points or solutions or different sets of non-unique solutions based on their parameter values (i.e. orientation in the parameter space). Continuing with the traditional neuron model example, there may be several different neuronal behaviors, which we desire to characterize, such as bursting, amplification, or bistability, and each behavior can potentially have its own parameter value set(s) and target output values.

An additional benefit of searches is that, by requiring that the quantitative output metrics be the same (within convergence or specified error criteria), searches are an excellent

vehicle for examining the differences between different model or sub-model implementations. Such an analysis can be invaluable for determining the implications of both the level of complexity and the type of mechanism(s) or concept(s) to be included in the model. Thus, the relational analysis of several prospective models can be compared to a relational analysis of an experimental data set such that the model with the closest match is chosen to represent the real system. A detailed example of such a comparison is given in the glutamate spillover test case where the simpler, 5-state Lester and Jahr NMDA receptor model compared to the more complex, 8-state Banke and Traynelis NMDA receptor model both intrinsically and extrinsically within the context of a glutamate spillover model.

When should a search be performed? Searches work best in a mechanistic model, but they can also be of aid in a conceptual model. Searches are particularly helpful for models that have either a large number of inputs or parameters or multiple "operating points" that exemplify different system properties or behaviors.

What should be included in a search? At first, the answer to this question may seem painfully obvious—parameters, of course. But actually, it can be more complicated. How many parameters should be searched at once? How does one go about choosing which parameters to search? When should a particular parameter be searched? These are just a few questions that relate to what to search. There are not precise answers to these questions. In fact, the best rule of thumb is 'when in doubt, try it'. If analyzing a single model, we typically begin by searching for every parameter within the model. The

advantage of this is that searching every parameter gives greater insight into the sensitivity and robustness of the parameter and its overall impact on the system at different operating points.

However, there is also great value in dividing the parameter set and only searching for a specified segment of parameters. Parameter segregation is particularly advantageous when comparing and contrasting sub-models or components of the system. It is analogous to 'doing an experiment' on a sub-model or component. Just like an experimentalist typically only varies one variable at a time when performing a test to determine the impact of an experimental factor, a modeler can also vary one component or sub-system at a time to determine its impact on a system. This is precisely what was done in the spillover test case to compare the LJ and BT NMDA-R models within a spillover model. However, there are other possible ways of segregation that are not on a strictly component or sub-model basis. One example is to do it on a factor basis. For example, in a neuron model, one may choose to vary every parameter that directly affects calcium. Thus, calcium parameter values would be changed in perhaps the calcium channel(s), calcium pump(s), and the calcium buffer(s), with each of the aforementioned three being considered its own 'component' or sub-model.

How is a search performed? While not the focus of this particular work, much research has gone into determining the best ways or methods to search. Basically, no one search or 'optimization' method or technique is perfect for every problem. All techniques have

their advantages and disadvantages. However, all optimization techniques follow the same basic workflow:

1) *Start.* Choose a random starting point for input(s) or parameters to be optimized. This starting point may or may not be bounded within a pre-determined range. Choose a desired set of metric and values to serve as the target output values and a set of convergence criteria, which state how closely the search must match the target output values.

2) *Evaluate.* The model is run at the starting point values. A 'cost function' or equation, which determines the 'error' in the outputs, their deviation from the target output values, is used to correct the search variable(s). The cost function may or may not be 'weighted' such that one or more outputs are deemed more 'important'. Depending on the technique, one or more variables may be moved at a time.

3) *Correct.* The details of this step depend largely on the search algorithm or technique. Essentially, the algorithm corrects one or more search variables by moving them in the appropriate direction(s) toward the target output values.

4) *Iterate.* Repeat steps 2-3 for all search variables.

5) *Stop.* There are different forms of stop criteria. Most set the stop criteria to the convergence criteria, but if the search has not converged on a solution, or homologue, after a specified number of iterations, then the

search either stops completely or starts over at step one with a new starting point.

Considerations to be made in choosing a search or optimization technique include the stability and robustness of the model, the properties of the underlying model mathematics, the number of parameters included in the search, computational requirements, and ease of implementation. Different types of techniques include gradient descent, genetic or evolutionary algorithms, bifurcation analysis, or hybrid methods. While it is best to choose an optimization technique that best fits the properties of your particular model or problem, like any given technique or set of techniques, individual researchers tend to have their favorite or preferred methods of searching. Our preferred method, which works well in our models and in neural models in general, happens to be gradient descent. A gradient descent type of search was used in our work with the spillover test case.

Survey

Surveying a model is very similar to surveying a construction site. The purpose of surveying the model is to determine the topology or characteristics of the model under a particular set of conditions, or model operating point. Surveying a model, just as in an actual construction site survey, consists of two parts: data collection, which includes quantitative measurements of the variability around the model operating point and visualization through a blueprint or map, which comprises the output relationships of the

model. The data collection process is performed via sensitivity analyses and the visualization is performed via the formation of the model landscape.

Sensitivity Analysis

The sensitivity analysis (SA) is typically defined as the study of how the variation or uncertainty in the output of a mathematical model can be apportioned, qualitatively or quantitatively, to different sources of variation in the input of a model. However, this definition need not be restricted solely to true 'input'. That is, this definition can extend to parameters as well since parameters can also greatly affect model output. To modelers in other fields, particularly sociology and economics, the SA is quite commonplace. However, it has been used to a lesser extent in biological models.

Typical SA's vary inputs or parameters or both over varied ranges that are typically set to one to two experimental standard deviations. Typically one input or parameter is varied at a time and the change that input or parameter has on the output is recorded, typically graphically. Therefore, we define the sensitivity itself as the linear relationship between a parameter and its output. Thus, the sensitivity is often characterized as a slope. An output that is sensitive to a particular input or parameter will reflect a steep slope in its sensitivity analysis.

Why perform a sensitivity analysis? Typically, an SA, when performed over what is thought to be an experimental or valid input or parameter range, is as much a necessary

validation technique as it is an analytical technique. Questions the SA helps to address include: Can the model hold up under some uncertainty or does it fall apart? Is the model as robust as the complex biological system, or more specifically, the experimental preparation, which it is supposed to simulate? While the SA still serves as a validation technique as one of its functions, it's primary purpose within relational analysis, and specifically the search-survey-and-summarize technique, is as the name implies, to 'survey' the system or model.

The only way to survey the model is to see how it responds. However, with most models, unless the model is stochastic or already has some degree of variability built into it such as 'white noise', the model will always produce the same quantitative output values with a given input or parameter set. Thus, to survey the model, we have to introduce some variability into the system by the way of altering inputs and parameters. Surveying the model via a SA allows the model dynamics to be characterized within the landscape by providing the data sets from which relationships are extracted among the outputs.

When should a sensitivity analysis be performed? The answer to this general question is rather simple, always! A SA is a necessary part of both the model validation and analysis process, regardless of the type of model or system. However, in regards to relational analysis technique of S^3, a SA should be performed of every homologue from the search. Note that as part of some searches, such as the searches we perform, SA's are embedded within the search and are used to 'guide' the search by surveying the landscape around the starting point and directing the search in the appropriate direction towards values that

are closer to the target output value(s). These SA's are specifically for the purposes of the search. Since they are done at the beginning or during the search, they typically are sensitivity analyses of a set of inputs or parameters, which do not produce the target output values. Therefore, these intermediate SA's do not replace the 'final SA', which is performed around the product of a single successful search, the homologue that produces the target output values. It is these final SA's, the sensitivity analyses of the homologues, that are used in relational analysis to make the landscape. If a search is not performed on the model, then a SA is done on every input and/or parameter set, which produces the target output values.

What should be included in a sensitivity analysis? In this respect, the SA is similar to the search. Typically, we begin by performing an overall SA in which every input or parameter is varied, depending on the requirements. (Note that for the test cases included in this work, the SA was always for parameters.) However, as was also the case in the search, there are additional benefits to performing the SA simply on one segment of the model, such a single component or factor that is of interest (see Chapter 5).

How to perform a sensitivity analysis? Many modelers simply hand tune their models by manually moving one input or parameter at a time and recording the output values. However, the easiest method is to automate the SA. Our typical method is to simply specify a deviation interval and set up a script that runs the model at specified points within the interval. Precisely what the analysis interval is will depend on the specifics of the model, particularly its robustness, but also on the availability of experimental data.

For the spillover model, the interval was equal to two experimental standard deviations. For the spinal cord injury model, experimental deviations were not known. Though the parameter ranges were not precisely known, they were known to be quite large. Thus, a SA was performed by varying each parameter individually by a specified interval of ± 50%, and the sensitivities were calculated by evaluating the model in eight 6.25% increments. While we use linear SA's in the test cases presented in this dissertation, a non-linear method SA could be implemented. The type of SA utilized will not affect the outcome of S^3.

When determining what interval over which to perform the SA for relational analysis, one has to remember both the purpose of the SA and the purpose of the model landscape. The purpose of the SA is to provide the data from which relationships are extracted in the model landscape, and the purpose of the model landscape is to access the system's inner working and dynamics. Thus, the data included in the landscape from the SA needs to be robust in that it needs both quantitatively measurable and meaningful variability in the outputs in order to effectively illustrate the output relationships. Since the correlation technique to make the landscape uses the differences between values and not the values themselves, too much or too little variability can alter the landscape both qualitatively and quantitatively. Too little variability (i.e. too small of a SA interval) and the landscape will either not reveal any relationships or it could vastly under or overestimate them due to the differences in small numbers. Too large of a variability (too large of a SA interval), and the landscape may 'average out' relationships or show a relationship average which quantitatively skews the relationships in one direction or the other.

There are a few ‘rules of thumb’ tests to check the SA interval. First, look at the differences in the output. Use intuition and knowledge of the model’s robustness to get a feel if the differences seem comparatively small or large. Also, check the magnitudes and signs of the slope. Are they consistent? If the sensitivities are plotted, do they appear linear? Are the signs all the same (i.e. do they go positive say, for example, 4 of your 6 points and negative for the remaining 2 points)? If the slopes are not consistent in magnitude or sign or they have large ‘gaps’ or ‘jumps’ in magnitude, the SA interval may be the wrong size. Typically, if the aforementioned is true, the SA interval would be too large, but if the differences themselves are extremely small (e.g. out past the decimal point), then one might suspect the SA is too small; thus, the differences being measured are really just stochastic or rounding error. If the model’s tolerance to variability is just inherently small and therefore the SA must be kept proportionately small, it is sometimes helpful to increase the sample size over the SA interval. Furthermore, if the model has built-in variability, as in a stochastic model, then the sample size will definitely need to be larger, and the SA interval may need to be on the larger side.

However, it should be noted that there might be cases where inconsistencies in magnitude or sign of the slopes are permissible. An example of such a case is when an ‘overall’ landscape of the ‘average’ system dynamics is desired over a determined operating range. In that particular case, the SA interval would likely be an interval that is known to be a viable operating range for the complex system being modeled, perhaps an experimentally determined range. Over such a range changes in sign or magnitude of the relationships might naturally occur.

Model Landscape

Why make a model landscape? A model landscape allows the output relationships of the system to be easily visualized, both in magnitude and/or sign. It is the underlying premise of relational analysis that based on complex systems philosophy, these relationships represent the inner workings and dynamics of a system. Thus, the landscape is both a critical and central product of relational analysis. It is from the model landscape or a set of model landscape(s) from which summarizing with exploratory data analysis techniques leads to new hypotheses regarding system mechanisms, behaviors, and/or functions. Visualizing these output relationships in a systematic way via a landscape allows their impact, influence, and overall interacting dynamics to be more easily identified and evaluated. This is particularly true in models where there are many outputs.

When to make a landscape? When performing relational analysis, their should always be at least one landscape which illustrates the relationships of the outputs under the primary set of specified conditions, or the primary operating point. However, landscapes 'have power in numbers'. The ability to compare and contrast landscapes is what makes relational analysis truly powerful. For ideas of different types or sets of landscapes which are particularly helpful in model analysis, see the "How should one summarize?" section of text.

What should be included in the landscape? Granted, there are different possible types of landscapes and thus what goes in the landscape depends on what type of landscape it is—

output landscape, parameter landscape, etc. However, landscapes have one thing in common—they all reveal relationships among the variables that they visualize. The main type of landscape is the model output landscape. The landscapes included in this work in the test cases are all model output landscapes but are simply referred to as the 'model landscape'. Model landscapes are the cross-correlation of the model output values obtained from a set of sensitivities extracted from a parameter sensitivity analysis. The standard model output landscape includes all of the model outputs. However, there is also value in just viewing the landscape, or the cross correlation of outputs, of a specific component or sub-model.

How to make a model landscape? A landscape can be made by cross-correlating the calculated sensitivities for each set of output values to be included in the landscape or by cross-correlating the actual output values, themselves. Cross-correlation analysis can be performed in any statistical software such as MATLAB ™ or Systat ™. However, it is important to pay attention to which cross-correlation technique is used and any user-specified options. It is our experience that different cross-correlation methods and options produce subtle to negligible variability in the results. However, it is important that any set of landscapes that are to be compared or contrasted be constructed using the same cross-correlation technique and options.

While there is no maximum on the number of 'runs'/model evaluations/sets of model output values to be included in the landscape, there can be a minimum. The 'minimum' number of model evaluations to include depends on the variability among the runs within

the group. Bootstrap analysis, a re-sampling technique, can be used to determine the minimum number of model evaluations in order for the landscape to be significant. This is discussed in greater detail in Chapter 5. The definition typically used as 'significant' for any particular landscape that is based on a segmented set of model evaluations is that the standard deviation of the magnitude of all the individual relationships within the segmented data set landscape must be less than the standard deviation, and preferably less than 50% of the standard deviation, of the landscape for the full data set. As a general rule, it is best to include at least 8 different model evaluations or sets of model output values in each landscape.

Note that quantitative correlations for any given cross-correlation matrix, or landscape, should range from -1 to +1 inclusive. The higher the absolute value of the cross-correlation, defined as the correlation magnitude, the greater the degree of correlation between two outputs. The sign of the correlation simply indicates its direction. Thus, a cross-correlation of positive one (+1) indicates that the two outputs are completely, positively correlated, a cross-correlation of negative one (-1) indicates that the two outputs are completely, negatively correlated, and a cross-correlation of zero (0) indicates no correlation between the two outputs. In some systems, the sign of the relationships are either arbitrary to the output definition, not particularly meaningful, or are simply 'confusing' to the analysis. For those cases, it can be best to remove the sign by taking the absolute value of the entire matrix.

Once the cross-correlations have been produced, they must be visualized graphically.

Typically, this is done with a 'heat map'. In a heat map, differences in magnitude are represented by different colors or hues of colors. The basic landscape of overall dynamics is best visualized using a grayscale heat map to avoid the confusion of many colors. In such a map, darker hues represent larger magnitudes (black is usually used to illustrate a correlation of 1) and lighter hues represent less correlation magnitudes (white is usually used to illustrate a zero correlation). However, if the intent of the analysis is especially focused on small differences in relationship magnitude, a color heat map may be necessary.

If it is not necessary to visualize the sign of the relationships within a certain landscape, it is best to take the absolute value of the cross-correlation matrix before plotting the graph. However, if differences in relationship signs are important in the system or analysis, there are three ways to both easily illustrate magnitude and sign. First, if very small differences in magnitude are not that important, plotting the positive relationships in one color (such as red) and the negative relationships in another color (such as blue) and using hues of either color to indicate magnitude is a good illustration technique. If grayscale is preferred, sign can be indicated by shape. However, if fine gradation is necessary to differentiate relationship magnitude, a heat map that has a colorbar for the entire positive and negative spectrum may be required.

Finally, there is great benefit to sorting the outputs on the axes. One sorting method that is beneficial, particularly when viewing a single landscape, is to sort such that the outputs that are the most related appear next to each other on the axes. This sorting helps to

identify patterns of relationship within a landscape. Such a sorting technique can be done manually by visualization, quantitatively by using the values of the cross-correlations themselves, or statistically using a technique such as cluster analysis. If a group of landscapes are to be compared, it is best to sort them such that the outputs appear in the same order on the axes of each landscape. Note that regardless of the method of sorting, sorting in no way changes the quantitative values of the relationships, their meaning or even what is in the landscape. Sorting only assists in evaluating and analyzing the landscape by giving different perspectives.

Summarize

Summarize is perhaps the least defined procedure in the S^3 technique. We loosely define 'summarize' as the analytical process by which we evaluate the 'pictures' (i.e the model landscapes) we have taken inside the pinch point to view the inner workings of our system. Thus, in general, 'summarizing' is the process of comparing and contrasting, performing multi-variate statistics, and posing hypotheses based on the model landscape(s).

Why summarize? If we do not summarize, or explore or put into perspective the results of our analyses, then our results are little more than statistical tests without biological meaning. Thus, without summarizing, we are simply left with general characterizations such as "the model exhibits parameter non-uniqueness" and "the model is or is not robust". It is the act of summarizing where the analytical techniques are applied to gain a comprehensive insight into the system. Summarizing is as much, if not more, of a

process of thinking, hypothesizing and evaluating, as it is a specific quantitative test or method.

When should one summarize? Based on why we summarize, the answer to this question is a resounding always! Regardless of the model type, complexity or the specifics of the number of outputs, homologues, or operating points or systems, the model (perhaps best stated as 'the system') should always be summarized. Summarizing is particularly helpful to analyze, compare, and contrast the dynamics of a model over time and at different operating points. It is also helpful in determining the differences between different model implementations or the contributions of different model or factor components.

What should one summarize? This is a question with an infinite number of answers. What is summarized often depends on the system specifics or what is desired from the analysis. In general, the landscapes should always be summarized and in as many ways as possible to hone as much information about the system. Summarizing by time, by component, homologue, target output values, and system factors are just a few ideas. Dimensionality is something else that can be summarized. A measurement of dimensionality is a measure of the 'degree of pinch' in the pinch point.

How should one summarize? Again, how to go about summarizing can be as varied as to what should be summarized. The key is to initially be systematic in summarizing. Set up a few different things or ways in which the system will be summarized. Then, be open in

letting the results of those initial summaries lead to other possible summaries from which more information can be honed. The act of summarizing is as much an art as it is a science. It is dependent on the generation of ideas to explore. However, coming up with such ideas is usually not difficult. The results of even one or two initial ideas or analyses typically generate many more. In general, we try to incorporate several different analytical or statistical tests as part of the summarizing process, such as factor or principal component analysis and bootstrap analysis. However, the way we go about summarizing is best described as exploratory data analysis. The goal is to use statistics and analytical techniques to explore or generate hypotheses rather than confirm them.

Rather than laying out a specific recipe for summarizing here, it is more beneficial to review the test cases themselves. Perhaps the best two examples to compare and contrast different ways of summarizing are the spillover and spinal cord injury model test cases. In the spillover case, summarizing focused on comparing and contrasting the differences between two different model implementations. In the spinal cord injury case, summarizing focused on characterizing the type and number of system interactions in the landscape and how those interactions changed with time (i.e. the analysis focused on hypotheses regarding system dynamics).

Below is a 'top 10' list of the most common ways to summarize:

1) Compare and contrast landscapes at different time points
2) Compare and contrast landscapes spatially (if model has spatiality)
3) Compare and contrast landscapes of different model components

4) Compare and contrast landscapes of different homologues
5) Compare and contrast the standard deviation in segregated group(s) of landscapes
6) Compare and contrast landscapes of different model or mechanistic implementations
7) Compare and contrast the landscapes of categories of model factors
8) Compare and contrast the dimensionality of different components
9) Compare and contrast the dimensionality of different model implementations
10) Compare and contrast the factor or principal component analysis of a landscape or group of landscapes

CHAPTER 5

COMPONENT ANALYSIS

The relational analysis presented in Chapter 4 uses the relationships within a system to determine the overall system dynamics and behavior and to make system-level mechanistic and/or clinical hypotheses. However, there are times in which scientists and engineers need to hone in on a specific aspect of a system, to essentially place a magnifier on a smaller segment, or component, while still being able to view such a component in terms of the full system. This need to view the inner workings of a system is no different than that of the mechanic who must raise the hood of a car to view the components of the engine, which are responsible for making the car run. The tool that we have devised to do precisely this task is *component analysis*. Whereas relational analysis allows us to pop the hood to view the 'engine' itself, component analysis allows us to go deeper and discriminate the relationships and contributions of individual engine parts. Another way to think about component analysis is that it allows one to 'peel off' the individual layers of a system, analogous to peeling away the layers of an onion. This peeling uncovers the embedded relationships and reveals the corresponding dynamics that are hidden from sight when the system is viewed simply at the outer-most level alone. This chapter serves as a user guide on when, why, and how to perform component analysis. Additionally, this chapter includes a detailed example of how component analysis can be used to extract component and system properties from experimental data.

Component analysis is a form of relational analysis that focuses on the relationships induced by an individual system component and reveals the impact of that component on the system landscape. That is, it is an analytical technique that quantifies the cross correlations, namely the system output cross correlations, which are specifically attributable to a system component. A component can be any segment of a model (e.g. such as subsystem or a category of factors or mechanisms that have a regulatory or functional commonality, etc.) or a portion or sub-set of experimental data within a single study (e.g. different cell types, cells with different properties, etc.). Examples of potential components:

- A factor or output that is affected by multiple mechanisms. For example, the 'calcium component' in a traditional neuron model may be defined as every 'mechanism' that has something to do with calcium, such as all calcium channels, pumps, and buffers.
- A single mechanism responsible for a specific function, such as the NMDA receptor model within a glutamate spillover model.
- Any category or group of similar factors, such as 'apoptosis' or 'free radicals' within the spinal cord injury model.
- A single factor or factor property that determines any given system-level property(ies): the conductance of a neuron, the glutamate concentration within the soma, the length of the axon, etc.
- A degenerate mechanism, whether mathematical (5-state receptor model versus 8-state receptor model) or biological (sodium channel Nav 1.3 versus sodium channel Nav 1.6).

Why and when to use component analysis

As stated above, the purpose of component analysis is to study a single component within the context and view of the larger system. Component analysis within a larger model, compared to isolated analysis of a component outside the system model, is analogous to the benefits of an in vivo experiment over an in vitro one. Just like an in vivo experiment, component analysis gives a more realistic picture of how a factor, mechanism or therapy affects the whole system by analyzing that component *within* the full system itself. Component analysis is an excellent tool for either general system analysis, in order to understand the deeper 'layers' of a system, or for a more specific or detailed analysis of the component itself. Thus, component analysis can be used with specific intent in order to go after a pre-existing hypothesis regarding a component or system function or it can be used to generate new hypotheses at both the component and system level. Thus, component analysis is an excellent tool for nearly every model type, and should be included as part of the relational analysis of any model.

How to perform component analysis

The general steps are the same regardless of the type of component to be examined and regardless of whether the data is of computational or experimental origin. Like regular relational analysis, component analysis closely follows the search-survey-and-summarize or S^3 technique. For details on S3, please see Chapter 4.

Step 1: Primary data collection, relational analysis, and landscape construction. Before beginning component analysis, it is best to have already collected the primary data set

and to have performed relational analysis on the overall set. That is, one should have already obtained the 'primary' system landscape, a cross-correlation of all the system outputs based on the primary data set. As stated in Chapter 4, typically this primary data set contains the sensitivity analyses of a model solution, which produces the target output values. This primary data set typically contains multiple sensitivity analyses, one for each homologue, if a search has been performed. However, it must contain at least one sensitivity analysis, which corresponds to at least a single solution that produces the target output values.

There are several reasons for starting with an overall or primary system landscape. First, having an initial primary landscape can be helpful for manual component identification using the summarize technique. Secondly, it is also necessary to aid in the validation of component analysis. Finally, it is necessary in order to compare the effect(s) of the component and separate those from the rest of the system.

Step 2: Determine the standard deviations of the correlations within the primary landscape. These standard deviations will be used to calculate what the maximal deviations in correlations are allowed to be within the component subset data. The standard deviation is simply calculated for every correlation within the primary correlation matrix or landscape from step 1 by bootstrapping. Bootstrapping is a statistical re-sampling technique, which allows properties, such as variance, to be measured from an approximating distribution (Hair, 2006). Bootstrapping allows one to gather many alternative versions of a single statistic, such as a standard deviation, that

would ordinarily be calculated from one sample. We cannot possibly obtain the sensitivity analysis for every homologue or model solution in order to calculate the true standard deviation of *all* possible homologues of the system. From our sample of data, only one value of a statistic can be obtained, i.e one mean, or one standard deviation etc., and hence we don't see how variable that standard deviation is for any particular homologue or set of homologues. When using bootstrapping, we randomly extract a new sample of N runs out of the sampled homologues or model operating points, where each homologue can be selected many times. By doing this several times, we create a large number of datasets that we 'might have seen' and compute the standard deviation for each of these datasets. Thus, we get an estimate of the distribution of standard deviations we might have seen. By taking the standard deviation of this distribution of standard deviations, we can determine what the 'allowable' standard deviation is for any set of homologues or model operating points. This allowable standard deviation determines the number of homologues or model operating points that must be included. Essentially, there must be enough data sets such that the standard deviation of the group is not above the calculated expected standard deviation for the set as determined by bootstrapping.

Step 3: Determine what to include as a component. Typically, there is a specific component that the modeler or experimentalist has already identified as 'interesting' or worthy of further examination either from the overall relational analysis from Step 1 or based on other analytical data or hypotheses in the field. However, if not, interesting components can be identified through a series of statistical tests using the correlations from the primary landscapes. Statistical tests that can be used to group potential outputs

in the landscape to formulate components include: factor analysis, cluster analysis, and categorical analysis, to name just a few. Categorical analysis and cluster analysis are perhaps the most preferable as they are best suited for the purpose of grouping relationships whereas factor analysis is best suited as a dimensionality assessment technique. For example, cluster analysis assigns objects (and in the case of component analysis on the cross-correlated outputs which comprise the landscape, the objects are the outputs) into groups called *clusters* so that the objects or outputs from the same cluster are more similar to each other than outputs from different clusters. Using cluster analysis, the major interesting components, which could be pursued, include the groups of outputs that form the nodes of the cluster.

Bootstrap analysis can be used to determine if there is anything that is both interesting and significant within the groups produced by the statistical tests. Using bootstrap analysis, the data is 'parsed' into distinct but random subsets for each identified group or component. These subsets can then be statistically compared to determine if specific correlation patterns are both evident and significant. If the patterns appear in multiple bootstrapped subsets, they may be worth pursuing. Bootstrap analysis can also reveal how many data sets are necessary to analyze a component using the process outlined in Step 2. This is also discussed further in Step 6.

Step 4: Obtain data for the component. The purpose of this step is to 'peel' away the component so that its effects on the system landscape can be visualized. This 'peeling' can occur by either sorting the existing data set used to formulate the primary landscape,

or by generating new data sets through either additional simulations or experiments, which directly separate the effects of the component. In essence, the goal is to isolate the variability and corresponding relationships, which are attributable to the component. Whether the data is simply sorted into segregated groups, which isolate the component in question or whether additional data is collected that isolates the component will depend on the nature of the component and the ease of which additional data can be obtained.

For component analysis on experimental data, this typically involves just segregating the data set by sorting by the properties, metrics, and/or outputs of the component. For example, in the motoneuron experimental input conductance component test case, the data was simply sorted by the measured input conductance magnitude. If such a sort is not possible or there is no variability among the metrics or outputs belonging to the component in question, additional experiments may need to be performed to obtain the variation in the component metrics and outputs such that their relationships to other system variables can be examined.

For a component analysis on computational data, usually a separate search or at the very least a separate sensitivity analysis will need to be run on the inputs and parameters which are directly related to the component. Using the example of a motoneuron calcium component mentioned previously, the parameters of all the calcium channels, pumps, and buffers would need to be varied to produce a data set that is simply a function of the 'calcium component'. This variation could be done through a search in an attempt to reach a particular target output, as was done in the comparison of the two NMDA

receptor models in the spillover test case, or it could simply mean doing a sensitivity analysis that varies all involved component inputs or parameters. Typically, unless comparing two degenerate models, a sensitivity analysis will suffice for the first pass at component analysis.

Step 5: Construct component landscape and determine standard deviation. To construct a landscape, simply cross-correlate all of the model or experimental outputs, using the data generated from Step 4 just as is done in Relational Analysis (see the landscape section in Relational Analysis, Chapter 4). Additionally, if multiple data sets (such as multiple homologues from a search or multiple sets of experimental data) are included in the aforementioned component landscape, cross correlate each data set independently to make a landscape for each data set and calculate the standard deviation of each correlation in the set of landscapes.

Step 6: Perform bootstrap analysis to determine the minimum number of points within a component. In this step, bootstrap analysis is used to determine either the minimum number of experiments or model simulations necessary to produce a 'significant' landscape for that component. To do this, the standard deviation, which was calculated during Step 2, is utilized. The criterion for significance is the number of points in the bootstrapped data set that results in an average standard deviation that is equal to total standard deviation of the overall landscape divided by the number of components into which the model has been separated. However, because the definition of a 'component' is somewhat subjective, particularly when using a non-mathematical definition, factor

analysis can be used to determine the number of dimensions in the data. The number of dimensions can then be taken as the number of components by which the overall standard deviation should be divided. However, a simpler rule of thumb if factor analysis cannot be readily performed is just to take the component landscape standard deviation 'cut-off' as being ~20-30% of the overall standard deviation because most systems rarely have more than 3-5 major dimensions in the data set. If the standard deviation of the data set of component sensitivity analyses for a set of homologues is within ~ 30% of the primary landscape standard deviation, the component is likely significant. However, due the limitations and assumptions of bootstrapping this significance must be manually verified as discussed in Step 7.

Step 7: Inspect the component landscape to verify component analysis significance/criteria. This is the final validation step to insure that component analysis has correctly and adequately 'peeled off' the intended layer. For example, in the motoneuron test case the intent was to 'peel off' size so that the relationships that lie 'under' the dominant 'size principle' correlations could be revealed. Thus, conductance relationships should be minimized within the individual component landscapes (i.e. the landscapes of the small, medium, and large motoneurons). If these correlations are still significant, then the intended layer has not been adequately peeled, and the component criterion for sorting needs to be re-evaluated. Typically, Step 6 will catch 'inadequate peeling', but Step 7 is an easy and effective check. For example, in the small motoneuron group landscape, Step 6 revealed that there were not enough points, and this

was visually evident in Step 7 as the landscape still showed significant conductance correlations, as shown in Figure 1A.

Step 8 (optional): Repeat for different model operating points. Just as in regular relational analysis, it is often beneficial to repeat the component analysis at different points of model operation or different sets of conditions. For example, repeating the component analysis at different times or under different input(s).

Step 9: Summarize. It is in this step that both component and/or system-level hypotheses can be either evaluated and/or identified. See Summarize section of Relational Analysis.

Step 10: Repeat or iterate for additional components. Often it is helpful to test the robustness of a component by comparing landscapes with other components such that the true contribution of a single component can be better compared and quantified in relation to other system components.

Component analysis to evaluate experimental motoneuron data

Motoneurons are classified according to their firing properties as: slow (type S) and fast (type-F). Type-F motoneurons can be further classified as fatigue resistant (type-FR), and fast fatigueable type-FF). The classification of motoneuron type is important because it is related to the overall function of the motoneuron within the neuromuscular system. Type-S motoneurons tend to respond to more stable inputs and participate in longer-term functions such as posture. Type-F motoneurons tend to respond to transient inputs and

participate in more short-term or 'active' movements. Elucidating the different intrinsic properties of these motoneuron types has been a key goal of scientists within the field. A common finding in both experimental data and in computational models is that the firing properties of motoneurons are highly related or correlated to the size of their conductance. Note that the conductance value is also directly proportional to motoneuron size or area. Lower conductance or smaller motoneurons are typically type-S whereas higher conductance or larger motoneurons are typically type-F. This size-based effect on the firing properties of motoneurons is often referred to as the 'size principle'. The size principle is typically the first noticeable trait of any landscape of motoneuron data, especially data generated from motoneuron computational models. In fact, because the properties of motoneurons are so closely tied with conductance, the conductance-based correlations end up dominating the landscape, making any other properties 'beneath the size principle' very difficult to reveal.

In this test case, component analysis is used to study in vivo cat spinal cord motoneuron experimental data from neurophysiology experiments performed by Dr. Robert Lee. The specific intent of this study was to analyze the underlying properties of motoneurons as a function of size. Thus, the purpose of performing component analysis for this study was to 'peel off' the conductance such that the underlying properties of these motoneurons, categorized by type, could be revealed within the landscape.

Since the component of interest had already been identified (input conductance), the data was automatically sorted using the input conductance measure (G_leak) into three

categories labeled as small, medium, and large. Figure 1 shows the conductance component analysis results for each of these three motoneuron sizes. As expected, component analysis was able to strip away the conductance layer of relationships, as noted by the absence of any correlations with input conductance (G_leak) in all panels of Figure 1.

The most apparent immediate observation is that the relationships among each group of motoneurons are in fact, different. This immediately supports the hypothesis that the motoneurons are not merely just different sizes of the exact same cell type. If this were the case, we would have expected the correlations to be very similar, with perhaps only a few small quantitative differences. Instead, we see that there are multiple differences in the sheer number of correlations, their magnitude, and their sign. The most striking difference at first glance is that there are far more correlations in the smaller motoneurons with the number of correlations decreasing with size.

Beyond the overall, holistic differences in the landscapes, there are many specific differences in the individual relationships, which suggest differences in regulation and function among the different motoneuron sizes. There are far too many notable correlations, both correlations that are similar among types and correlations that are very different, to mention each explicitly, but a few of the major ones are highlighted.

Major similarities among groups. Starting with the most recognizable pattern of correlation, there is a large block of strong, positive correlations (denoted in red) in all

three motoneuron groups that signify a potential 'excitability' mechanism. The group is composed of namely the spike properties (height, gain, slope, etc) and persistent sodium peak (Ifast peak). The number of factors included in this mechanism varies among the size groups, with strongest and greatest number of correlations appearing in the middle group, followed by the small group, and trailed by the large group, in which only a few of the correlations within the group remain. Another notable correlation similarity is the block of correlations relating the half-activation (GNaP_Vh and the AHP Bottom). Unlike the previous block of correlations, these correlations were not 'expected' and thus could potentially represent a mechanism or function that is yet to be determined.

Major differences among groups. The largest block of differences, other than the notable differences within the excitability block, are among the persistent sodium relationships (GNaP). In the small group, these correlations are numerous and strongly negative (denoted in blue) whereas in the middle group they are fewer but opposite in sign; finally, in the large group the same relationships are nearly non-existent, with only one or two major correlations showing up as strongly negative, namely the relationships between GNaP max (the peak of persistent sodium) and the GNaP rate (the rate of persistent sodium). Persistent sodium is known to have a strong effect on the types of firing, and thus, the relationships could be potentially meaningful in designating the mechanisms behind the firing of each group of motoneurons.

Finally, it should be noted, as is mentioned in step 7 of "How to perform component analysis", that the major correlations in the small group to conductance suggests that the

sample size is still too small for this group. The bootstrap analysis from step 6 had already suggested this, but it is apparent in the landscape as well by the appearance of these relationships, which should have been 'peeled off' or at the very least, minimized. To correct this, the input conductance magnitude inclusion criteria should be lowered and more cells that meet the new criteria should be included.

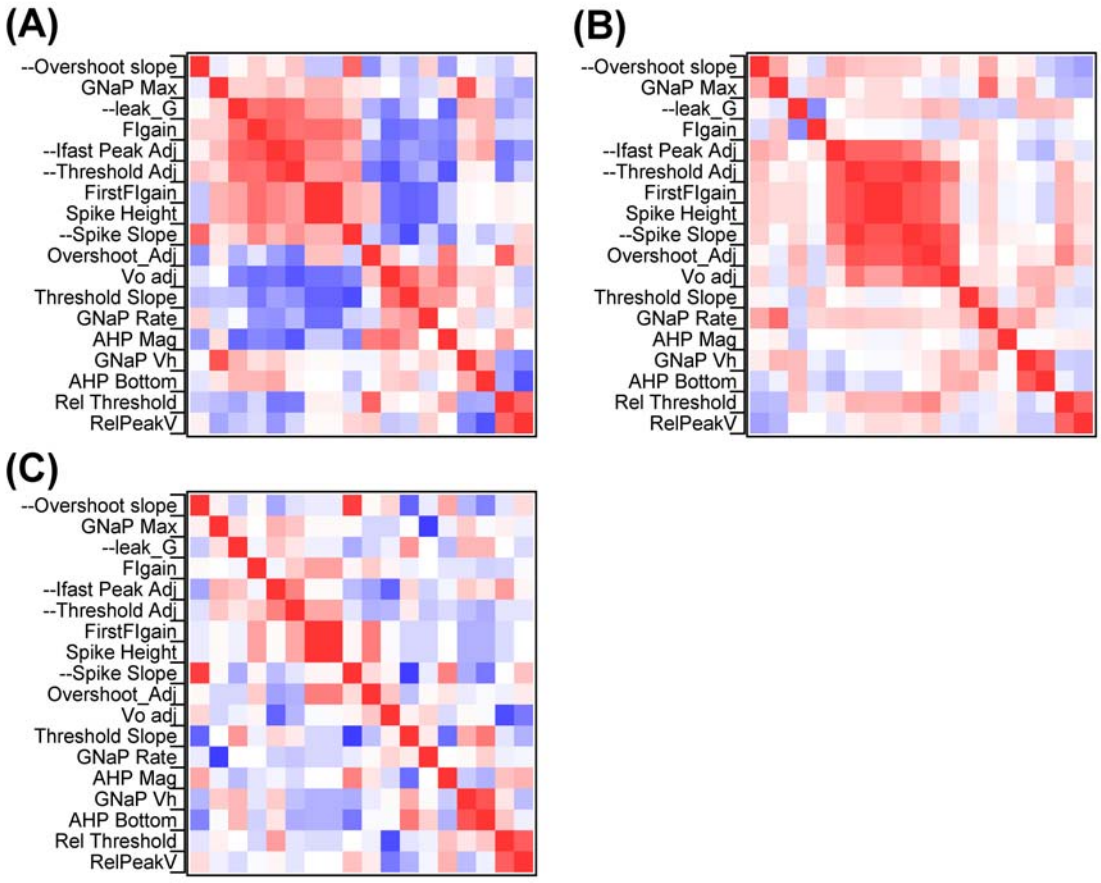

Figure 5.1. Input conductance component analysis landscapes for experimental motoneuron data (Mitchell and Lee, In prepartion). (A) Small conductance motoneuron landscape (B) Middle conductance motoneuron landscape (C) Large conductance motoneuron landscape

Component analysis to compare model implementations

As part of the spillover test case, two degenerate NNMDA receptor model implementations (the 8-state Banke and Traynelis model versus the 5-state Lester and Jahr model) are compared within the context of a larger neurotransmitter spillover model. In this test study, component analysis revealed the differences between the two models, including differences that were intended or expected as well as differences that were not. See Chapter 7 for details.

CHAPTER 6

RELATIONAL MODELING

As stated in the Introduction, the second key limitation that has prevented the use of the model as an exploratory tool is the inability to construct relevant computational models of physiologies and especially pathologies very early in the research process, a limitation largely attributable to the requirements of traditional model construction techniques requiring a vast amount of upfront knowledge of a system. That is currently modelers, analogous to map-making cartographers, must know with great detail what their system looks like before they can even begin to create their system maps. For example, the most common modeling technique, mechanistic modeling, requires that the modeler be able to both synthesize and construct the system at the most detailed or 'bottom' level, deriving and compiling mechanistic components from first principles. Other existing model construction techniques such as the traditional 'black box' modeling method and the relatively newer technique of conceptual modeling, require less detailed information regarding system mechanisms, but they do require a good deal of 'top' level knowledge and intuition regarding the overall properties of the system and its outputs. (For a review of traditional modeling methods see Background.)

The ideal system-level exploratory technique would not be at all reliant upon our current understanding but rather would rely on our naivety to the system such that our answers or

findings are not unintentionally preordained. Thus, such a method would neither require the holistic understanding of a top-down approach nor the detailed mechanisms of a bottom-up approach, but would instead utilize a 'middle-out' approach that simply incorporates the existing data of a system, such as the individual experimental studies/findings within the field. Whether in a relatively new physiological or pathological field or a long-standing field that lacks comprehensive understanding, there are typically numerous such 'findings' embedded in the literature of the field, literature that can range from 50 to 100 studies on the smaller end of the spectrum, to hundreds and even thousands on the larger end.

The method that we developed in order to construct models early in the research process is referred to as relational modeling. Relational modeling uses simply correlations (or relationships) and time constants extracted from experimental data to create a system of piece-wise linear first order differential equations that approximate the dynamics of a system. Note that the basics of this method are published within our spinal cord injury publication (Mitchell and Lee, 2008). Relational modeling fits all of the above criteria in that it simply aggregates and recapitulates the findings of numerous experimental studies of a physiology or pathology in order to provide a comprehensive, system-level view. Relational modeling, like relational analysis, is derived from complex systems philosophy in that it is based on the foundation that it is the system's relationships that result in the emergent properties and behaviors of that system. Furthermore, relational modeling exploits the fact that most individual experimental studies are detailed investigations of a single interaction between two system factors (often referred to in the

literature as the experimental correlation). Our general technique to develop and construct relational models is referred to as review-relate-refine (R^3): review the literature, relate the factors, and refine to meet validation criteria. The remainder of this chapter describes in detail the steps of this technique.

Review-relate-refine (R^3)

Relational modeling, using the R^3 technique, directly translates a system's numerous measured experimental relationships into a literal network or map of system factors and interactions, a map which can be further translated into a set of differential equations that can mathematically model the temporal and/or spatial dynamics of a system. The first step is to *review* the experimental literature/data to identify the known key aspects of a system, referred to as factors. Next is to *relate* the factors using their experimental correlations to create a network or 'map' of factors that illustrates all of their interactions and to translate this map into a system of mathematical equations. Finally, the translated factor network, or 'model', is *refined* to meet validation criteria by using relational analysis to identify areas that need improvement or further detail. Additional relationships and intermediate factors are added until a set of specified output criteria, as determined from the experimental literature, is reached. Once validation criteria are met, relational analysis can be used to make clinical and mechanistic predictions about the system. Thus, relational modeling using the R^3 technique enables 'scaffolding' models to be quickly and efficiently built. These system scaffolds can then be filled with either additional or more detailed relationships, or segments can be replaced with detailed mechanisms or concepts as research moves forward and information becomes available.

There are three major 'parts' to a relational model: factors, categories, and gains. Factors are distinct quantitative entities that represent the major parts or 'players' in the physiological or pathological system as defined by the literature in the field. For example, reactive oxygen species (ROS) and nitric oxide (NO) can be described as two potential factors of the pathology of spinal cord injury. Categories represent collections of factors commonly categorized or grouped together by scientists in the field. In the previous example, ROS and NO could be a part of a category called 'free radicals'. Last but not least, gains are quantitative metrics determined from experimental data, which represent the one-way interactions or relationships between factors. For example, the gain, $G_{NO\text{-}ROS}$, would determine how a change in NO would quantitatively impact ROS.

Figure 1a shows an example relational model for spinal cord injury where boxes denote factors and categories (energetics, excitotoxicity, free radicals, necro-apoptosis, inflammation, and other) are labeled and denoted by factor box color. Figure 1b illustrates the overall process of how experimental literature is used to extract gains that are translated into a system map. Essentially, one-way piece-wise linear correlations are exracted along with the time constant over which the correlation is valid. From this map, a set of first order differential equations are formed which reprsent the dynamics of the system. Using our relational and component analysis techniques, the system relationships are quantified and used to characterize and visualize emerging dynamics. Finally, the relationships and their resulting dynamics are used to make mechanistic and clinical predictions.

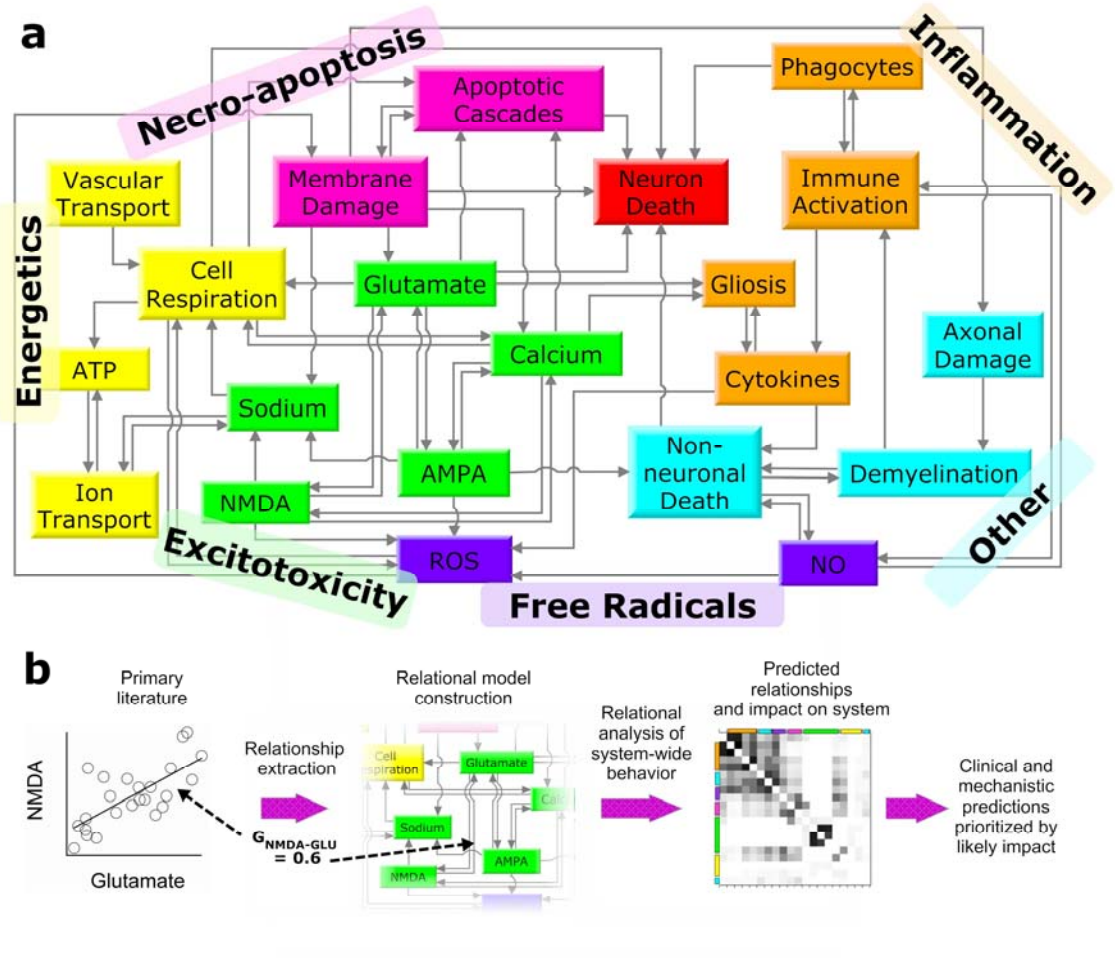

Figure 6.1. Construction of a relational model of spinal cord injury. (A) The boxes represents tracked factors. Necro-apoptosis, energetics, excitotoxicity, free radicals, inflammation, and other represent different categories as factors, indicated by color. (B) The relational model is developed by identifying important system factors (review), deriving experimentally determined relationships or gains from the literature and translating them into a network to construct a relational model (relate), and by performing relational analysis to analyze system wide behavior, make clinical and mechanistic predictions, and to improve the model (refine).

A relational model, like any model, is a form of map. In fact, it is most analogous to a map with which many engineers are familiar, a process flow diagram or a system control diagram. In R^3, the quantitative relationships extracted from the literature that are used to connect factors within the system map are referred to as 'gains', analogous to the proportional gains used in linear control systems. Just as in controls, the gain in a relational model specifies the output-input relationship between two factors. The gain in a control system is used to adjust the error between the current system operating point and the desired operating point. In a physiological system, the gain would likely have the same purpose. However, in a pathological system, the 'gain' may not always reduce the 'error' or the disease, but rather it may be a part of its propagation. At any rate, the gains, or the relationships between factors in a pathology, whether they help to reduce or to propagate, do determine the pathology's operating point. Figure 2 illustrates how the gains in a relational model are equivalent to the gains in a linear control system.

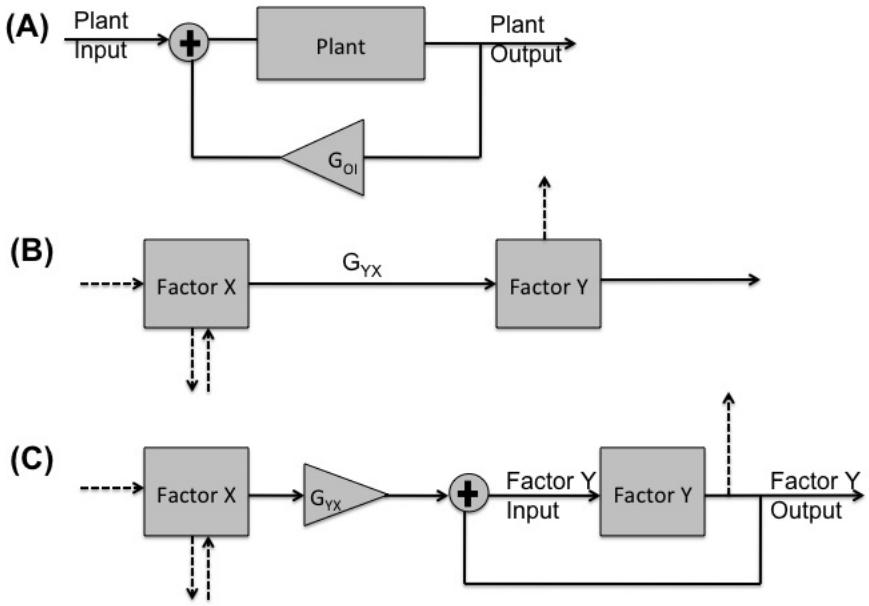

Figure 6.2. A relational model as analogous to a control system. The figure illustrates how a relational model uses experimentally determined relationships, or 'gains' between two pathological factors to determine the pathological output analogously to how and an engineered plant uses a proportional gain controller to alter its response. (A) A typical engineering 'plant' with proportional control feedback, as indicated by the output-input gain, G_{OI}. The gain is used to adjust the error between the current output and the desired or target output by altering the plant's input. (B) The diagram illustrates a portion of a generic relational model and exemplifies how Factor X impacts Factor Y via the experimentally determined relationship or gain, G_{YX}. The dotted lines represent connections to factors not shown. (C) The diagram 'converts' the relational model map to the equivalent control diagram having equivalent mathematics. Note the dotted line that was exiting Factor Y in (B), was moved to show that it has the same quantitative value as the solid line labeled Factor Y output.

Review

As with any literature review, the key is to be systematic and agnostic. With a relational model, it is important to be open and objective, to 'pull' out or away one's own knowledge and opinions of the system, such that the entirety of literature in a system or the system's field can be reviewed without bias or a tendency to 'pick and choose' what goes into the relational model. The great advantage of a relational model is that it can bring a system into focus, highlighting the 'key' or most important or highest-impacting factors. Thus, it is important not to unintentionally blur or skew this advantage by over-filling the model with a certain type or kind of factors, which from the beginning, points or leans toward a certain preconceived idea or theory. Once an overall system has been made and the most important factors objectively identified, then additional detail and filling may be done with certain system aspects or factors, which support an identified theory or mechanism.

Step 1a: Creating the database. One of the most important steps to success in a relational model is superb recordkeeping. It is nearly impossible to hold hundreds of papers in one's head, particularly long term. Thus, before one even begins to look at a single paper, it is important to create an initial database. Typically, we would recommend three databases. One database, the primary database, keeps track of every article that one finds interesting enough to download at least its abstract, whether or not that article is eventually read or used directly in the model does not matter. For this big database, EndNote™ or other similar reference managing system is excellent. EndNote™, for example, can store and sort by all of the typical author, date, and journal

information, stores the abstract, and it can be used to directly search and download references from a source such as PubMed (www.pubmed.gov). Furthermore, a downloaded pdf version of the paper can be stored with is entry in the EndNote™ library. All literature searches should be performed within this primary database (e.g. the EndNote™ library).

The second database is referred to the literature database. This database contains all of the papers that are downloaded or either partially or fully read, regardless of whether direct information or values is used from them in the final model. However, more importantly, this literature database has important summary information about the papers, which could potentially be incorporated into the model. The literature database, probably best implemented in either Microsoft Excel™ or Access™ gives each paper a primary and secondary category name. Additionally, it keeps track of important specific information pertinent to the system or pathology being modeled. For example, in the SCI model, we kept track of which nervous system the data was derived (CNS or PNS), whether it was from (brain, spinal cord or other), experimental type (in vivo or in vitro), experimental preparation (cat, rat, mouse, co-culture, human, etc). In the preliminary ALS model, we added database columns that kept track of particular ALS forms (familial or sporadic), the type of mutation involved (G93A, G85, etc). In addition, it is important to keep track whether or not the article is a 'review' article. Finally, besides the category assignments, perhaps the most important entry for each article in the database is a short one-line summary highlighting the major factors, a correlation or other quantitative finding of the article. The third and final database is simply the 'model database'. This

database keeps track of all the quantitative values used in the model (i.e. the gains, time constants, equation forms) and all of the values used as validation criteria (factor output values at certain time points, experimental correlations, etc). Like the literature database, Excel™ is a good platform because it also can allow for easy quantitative manipulation and calculation. With each recording, pertinent information regarding the source is also kept in addition to a one-line description of how the value was determined (figure number, graphical estimation, etc).

Step 1b: Reviewing the reviews. This step consists of reading the major literature reviews done within the system or the system's field within about the last decade. The purpose of this step is to get familiar with the field, particularly if it is a system in which you have no prior knowledge, as was the case with the two relational modeling test cases in this work for spinal cord injury and amyotrophic lateral sclerosis. However, this step is important even if one does have a good deal of initial knowledge. Reading several different reviews gives different perspectives of the system, aiding both the familiar and unfamiliar modeler to obtain a multi-perspective, balanced view. Furthermore, it is important to read not simply the most current review but also some older reviews. There is some truth to the saying that 'your first instinct is usually correct'. Thus, there are often some ideas in older literature that have much value. Unfortunately, such ideas are often dismissed or cast aside due to one or two studies, which have results that suggest an alternative or different view. This is not to say that the older view is correct and the newer one is not or vice versa. It could very well be that both views are correct and represent different aspects of an emergent property of the system. Remember that the goal of the relational

modeling process is not to pick the 'right' view from the onset but rather incorporate all views by tying together the experimental research pieces, the relationships or correlations, that represent each and let the relational analysis process bring the system-level or big-picture view into focus.

Thus, as a general rule of thumb it is important to read at least 5-10 comprehensive system reviews of the physiology or pathology to be modeled, if available. Additionally, particularly if the system is a pathological or diseased-state system, it is helpful to read a few clinical reviews or even case studies to really connect at both a scientific and human level to the pathology. Furthermore, reading both the experimental or preclinical literature in addition to the clinical literature helps to identify relationships between the two particularly later on. Being able to relate experimental factors to clinical outputs or effects is critical in the analysis of a pathology. Be sure to record to the primary and literature databases as appropriate.

Step 2: Initial identification of major categories. Using these initial reviews, obtain a list of 'categories'. These categorical groups or classifications will later be used to organize individual factors that describe a system function, mechanism, intermediate process, pathway or theory. Note that while 'categories' of factors are typically more easily or readily identified than individuated factors, particularly within reviews, it is both possible and allowable to reverse steps two and three, and thus identify a list of the most pertinent factors first and then subsequently classify those factors into categories.

Step 3: Identify initial factors within major categories. Use the initial reviews to identify factors within the major categories. These initial factors are typically more obvious in their association with a category. For example, caspase would be a factor in the category of apoptosis.

Step 4: Review detailed reviews of categories and/or individual factors. In this step, seek out literatures reviews, which are more detailed or specific. Such reviews will typically focus on a single aspect of a pathology, typically a category or a factor. Use these reviews to understand the more detailed workings of the system and to 'fill in gaps'. Be careful to record all pertinent information to the appropriate databases.

Step 5: First expansion of factors and/or categories. Use the information from the detailed reviews to expand the list of initial factors and/or categories. To aid in deciding what to include as categories and factors, it's often helpful to map out the process or cascade or theory presented in each detailed review. Often times, such maps are already presented within a figure in the review. If so, use the figure given. Within the map, every major 'block' typically becomes a factor and the map itself typically becomes a category.

Step 6: Key word searches for factors and categories. In this step, key word searches are initiated to find actual experimental and clinical studies that are not simply literature reviews. Typically, two key word searches are done for every factor. The first keyword search utilizes the pathology name as one keyword, for example "amyotrophic lateral

sclerosis", the factor's category name as the second keyword, for example "apoptosis" and the third keyword is the factor name, itself, such as "caspase". The second keyword search expands the search to include just the first and third keywords from the first search, that is simply the pathology and factor names, such that the expanded search can find studies in which caspase was studied but perhaps not as part of apoptosis or not exclusively as part of apoptosis. The Boolean operators (and, or, not) can also be helpful. This expanded search is critical to aid in finding indirect 'paths' where a factor ties in to other factors or categories.

With some pathologies, the number of searches turned up may still be overwhelmingly large. If this is the case, it may be helpful to limit the scope of the search again by another criteria, such as experimental preparation or mutation. For example, in the case of ALS, one criteria used was 'G93A' to represent a certain mutation known to cause ALS that is used to create an ALS mouse model that is a common experimental preparation.

Another helpful search tactic is to use the abstracts to manually cull through the pile, looking for studies that appear largely quantitative or focus on a specific output, factor relationship or correlation or a 'finding' or property of the pathology that is found at a certain time point. Remember that, other than output criteria, which state the specific value of a certain factor at a certain time, the relational model is a collection of relationships, and thus, the majority of the literature search should be focused on finding relationships. While the quantitative identification of relationships (i.e. the numerical

value of the factor gains) does not occur until the relate process, it is important that the papers identified during the review process contain these relationships. By knowing what words signify a possible experimental relationship, one can generally just use the abstract during the review process to collect potential papers for the literature database. Typical relationship-signifying words or phrases to look for in the abstract include: in relation, correlate, increase, decrease, compared to, etc. Examples of such statements found in actual abstracts from papers included in a literature database for ALS are compiled below, with the relationship-signifying word(s) in bold italics:

- "Compared to sham-treated G93A animals, 30-day calcium blocker infusions markedly ***diminished*** the loss of both motoneurons and of astrocytic GLT-1 labeling. (Yin 2007)"
- "Treatment with the antioxidant 5,5-dimethyl-1-pyrroline N-oxide resulted in inhibition of protein oxidation and ***decrease*** in proteasome activity to the basal levels. (Aquilano 2003)"
- "The temporal ordering of ***changes in*** cytoplasmic and intramitochondrial calcium levels ***in relation*** to mitochondrial reactive oxygen species accumulation and membrane depolarization was examined in cultured neural cells exposed to either an apoptotic or necrotic [modulator]. (Kruman 1999)"
- "These findings suggest a ***causal relationship*** between enhanced oxidative stress and mutant SOD1-mediated motor neuron degeneration, considering that enhanced oxygen free radical production results from the SOD1 structural alterations."(Liu 2002)

- This process accounts for up to ***50%*** of the glutamate accumulation during energy deprivation. Enhanced action potential-independent vesicular release also contributes to the ***increase*** in glutamate, by ***50%,*** but only once glutamate uptake is inhibited. (Jabaudon 2000)
- Here, we show that the ***increased*** denitrosylase activity of SOD1 mutants ***leads to*** an aberrant ***decrease*** in intracellular protein and peptide S-nitrosylation in cell and animal models of ALS. (Schonhoff 2006)
- While intra-mitochondrial calcium levels were elevated in SOD1G93A motoneurons, changes in mitochondrial function did not ***correlate*** with [Ca2+].

Typically, such direct qualitative and sometimes even quantitative relationship findings, as in the last bulleted point, are highlighted in the abstract. A paper that lists a key quantitative finding is a definite keep to file in the EndNote™ and literature databases. However, if an abstract has direct or indirect qualitative relationships in the abstract, as shown by the majority of the examples above, it should also be included in the EndNote™ and literature databases. While many authors are not completely forward with the quantitative value of such a mentioned qualitative relationship or a factor's gain either in the abstract or within the paper itself, typically data is presented from which the quantitative values can be extracted (this process is explained in the relate section). Finally, note that at this point, the date of publication range can be quite large. A preferred range may include studies within the last 10-15, but with some factors, including studies done over 20 years ago is not uncommon. Regardless of whether a

study has a factor or data point that you think you will want to include, record it to the EndNote™ database.

Step 7: Second expansion of factors and/or categories. Review the literature found as a result of the searches. Use the key word searches from step six to identify and expand especially new factors but also factor categories. At this point, it's good to have between 6-10 papers for each factor, if possible. Similarly, for something as complex as a pathology, there are typically between 5-10 obvious categories. The decision on what is a category can be defined by a function (such as apoptosis), a malfunction (such as excitotoxicity), a physiological process (such as axonal transport), or other obvious commonality among a group of factors (such as 'systemic effects', which represents all of the external effects on all bodily systems other than the one being modeled). Making and splitting categories is subjective, but the relational analysis during the refine process will be able to pick up on whether a factor has been wrongly categorized since factors of the same category typically have a high degree of correlation among themselves. Typically at this point, for an initial relational model, there are between 6-10 categories. Note that the number of categories will depend on the breadth of the pathology and the literature review, whereas the number of factors typically depends on the level of detail in the field and the literature review of the field.

It is difficult to assign a standard number of factors for a category. The number of factors within a category could easily range from 2-6, but could be as high as 10 or more. The rule of thumb for an initial model is there should be at least one factor for each major

'output' of the category (an example is cell death for apoptosis) and one factor for each of the major players in the category. Using apoptosis as an example, there could be factors for the two end or decision points, which determine apoptotic initiation, caspase and Bcl-2; factors to represent each receptor type in the pathway such as the cytokine EGF receptor, survival/growth RTK receptor, chemokine or GPCR receptor, death or Fas receptors, etc; or more general factors that represent specific apoptosis initiators such as calpain, calcium, gene regulation, etc. A modeler may choose to represent apoptosis with one or all of those schemes, depending on how apoptosis is presented in his/her system. Continuing with our apoptosis category example, intermediates, such as p53, FADD, mt and other apoptotic-associated signals that occur in mid-cascade, are generally not included as factors at this point. Admittedly, sometimes it is difficult to distinguish a 'major player' from an 'intermediate'. However, this determination becomes more evident during the relate process. During the relate process, when relationships are being identified and extracted from the literature, what one may think of as an 'intermediate' may actually need to be included as a factor since intermediates are often used as metrics of comparison or correlation to the main player, determining the main player's or factor's response. Because such intermediates will be used to alter the main players in the model through their gains, it will be necessary at that point to add in intermediates as actual factors.

What ends up being a factor for any particular category ultimately ends up being whatever the field defines as a 'major player' via what they measure as part of the experiments. Whether the factor is truly a 'major player' in terms of impact, as defined

by the field, will be determined by the relational analysis and not by the decision to include it in the model. Thus, if in doubt, include as many factors as there is relationship data during this second expansion. Once the factors are translated into a map, it will become apparent if there are interactions that will warrant keeping these questionable or extra/extraneous factors.

Finally, a critical part of this step is once again good record keeping. Carefully record all pertinent information to the primary and literature databases. Keep an, active up-to-date list of factors and categories.

Relate

It is in this step that all of the real work and 'magic' happens because it is here where the model really starts to come together and where major decisions are made. In this step, the relationships that represent the inner workings of the system are identified from the literature for each factor and are translated into a map or network of factors, which are connected by their relationships, or interactions. Typically, such a map looks very much like a process flow diagram, commonly used by chemical engineers to represent a power plant or refinery or a systems control diagram, commonly used my control engineers to operate such a plant. Every line connecting two factors is called a 'gain', where the gain is the one-way quantitative value of the relationship or correlation between two factors, as taken from the experimental literature. This gain can be thought of as either a slope or sensitivity that represents the linear change between two factors, X and Y, such as the gain imposed on X by Y is equal to dY/dX. Conversely, the gain imposed by X on Y is

dX/dY. However, note that these two gains do NOT have to be reciprocals of one another nor do the two gains need to have any quantitative relationship of any kind in respect to one another. In fact, two factors may have only a single one-way relationship in which factor X causes a change in factor Y but factor Y does not cause a change in factor X.

The primary intent of the relate process is to create a relational model that connects and illustrates factor relationships. However, as part of that process, it can be helpful to first go through the relate process with only categories. That is, in essence, make a relational model based only on categories. A category model uses very rough or 'back-of-the-envelope' estimates to determine the relationship or gain that each category has on every other category and to determine the corresponding time constant associated with each category. These category gains and time constants are essentially aggregated factor gains and time constants, which can be very roughly estimated from the literature.

The benefit of a category model is that, because there are fewer things to quantify, it can be very quickly constructed, and thus provide very fast feedback and insight into a system. The insight gained from a category model can then be used to hypothesize which parts of the relational model have the highest impact and when that impact occurs. This insight, in turn, can be used to determine which categories may require the most detail (i.e. additional factors), and when the most detail is needed (i.e. an estimate in the number of time constants required—see step 10). Furthermore, the category model can give insight into what additional factors may be needed to compensate within a category such

as, for example, factors which will provide negative feedback on the category to aid in making the pathology or system more stable.

One critical reminder, however, is that one must keep in mind that the category model is simply a very rough estimate. It cannot possibly represent all of the dynamics of the factor model. Once factors are inserted and a true relational model of factors is constructed and simulated, the factor model could show different or even contradicting results. However, this comparing and contrasting can be enlightening and beneficial in and of itself, helping to further stimulate hypotheses and conceptual system insight. The major steps of the relate process as described below are the same overall steps whether making a category or factor model. However, there are some specific details, which differ between the two. The major difference being that quantitative data for factors are taken directly from literature whereas the quantitative data for categories are roughly estimated by the modeler using his/her aggregated insight obtained from reading the literature. Thus, this distinction between factor and category model details is made clear in each step.

Step 8: Determine the relationships. In this step, the specific relationships are identified. That is, every 'line' or 'arrow' connecting the categories or factors is identified.

For factors, this means first connecting every direct relationship. The 'direct' relationships are those that are directly stated or measured from the literature. For

example, “an increase in calcium resulted in a subsequent increase in free radicals.” However, one must be wary of relationships that are not directly apparent from the literature. In fact, it may be the modeler who actually identifies an indirect relationship by combining the results of two different studies, which have a common thread. Also, there may be times when an apparent relationship is obvious from what is known about the non-diseased physiology, but such a relationship may not have yet been directly measured in the pathological literature in which case it must be estimated using other literature or data points. In summary, it is up to the modeler to synthesize all of the literature and identify all pertinent relationships.

For categories, determining the relationships simply means asking the question “Does Category A in any way have an effect on Category B?” The answer to this question can be very complicated and daunting, and it’s easy to miss especially smaller or indirect effects. This is why it is important to keep in mind that the category model is simply an estimate. Thus, simply recognizing obvious or direct effects is enough for a model at this very rough, category level. Determining the relationships between categories involves synthesizing what is known about both the normal physiology and the diseased pathology. For example, in the normal motoneuron axonal transport physiology it is known that the energetics category affects the axonal transport category. Thus, whether there is a pathological ALS study that directly quantifies the effects of these two categories does not matter. The relationship would be inferred from the physiology and thus recorded as ‘present’ in a category model of ALS. Another pointer is that it may be helpful to think in terms of factors. Is there any factor in Category A that impacts any

factor in Category B? If yes, then there is likely a relationship between the two categories, however big or small it may be does not matter, since the primary intent of this step is simply to identify relationships.

Step 9: Determine the direction of the relationships. The purpose of this step is to determine the direction of each one-way gain, 'up' (positive or increasing) or 'down' (negative or decreasing). This gives more intuition as to how each factor or category affects the movement of another factor or category. It also aids in determining the sign convention of a factor or category, as in whether the feedback is positive or negative. For factors, this sign convention will come directly from experimental data. It will typically follow a shown graphical or visual trend. Thus, there is typically nothing tricky about determining the sign of a factor gain. The exception is when factor have resource constraints or multiple feedbacks that have different signs. For example, glutamate can be increased by NMDA activation and decreased by uptake by glutamate transporters. The overall sign of glutamate will depend on which relationship or interaction is 'winning' at the measured time point. The possibility of a direction switch should be denoted at this time such that it is not forgotten later. But, at this point, the direction can simply be taken as the direction that causes the highest degree of pathological impact. For example, in the case of glutamate, increasing glutamate via NMDA causes excitotoxicity whereas decreasing glutamate, for most part, does not impose a pathological effect. Thus, the sign of glutamate would be recorded as positive.
For categories, the sign can be trickier since different factors within a category can potentially push the category different ways, similar to the factor case described with

glutamate above. Again, the rule of thumb is to go with what the majority of the factors within the category do to increase the pathological effect(s) on the system.

Step 10: Determine the time constant for a factor or category. The time constant is used to determine the time-dependent behavior of a factor or category. It is a necessary component to translate and construct the differential equations, which describe the network of factors.

For factors, a time constant is determined directly from experimental data using the peak or maximal impact as the point of measurement. For example, if the peak glutamate concentration occurred at 1 hour, the time constant, as typically defined by engineers, would be 67% of 1 hour, or ~ 40 minutes.

Of note, is that a factor may need to have multiple time constants. Since the relationship gain being taken from literature is assumed to be linear over a short period of time, there may need to be several 'pieces' of time which the factor is modeled with a different time constant. This is analogous to having a smaller mesh size or time step for a differential equation solver in areas in which a function is experiencing frequent or high degrees of change. If a factor's gain significantly changes with time, such as the glutamate case described in step 9, then there must be a time constant to represent each piece-wise change represented.

In general, the model must be split in order to accommodate these piece-wise changes. For example, in the SCI model, there are two such splits. There are time constants to represent the 'acute' period, the first hour post-insult, and time constants to represent the 'sub-acute' period, hours 2-16 post-insult. These splits can only be determined by validating the factor values at known time points to experimental data during the refine process. If a factor's output values track experimental data well at first but then begin to not follow the experimental data over longer time periods, then there needs to be a split and another time constant to be identified and used when the significant deviation from experimental values occurs. Essentially, the number of time constants and time splits required will depend on the system and the relationships of its individual factors. While this process is *not* a curve fit, it is analogous to the piece-wise process used to fit different parts of a function during a curve fit.

For categories, the time constants can be estimated based on when the main outputs or factors of the categories express their peak impact. Thus, the estimate is based on the 'majority' of impact within the category. Typically, this is not a difficult estimate as factors within a category are typically very inter-related and thus have similar time constants; thus, the aggregated time constant for the category is comparable to the factor time constants. Such an estimate definitely does not require knowing each factor's time constant. Typically, most experimental papers, and particularly high-level overall physiology or pathology reviews, such as those used in step 1, are forthcoming in making statements that hint to a category's time constant. For example, a review in ALS may

state the following: “Axonal transport defects are evident by day 60 in the G-93 mouse model.”

For a physiology or pathology with a large number of categories, it may be helpful to simply divide the time constants into ‘fast’, ‘medium’ and ‘slow’. For example, a relational category model of ALS uses time constants that indicate key pathological presentations of the G93A mouse model at 60, 90, and 120 days. A quantitative value, based roughly on data for the system can be assigned to each time constant speed. For the purpose of getting a preliminary system overview, obtaining more gradated or accurate versions of the time constant magnitudes does not add a considerable amount to the analysis since there the entire category model will be based largely on estimation.

Step 11: Translate the relationships into a relational map. It is at this point where overall system map can be constructed. As in the example shown in Figure 1 for spinal cord injury, a box should represent every factor and an arrow in the appropriate direction between two factors should indicate every relationship or ‘gain’. Using the number of total connections to each factor can help with ideal spatial placement of factors in order to minimize the number of line crossings and clutter. The factors with a higher number of relationships should be placed more towards the middle of the map.

Step 12a: Determine the magnitude of the relationships or ‘gains’. It is in this step that the literature relationships are turned into quantitative values that can be used in Step 14 to form differential equations.

Determining the magnitudes for gains of factors can be either extremely easy—a matter of simply reading the text and extracting the stated value or it could be as difficult as synthesizing multiple studies, crudely measuring, comparing, or averaging a handful of things and then making a determination. However, the majority of the time, the value is *not* simply stated. Even if a factor's relationship *is* directly stated, it definitely does not appear in the paper as "The gain of factor X on factor Y is 3.2". Unfortunately, the majority of the time, it takes a good amount of 'work' to find a gain in the text or even obtain the data necessary to 'calculate' a gain, particularly for the first 10 or so gains for any given system. In general, scientists in a particular field tend to present their data in a similar way and, within reason, they even organize their findings in specific ways (e.g. explicit types of graphs or visualizations) or patterns within the journal article (e.g. location and organization of data within the results section). Thus, once one has become more familiar with such ways and patterns of a particular field, gains are determined more easily and efficiently as the extraction process continues.

The most important thing to keep in mind or remember whether trying to cull the literature text to find the quantitative values directly or using the presented data to calculate a value, is the definition of what the gain is: the gain is most simply stated as the slope between two factors. Another way to think about it is like the proportional gain on a controls diagram. The gain allows the change in a factor to be calculated, and within the model this change can then be added back to the previous value of the factor to determine the new factor value.

If a gain is directly quantitatively stated in a paper, it often appears in a figure caption that describes the data being measured or near where a figure is cited in the text. For example, "Figure 1 illustrates a *five-fold increase* in glutamate at 15 minutes post-insult". Note that the same relationship-signifying words as previously mentioned during the review process in Step 6 still apply when looking for actual quantitative values within the text. However, there is one important warning to be aware of when taking what appear to be quantitative values or relationships from the text. Typically, papers do not present factor relationships as an actual 'gain' or slope. Instead, they present a gain as a proportional difference in a factor between two different points of measurement, as in the example above. That is, the relationship presented is usually a dX or dY and not the slope dY/dX or dX/dY, which is required for a relational model. This can be easily corrected by using the dX or dY given in combination with 'base' value points of X and Y or the experimentally varied points of X and Y to calculate a slope. 'Base' values, if not shown in the data presentation (table or figure) often appear in the methods. Also, 'base' values can have many potential names or descriptions within the literature such as physiological, non-diseased, normal, wild type, sham, or control. Another cautionary reminder is to be careful of not flipping the gain the wrong way; this is a particularly easy mistake to make for two factors which have a two-way relationship to each other.

There are quite possibly a nearly infinite number of ways for a relationship or 'gain' to be presented within the data of a paper. The most common data presentations from which gains can be extracted are listed below. However, it is important to keep in mind that a couple of different data sources, whether within the same paper or whether from different

papers but comparable studies, may be needed in order to determine quantitative gains. For example, one experiment may identify that a relationship between Factor X and Factor Y simply exists, while the results of another experiment presented in one or more graphs may enable the change or slope to be calculated.

- *Bar graphs.* Bar graphs are probably the most highly favored data presentation technique of experimentalists, mainly because most experiments aim to directly compare a relatively few number of points. Such graphs typically have multiple bars to show either different factors or different experimental variations of a factor. If making measurements about the pathology in its native environment, most will compare the values of two different pathological factors over time. A slope can easily be extracted from data in this form. However, it is not uncommon for factors to have different gains over time. Thus, one should check the gain at multiple time points, if possible. An example gain extraction is given in Figure 3: Qualitatively, the slope between the 0 and 4 hour time points is about the same as the slope between 4 and 8 hour time points. However, the slope is visually different between between the 8, 12, and 15 hour time points. Thus, there would be two gain extracted for this data, one gain for hours 0-8 and another gain for hours 8-16. The gain dY/dX or G_{YX} would be ~ 2 for hours 0-8. This gain can be obtained by averaging the slope between 0 and 4 hours and 4 and 8 hours or by taking the slope across the entire 0-8 hour interval. Taking the slope across the entire interval, the slope dY/dX or G_{YX} calculation is: (3-2) / (1-0.5), where 3 and 2 correspond to the values of Factor Y and 1 and 0.5 correspond to the values

of Factor X at the time points of 8 and 0 hours, respectively. Using the same process, the gain can be calculated for hours 8-16 to be approximately 5. In summary, this is an excellent example of when a model 'split' with two time constants may be needed, as described in Step 10.

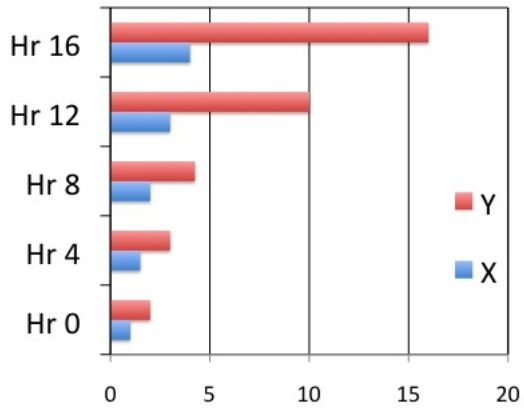

Figure 6.3. Two-factor temporal bar graph. The figure illustrates one of the more common bar graph presentation forms from which a gain can be extracted. In this particular example, two factors of a pathology are measured at different time points. For this example, assume that it is given in the literature that Factor X has a one-way relationship which impacts the value of Factor Y. Using this information, we know which direction the slope must be calculated. By simply looking at the figure, it is evident there are two different gains—one gain that remains fairly constant from 0-8 hrs and another quantitatively different gain that represents the relationship between Factor X and Factor Y from 8-16 hrs. The slope can be calculated between each of the two sets of points. Slopes of similar magnitude can be averaged to determine the average gain over a time frame.

Another common bar graph presentation is to illustrate how an experimental variable, such as Factor Y, responds to a controlled level of another impacting factor, such as Factor X (see Figure 4 below). This is a typical presentation especially in in vitro experimental studies where individual factors can be more easily controlled. It is also a very common data presentation form for a therapeutic study or a study where a drug, such

as receptor blocker or antagonist, is used to measure the response of one or more pathological factors. A slope can still be calculated as long as the control values are given.

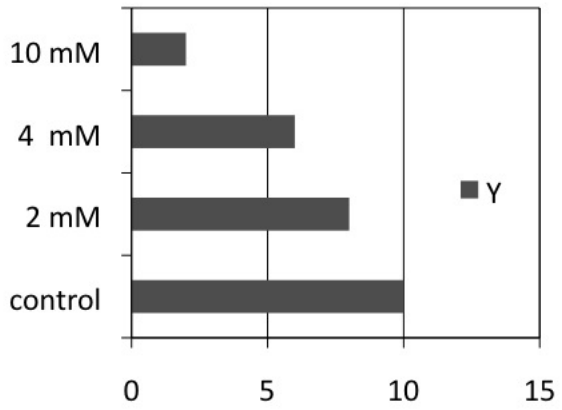

Figure 6.4. Single factor or therapy bar graph. This example illustrates two data presentation possibilities. One possibility is that the categories presented represent an experimentally controlled concentration of Factor X, and thus, this graph alone can be used to determine the slope or gain of the impact of Factor X on Factor Y (dFactorX/dFactorY). Taking the slope between the control and 2mM of Factor X, the gain would be (2-0)/(8-10) = 2/(-2) = -1. The negative sign indicates that Factor X decreases Factor Y. Another possibility is that the example represents the change in Y when exposed to a therapeutic. If it were a therapeutic example, unless the therapy itself actually represented Factor X, then another data presentation form would be necessary to determine the presence of a relationship between X and Y and to determine the change in X with the same therapeutic or within the same experimental preparation. Combined, the latter two data forms could be used to determine the gain imposed by Factor X on Factor Y.

- *Traditional scatter plots.* Such plots typically will either directly plot the relationship, Factor Y vs Factor X, (as shown in Figure 4) or will plot a single factor (Y or X) over time. The factor versus time plots are the easiest for obtaining output validation criteria at multiple time points and for determining when the model will need to be 'split' with multiple factor time constants. If a

single factor is plotted, data may need to be combined with another data source in the same paper or from a different paper.

- *Tables.* Sometimes quantitative data is presented in tables. This data presentation form is typically very accessible for calculating a gain. However, it often requires reading the text to determine which and how what factors are related in the table.
- *Gene microarrays.* These typically just give a 'fold difference' increase or decrease in the expression of a gene or other marker. If the 'mechanism' or how two factors are related is known (either from experiment or from the normal physiological system), two microarray correlations can be combined to obtain a one-way factor gain.
- *Protein gels (western blot).* These are largely qualitative and simply show if a relationship is present. However, they are often combined with other analytical tests and visualization methods that do quantify the fold-difference. Thus, they can be combined with such aforementioned tests or other analytical tests to determine a gain.
- *Histological micrographs.* These are by far the most difficult to obtain gains from because very often they are heavily qualitative. Typically, relationships are obtained when a drug, such an agonist or antagonist, is applied to increase or decrease a factor, such as Factor X, so that the corresponding qualitative change in Factor Y can be determined by change in dye 'color intensity'. However, there are a few cases in which quantitative gains can be extracted when no other data source is available. The primary example is when the factor is manually 'countable', as in the case of detecting the presence of macrophages or microglia.

If two micrographs of the same magnification are shown (either a before and after treatment or two different time points), then counting within each micrograph enables a factor difference obtained. This difference can then be combined with data from another factor, either from the micrographs themselves (such as treatment levels) or another data format. Another example is if the geometric area of the micrograph covered by a certain color is the qualitative indicator, then this area can be measured in order to compare micrographs and obtain a factor difference, which like in the previous example, can be used in the construction of a gain.

- *Electrophysiology.* Traces of neural activity can be difficult to compare in and of themselves. Metrics from such traces like frequency, firing rate, and amplification provide the best means of comparison to calculate a relational model gain or slope. The appropriate metric to choose will depend on what relationship one is trying to illustrate.
- *Combining data sources.* There are a few intuitive pointers to keep in mind when combining data sources. First, one must know how and when the relationship exists between two factors. Knowing the how and when allows one to decide what data is valid to measure a relationship or gain. Second, to the fullest extent possible, it is best if the two data sources were measured at the same conditions (same protocol, preparation, etc). This usually means that it is preferable to use data that is within the same study or paper. However, there may be times when using data from the same study is simply not feasible. In those cases, one must simply match data sources as best as possible.

As values are recorded, it is important to keep track of them in the model database. Minimally, one must record the gain type, its value and the source. However, because obtaining gains can be subjective and they can vary at different experimental conditions, it is also important to keep more details such as the figure or table number from which it was extracted, the time points used, the numbers used in calculating the slope (if applicable), and how the gain was determined. Additionally, finding and recording a rough estimate of both the standard experimental error (mean or deviations) is helpful and can be used during the refine process. Also, making a note of the general accuracy of how the gain was extracted is helpful. For example, there is much more error by the modeler in obtaining a gain from micrographs compared to graphical or tabular data. Finally, upon reviewing and reading the literature in the current EndNote™ and literature databases, one may find that there are still quantitative values that are missing for some of the gains illustrated on the relational map and one may even find that there are possible relationships that have not been appropriately illustrated on the map. If more data is needed to fill these gaps, go to Step 12b.

Step 12b: Third expansion of factors—after reading this step, return to Review step 7. Sometimes it becomes apparent during Step 12a that there are documented relationships that have no current papers in the EndNote™ or literature databases that have measured the relationships in a way that a quantitative gain can be identified or extracted. This especially tends to happen when there are indirect relationships in a model that have been inferred from a physiology or when a quantitative measurement has not been made of the

pathological relationship. If this is the case, the literature review must be expanded beyond the pathology to other sources of information---either literature of the normal physiology or a related pathology. For example, in the spinal cord injury relational model, traumatic brain injury data was often used as the 'next source' when useable, quantitative data for a particular relationship was not available in the SCI literature. For 'normal' physiology data in the SCI model, central nervous system data was used. Ultimately, a number from an expanded source is better than no number at all or a complete guess. However, as with any review, one must set and record inclusion and exclusion criteria for gain data sources for accuracy and consistency.

It is also at this point when the factors are reviewed to determine which ones of the 'questionable' or 'intermediate' factors identified from Step 7 should remain included in the model and which ones should be excluded from the model. There is a rule of thumb: In general, each factor in question should have at least two relationships, one of which must induce feedback. Two exceptions are if a factor is a major input or output of the system, like an input used to 'initiate' the pathology (as shown in Figure 5D), such as a gene mutation, or an output used to validate the model (as shown in Figure 5E) or represent a clinical presentation. The most common example of an intermediate that should be *excluded* as a factor is shown in Figure 5A, where the intermediate simply serves to connect two factors, but the intermediate has no feedback. For such a case where there is no feedback, the intermediate can be excluded from the relational model because the information extracted from the literature to obtain G_{IX} and G_{YI} can be used to determine G_{YX}. As long as the intermediate in question has feedback, whether external

(Figure 5B) or internal (Figure 5C), then the intermediate should be *included* as a factor in the relational model.

Note that there may be other cases not shown in Figure 5 in which there is no feedback but an intermediate may wish to be included, such as an intermediate that has relationships to multiple factors. While there is no 'harm' in including intermediates as actual factors, frequently doing so unnecessarily can make the model more cumbersome and computationally slower. However, most importantly, unnecessarily including every intermediate as a factor will make the model more difficult to analyze and interpret by adding extra 'clutter', particularly in pathologies that already have a very large number of factors that must be tracked and visualized.

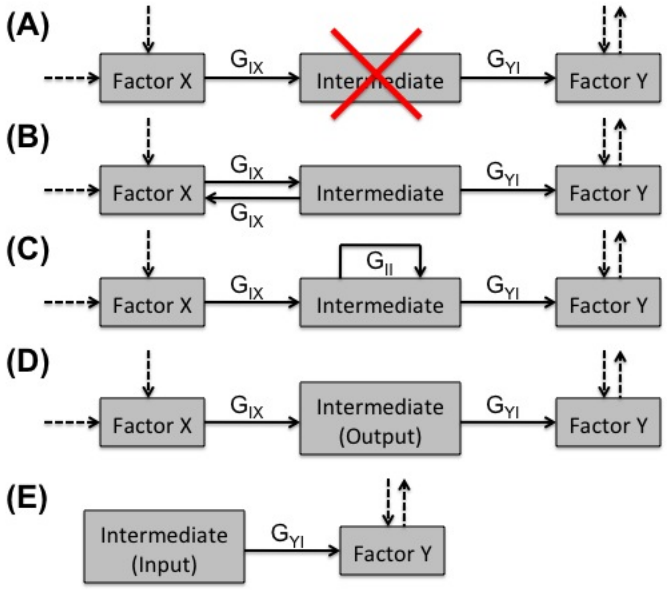

Figure 6.5. Determining when to make an intermediate an actual factor in the model. Note that dotted arrows represent relationships to factors not shown. A. This example illustrates the most common example of when an intermediate should be excluded as a factor. This 'linear' scenario has no feedback and thus there is no reason to include it. B. This example illustrates an intermediate with external feedback that should be included as a factor in the relational model. C. This example illustrates an intermediate with internal or self-feedback that should be included as a factor in the relational model. D. This example illustrates an intermediate that also serves as a model output, and thus, should be included as a factor in the relational model. E. This example illustrates an intermediate that also serves as a model output, and thus, should be included as a factor in the relational model.

For categories, once again, the values must be estimated. However, as before with the time constants, reviews provide a good source to obtain some estimates as to what a category of aggregated factor gains might look like. Similar to the recommendation made in Step 10 for category time constants, category gains can also be assigned as having magnitudes that are 'small', 'medium' or 'large'. These magnitudes are assigned relative to one another. Since the goal of a category model is to get an idea of system behavior and not to precisely match quantitative values, keeping the category gains in

roughly the correct proportions relative to one another is more important the actual values used.

Step 13: Determine the 'output' value criteria. When it comes to output criteria, more is better as additional outputs only help to further analyze and validate the model. Remember that the relational analysis techniques actually perform better with larger numbers of outputs. There are not very many rules when it comes to outputs. The one rule is that there needs to be at least some outputs which come from data sources that are not used to construct the model. This keeps the validation from becoming 'biased'. However, given the availability of data it is practically impossible to have an external output for every factor. In fact, a good majority of the outputs may in fact come from the same study from which the factor's gain and/or time constant was taken. Thus, it is important to keep track of where the outputs come from exactly, including the paper, figure number, etc. Furthermore, it is helpful to categorize outputs such as 'primary', 'secondary', and 'tertiary'. Primary outputs are completely external to the model. Secondary outputs may have come from a study in which indirect information was extracted for the model, taken either from different sub-study within the publication or from a study in which only factor time constant information was extracted (since factor time constants are less study-specific compared to factor gains). Tertiary outputs come from papers or studies in which one or more factor time constants were extracted. Despite being 'closest' to the model, tertiary outputs are often still not completely internalized because there are typically many factor gains that go into the calculation of a factor. Thus a tertiary reference only contributes to a portion of the factor's output value.

For categories, there is little to be done in getting actual category output validation criteria in terms of quantitative values since such data typically is not readily available from the literature or even in the reviews. Thus, categories must be analyzed relative to one another and based on their time courses rather than their actual quantitative output values/magnitudes.

Step 14: Determine the form of the equations for each factor or category. Although this entire step is written in terms of factors, please note that the mechanics of this step are the same whether doing a factor or category relational model. The form of the equations for individual factors can be of any type and each factor can have a different form if one so chooses. However, in general, the expected value for most factors, $F_{expected}$, can be determined using this simple linear form where the gain of the influencing factor, $G_{i\text{-}Factor}$, is multiplied by the influencing factor value, $Factor_i$, and all such products for all influencing factors one through N are summed:

$$Factor_{expected} = \sum_{i=1}^{i=N} G_{i-Factor} \cdot Factor_i \qquad \textbf{Equation 6.1}$$

There are exceptions where the above does not work well. One example of a factor that was not well represented by the above was the Na-K-ATPase pump in the SCI model, in which the above equation had to be altered (see Methods of the SCI test case in Chapter 8). It is possible that the above only works well for factors that are unidirectional in sign over the selected model time 'split' or time constant. The SCI test case supports this

hypothesis as the Na-K-ATPase pump was the only factor in the SCI model which had a significant change in sign during a single time split.

Typically, the differential equations, themselves, for most factors can be represented in typical Euler form where the subscripts expected and previous denote the expected and previous factor values, usually in terms of time:

$$\frac{\mathrm{d\,Factor}}{\mathrm{dt}} = \frac{\mathrm{Factor}_{\mathrm{expected}} - \mathrm{Factor}_{\mathrm{previous}}}{\tau_{\mathrm{Factor}}} \qquad \textbf{Equation 6.2}$$

Step 15: Construct and simulate a relational model. The construction part of this particular step is really no different then implementing any other computational model. The modeler can pick his/her favorite modeling platform such as MATLAB (The MathWorks, Inc.), C/C++, Pascal, or FORTRAN.

As for the simulation part, review the chapter on relational analysis methodology. The model will need to be simulated at multiple operating points. Some helpful pointers include: separating the time 'splits' such that their results or outputs can be viewed separately, automating sensitivity analyses for factor gains and/or time constants, and automating the relational analysis landscapes.

Refine

Step 16: Perform relational analysis. See the relational analysis instructions (Chapter 4.) Note that, in general for a relational model, only the survey and summarize parts of the S^3 relational analysis technique can be used on a relational model. Use the recorded standard experimental errors (means or deviations) to aid in the sensitivity analysis ranges.

Step 17: If possible, validate the relationships with experimental correlations. This step is usually done jointly with Step 18, although it easier to start with validating correlations before trying to obtain specific values. See the relational analysis instructions and particularly the landscape text. Check the correlation of each factor at its experimentally determined time. Ask the following questions: Does the model show the expected correlations? Do the sign and/or magnitude(s) change with time? For the predicted correlations, do they make sense? Can a mechanism be hypothesized?

If there are known differences in the model and experimental data, these differences will need to be addressed. First check to see if the simulated factor correlation was sampled at the same time period as the experimental data since correlations can actually change with time. If not, then re-do the landscape at the experimental time frame for the factor in question. Once the time frames are the same, check the factor gains including their directionality (impact of X on Y vs impact of Y on X, if applicable), magnitude and sign. If these are all correct, more detail may be needed (see Step 19). If these are incorrect, make a series of landscapes over time. If and when do any of the series of landscapes have the correct correlation? Next, check the time constants to see if they need to be

split. This is usually evidenced by a factor following the proper trend for a while and then suddenly falling away from the experimental trend. Next, check the form of the factor-gain equation to see if it adequately represents the trend of the experimental data. Finally, sample the space with a broad-based sensitivity analysis to check the robustness of the factor and its broader behavior and stability.

Step 18: Validate values by comparing single factors with experimental data. There are a multitude of ways to go about refining the model to obtain the proper output values. If the correlations are correct over time (from Step 17), the first thing to check is the relative trend of the factor. Does it look like its experimental counterpart? If not, return to the troubleshooting tips in Step 17. If all of those criteria have been met, then the model may simply need more detail (see Step 19), both in terms of time constants and/or factor gains. If the trends are correct, but the quantitative values are merely wrong, perform an extended sensitivity analysis using the standard experimental error and approximated error during the gain extraction process. This allows the proper gain to be 'tuned' to the correct value.

Step 19: Determine which categories or factors need more detail. Steps 17 and 18 outlined many trouble shooting tips for factors, which did not in one way or another meet some portion of the validation criteria. Once the factors are 'close' to experimental correlations, the best way to determine if a category or factor needs more detail is to perform relational analysis and component analysis on specific factors by both subtracting and adding more detail (i.e. making the model bigger by adding in more

factors or intermediates and smaller by subtracting them). Once the model gets to the point to where both qualitative and quantitative changes seem tolerably small and the top 5 or so influencing factors are stable (in that they are the same regardless of model operating point), it can be safely assumed that the model has sufficient detail to make system-level hypotheses about dynamics. In the case with SCI, there was little difference between the final implementation versus the version before it, which included about 25% fewer papers. Thus, a stopping point was reached for the first system-level model of SCI. This is not to say that more detail or outputs and such could not be added and more insight gained. The 'stopping point' simply means that the answers the model produced could be trusted.

Step 20: Iterate until the appropriate relationships and criteria have been satisfied.

Expect around 3 iterations to get a base model up and running.

If doing a preliminary or category model, return to step eight to make a factor model.

CHAPTER 7

NEUROTRANSMITTER SPILLOVER

Neurotransmitter spillover was chosen as the first system test case. It was a reasonable 'starter system' in that it is a system in which we have some prior familiarity, and is scientifically interesting in that it re-opens the long-standing debate in neuroscience that synapses are truly independent. In section one of this chapter, the 'base' neurotransmitter spillover model is developed and the system is analyzed using traditional analytical techniques such as a parameter sensitivity analysis. In section two of this chapter, degenerate versions of the neurotransmitter spillover model are developed in order to refine our relational analysis technique of search-survey-and-summarize (S3) and to develop the related component analysis technique.

Neurotransmitter spillover was chosen as the methodological development system for three reasons: 1) It is a relatively simple system that can be modeled as two sub-systems or components which can be independently analyzed, a glutamate diffusion model and a neurotransmitter receptor model; 2) A neurotransmitter spillover model is a mechanistic model, the most common type of model implementation, and its diffusion and kinetic mechanics are representative of a large portion of traditional biological models and 3) While the sub-system or component properties are well-characterized, the dynamics or properties emerging from the interaction of the two sub-systems are not; thus, there were

opportunities to "check" the method for what was known and to "test" the predictability of the method to identify dynamics and/or mechanisms which were unknown.

The first study of spillover in the cerebellar glomerulus, the mechanistic model of the system, was implemented and the amount of spillover seen within the cerebellar glomerulus was calculated under a wide range of physiological parameters. This study utilized a sensitivity analysis of the geometric parameters to determine the percent contribution of NMDA-R activation to spillover at the cerebellar glomerulus. The major finding of the study was that spillover results in NMDA-R open probabilities that are 79% of what is seen during a direct release. The paper, "An analysis of glutamate spillover on the N-methyl-D-aspartate receptors at the cerebellar glomerulus", as published in the *Journal of Neural Engineering* 4(3): 276-282 (Mitchell et al, 2007), is presented in its entirety.

Study two focuses on the methodological development of the relational analysis technique. In this study, relational analysis is used to discern the difference between two degenerate models—the 8-state BT NMDA-R model and the 5-state LJ NMDA-R model, both individually and within the context of the larger spillover model. The underlying thought was that the ability to discern between two models capable of producing the same output [i.e. two degenerate models] would be a critical test of the robustness and effectiveness of the relational analysis method to reveal complex system dynamics. Furthermore, the study was an interesting exercise in determining the necessity of

complexity within a model—a judgment that must often be made by modelers to balance computational requirements, run time, and model robustness.

Ironically, the idea to compare the two degenerate versions of the NMDA-R model was spurred by the comments of a reviewer of the first spillover paper who stated in his review: "Why is the Banke and Traynelis model used instead of the Lester and Jahr model? I see no need to implement the more complex BT model over the LJ model as they both accurately model NMDA-R behavior." His reasoning was similar to that of most modelers—if a model produces the right "answer" (i.e. it meets the appropriate quantitative output criteria), then it is "good enough" and there should be no need for additional model complexity.

However, the findings of this study illustrates that there is much more to a model and its dynamic behavior than simply meeting target output criteria. Using the developed relational analysis technique of search-survey-and-summarize, this paper highlights how relational analysis is able to "raise the hood of the model" to view the important dynamics that lie beneath that contribute to the model's robustness and ability to predict unknown or emergent behavior using the product of relational analysis, the model's landscape, which consists of a visual representation of its quantitative output relationships. The key result of the paper, in regards to spillover, is that though both the BT and LJ NMDA-R models are able to reproduce overall spillover model target output criteria, the BT model more accurately represents the dynamical relationships of synaptic geometry, a critical predictive feature particularly once spillover analysis is moved from

the well-characterized geometry of the cerebellar glomerulus to less-characterized synapses. Furthermore, the presence of a "pinch point" or dimensional reduction within the spillover model is determined and characterized. The paper "Output-based comparison of alternative kinetic schemes for the NMDA receptor within a glutamate spillover model" as published in the *Journal of Neural Engineering* 4(4): 380-389 (Mitchell and Lee, 2007) is given in its entirety.

System Background: Neurotransmitter spillover

The concept of synaptic independence has been a long-standing theorem in neuroscience upon which nearly all mechanistic single cell and neural network models are based. In fact, the very foundation of our neuroscientific thought hinges upon the dogma that synapses are truly independent. However, increasing experimental and theoretical evidence has suggested that this may not be the case. Synaptic neurotransmitter spillover, defined by Diamond (2002) as the escape of neurotransmitter from a synapse of an intentionally or directly activated neuron to a neighboring, quiescent synapse resulting in the neighbor's indirect activation (see Figure 1), has remained a topic of much debate. Whether intentional whereby spillover has the potential to increase transmission reliability or network synchronization (Nielson, 2004) or unintentional whereby spillover has the potential to trigger pathological responses such as aberrant firing (Rusakov and Kullmann, 1999), spillover most certainly impacts and adds additional layers of complexity to neuronal dynamics and firing properties. The significance of spillover to experimental and theoretical neuroscientists alike is without question, and as such,

neurotransmitter spillover makes for an interesting test case from which further system exploration using complex systems based methods is both necessary and warranted.

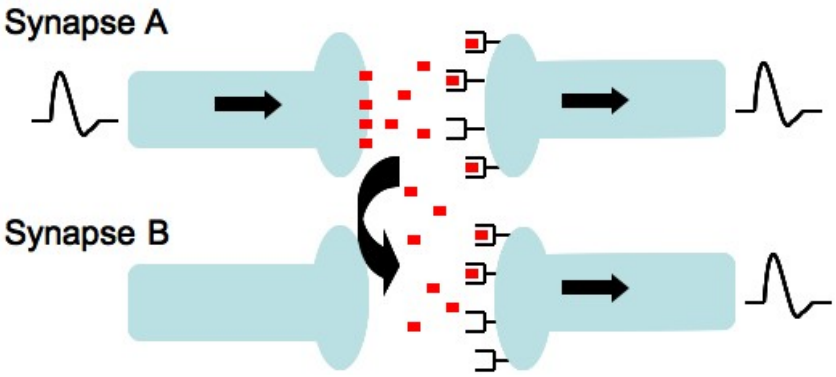

Figure 7.0.1. Diagram of neurotransmitter spillover. The pre-synaptic terminal of Synapse A is intentionally activated, resulting in the release of neurotransmitter from its synaptic cleft (denoted by the red boxes). Under the theory of true synaptic independence, this neurotransmitter simply diffuses across the synaptic cleft of Synapse A, resulting in receptor activation in the post-synaptic terminal and subsequent action potential initiation. However, when neurotransmitter spillover occurs, the neurotransmitter from Synapse A escapes, diffuses into neighboring Synapse B, and results in indirect receptor activation of the post-synaptic terminal of Synapse B and subsequent action potential initiation.

The properties of neurotransmitter spillover, and neural transmission in general, are largely dependent upon the specific properties of the synapses being studied including geometry, intrinsic properties, uptake transporters, etc. In order to keep our analysis tractable, both for the sake of understanding the system being explored and to assist in methodological development, we chose to model the cerebellar glomerulus for which much data already exists. The glomerulus consists of a relatively enclosed complex of synapes having a mossy fiber at its core synapsing with axons of Golgi type II neurons

tractable, both for the sake of understanding the system being explored and to assist in methodological development, we chose to model the cerebellar glomerulus for which much data already exists. The glomerulus consists of a relatively enclosed complex of synapes having a mossy fiber at its core synapsing with axons of Golgi type II neurons and dendrites of granule cells (Kandell et al, 2004). Because of it relatively large size, its geometric properties have been thoroughly experimentally examined. An additional advantage is that uptake of the active neurotransmitter, glutamate, is accomplished by an enclosed sheath around the complex that houses glutamate transporters (Overstreet et al, 1999). Because nearly all glutamate uptake occurs at the boundary of this sheath, there is little need to model individual glutamate transporters. Instead, glutamate uptake can be modeled using its residence time; when glutamate reaches the sheath, it is extracted from the active synaptic system.

The synaptic transmission itself is accomplished via the activation of the glutamatergic receptors, the N-methyl-D-aspartate receptor (NMDA-R) and alpha-amino-3-hydroxy-5-methyl-4-isoxazolepropionic acid receptor (AMPA-R). The role of AMPA-Rs had been both experimentally and theoretically characterized by previous studies (DiGregorio et al, 2004; Saftenku, 2005). However, while no prior theoretical study had been conducted to characterize the role of NMDA-Rs, prior experimental studies showed conflicting results regarding the impact of NMDA-Rs in neurotransmitter spillover (Rossi et al, 2002, Sargent et al, 2005; Cathala et al, 2003).

With these simplifications in mind, a neurotransmitter spillover model which explores the synaptic spillover of glutamate within the cerebellar glomerulus consists of two sub-models: 1) a diffusion model which simulates the diffusion of glutamate between the synapses within the cerebellar glomerulus and its uptake at the outer ensheathing boundary and 2) a receptor kinetics model which simulates the binding and activation of synaptic NMDA-Rs responsible for neural transmission. We chose to use existing theoretical models, which accurately represented each sub-model system. The implemented diffusion model was that developed and used by Saftenku (2005) to study the effects of glutamate spillover on AMPA-Rs at the cerebellar glomerulus. The implemented NMDA-R model was one of two published models: the 5-state Lester & Jahr (LJ) model (Lester and Jahr, 1992) and the 8-state Banke and Traynelis (BT) model (Banke and Traynelis, 2003).

This chapter is divided into two sections, each representing one of two published papers on spillover at the cerebellar glomerulus. The first section or paper highlights the spillover model development and the major conclusions regarding the impact of glutamate spillover on the activation of NMDA-Rs at the cerebellar glomerulus. The second section or paper highlights the methodological development of the search-sensitivity-and-summarize technique of relational analysis and illustrates the effectiveness of the method to identify complex system dynamics by using the method to discern between two degenerate models (i.e. the BT and LJ NMDA-R models) within the context of the larger spillover model.

An analysis of glutamate spillover on the N-Methyl-D-Aspartate receptors at the cerebellar glomerulus

Journal of Neural Engineering 4(3):276-282

doi: 10.1088/1741-2560/4/3/013

http://www.iop.org/EJ/abstract/1741-2552/4/3/013/

Contributions of the authors

Cassie Mitchell developed and implemented the model, performed the simulations and analysis, and wrote the manuscript. Steven Feng contributed to model code development. Dr. Robert Lee provided valuable project input and co-edited the manuscript.

Abstract

Glutamate spillover is thought to play a significant role in increasing neural transmission at the mossy fiber/granule cell cerebellar glomerulus. Glutamate spillover has been shown to activate AMPA receptors at the glomerulus, and here we complete the characterization of spillover at the glomerulus by investigating the role of glutamate spillover in N-methyl-D-aspartate receptor (NMDA-R) activation. We present a quantitative model of glutamate spillover combining recent models of glutamate diffusion and NMDA-R binding to determine the open probabilities of NMDA-Rs over time at a neighbor synapse. Simulation results from a baseline set of physiologically realistic

parameters show that glutamate spillover onto a single neighbor synapse, created by glutamate that diffuses from a point source into a restricted fractional 2D-3D space and the glutamate concentration created by neighboring glutamate release sites, is sufficient to elicit an NMDA-R peak open probability of 0.23, approximately 79% of that obtained by a direct release (peak open probability of 0.29). Thus, it would appear that glutamate spillover at the glomerulus at NMDA receptors is even more substantial than that seen at AMPA receptors.

Keywords

synaptic crosstalk, NMDA receptor, cerebellar glomerulus, computer model, extrasynaptic diffusion

Introduction

Glutamate spillover, defined as the escape of neurotransmitter from the synapse into which it is released to neighboring, quiescent synapses thereby activating receptors (Diamond 2002), is thought to play a critical role in synaptic transmission at the cerebellar glomerulus, a complex structure surrounded by a glial sheath where the mossy fiber terminal forms glutamatergic synapses on the dendrites of granule cells (Palay and Chan-Palay 1974). Glutamate spillover has the potential to increase transmission reliability (Saftenku 2005; Sargent et al. 2005) and to help synchronize granule cell firing (DiGregorio et al. 2002). Most previous experimental and theoretical work has focused on glutamate spillover on AMPA receptors (DiGregorio et al. 2002; Nielsen et al. 2004; Saftenku 2005) which have shown considerable activation, >50%, via glutamate

spillover. Since NMDA receptors have a higher affinity for glutamate than AMPA receptors, it is plausible that they, too, would be greatly influenced by glutamate spillover. Thus, it has been hypothesized that glutamate spillover on NMDA does occur at the cerebellar glomerulus. However, current experimental results looking at the effects of glutamate spillover on NMDA receptors at the cerebellar glomerulus are mixed. NMDA receptors contribute to quantal excitatory post synaptic currents (EPSCs) at immature granule cell synapses, but multiquantal release was required to activate NMDA receptors at mature synapses (Cathala et al. 2003). Consequently, further investigation is warranted.

We examine the spillover of glutamate on NMDA receptors (NMDA-R) located at the mossy fiber/granule cell synapse in the cerebellar glomerulus. A quantitative model of NMDA spillover at the cerebellar glomerulus will complete the characterization of spillover at this synapse. Using known glomerulus geometry from electromicrographs and combining two published models of glutamate diffusion (Saftenku 2005) and NMDA receptor kinetics (Banke and Traynelis 2003), we present spillover in terms of glutamate concentration profiles and NMDA receptor open probability profiles. Specifically, we explore the role of geometry, glutamate diffusion and uptake, receptor properties, and cumulative glutamate release from multiple neighboring synapses. Additionally, the effects of quantal release, receptor number per synapse, number of release sites, the effective diffusion coefficient, nerve diameter, and location of glutamate uptake are investigated.

Our results indicate that the effects of glutamate spillover on NMDA receptors of the cerebellar glomerulus are substantial with approximately 79% of the response obtained by "normal" direct release.. Sweeps of model parameters indicate that substantial glutamate spillover occurs in the majority of cases, including the cases that would currently be considered physiological, suggesting that some level of spillover is the norm rather than the exception in the cerebellar glomerulus.

Methods & Materials

Diffusion Model

The Saftenku diffusion model (Saftenku 2005) was chosen because it includes several key features that limit the number of unknown parameters, and has already been successfully used to characterize AMPA receptors at the cerebellar synapse. The more complex, bounded cylindrical geometry well represents the actual neural environment based on electron micrographs of the cerebellar glomerulus measuring the geometric distances and parameters. Also, glutamate uptake is handled by an absorbing boundary derived from the residence time of the glutamate in the extracellular space (Trommershauser et al. 1999). Additionally, this model integrates the probability of glutamate release from multiple neighboring synapses. Finally, the analytical nature of this model allows for rapid computations (91 seconds per 60 ms simulation).

The glomerulus contains a mossy fiber at its center that is 3-4μm in diameter (R_{MF}) and 6.5-10μm in length; the glial sheath is about 1-1.5μm from the mossy fiber terminal (Xu-

Friedman and Regehr 2003). Hence, the absorbing boundary in the radial direction, r_{abs}, is 2.5-3.5μm measured from the center of the mossy fiber. The normal direction absorbing boundary (R_{dd}) is equal to the difference between r_{abs} and R_{MF}. When glutamate molecules reach r_{abs} in a radial direction or R_{dd} in the normal direction, they are absorbed by the glial sheath.

The diffusion model assumes instantaneous release of glutamate with an initial concentration, c_0, of 8.77mM, equivalent to one vesicle containing 4,000 molecules of glutamate corresponding to a vesicle concentration of 100mM. Multi-vesicle release is simulated by varying c_0 at 4.385, 8.77, and 17.54mM to represent 0.5, 1, and 2 vesicles, respectively. There are many citations for possible diffusion coefficient values (Nicholson and Sykova 1998; Saftenku 2005), etc. Accounting for the effects of macromolecule obstacles and overcrowding, the glutamate diffusion coefficient is 0.2μm^2/ms (Saftenku 2005). The highest diffusion coefficient, describing diffusion within the synaptic cleft, is thought to be 0.76 μm^2/ms (Barbour 2001). The value of 0.41 μm^2/ms represents the aqueous glutamate diffusion coefficient corrected for temperature and a brain tortuosity of 1.6 (Nicholson and Sykova 1998). **Table 1** lists the diffusion model parameter base values, physiological ranges, and references. Note that to be conservative in our estimate of spillover, we use slightly different base case parameter values than those used by Saftenku 2005. However, our base case parameter values lie closer to the mean of the experimentally determined values shown in Table I, and most of the parameter values used by Saftenku 2005 lie within the parameter ranges we test (see Table 2).

Table 7.1.1. Diffusion model parameter definitions, values and references.

Description	Name	Base Value	Physio-logical Range	Reference
Mossy fiber radius (μm)	R_{MF}	1.5	1.5-2	(Hamori et al. 1997; Xu-Friedman and Regehr 2003)
Distance from center of mossy fiber to glial sheath (μm)	r_{abs}	3.0	R_{MF}+1.5	Xu-Friedman & Regehr, 2003
Distance from mossy fiber to glial sheath (μm)	R_{dd}	1.5	1-1.5	Saftenku, 2005
Radius of circle containing one release site $= \sqrt{v_s \pi}$ (μm)	r_{MD}	2.17	1.25-2.8	Saftenku, 2005 (equation) See v_s references
Initial glutamate concentration (mM)	C_0	8.77	4.39-17.54	Xu-Friedman & Regehr, 2003
Effective diffusion constant ($\mu m^2/ms$)	D_{eff}	0.41	0.41-0.76	Saftenku, 2005 ; Barbour, 2001 ; Nicholson & Sykova,1998 ; Nielson, 2004.
Average release site density (μm^{-2})	v_s	1.5	1.5-3.5	(Rusakov et al. 1999; Sorra and Harris 1998; Xu-Friedman and Regehr 2003)
Average radius of post-synaptic density (μm)	a	0.11	0.11	Xu-Friedman & Regehr, 2003

NMDA-R Binding Model

To investigate glutamate spillover, we examine the binding kinetics of the two NR2 subunits, even though co-agonist binding is necessary to open the ion channel. Each NR2 subunit can independently bind glutamate, and glycine concentration is assumed to be high enough such that the NR1 subunits are saturated. To simulate NMDA-R activation,

the diffusion profile concentrations were fed into the Banke and Traynelis model (Banke and Traynelis 2003)

The Banke and Traynelis model incorporates two desensitized receptor states and two transition states representing a fast and a slow conformation change. The 2-glutamate bound state, the two transition states, and the activated receptor state comprise a loop **(Figure 1)** which allows for two conformational changes to proceed before receptor activation.

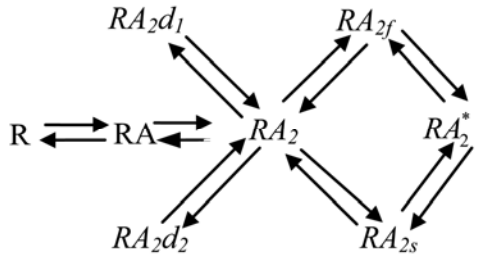

Figure 7.1.1. Banke and Traynelis NMDA-R binding model. The desensitized states are labeled RA_2d_1 and RA_2d_2, and the transition states are labeled RA_{2f} and RA_{2s}. The activated state is RA_2* (Adapted from Banke and Traynelis, 2003).

Spillover Model Analysis

Model output is in the form of glutamate concentration profiles and open probability profiles. Given a parameter set, glutamate concentration profiles show the time course of glutamate concentration, at a distance of 0.46μm from the center of the cleft, arising from summary contribution of spillover from all neighboring release sites. Similarly, the open

probability profiles show the time course of open probability when a synapse at the aforementioned distance is exposed to a given concentration profile.

The implementation of the diffusion model was confirmed by comparison of the base $[Glu]_{ts}$ profile to that reported by Saftenku (not shown); note that the glutamate concentration traces shown in this work (Figure 2) appear different than Saftenku because of the differences in parameter values chosen (to keep the spillover estimate more conservative) The implementation of the Banke and Traynelis NMDA-R model was verified by comparison of the NMDA-R open probability (P_O) distribution generated when exposed to 1000μM glutamate to that reported by Banke and Traynelis (2003) (not shown). The model is implemented in MATLAB R14 and runs at a time step of 10μs. Use of smaller time steps has negligible impact on the results.

A sensitivity analysis was performed by varying parameters independently. The individual effects of D_{eff}, $r_{abs,}$ R_{MF}, c_0, v_s, and receptor number on the concentration and open probability profiles are assessed while using base values for the rest of the parameters.

Results

A summary of effects of each parameter on peak glutamate concentration, peak open probability, and the time point of the peak open probability are presented in **Table 2**. Simulation of the model with the midpoint physiological parameter values (base values in

Table III) led to a peak glutamate concentration (peak $[Glu]_{ts}$) of 126μM and a peak open probability (peak P_O) of 23% occurring 16.47ms after initial glutamate release. Exploration of the details of the results is presented below.

Table 7.1.2. Summary of simulated parameter values and their effects on peak $[Glu]_{ts}$, peak P_O, and time of peak P_O.

Name	Base Value	Simulated Range	Peak [Glu] (μM)	Peak [Glu] Trend	Peak P_O	Peak P_O Trend
R_{MF} (μm)	1.5	1-2	102-131	Mixed	0.16-0.24	Mixed
r_{abs} (μm)	3.0	2-3.5	103-126	↑ r_{abs} = ↑ [Glu]	0.06-0.25	↑ r_{abs} = ↑ P_O
c_0 (mM)	8.77	4.39-17.54	63-252	↑ c_0 = ↑ [Glu]	0.14-0.28	↑ c_0 = ↑ P_O
D_{eff} ($\mu m^2/s$)	0.41	0.2-0.76	126	↑ D_{eff} = ↓ [Glu]	0.15-0.28	↑ D_{eff} = ↓ [Glu]
v_s (μm)	1.5	0.5-2.5	23-246	↑ v_s = ↑ [Glu]	0.04-0.28	↑ v_s = ↑ [Glu]

Concentration Profiles

The glutamate concentration profile versus time was examined as a function of the various model parameters within their respective physiological ranges (**Figure 2**). The base case (**Figure 2A)** represents the mid-range of the physiologically relevant parameters and, as previously stated, generates a peak $[Glu]_{ts}$ of 126μM. Peak $[Glu]_{ts}$ is relatively insensitive to varying the effective diffusion constant (D_{eff}), the distance from the center of the mossy fiber to the glial sheath (r_{abs}), or the radius of the mossy fiber (R_{MF}) (**Figure 2B-D**). However, the time course of $[Glu]_{ts}$ is substantially affected by the parameters, particularly D_{eff}. Decreasing D_{eff} delays the arrival of glutamate at the glial sheath, resulting in a prolonged concentration increase. Increasing r_{abs} increases the

distance the glutamate must travel before being taken up by the glial sheath thereby lengthening the time course. Varying R_{MF} has a mixed effect: at an R_{MF} = 1.5μm peak $[Glu]_{ts}$ is higher than that at an R_{MF} = 1μm, and the time course of uptake is dominated by the effect of the increased number of release sites, making it slower. (Increasing R_{MF} increases the surface area of the mossy fiber which in turn increases the number of glutamate release sites.) At an R_{MF} = 2μm the peak $[Glu]_{ts}$ is lower and the time course of uptake is dominated by the effect of the shorter distance to the glial sheath, making it faster. Thus, the distance glutamate must travel to reach the glial sheath decreases as R_{MF} increases and glutamate is taken up more quickly.

Conversely, both the initial glutamate concentration (c_0) and the number of glutamate release sites (v_s) significantly alter peak $[Glu]_{ts}$, but neither has a significant impact on the concentration time course (**Figure 2E-F**). The effects of c_0 and v_s on peak $[Glu]_{ts}$ are scaled. Increasing either parameter results in a proportional increase in peak $[Glu]_{ts}$.

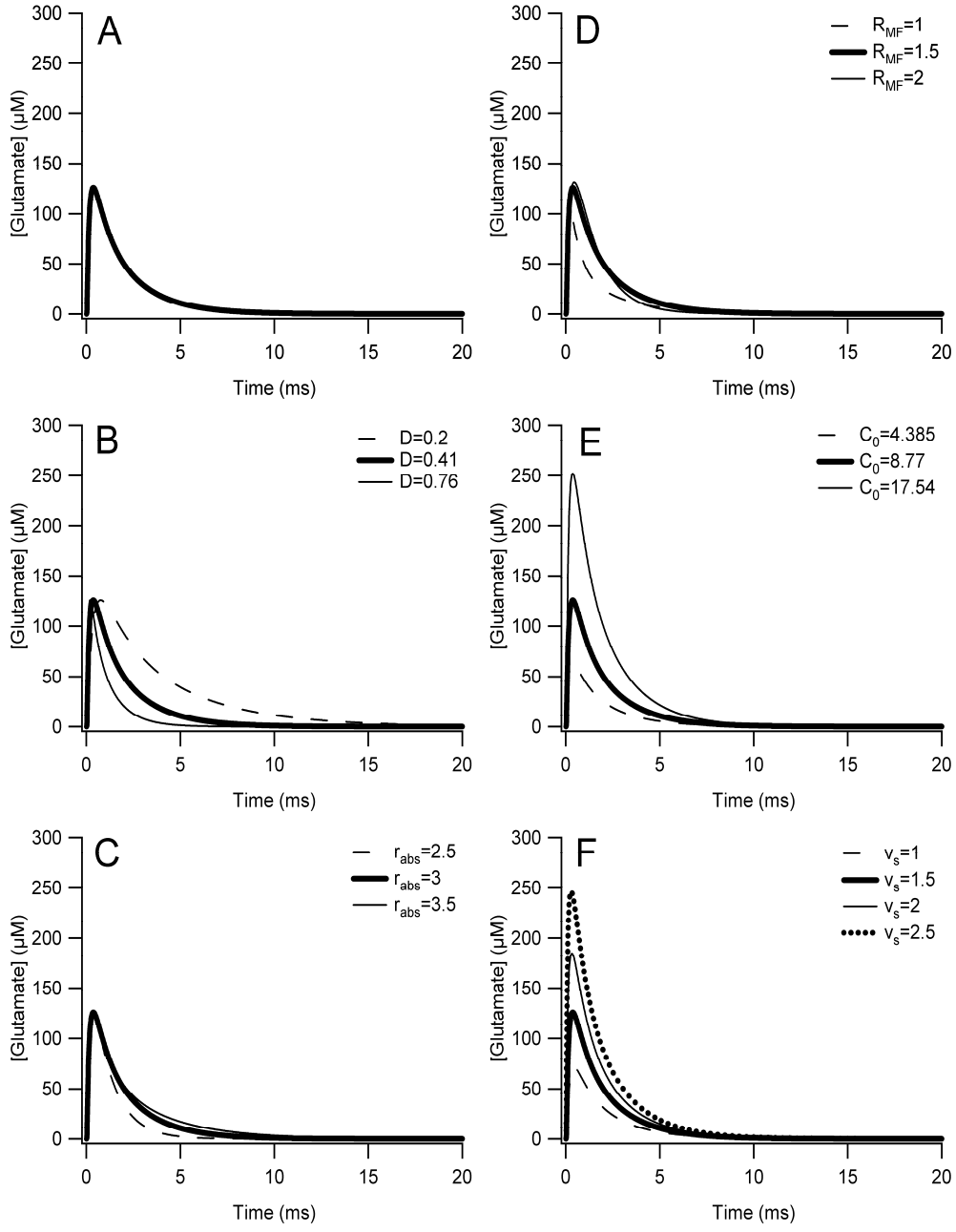

Figure 7.1.2. Glutamate concentration profiles for parameters varied within the physiological range. *A.* The base case concentration profile. *B.* The effect of D_{eff}, the effective diffusion constant. *C.* The effect of r_{abs}, the distance from the center of the mossy fiber to the glial sheath. *D.* The effect of R_{MF}, the radius of the mossy fiber. *E.* The effect of C_0, the initial concentration. *F.* The effect of v_s, the number of release sites.

Open Probability Profiles

Ultimately, it is the action of glutamate on receptors that determines the relevance of spillover. Thus, open probability (P_O) versus time was examined as a function of the various model parameters within their respective physiological ranges (**Figure 3**). The base case (**Figure 3A)** generates a peak P_O of 0.23. However, the P_O remains above 0.15 for up to 60ms.

All of the parameters included in the parameter analysis have a meaningful impact on peak P_O. In general, the greater the impact the parameter has on the $[Glu]_{ts}$ profile, the greater its impact on peak P_O. The geometric parameters (r_{abs}, R_{MF}) when varied within the physiological range have less of an impact than the intrinsic parameters (D_{eff}, c_0, and v_s). Variation of r_{abs} within the physiological range results in peak open probabilities between, 0.19 and 0.25, increasing as r_{abs} is increased (**Figure 3B**). The mixed effects of varying R_{MF}, as discussed previously for the $[Glu]_{ts}$ profiles, are again apparent in the P_O profiles (**Figure 3C**). The higher peak $[Glu]_{ts}$ seen with an R_{MF} = 1.5μm results in a higher peak P_O than when R_{MF} =2 μm. Receptor number (varied between 250 and 1,000) has no effect on peak P_O (not shown).

The parameters that have the highest impact on peak P_O when varied within their physiological range are D_{eff}, c_0, and v_s. Variation of either c_0 or D_{eff} within the physiological range results in a peak P_O from approximately 0.14-0.28 (**Figure 3D-E**). The effect of varying v_s within its physiological range from 1-2.5μm^{-2} results in a peak P_O range of 0.16 to 0.28 (**Figure 3F**).

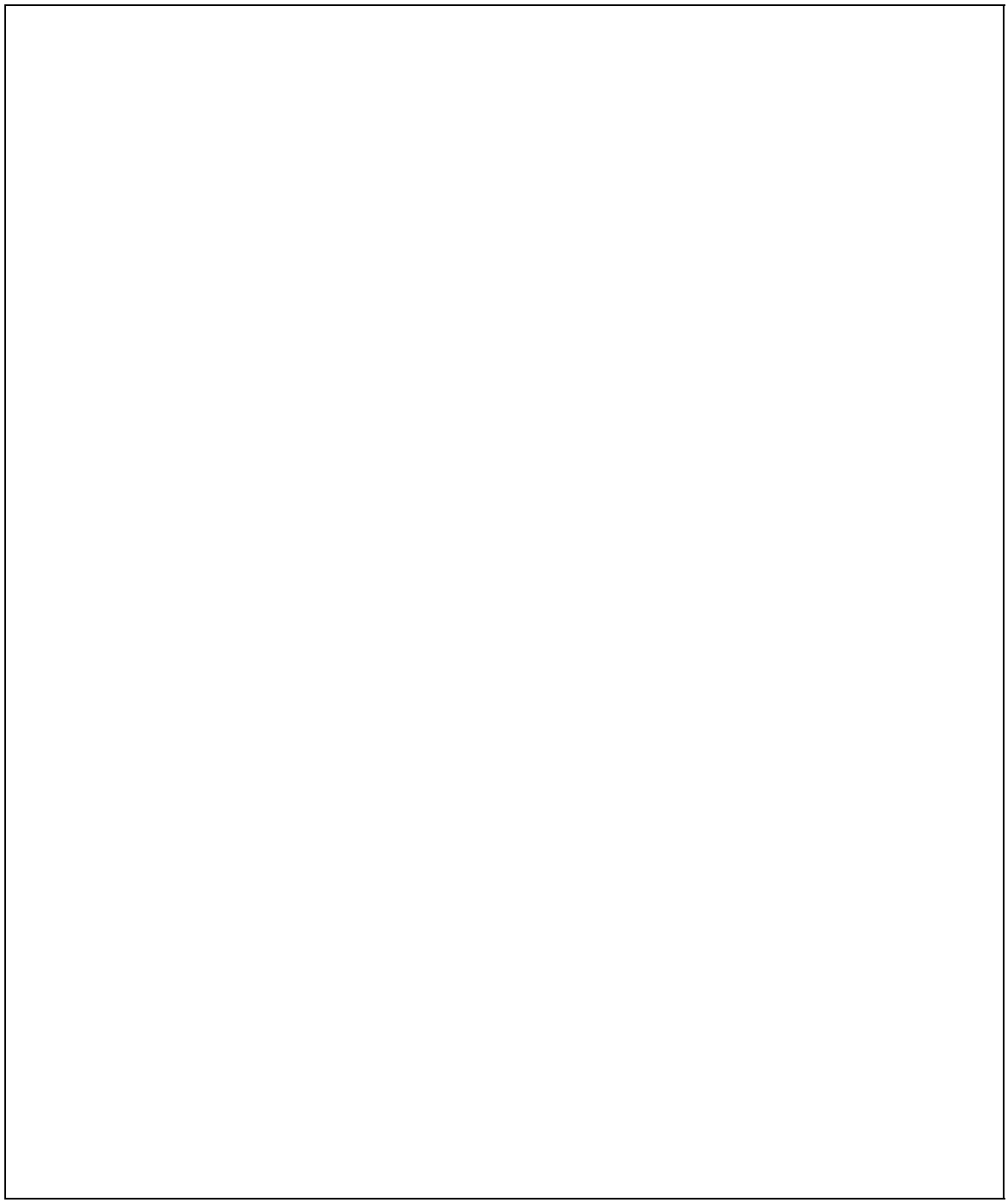

Figure 7.1.3. Open probability profiles for parameters varied within the physiological range. *A*. The base case open probability. *B*. The effect of r_{abs}, the distance from the center of the mossy fiber to the glial sheath. *C*. The effect of R_{MF}, the radius of the mossy fiber. *D*. The effect of D_{eff}, diffusion coefficient. *E*. The effect of C_0, the initial concentration. *F*. The effect of v_s, the number of release sites.

Limiting Cases

The lowest peak P_O found by varying model parameters one at a time within their physiological ranges was 0.15 (D_{eff} = 0.76). To even reach a peak open probability of 0.05 (approximately 15% of the direct release open probability of 0.29 in the Banke and Traynelis model) multiple parameters had to be varied to their minimizing limit within their physiological range (D_{eff}, v_s and r_{abs}). Of course, with expanded parameter ranges beyond the stated physiological range it is possible to achieve a P_O at or below 0.05 with several combinations of parameter values. However, the plausibility of these combinations is highly questionable given the extent to which multiple parameters would need to be beyond their established physiological ranges.

Comparison to Direct Release

To determine the impact of spillover, the base case open probability profile for the NMDA-R was simulated using only direct release as was done by Saftenku (2005) for the AMPA-R. The spillover peak open probability for direct release on NMDA is 0.29 compared to spillover release which results in a peak open probability of 0.23. Thus, in this model, spillover can generate up to 79% of the NMDA-R open probability see from direct release.

Discussion

Our results demonstrate that glutamate spillover on NMDA-Rs does result in significant open probabilities. Our base case exhibits a peak NMDA P_O that is roughly 79% of that

associated with direct release (base case $P_O = 0.23$, direct release $P_O = 0.29$). The higher percentage of peak NMDA P_O in comparison to AMPA (Saftenku 2005) may be attributable to the receptor's higher affinity for glutamate and could also be responsible for spillover activation of extrasynaptic NMDA receptors. Our results support the hypothesis that spillover plays an important role in synaptic transmission in the cerebellar glomerulus. While it is not surprising that spillover on NMDA-Rs is probable at this synapse, the magnitude of effect, as predicted here, is remarkable.

Comparison to Experiment

Previous experimental work (DiGregorio et al. 2002; Nielsen et al. 2004) and theoretical work (Saftenku 2005) has shown that AMPA is activated by spillover of glutamate at the cerebellar glomerulus. Given the NMDA receptor's higher affinity for glutamate (Diamond 2002) and the restricted area for diffusion in the glomerulus, perhaps our results are not too surprising. The closed cerebellar glomerulus geometry and relatively large size may explain why much higher open probabilities can be obtained via spillover compared to smaller, isolated synapses such as hippocampal or pyramidal cells (Barbour 2001; Diamond 2001; Rusakov et al. 1999).

Unfortunately, no direct comparison of the spillover calculation with experiment is possible (the inability to directly measure open probabilities associated with glutamate spillover is what originally spurred this modeling work). Rossi et al (2002) measured the EPSCs associated with spillover, but had no way of knowing the relationship of each of the neighbor synapses which was contributing to the EPSCs. That is, was there one

neighbor or five, etc? Without this geometric information there is no way to convert the data generated by the EPSC into a calculation that is directly comparable to the geometry-specific open probabilities generated by this work.

Furthermore, experimental work on some mature mossy fiber granule cells has suggested that NMDA-Rs are located outside the synapse (Cathala et al. 2003). If this were the case, glutamate spillover may be the only means of activation. In fact, Rossi et al found that extrasynaptic NMDA receptor-mediated EPSCs activated by glutamate spillover contribute 23% of the synaptic charge of single NMDAR EPSCs (Rossi et al. 2002).

Model Limitations

One of the key limitations of the spillover model presented here is that the Saftenku diffusion model we implement lacks glutamate transporters. Experimentally it has been shown that inhibiting transporters has little effect on the spillover-mediated component of single EPSCs which suggests that glial transporters in mossy fiber–granule cell synapses are not interposed between release sites and granule cell dendrites, but are situated mainly at a distance from the mossy fiber terminal on the glial sheath, which surrounds the glomerulus. Hence, most of the uptake transporters are located at this outer boundary (Saftenku 2005) where 100% absorption of glutamate is assumed. The glial transporter subtype GLAST is suggested to be most responsible for glutamate uptake within this structure (Overstreet et al. 1999) but, unfortunately, we know little about the actual parameters of uptake as the author of the cerebellar glomerulus diffusion model states

(Saftenku 2005). Since transporters are not perfectly efficient, the absorbing boundary assumption may overestimate the actual amount of uptake.

Implications

This work completes the preliminary theoretical characterization of glutamate spillover at the cerebellar glomerulus. Although the results of this work can only be applied to the cerebellar glomerulus, it does revive the long-debated topic of neurotransmitter spillover and synaptic independence. Although the geometry and transporters at this synapse suggest that spillover could very well be intentional to help aid in neurotransmission, it remains to be seen how spillover could affect other synapse types. Pursuit of spillover studies in other synapse types, both theoretical and experimental, will aid in our ability to understand synaptic cross-talk and the implications it has in our current neuron models and neuroscientific thought.

Acknowledgements

This work is supported by National Science Foundation IGERT program (DGE-0333411) and by the Human Brain Project (NINDS, NIMH and NIBIB NS046851). In addition, we would like to thank Stephen Traynelis, PhD and Jeffrey Diamond, PhD for their comments and consultation

References

Banke, T. G. and S. F. Traynelis (2003). "Activation of NR1/NR2B NMDA receptors." Nat Neurosci 6(2): 144-52.

Barbour, B. (2001). "An evaluation of synapse independence." J Neurosci 21(20): 7969-84.

Cathala, L., S. Brickley, et al. (2003). "Maturation of EPSCs and intrinsic membrane properties enhances precision at a cerebellar synapse." J Neurosci 23(14): 6074-85.

Diamond, J. S. (2001). "Neuronal glutamate transporters limit activation of NMDA receptors by neurotransmitter spillover on CA1 pyramidal cells." J Neurosci 21(21): 8328-38.

Diamond, J. S. (2002). "A broad view of glutamate spillover." Nat Neurosci 5(4): 291-2.

DiGregorio, D. A., Z. Nusser, et al. (2002). "Spillover of glutamate onto synaptic AMPA receptors enhances fast transmission at a cerebellar synapse." Neuron 35(3): 521-33.

Hamori, J., R. L. Jakab, et al. (1997). "Morphogenetic plasticity of neuronal elements in cerebellar glomeruli during deafferentation-induced synaptic reorganization." J Neural Transplant Plast 6(1): 11-20.

Nicholson, C. and E. Sykova (1998). "Extracellular space structure revealed by diffusion analysis." Trends Neurosci 21(5): 207-15.

Nielsen, T. A., D. A. DiGregorio, et al. (2004). "Modulation of glutamate mobility reveals the mechanism underlying slow-rising AMPAR EPSCs and the diffusion coefficient in the synaptic cleft." Neuron 42(5): 757-71.

Overstreet, L. S., G. A. Kinney, et al. (1999). "Glutamate transporters contribute to the time course of synaptic transmission in cerebellar granule cells." J Neurosci 19(21): 9663-73.

Palay, S. L. and V. Chan-Palay (1974). Cortex: Cytology and Organization. New York, Springer-Verlag.

Rossi, P., E. Sola, et al. (2002). "NMDA receptor 2 (NR2) C-terminal control of NR open probability regulates synaptic transmission and plasticity at a cerebellar synapse." J Neurosci 22(22): 9687-97.

Rusakov, D. A., D. M. Kullmann, et al. (1999). "Hippocampal synapses: do they talk to their neighbours?" Trends Neurosci 22(9): 382-8.

Saftenku, E. E. (2005). "Modeling of slow glutamate diffusion and AMPA receptor activation in the cerebellar glomerulus." J Theor Biol 234(3): 363-82.

Sargent, P. B., C. Saviane, et al. (2005). "Rapid vesicular release, quantal variability, and spillover contribute to the precision and reliability of transmission at a glomerular synapse." J Neurosci 25(36): 8173-87.

Sorra, K. E. and K. M. Harris (1998). "Stability in synapse number and size at 2 hr after long-term potentiation in hippocampal area CA1." J Neurosci 18(2): 658-71.

Trommershauser, J., J. Marienhagen, et al. (1999). "Stochastic model of central synapses: slow diffusion of transmitter interacting with spatially distributed receptors and transporters." J Theor Biol 198(1): 101-20.

Xu-Friedman, M. A. and W. G. Regehr (2003). "Ultrastructural contributions to desensitization at cerebellar mossy fiber to granule cell synapses." J Neurosci 23(6): 2182-92.

Output-based comparison of alternative kinetic schemes for the NMDA receptor within a glutamate spillover model

Journal of Neural Engineering 4(4):380-389
doi: 10.1088/1741-2560/4/4/004
http://www.iop.org/EJ/abstract/1741-2552/4/4/004/

Contributions of the authors

Cassie Mitchell developed and implemented the spillover model(s), developed the application and implementation of the search-survey-and-summarize technique, developed the ideological application and implementation of component analysis, performed the simulations and analysis, and wrote the manuscript. Dr. Robert Lee contributed the primary ideological and philosophical development of the search-survey-and-summarize technique, provided invaluable advice in regards to technique application and implementation, and co-edited the manuscript.

Abstract

Recent experimental and theoretical work continues to explore the mechanisms and implications of neurotransmitter spillover. Here we examine N-methyl-D-aspartate receptor (NMDA-R) kinetics to determine their implication(s) in glutamate spillover by comparing two mechanistically different NMDA-R models, the 5-state Lester and Jahr

(LJ) model and the 8-state Banke and Traynelis (BT) model, within the context of a glutamate spillover model. We employ a search-survey-and-summarize strategy to analyze the relationships within model behavior (model relational analysis) and form a model output landscape. Our results indicate that model relational analysis can reveal differences in models whose outputs would be considered the same. The analysis reveals that the BT model, with its more complex kinetics, is less reliant on diffusion compared to the LJ version, resulting in differences in the relationships between open probability and glutamate concentration despite the fact that both model versions were able to produce the same target output values. Additionally, model relational analysis is able to distinguish between the BT and LJ NMDA-R model versions even though factor analysis indicates that the overall model output space dimensions are the same for both NMDA-R models. Furthermore, the work presented here suggests that model relational analysis may be broadly applicable as a means to examine the complex interactions hidden within overall model behavior.

Introduction

There has been a recent resurgence of interest in synaptic cross-talk or "neurotransmitter spillover" with the mechanisms and implications of spillover being examined on many fronts (e.g. DiGregorio et al. 2007; Logan et al. 2007; Marcaggi and Attwell 2007; Mitchell et al. 2007; Sun and June Liu 2007; Szapiro and Barbour 2007; Waxman et al. 2007). Glutamate spillover is defined as the escape of glutamate from the synapse into which it is released to neighboring, quiescent synapses thereby activating receptors (Diamond 2002). Thus, our spillover model (Mitchell et al. 2007a) includes both a

glutamate diffusion model to provide time-dependent glutamate concentration and an NMDA-R kinetic model to produce time-dependent receptor open probabilities. Many different kinetic models have been proposed for NMDA-Rs, two of which include the 5-state Lester and Jahr (1992) model and the 8-state Banke and Traynelis (2003) model. At first appearance, it would seem plausible and it has therefore been suggested that in the case of glutamate spillover, the type of NMDA-R model implemented is unimportant. The work presented here examines this supposition to determine the implications of NMDA-R kinetics based on a relational analysis of model behavior (i.e. an analysis of the inherent relationships exhibited by a model, independent of output values). Specifically, we address the question "Is matching output sufficient to declare that different internal mechanisms are functionally the same?"

Degeneracy (i.e. the ability of elements that are structurally different to perform the same function), is a prominent property of many biological systems, including neural networks (Price and Friston 2002; Tononi et al. 1999) and is thought to increase the system's robustness (Csete and Doyle 2002). Just as degeneracy is present in real biological systems, it is also present in computational models (Marder and Prinz 2002) in that often two mechanistically different models can often produce the same output. However, like the physiology that the models represent, producing the same output at a single functional point of assessment may not equate to the models actually being the same.

Here we explore degeneracy in the context of spillover using a "search-survey-and-summarize" strategy to perform a model relational analysis to compare the more complex

BT NMDA-R model to the simpler LJ NMDA-R model. Our approach consists of performing multiple automated parameter searches ("search"), parameter sensitivity and multivariate correlation analyses ("survey"), and population statistics ("summarize") to obtain a landscape of the model based on output relationships. Our data indicate that this landscape can reveal inherent output relationship differences in models whose outputs would otherwise be considered the same.

Methods

The cerebellar glomerulus glutamate spillover model employed here (Mitchell et al. 2007a) consists of the Saftenku glutamate diffusion model (Saftenku 2005) and an NMDA-R kinetic model, either the Banke and Traynelis (2003) or the Lester and Jahr (1992) model. The glutamate concentration profile produced by the diffusion model is fed into the NMDA-R kinetic model to obtain an open probability profile. We utilize 10 outputs that describe the glutamate diffusion and open probability profiles (Table 1). Metrics 3-4 and 8-10 correspond to outputs derived from the glutamate concentration ([Glu]) profiles, which are only dependent upon the diffusion model, while metrics 1-2 and 5-7 are derived from the open probability (Po) profiles, which are functions of both the diffusion and NMDA-R models. The output values in Table 1 are deemed the "target" output values, or simply the target, because they are the output values of the previously published physiological base case cerebellar glomerulus glutamate spillover model (Mitchell et al. 2007a).

Table 7.2.1. *Target output values.*

No.	Output Metric	Value
1	Peak open probability	0.24
2	Half-peak open probability	0.12
3	Peak glutamate concentration (μM)	126.0
4	Half-peak glutamate concentration (μM)	65.82
5	Time of peak open probability (ms)	16.47
6	Time of half-peak open probability (ms)	4.22
7	Time of decay half-peak open probability (ms)	99.74
8	Time of peak glutamate concentration	0.37
9	Time of half-peak glutamate concentration (ms)	0.10
10	Time of decay half-peak glutamate concentration (ms)	1.60

Saftenku Cerebellar Glomerulus Glutamate Diffusion Model.

The Saftenku glutamate diffusion model utilizes a cylindrical geometry to represent glutamate diffusion from a point source that includes neighbor synapse contributions and a simple residence time based method for glutamate uptake to represent the transient glutamate concentration at a single neighbor synapse. Glutamate diffuses from the mossy fiber until it is taken out of the glomerulus by the glial sheath which surrounds the mossy fiber. The model has six free parameters: the initial glutamate concentration released from the activated neighbor (C_0), the radius of the mossy fiber (R_{MF}), radius from the center of the mossy fiber to the glial sheath (r_{abs}), the effective diffusion constant (D_{eff}), the release site density (v_s), and the number of NMDA-Rs (R). The diffusion model base parameters are given in Table 2A and are the same as those used in the previously published spillover model (Mitchell et al. 2007a).

Banke and Traynelis NMDA-R model

The Banke and Traynelis (BT) model incorporates two desensitized receptor states and two transition states representing a fast and a slow conformation change. The 2-glutamate bound state, the two transition states, and the activated receptor state comprise a loop (Figure 1B), which allows for two conformational changes to proceed before receptor activation. Each NR2 subunit can independently bind glutamate, and glycine concentration is assumed to be high enough such that the NR1 subunits are saturated. Rate constants are the free parameters and are as denoted in Figure 1B with base values taken as published in ChanneLab (software by Stephen Traynelis) in Table 2B.

Lester and Jahr NMDA-R model

The Lester and Jahr (LJ) model is similar to the Banke and Traynelis model. The key difference is the absence of transition states and presence of only one desensitized state (RA_2d) instead of two (Figure 1A). Rate constants are as illustrated. The base values of the LJ kinetic rate constants are taken from Lester and Jahr (1992) in Table 2C.

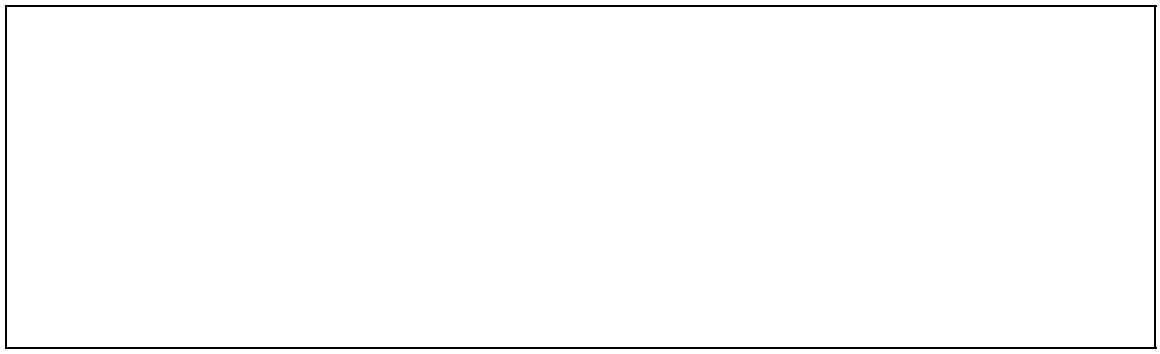

Figure 7.2.1. *Comparison of the LJ and BT NMDA-R Models. A. Lester and Jahr, 1992.* The simpler LJ model contains an unbound receptor, R; 1-glutamate bound state, RA; a 2-glutamate bound state, RA_2; a single desensitized state, RA_2d; and an open state, O. *B. Banke and Traynelis, 2003.* The more complex BT model contains the same states as the LJ model except that there are two desensitized states, RA_2d_1 and RA_2d_2, and two transition states, RA_2s (slow conformation change) and RA_2f (fast conformation change).

Overview of the S^3 Method

As the name implies, the search-survey-and-summarize (S^3) method contains three basic steps: search for a set of parameter values that give rise to the selected target output values (we define each set as a homologue), survey the model output landscape by cross-correlating sensitivity analyses for each homologue, and summarize by statistical analysis of the population of homologue landscapes. The steps of this general method are presented below.

Search

1) Determine a list of model output values to serve as the point of assessment (base case).
2) Segregate parameters into regions of interest (e.g. intrinsic vs extrinsic)

3) Randomly determine a set of starting point parameter values for the search.

4) Perform an initial sensitivity analysis around the starting point

5) Use an optimization method to search for a parameter value set that generates the chosen base case output values (i.e. a homologue to the base case)

Survey

6) Perform a final sensitivity analysis of the homologue.

7) Generate a model output landscape based on a cross-correlation (output vs output) matrix from the sensitivity analysis, to obtain the model output landscape.

Summarize

8) Repeat steps 3-7 to generate additional homologues

9) Examine the variation of the model output landscapes by determining the standard deviation of each point in the matrix across the set of homologues.

10) Perform multi-variate statistics on the population of homologues.

Sensitivity analyses

A sensitivity analysis is performed by varying each parameter individually by a specified amount to measure its effect on the model output values. The sensitivity is defined as the linear relationship of a parameter to its output. We perform sensitivity analyses before and after the search with the final sensitivity analysis being used in the calculation of output cross-correlations for the model output landscape.

Partitioning of parameter set

Parameters are divided into "intrinsic" (parameters that are internal to the NMDA-R model, i.e. the NMDA-R model kinetic rate constants), and "extrinsic" (parameters that are external to the NMDA-R model, i.e. the diffusion model parameters). Note, we use the term "full" to denote to the entire set of parameters (i.e. intrinsic plus extrinsic). Segregating the parameter sets this way allows the contributions of each respective NMDA-R model to be compared separately from the diffusion model.

Automated Parameter Search

Before the two models can be compared, they must be made equivalent in that they must be forced to produce the target output values. To accomplish this, an automated parameter search is used to obtain multiple homologues, parameter value sets that produce the target output values within a specified error set by the convergence criteria. Each homologue produces the same output values using the 10 metrics described previously but from a different parameter value set. For the purposes of the analysis presented here, we obtain multiple homologues by either varying the intrinsic or extrinsic parameters, but not both simultaneously.

The general optimization method is a gradient-based search algorithm that utilizes a modified secant method (Reklaitis et al. 1983) to obtain a set of homologues. The secant method fits a second order polynomial to a function whose x-coordinate consists of the parameter value and the y-coordinate is the corresponding cost function value. The cost function value is defined as the sum of the square of the difference in the "target" output

values to the output values of the homologue generated by the search. The first derivative of the fitted polynomial is used to minimize the cost function over a parameter range. The entire parameter set is optimized by tuning each parameter, one at a time.

The algorithm details are as follows: Initial starting point parameters for the search are randomly determined and allowed to vary +/- 15% from the base values; this range insures good coverage of the parameter space but is still tight enough to allow for good convergence. Since parameters are varied individually, the order of parameter evaluation is randomly determined at the beginning of each search. This insures good coverage of the parameter space so that the search is not biased towards moving the same parameter the same way each time. An initial sensitivity analysis is run to determine the baseline sensitivity and to point the search in the right direction. Six different parameter values which range between +/-10% of the starting point values are evaluated for each parameter for the sensitivity analysis, and those points and their respective cost function values make the polynomial for the first secant minimization. After each secant minimization, the model is re-evaluated, and the new parameter value and its cost function value are included in a new polynomial which is re-fitted and re-minimized; this continues for a maximum of ten secant minimizations. Note that extrinsic parameter search values are bounded by their physiological ranges, approximately +/-50%, and intrinsic parameter searches are bounded by their published experimental standard deviations, approximately +/- 35%. After each parameter is tuned, the parameter set is updated, and a new single-parameter sensitivity analysis is run for the next parameter to be evaluated to start its secant minimizations. This is repeated for all parameters remaining in the parameter set.

Convergence criteria are based on a standard sum of squares cost function with the 10 output metrics. Scaling factors are often used to "weight" certain outputs in the cost function by making the error between the target output value and the search output value appear bigger by multiplying the square of the difference of an individual output value by a scaling factor. For all searches in this work, the cost function weights for all outputs were set to be equal. However, the convergence criteria for the outputs were not equal. The tightest convergence criterion is on peak open probability which is allowed to vary between +/- 3% from the target output value while all other outputs can vary by +/- 5%. However, since the most sensitive output tends to be peak open probability, practically all homologues result in the remaining outputs varying by less than 3%. Regardless, the convergence criteria result in outputs that are qualitatively indistinguishable.

Cross-correlation Matrix

Cross-correlation analysis has been used in applications for DNA fingerprinting (Arnold and Reilly 1998); here we propose cross-correlation analysis as a form of model fingerprinting to obtain the model output landscape. A correlation matrix is a statistical measure that shows the strength of the interrelationships among variables (Hair et al. 2006) or in our case, outputs. Individual correlations can range from +/-1. The sign indicates the direction (positive or negative) of the correlation. The magnitude indicates the strength of the correlation with one being completely correlated and zero completely uncorrelated. The correlation matrix, which forms the landscape, consists of the correlation values obtained by correlating all outputs against one another based on the sensitivity analysis data. Since any given output will correlate perfectly with itself, the

correlation matrix contains a diagonal line of identity and is symmetric along the diagonal axis of the square. Since each homologue can generate such a matrix, the average and standard deviation of each correlation value within the matrix is determined to assess the robustness of the matrix with respect to position within the parameter space.

Output Space Dimensionality

Another means of comparing the model output spaces is to look at the relative size, or dimensionality, of the output space instead of just examining individual outputs. One way to examine dimensionality is using the multi-variate statistical technique, factor analysis. In factor analysis, linear combinations of the original variables (or in this case, model outputs), called factors, are used to represent underlying dimensions. Specifically, we use a form of factor analysis called principal component analysis. Typically the Eigenvalue (sometimes called the latent) of each factor generated by the factor analysis is used to determine the number of dimensions; a plot of each factor's Eigenvalue versus the factor number is called a scree plot. The cut-off for what is "significant" enough to be a dimension is somewhat subjective. Two possible criteria that are commonly used alone or in combination are: 1) All factors whose Eigenvalue is greater than one are counted as dimensions 2) Factors shown to have substantial amounts of common variance (i.e. factors before the inflection point or natural "break" of the scree plot) (Hair et al. 2006) are counted as dimensions.

Implementation

The entire spillover model, automated parameter search, sensitivity analyses, and cross-correlation analysis is implemented and performed in MATLAB R2006b (The MathWorks Inc). Factor analysis is performed in the statistical software program Systat (Systat Software Inc.). Simulations were run on Windows personal computers (Core 2 Duo Intel processor, and 2 GB RAM).

Results

Based on the automated parameter search process, multiple homologues were generated that met the convergence criteria. For our main example, we use four cases that produce the target output values listed in Table 1. Each test case required its own set of searches and resulted in its own set of homologues. These four cases consist of using either the BT or LJ NMDA-R model inside the spillover model and varying either the extrinsic (diffusion model parameters) or intrinsic (NMDA-R rate constants) parameter sets. Approximately 100 searches were run for each test case; the exception was the LJ intrinsic case for which 200 were run due to the low rate of convergence. The convergence rate for the BT and LJ extrinsic models were 95% and 40%, respectively. The intrinsic convergence rates were substantially less, 58% for BT and 7% for LJ. Initially, all homologues were included in the cross-correlation analysis. Bootstrapping, a re-sampling technique that can estimate variance based on an approximating distribution (Efron 1979), was performed in Systat (Systat Software Inc.) to determine the appropriate number of homologues required to construct the correlation matrix; "appropriate" was defined as the number of homologues required such that the no correlation was changed

beyond its standard deviation, approximately less than +/-0.2. The required number of homologues, as determined by bootstrapping, was six. However, we include twelve, randomly chosen, for each landscape presented. The base case parameter values and the maximum, minimum, median and standard deviations are shown for the converged parameter sets in Table 2. Examples of model output using two randomly chosen homologues are shown for both the BT and LJ models in Figure 2. Note how the solutions are qualitatively indistinguishable.

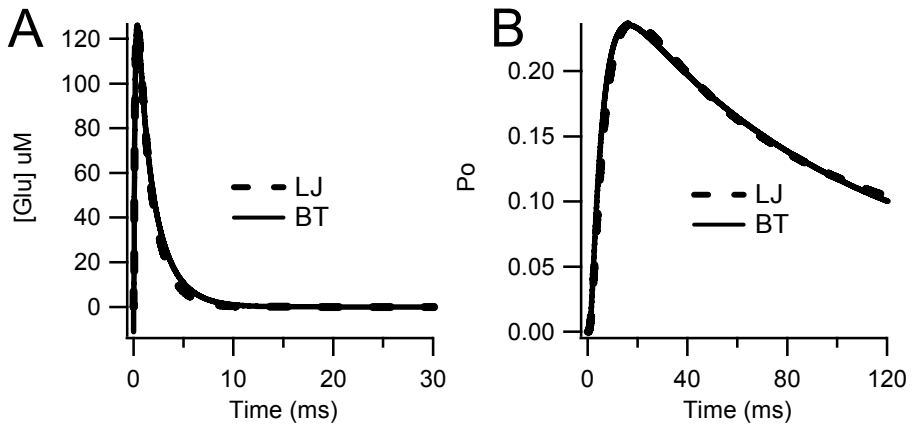

Figure 7.2.2. *Comparison of homologues generated by the parameter search.* These two figures illustrate that the search can find parameter sets that result in qualitatively indistinguishable spillover models outputs using either the LJ or BT NMDA-R models. *A.* Glutamate concentration ([Glu]) profiles. *B.* Open probability profiles (P_o).

Table 7.2.2. *Extrinsic and Intrinsic Parameter Values.* All base values are in parentheses. The maximum (max), minimum (min), median (med), and standard deviation (SD) are given for the converged parameter sets for each case.

A

	BT Extrinsic				LJ Extrinsic			
Extrinsic Parameter	Max	Min	Med	SD	Max	Min	Med	SD
initial concentration (8.77mM), C_0	9.38	7.69	8.66	0.41	10.80	7.85	9.01	0.99
radius from center of mossy fiber to glial sheath (3 um), r_{abs}	3.28	2.92	3.04	0.08	3.13	2.80	2.95	0.11
diffusion constant (0.41 um2/ms), D	0.45	0.38	0.42	0.01	0.48	0.43	0.44	0.02
radius of mossy fiber (1.5 um), R_{MF}	1.64	1.42	1.51	0.05	1.65	1.28	1.50	0.13
receptor number (500), R	915	418	525	69.6	551.9	350	416	75
release site density ($1.5um^{-2}$), v_s	1.84	1.29	1.52	0.09	1.62	1.50	1.57	0.05

B

Intrinsic	BT Intrinsic			
Parameter	Max	Min	Med	SD
k1 ($9.5\ \mu M^{-1}s^{-1}$)	9.42	8.11	9.06	0.45
k2 ($29\ s^{-1}$)	33.82	29.06	30.30	1.67
k3 ($45\ s^{-1}$)	56.88	45.55	49.18	4.22
k4 ($0.5\ s^{-1}$)	0.57	0.45	0.54	0.04
k5 ($70\ s^{-1}$)	73.20	52.13	71.66	8.11
k6 ($2.8\ s^{-1}$)	3.72	2.78	2.94	0.36
k7 ($1557\ s^{-1}$)	2296.24	1557.73	1644.33	257.40
k8 ($182\ s^{-1}$)	236.50	169.21	188.77	21.57
k9 ($89\ s^{-1}$)	99.37	86.36	92.58	4.00
k10 ($135\ s^{-1}$)	141.89	134.91	137.87	2.99

C

Intrinsic	LJ Intrinsic			
Parameter	Max	Min	Med	SD
k1 ($5\ \mu M^{-1}s^{-1}$)	5.10	4.21	4.36	0.17
k2 ($6.6\ s^{-1}$)	7.56	6.19	6.77	0.34
k3 ($15.2\ s^{-1}$)	18.38	8.46	16.21	2.62
k4 (9.4 s-1)	10.87	9.61	10.23	0.40
k5 ($83.8\ s^{-1}$)	92.16	82.38	84.89	2.96
k6 ($83.8\ s^{-1}$)	96.88	81.65	85.66	4.14

Determining model output landscape

We determine the model output landscapes for four different cases (BT extrinsic, LJ extrinsic, BT intrinsic, and LJ intrinsic) which produce the target output values listed in Table 1. The landscapes for the cases where the extrinsic parameters are varied give the full landscape for all ten outputs. Since the NMDA-R model does not change the outputs

associated with glutamate concentration, there are only five outputs which appear in the intrinsic case landscapes and also later in the intrinsic dimensionality assessment. Thus, the landscapes for the cases where intrinsic parameters are varied show only the contribution of the NMDA-R model to the total landscape.

The landscapes for all four cases are presented in Figure 3 along with the landscapes for the full parameter sets . The numbers on the axes identify the outputs based on their given output identification number in Table 1. Looking at each correlation individually, we can gain insight into the inter-relatedness of the outputs. Although there are some characteristic features shared across all cases, there are also some unique features depending on the NMDA-R model (BT vs LJ) and the parameter set varied (extrinsic versus intrinsic). These differences are consistent for each case as shown by the small standard deviation for the BT Extrinsic case (Figure 3E). The standard deviations for each of the cases are quite small and look very similar to the representative example shown in Figure 3G.

Similarities in landscape across partitioned cases

It is immediately noticeable that all the cross-correlation matrices have a wide swath of high cross-correlation near the diagonal line of identity (Figure 3). This structure was imposed by sorting the outputs to group correlated outputs near one another (see table 1 for a listing of the outputs). These "blocks" of correlations represent each of the four main categories of output types that make up the ten output metrics: 1,2-peak open probabilities, 3,4-peak glutamate concentrations, 5,6,7-times of peak open probabilities,

and 8,9,10-times of peak glutamate concentrations. Within these category blocks, the outputs correlate well with one another across all cases. For example, it is evident that 1,2-peak open probabilities correlate well to each other as do 3,4-peak glutamate concentrations.

Differences in landscape across partitioned cases

While some cases look qualitatively similar, there are many quantitative differences between the correlations matrices of the four cases illustrated in Figure 3. These differences are too numerous to list individually. Below we focus on the major differences.

At first glance, the most obvious difference seen between the two models (LJ vs BT) whether varying intrinsic (kinetic parameters) or extrinsic (diffusion parameters), is seen in the cross-correlations involving times of occurrence in open probability (5-time of peak, 6-time of half-peak, and 7-time of decay). The correlations of 5,6-open probability times to 1,2-peak and half-peak open probability are substantial in the LJ-E model compared to the minimal, opposite in sign, correlations seen in the BT-E model. Similarly the second major difference seen between the two models consists of the correlations which relate the 5,6-times of occurrence in open probability to the 8,9-times of occurrence of the peak and half-peak glutamate concentrations. The LJ model has substantially higher correlations for these relationships compared to the BT model, and also notable is that there are differences in the direction, or sign, of the correlation, particularly for the correlations involving 7-time of the decaying half-peak open

probability. Thus, the LJ model tends to have stronger correlations that relate outputs which are dominated exclusively by the diffusion model and the extrinsic parameters while most of the strong correlations seen in the BT model are to outputs that are affected by both the diffusion and NMDA-R model. (Note that unlike the diffusion model, there is no output metric that can be solely attributed to the NMDA-R model itself.)

By dividing the searches into intrinsic and extrinsic parameters, we are able to see which part(s) of the model are contributing where. The spillover model makes an excellent test case for this because there are only two sub-models, the independent diffusion model and the diffusion-dependent NMDA-R model. For example, we can see that the strength of the relationships among 1,2-peak open probabilities, themselves, and between 1,2-peak open probabilities and 5,6,7-times of peak open probabilities is intrinsic to the receptor models and projected from there into the extrinsic parameter correlations.

In the case of the NMDA-R models, it is actually known what the difference between the LJ and BT model is "supposed to be", and we can use this knowledge to test the ability of our S^3 method to find the difference. The motivation for the additional states (2 transition states and an additional desensitized state) in the BT model compared to the LJ model was to better fit the receptor shut times (Banke and Traynelis 2003). Our closest output which would account for shut time is 7-time of the decaying half-peak open probability. In the BT model, there are strong correlations between the 7-time of the decaying half-peak open probability and 5-time of the peak open probability and 6-time of the half-peak open probability. However, in the LJ model the correlation for 7-time of the decaying

half-peak open probability is much stronger with 3-peak glutamate concentration and 4-half-peak glutamate concentration. So, basically, "control" over correlations involving 7-time of the decaying half-peak open probability is shifted from exclusively the diffusion model in the LJ model to both the diffusion and NMDA-R models in the BT case. That is, the BT model is better able to control the time of decaying half-peak open probability, just as it was intended. However, changes in the relationships with 7-time of the decaying half-peak open probability were not the only correlation changes seen in the entire spillover landscape, as previously illustrated. Thus, it can be concluded that the S^3 generated landscape is capable of picking up changes that we would expect to see between the two different NMDA-R model versions as well as changes that we might not expect to see, or at the very least, changes that are not obvious until we "look backwards" after performing the relational analysis.

Partitioned landscapes versus the full landscape

Comparing the four cases to the landscapes for the full parameter set, it can be seen that the effect of extrinsic parameters dominate the full landscapes with the exception of 7-time of peak open probability, which appears to be dominated by the intrinsic parameters.

Other test cases

To test the robustness of the S^3 method, other model variants and simulations using different target output values were used. For brevity and simplicity, the results of these test cases will only be discussed below and not shown.

Just as two mechanistically different NMDA-R models can be distinguished based on landscape, two mechanistically different diffusion models can also be distinguished using model relational analysis. A simplified version of the Saftenku diffusion model, basically a model without glutamate uptake, was compared to the original Saftenku diffusion model using the S^3 method. Since glutamate uptake actually ends up being a critical aspect to the diffusion model, convergence of the no-uptake model to the target output metrics listed in Table 1 was practically negligible. Regardless, the two model landscapes comparing the original Saftenku diffusion model and the no-uptake model were vastly different, as expected.

To test how the functional point of assessment affects the analysis, target output values were chosen such that each output value was within 5% of the original value shown in Table 1. The new output values became the new target for the parameter search. Convergence was less than with the original target output values, but still good, >40% in most cases. The landscapes revealed that models could be differentiated not only based on model type and parameter set varied, but also by there functional point of assessment. That is, models which are analyzed at two different target output values can have two different landscapes; hence, the sensitivities of the outputs can be different at different model operating points. This is also supported by the fact that there is, though small, a standard deviation seen between the sensitivities generated between different homologues as shown in Figure 3G.

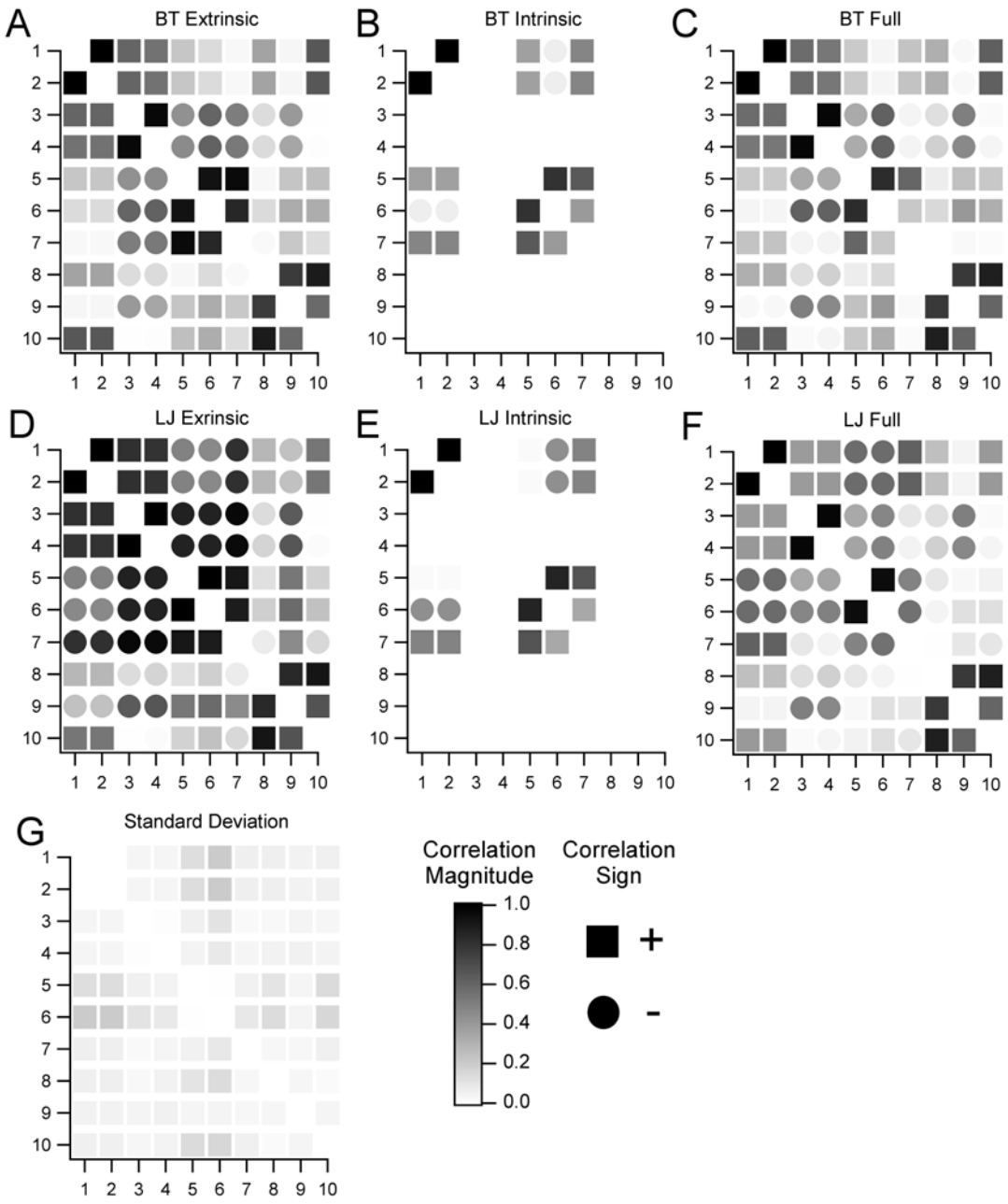

Figure 7.2.3. *Comparison of Model Output Landscapes.* Color intensity represents the correlation magnitude (i.e. darker colors represent stronger correlations) while the shape represents the correlation sign (i.e. squares represent positive correlations and circles represent negative correlations). Note the correlations which lie on the diagonal line of identity (cross-correlations of an output to itself) have been removed for clarity. The numbers on the axes identify the outputs based on their given output identification number in Table 1. *A-C.* Landscapes utilizing the BT NMDA-R model. *D-F.* Landscapes utilizing the LJ NMDA-R model. *G.* Representative standard deviation of a typical spillover model landscape (using the standard deviation of BT Extrinsic as the example).

Output Space Dimensionality

Dimensionality assessment provides a means to compare the size of the output spaces as whole. We compute the output dimensionality of the entire spillover model and the contributions of the diffusion and NMDA-R models by performing factor analysis using Systat (Systat Software Inc.). Several factor rotation methods were tried, but all resulted in approximately the same Eigenvalues, within +/- 0.1. Like the full parameter set cases, the extrinsic cases can have a maximum of ten factors (or dimensions), potentially one factor for every output. The intrinsic cases can only have a maximum of five potential factors, potentially one factor for each of the NMDA-R model outputs (the diffusion model outputs are constant for the intrinsic cases and therefore cannot be included in the factor analysis). Looking at the scree plot it is evident that the extrinsic cases carry an additional dimension compared to the intrinsic cases (Figure 4). Careful comparison of the extrinsic cases to the full parameter sets reveals that the full parameter sets carry about an extra one-half to one dimension (seen in between factors 4 through 6). Thus, it can be concluded that the extrinsic parameter set is contributing most of the dimensionality to the model output space. In fact, the model output space is severely sublinear. That is, the dimensions imposed by the extrinsic parameter set (~ 4) and the intrinsic set (~ 3) are not linearly additive. The full parameter set has only 4.5-5 dimensions instead of 7. Of particular note is the lack of difference in dimensionality between the BT and LJ models for intrinsic, extrinsic or the full parameter sets.

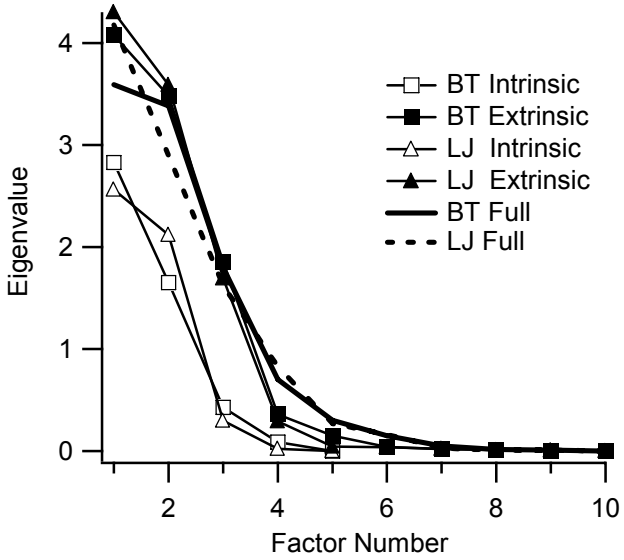

Figure 7.2.4. *Scree plot.* Comparison of factors (or dimensions) for the four different cases.

Discussion

Here we perform a model relational analysis to obtain a model output landscape using the search-survey-and-summarize (S^3) method. Based on the results, the two receptor models, in the context of the larger spillover model, can result in the same overall model output but yield differing sensitivities and therefore different cross-correlations of outputs or landscapes. For the case of spillover, we are able to pick up the subtle differences purposely imposed by the BT NMDA-R model, the ability to improve shut time, as well as other differences, which were not intentional. In fact, utilizing the model output landscape, we were able to differentiate between models that produce the same quantitative output based on: 1) model type (BT versus LJ), 2) parameter set varied

(extrinsic versus intrinsic), and 3) target output values. What does this mean for spillover? The true differences in the NMDA-R models appear benign if only looked at in the context of the NMDA-R models themselves; however, the differences imposed by the NMDA-R model type in the larger, more complex spillover model become very apparent in the landscape. In the case of spillover, the BT model does do what it was intended to do, and it is less reliant on the diffusion model parameters to do so. Thus, in this specific study of spillover at the cerebellar glomerulus either the BT or LJ NMDA-R model could be safely used to simply determine the presence of spillover, but the BT model will give a better picture of what is happening at the mechanistic level without being quite as dependent upon diffusion and geometric parameters. This could be advantageous when spillover analysis moves beyond the well-studied geometry of the cerebellar glomerulus to less known synaptic geometries in the brain.

Applications of model relational analysis

Systems biology has pushed computational models from being reduced to complex and hypothesis driven (Baldi et al. 1998; Lee 2007; Shapiro and Lee 2007). There is an increasing desire to use computational models to reveal deeper understanding into cellular and system organization and interactions and their respective implications (Coveney and Fowler 2005). Thus there is increasing need to balance computational load induced by these large models as well as the need to be able to meaningfully analyze such models where often many of the parameters are unknown.

Previous attempts to characterize models have focused on parameter relationships via careful and methodical tuning of the model (Achard and De Schutter 2006; Prinz et al. 2004; Vanier and Bower 1999). A model analysis that relies solely on parameter relationships has the potential to be somewhat difficult to interpret given the known existence of parameter non-uniqueness (Goldman et al. 2001; Hooper 2004) , i.e. the presence of homologues. Furthermore, not all parameters can be experimentally validated nor is their physiological range always known. Here we propose to analyze models based on their inherent output relationships by exploiting parameter non-uniqueness. We believe model relational analysis using the S^3 method to be advantageous because 1) output relationships can provide a unique, distinguishable landscape and 2) since most model outputs are derived from experimental outputs or metrics, output analysis can be used on model and experimental data as a basis for an additional layer of analysis, comparison, and/or validation.

The ability to distinguish between mechanistically different model implementations solely based on output relationships is a useful tool that opens the door to higher level analysis. There are times when several degenerate models may describe a system, and the "best" model may not always be the "correct" model (Judd and Nakamura 2006). When possible, landscapes to various computational models of a system can be compared to the experimental output landscape (i.e. cross-correlations of experimental outputs) to help decide which model is "best" (fits the data) and "correct" (accurately represents the underlying mechanisms and interactions) for a given system or application. Additionally, landscapes can be used to determine the most appropriate model for the desired

computational load. Modelers can "see" what the difference is between models and decide what differences in landscape are tolerable for a given problem to save on computation time. Finally, it is possible that landscapes could be used to help identify new correlations which can be used to guide further model development or experimental work.

Dimensionality assessment is another potentially useful tool which can be used in conjunction with model output landscapes as part of the model relational analysis. Dimensionality assessment has been employed in various forms in biological science to analyze and categorize different forms of multi-variate data sets (Cangelosi and Goriely 2007; Lin et al. 2003; Ly and Tranchina 2007). The ability to determine how various model interactions and sub-components are contributing to the dimensionality of a system is helpful in understanding complex interactions. For example, we were able to use dimensionality assessment to determine that the majority of output space size is coming from the extrinsic parameter set.

It has been suggested that a simplified model can exhibit dimensional reduction (Gallagher and Appenzeller 1999; Ricard 2006; Teodoro et al. 2003). In the case of the spillover model, the apparent reduction from 7 to about 4.5 dimensions noted in Figure 4 would seem to support this assertion. However, it is difficult to see the reduction in dimensionality from the slightly more complex BT model compared to the slightly simpler LJ model because the models are so mechanistically and structurally similar. In contrast, the model output landscape can detect these differences. We suggest that the

dimensionality of the model output space is analogous to the size of the output space while the landscape is analogous to the shape of the model output space. The dimensions imparted by the NMDA-R model have already been collapsed to the point that no difference can be seen between the BT and LJ models and therefore their output spaces remain the same size. However, the shape of the spaces is different, and this difference is detected by the landscape.

Applications to Degeneracy

As has been discussed previously, there are many reasons why a modeler may desire to differentiate between two different degenerate models. Three common such reason include: 1) to aid in model selection and construction 2) to balance computational load 3) to validate a mechanistic model implementation. However, what underlies the differences imparted by mechanistically different models? It is likely that the differences seen between two degenerate models are largely a function of the difference in their sensitivities to input parameter sets and parameter values. These differences in sensitivities, which are apparent in the model output landscapes, likely determine the robustness of the model. The model's ability to alter its sensitivities is probably a function of its complexity. More parameters and dimensions (i.e. degrees of freedom) allow the model to adjust to conditions that extend beyond its optimal base case. In essence it can be hypothesized that more complex degenerate models will have larger possible output ranges. The BT model's ability to better control its own properties intrinsically and its higher rate of convergence to multiple target output values supports this hypothesis.

Limitations

As with any form of data analysis, model relational analysis cannot be simply used blindly. If there are not enough model outputs or if there is a "wrong" or "missing" output, model relational analysis may not accurately represent the model. Additionally, intuition must be used as a sanity check in viewing the cross-correlation values in the model output landscape. The landscape is based on cross-correlation coefficients which are a function of output variance; an output that generally always has a small variance (i.e. an output that remains relatively constant) may have an exaggerated correlation coefficient (usually either approximately 1 or 0) that is not representative of model behavior. Alternatives to using cross-correlation coefficients are possible and would involve normalizing regression slopes based on something other than variance (e.g. subjective scaling factors). Finally, as mentioned previously, there are limitations to factor analysis. Factor analysis assumes orthogonality, and there is subjectivity in determining the number of factors.

Acknowledgements

This work is supported by the National Science Foundation IGERT program (DGE-0333411), the NSF Graduate Research Fellowship Program (C.S.M.), and by the Human Brain Project (NINDS, NIMH and NIBIB NS046851).

References

Achard P, De Schutter E (2006) Complex parameter landscape for a complex neuron model. PLoS Comput Biol 2:e94.

Arnold RJ, Reilly JP (1998) Fingerprint matching of E. coli strains with matrix-assisted laser desorption/ionization time-of-flight mass spectrometry of whole cells using a modified correlation approach. Rapid Commun Mass Spectrom 12:630-636.

Baldi P, Vanier MC, Bower JM (1998) On the use of Bayesian methods for evaluating compartmental neural models. Journal of Computational Neuroscience 5:285-314.

Banke TG, Traynelis SF (2003) Activation of NR1/NR2B NMDA receptors. Nat Neurosci 6:144-152.

Cangelosi R, Goriely A (2007) Component retention in principal component analysis with application to cDNA microarray data. Biol Direct 2:2.

Coveney PV, Fowler PW (2005) Modelling biological complexity: a physical scientist's perspective. J R Soc Interface 2:267-280.

Csete ME, Doyle JC (2002) Reverse engineering of biological complexity. Science 295:1664-1669.

Diamond JS (2002) A broad view of glutamate spillover. Nat Neurosci 5:291-292.

DiGregorio DA, Rothman JS, Nielsen TA, Silver RA (2007) Desensitization properties of AMPA receptors at the cerebellar mossy fiber granule cell synapse. J Neurosci 27:8344-8357.

Efron B (1979) 1977 Rietz Lecture - Bootstrap Methods - Another Look at the Jackknife. Annals of Statistics 7:1-26.

Gallagher R, Appenzeller T (1999) Beyond Reductionism. Science 284.

Goldman MS, Golowasch J, Marder E, Abbott LF (2001) Global structure, robustness, and modulation of neuronal models. J Neurosci 21:5229-5238.

Hair J, Black W, Babbin B, Anderson R, Tatham R (2006) Multivariate Data Analysis, 6 Edition: Pearson Prentice Hall.

Hooper SL (2004) Multiple routes to similar network output. Nat Neurosci 7:1287-1288.

Judd K, Nakamura T (2006) Degeneracy of time series models: the best model is not always the correct model. Chaos 16:033105.

Lee EK (2007) Large-scale optimization-based classification models in medicine and biology. Ann Biomed Eng 35:1095-1109.

Lester RA, Jahr CE (1992) NMDA channel behavior depends on agonist affinity. J Neurosci 12:635-643.

Lin FH, McIntosh AR, Agnew JA, Eden GF, Zeffiro TA, Belliveau JW (2003) Multivariate analysis of neuronal interactions in the generalized partial least squares framework: simulations and empirical studies. Neuroimage 20:625-642.

Logan SM, Partridge JG, Matta JA, Buonanno A, Vicini S (2007) Long-lasting NMDA receptor-mediated EPSCs in mouse striatal medium spiny neurons. J Neurophysiol.

Ly C, Tranchina D (2007) Critical analysis of dimension reduction by a moment closure method in a population density approach to neural network modeling. Neural Comput 19:2032-2092.

Marcaggi P, Attwell D (2007) Short- and long-term depression of rat cerebellar parallel fibre synaptic transmission mediated by synaptic crosstalk. J Physiol 578:545-550.

Marder E, Prinz AA (2002) Modeling stability in neuron and network function: the role of activity in homeostasis. Bioessays 24:1145-1154.

Mitchell CS, Feng SS, Lee RH (2007) An analysis of glutamate spillover on the N-methyl-D-aspartate receptors at the cerebellar glomerulus. Journal of Neural Engineering 4:276-282.

Price CJ, Friston KJ (2002) Degeneracy and cognitive anatomy. Trends Cogn Sci 6:416-421.

Prinz AA, Bucher D, Marder E (2004) Similar network activity from disparate circuit parameters. Nat Neurosci 7:1345-1352.

Reklaitis G, Ravindran A, Ragsdell K (1983) Engineering Optimization: Methods and Applications: John Wiley & Sons, Inc.

Ricard J (2006) Emergent collective properties, networks, and information in biology.: Elsevier.

Saftenku EE (2005) Modeling of slow glutamate diffusion and AMPA receptor activation in the cerebellar glomerulus. J Theor Biol 234:363-382.

Sargent PB, Saviane C, Nielsen TA, DiGregorio DA, Silver RA (2005) Rapid vesicular release, quantal variability, and spillover contribute to the precision and reliability of transmission at a glomerular synapse. J Neurosci 25:8173-8187.

Shapiro NP, Lee RH (2007) Synaptic amplification versus bistability in motoneuron dendritic processing: a top-down modeling approach. J Neurophysiol 97:3948-3960.

Sun L, June Liu S (2007) Activation of extrasynaptic NMDA receptors induces a PKC-dependent switch in AMPA receptor subtypes in mouse cerebellar stellate cells. J Physiol 583:537-553.

Szapiro G, Barbour B (2007) Multiple climbing fibers signal to molecular layer interneurons exclusively via glutamate spillover. Nat Neurosci 10:735-742.

Teodoro ML, Phillips GN, Jr., Kavraki LE (2003) Understanding protein flexibility through dimensionality reduction. J Comput Biol 10:617-634.

Tononi G, Sporns O, Edelman GM (1999) Measures of degeneracy and redundancy in biological networks. Proc Natl Acad Sci U S A 96:3257-3262.

Vanier MC, Bower JM (1999) A comparative survey of automated parameter-search methods for compartmental neural models. Journal of Computational Neuroscience 7:149-171.

Waxman EA, Baconguis I, Lynch DR, Robinson MB (2007) N-methyl-D-aspartate receptor-dependent regulation of the glutamate transporter excitatory amino acid carrier 1. J Biol Chem 282:17594-17607.

CHAPTER 8

SPINAL CORD INJURY

In addition to being an amenable test case to our set of complex system-based analytical techniques, referred to as relational analysis, secondary SCI is a system that was ideally suited for the development and implementation of our complex-systems based modeling technique, referred to as relational modeling. Typical of most pathologies, no comprehensive computational model of secondary SCI had previously existed. The under-utilization of models in pathologies like SCI directly corresponds to both our lack of understanding of pathologies and the lack of detailed information that is typically required to make traditional mechanistic computational models. However, in the case of secondary SCI, where detailed experimental research of several individuated factors or mechanistic concepts has yet to translate into reliable and predictable clinical therapies (Hall and Springer, 2004) and where numerous possibilities for additional research and combinations of therapeutic trials seems infinite (Faden and Stoica, 2007), the empowering ability of a computational model as an exploratory tool to predict and prioritize was quite needed.

In this published study (Mitchell and Lee, 2008) the relational modeling methodology is developed and implemented to produce a comprehensive computational model of secondary SCI by simply aggregating and translating experimental literature-derived relationships or correlations into a network of time-varying factors. This network

exhibits the same output relationships and dynamics of the real system and provides a means or test bed by which comprehensive mechanistic and therapeutic theories can be identified, explored, and analyzed. Using the relational modeling methodology of review-relate-refine, we successfully developed the first comprehensive model of SCI, which recapitulated the findings of over 250 experimental papers. Using relational analysis to analyze the underlying dynamics and relationships illustrated within the model landscape, we were able to generate novel mechanistic, dynamical, and therapeutic insights (Mitchell and Lee 2008). The results of this study challenge pre-existing hypotheses surrounding the pathology dynamics of SCI and the subsequent therapeutic direction of the SCI field. Our quantitative assessment of thousands of potential therapeutic strategies has resulted in new and exciting ideas for potential therapeutic alternatives. As such this initial relational model serves as a "scaffold" from which further relational, conceptual or mechanistic modeling can be used to investigate areas of interest in more detail. The papers "Pathology dynamics predict spinal cord injury therapeutic success" as published in the *Journal of Neurotrauma* 25(12): 1483-1497 is presented in its entirety (Mitchell and Lee, 2008).

Background: Secondary Spinal Cord Injury

The spinal cord serves as a conduit for over 13 million neurons, which directly conduct signals from the brain to the rest of the body (Kandel et al, 2000). Spinal cord injury can result in a devastating loss of function below the level of insult, including the inability to breathe (in upper level C1-C3 cervical injuries), the loss of sensation, the loss of voluntary motor control, and the loss of bladder and bowel control, to name just a few of

the primary consequences. To date, despite promising in vitro and in vivo experimental studies, there are no effective and reliable therapies to directly address the neural damage and subsequent functional losses associated with SCI (Hall and Springer, 2004). With over 11,000 new injuries each year in the United States alone that result in these aforementioned catastrophic clinical consequences (according to the 2008 National Spinal Cord Injury Database), SCI is both a relevant and significant clinical pathology worthy of further system exploration. Notably, much of the damage associated with SCI occurs post-insult as a result of a complex cellular cascade referred to as "secondary injury" in which the body's own response to the mechanical insult, including the failure of cellular respiration, the accumulation of excitotoxic and free radical factors, the initiation of necrotic-apoptotic cascades, and the activation of the immune system, results in an increase in lesion size over the following weeks and months (Schwab, 1996; Park, 2004). This increase in lesion size can have perilous effects on the outcome of SCI that results in the accumulation of additional permanent losses (Hall and Springer, 2004; Schwab, 2006). The large number of interactions among these pathological factors across multiple physiological and time scales makes both the experimental and theoretical characterization and examination of secondary injury as a whole extremely difficult. However, such an interactive and truly complex biological system is the ideal test case for employing complex systems-based analytical methods.

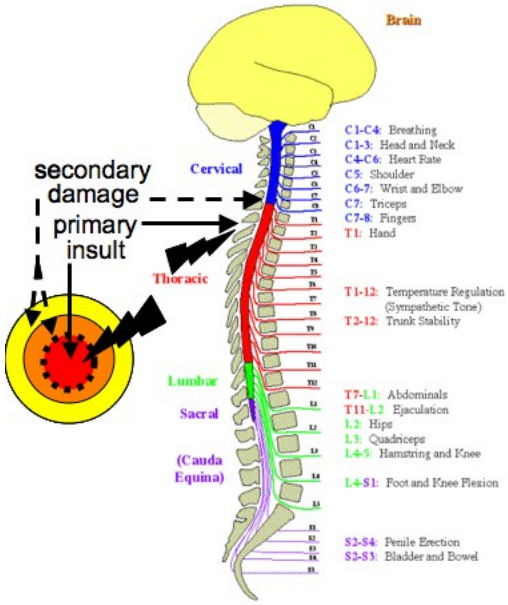

Figure 8.0.1. Propagation of Spinal Cord Injury. The figure illustrates SCI lesion expansion from the initial primary mechanical or traumatic insult due to "secondary injury", damage that is initiated from within the cellular environment of the primary injury. Secondary injury can expand a couple of vertebrae above and/or below the primary insult, resulting in additional sensory and/or functional losses. Image credit: the brain and cord figure is adapted from IC Irvine Reeve-Irvine Research Center. Anatomy 101: Spinal Cord and Central Nervous System. Website: www.reeve.uci.edu/anatomy/images/scns_1b.gif Downloaded on1/19/2009.

Pathology Dynamics Predict Spinal Cord Injury Therapeutic Success

Journal of Neurotrauma 25(12):1483-1487

doi:10.1089/neu.2008.0658

http://www.liebertonline.com/doi/abs/10.1089/neu.2008.0658

Contributions of the authors:

Cassie Mitchell was responsible for the ideological development, application, and implementation of the relational modeling technique of review-relate-refine; performed the literature review, created the literature database, and extracted the qualitative and quantitative relationships used as model parameters; developed and implemented the SCI model; performed the simulation and analysis of the SCI model; and wrote the manuscript. Dr. Robert Lee contributed to the ideological development of the relational modeling methodology, provided invaluable insight and assistance into the dynamical analysis including the creation of the "fire-flood" dynamical analogy, created all of the illustrations/figures, and co-edited the paper.

Abstract

(Secondary injury, the complex cascade of cellular events following spinal cord injury (SCI), is a major source of post-insult neuron death. Experimental work has focused on the details of individual factors or mechanisms that contribute to secondary injury, but

little is known about the interactions among factors leading to the overall pathology dynamics that underlie its propagation. Prior hypotheses suggest the pathology is dominated by interactions, with therapeutic success lying in combinations of neuroprotective treatments. In this study, we provide the first comprehensive, system-level characterization of the entire secondary injury process using a novel *relational model* methodology that aggregates the findings of ~250 experimental studies. Our quantitative examination of the overall pathology dynamics suggests that while the pathology is initially dominated by "fire-like", rate-dependent interactions, it quickly switches to a "flood-like", accumulation-dependent process with contributing factors being largely independent. Our evaluation of ~20,000 potential single and combinatorial treatments indicates this flood-like pathology results in few highly influential factors at clinically realistic treatment time frames with multi-factor treatments being merely additive rather than synergistic in reducing neuron death. Our findings give new fundamental insight into the understanding of the secondary injury pathology as a whole, provide direction for alternative therapeutic strategies, and suggest that ultimate success in treating SCI lies in the pursuit of pathology dynamics in addition to individually involved factors.

Key Words

Secondary insult, spinal cord injury, traumatic brain injury, combination therapy, neuroprotection, therapeutic treatment window

Introduction

Despite their promise, translating in-vitro and in-vivo experimental SCI treatments into effective and repeatable clinical therapies has been problematic (Blight and Tuszynski 2006; Faden and Stoica 2007; Hall and Springer 2004). It is therefore often concluded that the progression of neuronal death in secondary injury must be dominated by complex interactions, rather than any given single factor, and that the solution must therefore lie in multi-faceted treatments aimed at simultaneously targeting several secondary injury factors (Faden and Stoica 2007; Hall and Springer 2004). However, the overall dynamics of the processes underlying the pathology remain unknown.

At a conceptual level, the secondary injury process is often thought to behave like a forest fire. That is, a propagating wave of death that results in a slowly expanding lesion, driven by multiple factors, often referred to as the necrotic-apoptotic continuum (PorteraCailliau et al. 1997). Thus, the assumption is that a critical intervention in one or more factors might arrest the propagation, thereby preventing subsequent damage. The most commonly pursued secondary injury factors can be categorized into excitotoxic, energetic, inflammatory, "necro-apoptotic", and free radical. The excitotoxic factors arise from a cascade originating from the initial mechanical insult, leading to the direct disruption of ion gradients (e.g. sodium, calcium) and the escape of neurotransmitters such as glutamate (Agrawal and Fehlings 1996; Park et al. 2004; Schwab and Bartholdi 1996). These effects, in turn, cause activation of metabotropic and ionotropic receptors, further increasing external glutamate and internal calcium concentrations, thereby perpetuating the excitotoxic response (Agrawal and Fehlings 1997; Park et al. 2004).

Energetic factors arise from the cell's attempt to maintain homeostasis in the face of the above cascade (Ahmed et al. 2002). Thus, cellular respiration falls off as mitochondrial dysfunction occurs (Sullivan et al. 2007) and local ATP concentrations decrease (Anderson et al. 1980), compromising the cell's energy supply (Sullivan et al. 2007) and hampering the ability of ionic pumping mechanisms, such as the Na-K-ATPase transporter (Faden et al. 1987; Li and Stys 2001), to restore ionic homeostasis. Free radical factors, including nitric oxide (NO) (Hamada et al. 1996; Merrill et al. 1993) and reactive oxygen species (ROS) (Hall and Braughler 1993), accumulate, damaging DNA. Necro-apoptotic (i.e. necrotic and apoptotic) factors arise from these damaged cells as well as those with increased membrane permeability (Farkas et al. 2006; Shi and Whitebone 2006) from membrane damage. Cells that do not die necrotically initiate apoptotic cascades (Crowe et al. 1997; Lu et al. 2000) via caspase and calpain activation (Crowe et al. 1997). Inflammatory factors are activated (Beattie 2004; Dusart and Schwab 1994), including microglia (Gomes-Leal et al. 2004; Merrill et al. 1993), macrophages (Giulian and Robertson 1990) and astrocytes (O'Brien et al. 1994), resulting in the production of pro-inflammatory cytokines (Bartholdi and Schwab 1997; Klusman and Schwab 1997; Pineau and Lacroix 2007). Other secondary injury factors include demyelination (Totoiu and Keirstead 2005), oligodendrocyte death (Crowe et al. 1997), and axon damage (Shi and Whitebone 2006).

Experimental investigation of individual secondary injury factors has resulted in a substantial, yet disparate pool of single factor data, making the interpretation of multi-factor effects difficult. Recently, we have developed a methodology (Mitchell and Lee

2007) that greatly facilitates pooling disparate data, enabling a novel, comprehensive view into the pathology of secondary injury across time points, preparations, and protocols. We developed a system-wide *relational model* of secondary injury by aggregating the relevant relationships between factors commonly believed to be involved in the progression of secondary injury from over 250 experimental papers. This relational model represents a comprehensive view of the progression of neuron death following mechanical insult by directly incorporating the literature-derived experimental relationships into a network of time-varying factors. Thus, the dynamics of the entire secondary injury process, including potential treatments, can be quantitatively examined. This systems-based relational modeling approach encompasses and recapitulates experimental data without having to assume the detailed and cumbersome mathematics of numerous unknown mechanisms.

Methods

General strategy

The secondary injury model is characterized as a *relational model* (see **Figure 1a**), which uses intrinsic relationships identified in the experimental data to aggregate and recapitulate the findings of hundreds of experimental findings to make predictions regarding pathology dynamics and interactions over time. Based on over 250 research articles, we constructed a 20-output, 26-differential equation, 85-relationship system that transformed the individual experimentally derived relationships into a model that exhibited the known behaviors of secondary injury in the spinal cord.

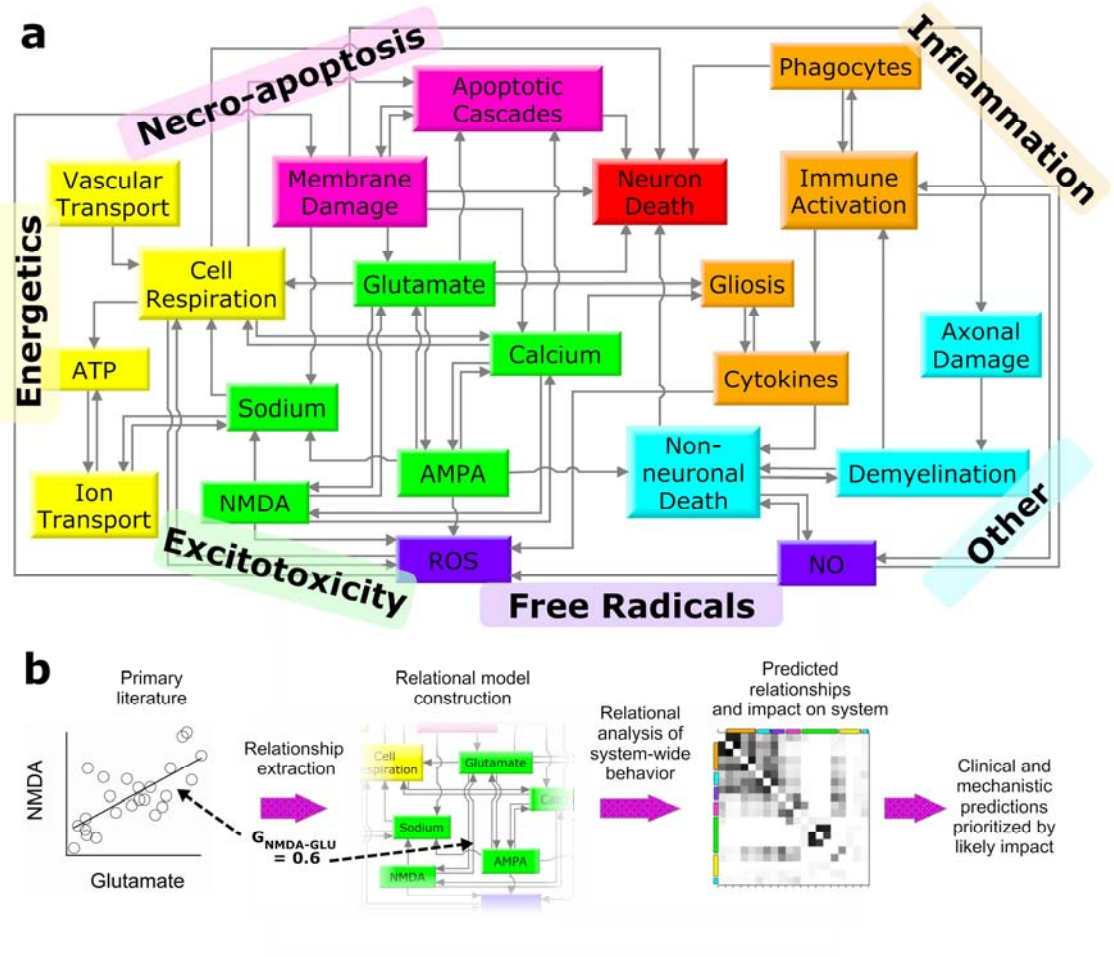

Figure 8.1.1. Comprehensive pathology of secondary injury post-SCI. **(a)** The diagram represents the structure of the relational model, which is an embodiment of the published literature. The model permits cross-factor examination of the pathology and treatment responses of the secondary injury process. Boxes represent tracked factors in the model. Categories of factors (shown in differing colors) represent established theories from the literature regarding secondary injury: necro-apoptosis, energetics, excitotoxicity, free radicals, inflammation, and other. **(b)** The figure illustrates how the extraction of experimental relationships results in a relational model capable of making clinical and mechanistic predictions. Each arrow in Figure 1a represents an experimentally derived relationship or "gain", which is extracted from the experimental relationship between 2 factors. Altogether, these gains are used to form the relational model's differential equations, which transcribe the relationships into a network of time-varying factors.

The general relational modeling strategy utilizes the review-relate-refine technique as summarized in **Table 1**: review the literature to identify pertinent factors, relate the factors into a map transcribing a system of differential equations, and refine the model to meet validation criteria. Specific methodological and analytical details central to the secondary injury relational model are outlined in the sections of text below. As an aid to the reader, **Table 2** summarizes pertinent terminology used to convey dynamical concepts, methodology, illustrations, and treatments, which appear throughout this article.

Table 8.1.1. Relational modeling technique: Review-Relate-Refine.

Review
1) Determine criteria for primary literature reference inclusion.
2) Determine a base list of references and system factors for inclusion
3) Record references, categorized by factor, in an annotated database.
4) Expand scope of literature base manual searches. Record new or additional factors.
Relate
5) Devise a "map" that illustrates how identified factors are related. Include relevant system output(s).
6) For each 2-way relationship, extract a value from the literature that quantitatively describes the relationship (e.g a gain).
7) Translate the map into a system of equations
Refine
8) Validate using experimental data
9) Repeat steps 3-7 for areas that need improvement

Table 8.1.2. Glossary of terminology used to describe dynamical concepts, methodology, illustrations, and treatments. Note that the treatment portion of Table 8.1.2 is continued on the next page.

Dynamical Concepts	
fire	Describes rate-dependent dynamics in which a high degree of interaction between factors drives the propagation of the secondary injury process.
flood	Describes accumulation-dependent dynamics in which the accumulation of independent factors drives the propagation of the secondary injury process.
Methodology	
relational model	Aggregates multiple 2-way experimental relationships at discrete time points to predict the interactions and dynamics of all involved factors over a continuous time frame.
relational analysis	Set of analytical techniques that evaluates and subsequently uses the relationships among parameters, variables, and especially model outputs to hypothesize process dynamics, mechanisms, and/or functions (for details see (Mitchell and Lee, 2007).
factor	Quantifiable entity or output that has a measurable impact on the process outcome.
factor category	Set of factors, which have been grouped together as 'similar' by scientists in the field, based on their function, mechanism, or impact on process outcome.
factor gain	Value that quantitatively specifies the one-way impact of an inter-related or interacting factor.
factor time constant	Calculated using the factor peak value over its experimentally measured range and used to form the factor's differential equation.
Dynamics Illustration	
landscape	Matrix of correlations, which quantifies the inter-relatedness of model outputs (or factors) and is representative of their degree of interaction (i.e. a measure of 'fire'.)
pathology diagram	A map/survey of the overall system operation, including the changes in factor size, impact, and "flow" (i.e. a measure of accumulation).

Table 8.1.2 (continued)

Treatments	
reducing treatment	Targets factor accumulation by reducing the existing factor (e.g. a free radical scavenger actively reduces existing free radicals)
inhibiting treatment	Targets the interactions by inhibiting formation of a factor (e.g a free radical anti-oxidant inhibits the formation of free radicals).
single [factor] treatment	A single treatment, either reducing or inhibiting, applied independently to target one factor.
combination treatment	An *n*-number of inhibiting or reducing treatments given in combination targeting *n*-number different factors.

Derivation of equations

Differential equations are of the standard Euler form. The derivative for each factor at each time step is calculated using its relationships to the other factors and then integrated numerically. Every arrow pointing to a specific factor in Figure 1 represents a relationship between the two factors (see **Figure 1b** for illustration of extraction method). For example, NMDA activation is mediated by calcium and glutamate. The relationships between factors are taken or measured from the experimental data, and are effectively linear gains denoted by 'G' (**Table 3**). Similarly, time constants for each factor, denoted by τ, are calculated from experimental data and represent the time constants for the acute and sub-acute secondary injury periods (**Table 4**). Therefore, for our example with NMDA we have:

$$NMDA_{\text{expected}} = G_{NMDA-Glu} \cdot Glu + G_{NMDA-Ca} \cdot Ca \qquad \textbf{Equation 8.1.1}$$

$$\frac{dNMDA}{dt} = \frac{NMDA_{\text{expected}} - NMDA_{\text{previous}}}{\tau_{NMDA}} \qquad \textbf{Equation 8.1.2}$$

The one non-linear exception to the form of Equation 1 is for the factor ATP, (Equation 3) which reflects the production of ATP by the mitochondria and the consumption of ATP by the Na-K-ATPase pump. However, the Euler differential equation still has the same form as the other factors as shown in Equation 2.

$$ATP_{\text{expected}} = 1 \Big/ \left(G_{ATP-Mito} \cdot Mito + G_{ATP-NaKATPase} \cdot NaKATPase \right) \qquad \textbf{Equation 8.1.3}$$

The model was split into two parts to better mathematically represent the fast or "acute" period (<1 hour after injury) and slow or "sub-acute" (>1 and < 16 hours after injury). The acute and sub-acute parts each have their own time constants (**Table 4**) to represent the changing dynamics seen experimentally between these two time periods. However, depending on a factor's split dynamics, it may only exhibit substantive changes in one period or the other. For a validated comparison between simulated factor values and experimental data, see **Table 5.** Note that by splitting the time constants into smaller time frames, the relationship equations, like Equation 1, can be safely approximated as piece-wise linear. However, this linear approximation does not specify that the resulting trajectories of factor values be linear, as shown in the Results in Figure 2.

Table 8.1.3. Table of model gains for the calculation of secondary injury factors. How to read the table: Each gain represents the relationship between two factors as shown in Figure 1. The first part of the hyphenated gain name states the name of the factor being calculated while the second part of the gain name states the influencing factor that the gain relates. See main text (equation 1) for the example with NMDA. A. Energetic gains. B. Excitotoxicity. C. Inflammation. D. Free radical. E. Necro-apoptotic. F. Other.

Table 8.1.3A. Energetics

Gain	Value	Reference	Invitro	Invivo	TBI	SCI	Other
ATP-Mitochondria	0.40	(Nicholls and Budd 2000)			x	x	
ATP-NaKATPaseFactor	1.00	(Green and Kroemer 1998)			x	x	
Blood-Blood	0.50	(Yanase et al. 1995)		x		x	
Glucose-Blood	0.50	(Anderson et al. 1980)		x		x	
Mitochondria-Calcium	0.10	(White and Reynolds 1996)	x			x	
Mitochondria-Glutamate	0.15	(Ankarcrona et al. 1995)	x		x		
Mitochondria-ROS	0.05	(Azbill et al. 1997)		x		x	
Mitochondria-Sodium	0.40	(Iwai et al. 2002)	x				x

Table 8.1.3B. Excitotoxicity

Gain	Value	Reference	Invitro	Invivo	TBI	SCI	Other
AMPA-Calcium	0.10	(Yanase et al. 1995)		x		x	
AMPA-Glutamate	0.55	(Saftenku 2005)					x
Calcium-AMPA	0.23	(Carriedo et al. 1998)	x		x		
Calcium-Calcium(uptake)	-3.50	(Wingrave et al. 2003)		x		x	
Calcium-Mitochondria	1.50	(Wingrave et al. 2003)		x		x	
Calcium-NMDA	0.28	(Carriedo et al. 1998)	x		x		
Calcium-Membrane Damage	0.25	(Yoshioka et al. 1996)	x		x	x	
Glutamate-AMPA	1.10	(Saftenku 2005)					x
Glutamate-Glutamate(uptake)	-3.50	(Xu et al. 2004)		x		x	

Table 8.1.3B (Continued) Excitotoxicity

Gain	Value	Reference	Invitro	Invivo	TBI	SCI	Other
Glutamate-NMDA	1.30	(Mitchell et al. 2007)					x
Glutamate-Membrane Damage	0.25	(LaPlaca and Thibault 1998)	x		x		
Glutamate-ROS	0.02	(Volterra et al. 1994)	x		x		
NMDA-Calcium	0.10	(Zhang et al. 1996)	x		x		
NMDA-Glutamate	0.60	(Mitchell et al. 2007)					x
Sodium-AMPA	1.10	(Agrawal and Fehlings 1996)	x			x	
Sodium-NaKATPase	1.00	(Agrawal and Fehlings 1996)	x			x	
Sodium-NMDA	1.30	(Agrawal and Fehlings 1996)	x			x	
Sodium-Membrane Damage	0.10	(Schwartz and Fehlings 2001)		x		x	

Table 8.1.3C. Inflammation

Gain	Value	Reference	Invitro	Invivo	TBI	SCI	Other
Astrocyte-Calcium	0.30	(Schnell et al. 1999)		x	x	x	
Astrocyte-Cytokine	2.00	(Gomes-Leal et al. 2004)		x		x	
Astrocyte-Glutamate	0.50	(Schnell et al. 1999)		x	x	x	
Cytokine-Astrocyte	1.20	(Klusman and Schwab 1997)		x		x	
Cytokine-Microglia	2.00	(Klusman and Schwab 1997)		x		x	
Macrophage-Microglia	4.50	(Tian et al. 2007)		x		x	
Microglia-Demyelination	0.33	(Blight 1985)		x		x	
Microglia-Macrophage	0.30	(Dusart and Schwab 1994)		x		x	
Microglia-NO	0.20	(Zhao et al. 2004)	x				x
Sodium-NaKATPase	1.00	(Agrawal and Fehlings 1996)	x			x	

Table 8.1.3D. Free Radicals

Gain	Value	Reference	Invitro	Invivo	TBI	SCI	Other
NO-Microglia	0.27	(Merrill et al. 1993)	x				x
NO-Oligodendrocyte	0.57	(Zhao et al. 2004)	x				x
ROS-AMPA	2.50	(Carriedo et al. 1998)	x		x		
ROS-Cytokine	0.40	(Hu et al. 1997)	x		x	x	
ROS-Mitochondria	0.20	(Azbill et al. 1997)		x		x	
ROS-NMDA	2.00	(Carriedo et al. 1998)	x		x		
ROS-NO	0.10	(Mattiasson 2004)	x				x

Table 8.1.3E. Necro-apoptosis

Gain	Value	Reference	Invitro	Invivo	TBI	SCI	Other
Caspase-Calcium	2.00	(Wingrave et al. 2003)		x		x	
Caspase-Glutamate	0.20	(Liu et al. 1999)		x		x	
Caspase-Mitochondria	0.20	(Krajewski et al. 1999)	x	x	x		
Caspase-Membrane Damage	1.00	Kacy Cullen, PhD and Michelle LaPlaca, PhD (unpublished data)	x		x		
Neuron-Caspase Factor	2.43	(Hartmann et al. 2000)		x			x
Neuron-Macrophage	2.03	(Tian et al. 2007)		x		x	
Neuron-Mitochondria	0.16	(Sullivan et al. 2007)		x		x	
Neuron-Oligodendrocyte	0.27	(Zhao et al. 2004)	x				x
Neuron-Membrane Damage	0.81	(Cullen and LaPlaca 2006a)	x		x		
Membrane Damage-Caspase	1.00	(Wingrave et al. 2003)		x		x	
Membrane Damage-ROS	1.00	(Mattiasson 2004)	x				x

Table 8.1.3F. Other

Gain	Value	Reference	Invitro	Invivo	TBI	SCI	Other
Axon-Microtubule	2.00	(Pettus and Povlishock 1996)	x		x		
Axon-Neurofilament	2.00	(Pettus and Povlishock 1996)	x		x		
Axon-Membrane Damage	0.20	(Pettus and Povlishock 1996)	x		x		
Demyelination-Axon	0.30	(Lovas et al. 2000)		x			x
Demyelination-Oligodendrocyte	3.00	(Kandel et al. 2000)					x
Neuron-Glutamate	0.09	(Ankarcrona et al. 1995)	x		x		
Oligodendrocyte-AMPA	0.89	(Yoshioka et al. 1996)	x		x	x	
Oligodendrocyte-Cytokine	0.50	(Louis et al. 1993)	x				x
Oligodendrocyte-Demyelination	0.20	(Yoshioka et al. 1996)	x		x	x	
Oligodendrocyte-NO	0.10	(Merrill et al. 1993)	x				x

Table 8.1.4. Time constants used in the model. Fast time constants are used for the acute (<=1 hr post-insult) and slow time constants are used for the sub-acute period (> 1 hr and < 16 hr).

Factor	Fast (hrs)	Slow (hrs)	Reference	Invitro	Invivo	TBI	SCI
NMDA Activation	0.33	3.35	(Zhang et al. 1996)	x		x	
AMPA Activation	0.33	3.35	(Goforth et al. 2004)	x		x	
NaKATPase Transporter	0.67	24.00	(Faden et al. 1987)		x		x
			(Anderson et al. 1980)		x		x
Reactive Oxygen Species (ROS)	2.5	24.0	(Hall and Braughler 1993)				x
			(Hamada et al. 1996)		x		x
Glutamate Concentration	0.22	3.35	(Xu et al. 2004)		x		x
			(Liu et al. 1999)		x		x
			(LaPlaca and Thibault 1998)	x		x	
Calcium Concentration	0.22	3.35					
Sodium Concentration	1.00	24.00	(Lemke et al. 1987)		x		x
			(Fehlings and Agrawal 1995)	x			x
Mitochondria Dysfunction	1.00	24.00	(Alano et al. 2002)	x		x	
ATP Concentration	0.67	24.00	(Anderson et al. 1980)		x		x
Membrane Damage	0.67	24.00	(Shi and Whitebone 2006)		x		x
			(Cullen and LaPlaca 2006b)	x		x	
			(Barut et al. 2005)		x		x
Microglia Activation	--	4.00	(Dusart and Schwab 1994)		x		x
			(Carlson et al. 1998)		x		x
			(Vela et al. 2002)		x	x	
Cytokine Concentration	--	12.00	(Pineau and Lacroix 2007)		x		x
			(Klusman and Schwab 1997)		x		x

Table 8.1.4. (continued)

Factor	Fast (hrs)	Slow (hrs)	Reference	Invitro	Invivo	TBI	SCI
Astrocyte Activation	6.7	5.00	(O'Brien et al. 1994)		x		x
Macrophage Activation	--	5.00	(Carlson et al. 1998)		x		x
			(Vela et al. 2002)		x	x	
			(Fleming et al. 2006)		x		x
Oligodendrocyte Death	--	12.00	(Crowe et al. 1997)		x		x
			(Totoiu and Keirstead				
Demyelination	--	24.00	2005)		x		x
Nitric Oxide (NO)	--	8.00	(Xiong et al. 2007)		x		x
Caspase Activation	5.4	24.00	(Springer et al. 1999)		x		x
			(Pettus and Povlishock				
Axonal Damage	--	12.00	1996)		x	x	
Neuron Death	1.4	12.00	(Gaviria et al. 2006)		x		x
		24.00	(Fujiki et al. 2005)		x		x

Table 8.1.5. *Factor validation comparison to experimental data.* The model is "unitless" in that the model generates factor values that are ratios to the baseline values, with all baseline values (values immediately post-insult) starting at one. For example, a factor value of three means that the factor value is three times the baseline value. References listed in **bold type** indicate primary (i.e. external or independent) validation criteria in which no data from the reference was used to calculate the corresponding validated factor value. References in *italic type* indicate secondary validation criteria from which only time constant information was extracted. Thus, these secondary references had no impact on their corresponding resulting factor relationships. The remaining references in regular type, with the exception of axonal damage, indicate tertiary validation criteria from which the indicated reference was only one of several references that data was extracted from as part of the calculation of the corresponding factor value. Thus, these tertiary references have only a partial role in determining the impact of their listed factor values and resulting relationships. Limitations imposed by the quantity, applicability and extractability of available data make the prediction and validation of axonal transport more difficult than the other factors.

Factor	Model Value	Exp. Value	Time Point (hrs)	Reference	Invitro	Invivo	TBI	SCI
NMDA Activation	2.53	2.5	< 1	(Zhang et al. 1996)	x		x	
AMPA Activation	2.31	2.2	< 1	*(Goforth et al. 2004)*	x		x	
		2.5	1	**(Li and Stys 2001)**	x			x
NaKATPase Transporter	0.67	0.7	24	(Faden et al. 1987)		x		x
		0.7	24	**(Li and Stys 2001)**	x			x
Reactive Oxygen Species (ROS)	5.11	4-5	1	*(Hall and Braughler 1993)*				x
	1.77	2.5	0.5	*(Hamada et al. 1996)*		x		x
Glutamate Concentration	4.1	4-7	0.75	(Xu et al. 2004)		x		x
Calcium Concentration	2.5	2.5-3	4	(Wingrave et al. 2003)		x		x
Sodium Concentration	2.43	2	1	*(Lemke et al. 1987)*		x		x
Mitochondria Dysfunction	1.3	1.2	6	**(Sullivan et al. 2007)**		x		x
ATP Concentration	0.8	0.7	1	*(Anderson et al. 1980)*		x		x
Membrane Damage	4.5	2-7	<1	**(Choo et al. 2007)**		x		x
Microglia Activation	3.6	3	6	(Dusart and Schwab 1994)		x		x
Cytokine Concentration	2.6	2-5	6	**(Bartholdi and Schwab 1997)**		x		x

Table 8.1.5 (continued)

Factor	Model Value	Exp. Value	Time Point	Reference	Invitro	Invivo	TBI	SCI
Astrocyte Activation	2.1	2-4	4	*(O'Brien et al. 1994)*		x		x
Macrophage Activation	11.1	11	16	**(Giulian and Robertson 1990)**		x		x
Oligodendrocyte Death	1.7	2	6	*(Crowe et al. 1997)*		x		x
Demyelination	2.7	~ 2.5	12#	*(Totoiu and Keirstead 2005)*		x		x
Nitric Oxide (NO)	1.5	2-5	6	(Merrill et al. 1993)	x			x
Caspase Activation	2.5,	3-3.5	4	(Wingrave et al. 2003)		x		x
	3.3		6	(Springer et al. 1999)		x		x
Axonal Damage	2.2	>2	6	(Pettus and Povlishock 1996)		x		

Parameter value extraction

When using experimental literature to obtain parameter values (Tables 4 and 5), primary reference selection was based on the quantifiability of the parameter. All parameters were extracted from central nervous system data, and when possible, data measured in the spinal cord and spinal cord injury. However, when insufficient quantifiable data was not available from the spinal cord literature, parameters were extracted from the traumatic brain injury literature. This distinction is made in the tables.

Justification for factor inclusion/exclusion

This model is based on what is already known about secondary injury. Therefore, factors included in the model were limited to those known to contribute to secondary injury

during the studied time frame and for which there was sufficient experimental data available for obtaining parameter values and validating results. Consequently, mediation factors (factors that mediate cell death), which have been understudied in this early time frame, are difficult to include. Thus, such explicit factors, like remyelination, were excluded from the relational model. Some factors of secondary injury, such as inflammation, are thought to have mediating as well as deleterious effects. In the model presented here, only the deleterious effects are explicitly included, mainly due to the lack of consistent, quantitative information currently available. Thus, it is implicitly assumed that the impact of mediation factors during the time frames examined in this study is negligible. However, we do not discount their potential importance; in the future, as more experimental information becomes available, inclusion may be appropriate.

In general, this study only includes *direct* factors for which experimental data among various studies is qualitatively consistent. If there was discordant experimental data for a factor, the factor was not directly or explicitly included, but rather implicitly modeled using related *indirect* factors and/or mechanisms for which experimental data was qualitatively consistent. For example, we recognize the potential importance of cell volume regulation, or edema, in the secondary injury process. However, conflicting experimental results make direct inclusion as an individuated factor very difficult. Several studies have documented a 2-3% change in spinal cord volume post-SCI, and each of these studies states to have reduced this volume change by approximately the same amount using very different methods corresponding to different potential mechanisms—by reducing NMDA receptor activation (Churchwell et al. 1996),

macrophage/microglia activation (Tian et al. 2006), ATP depletion (Jurkowitzalexander et al. 1992), and sodium (Ates et al. 2007), to name a few. Thus, in this study, we elect to model the effects of edema indirectly by inclusion of these aforementioned indirect mechanisms. Without a direct connection between edema and neuron death, it is possible that factors likely to contribute to edema, such as sodium, may have their impact on neuron death slightly underestimated, but the actual values of the indirect factors themselves remain in line with experimental data (see Table 5).

Other model assumptions and limitations

It is true that there are implicit assumptions with each factor that are inherently associated with the conditions, assumptions and limitations associated with the experiment from which each gain was extracted including the experimental model type, time frame of data collection, etc. (for a list of such publications, see Table 3). There are also limitations based on the information available for a certain factor. Another implicit assumption lies in the limitation imposed during data extraction from the literature. However, the more general assumptions of the model are: 1) A quantitative experimental correlation specifies an interaction which can be modeled in differential form resulting in both inherent and emergent predictions which reflect the interactive and temporal dynamics of the process. 2) No "events" occur between the discrete time points extracted experimentally, and thus temporal dynamics can be interpolated between discrete points by using an experimentally derived time constant in the translated differential equations.

Sensitivity analysis

A sensitivity analysis was performed by varying each parameter individually by a specified amount (± 50% in eight 6.25% increments) to measure its effect on the model output (i.e. factor and neuronal death) values. Sensitivity data was used to obtain the correlations between factors for the landscape. Additionally, the sign of the slope of the linear regression between each gain and neuronal death was used to calculate which direction a gain must be moved to minimize neuron death when specifying inhibiting treatments.

Secondary Injury Landscape(s)

The landscapes reveal the inter-relatedness of the factors and thus are illustrative of interaction dynamics. The correlation matrix, which forms the landscape, consists of correlation values obtained by correlating all outputs against one another based on the sensitivity analysis data. Note that landscapes are based on peak or maximal impact of each factor rather than ending impact. "Maximal impact" was defined as the minimum factor value occurrence over 12 hours for factors that decrease with neuron death (e.g. the Na-K-ATPase transporter and ATP) and the maximum factor value for the remaining 17 factors, which increase with neuron death. Neuron death values for each sensitivity analysis run were taken at their maximal value (i.e. at 12 hours).

Since any given output will correlate perfectly with itself, the correlation matrix contains a diagonal line of identity and is symmetric along the diagonal axis of the square. Correlations range from zero to one, with zero being completely uncorrelated and one

completely correlated (for method details see (Mitchell and Lee 2007)). The factors were sorted based on their correlation coefficients using hierarchical cluster analysis such that the most correlated factors were located near each other in the landscape. This sorting does not change the correlations in the landscape but rather makes correlations easier to illustrate and readily identifies "groups" of related factors based on correlation.

Pathology Diagrams

Pathology diagrams serve not only as a map but also as a survey of the overall system operation, including the changes in factor size, impact, and "flow". Since the purpose of the diagrams is to provide insight into the operation of the system as a whole, additional scaling was applied to determine line thicknesses/saturation levels etc. The overall intent was to scale in a manner that kept all lines and boxes visible and yet still provide meaningful individuation of effect. Qualitatively, greater intensity (darkness/saturation) indicates greater impact on neuron death with the scaling being roughly logarithmic. Thus, each increment in intensity is approximately a 2.5-fold increase in impact on neuron death. In contrast, size (box or line) is an indicator of magnitude. Box size (area) scaling is roughly linear with factor magnitude relative to its peak value. Line thickness is scaling is roughly logarithmic as impacts range over approximately 5 orders of magnitude. Thus, each increment in thickness is worth approximately a 2.7-fold increase in impact.

Inhibiting treatments

Inhibiting treatments (treatments that inhibit the growth of a factor) were simulated by co-varying all of the experimentally derived relationships (gains) directly governing a given factor (i.e. all parameters, excluding the time constants, appearing in the mathematical calculation of a factor) by a specified amount or "dose" in a direction that reduces neuron death. For inhibiting treatments, doses were simulated by moving the individual gains, G, that govern a factor or combination of factors between 1-95%. The direction that each individual gain must be varied to reduce neuron death was determined from a parameter sensitivity analysis.

Reducing treatments

Reducing treatments (treatments that directly reduce a factor) were performed by subtracting a factor-dependent 'dose', by multiplying the current factor value at each time step by a "reducing gain" that was roughly based on the sum of all gains ($G_{total, \text{factor}}$) for each factor. However, to facilitate comparison, the exact scaling of reducing gains was set so that reducing and inhibiting resulted in the same effect at very small dosing levels under the premise that reducing and inhibiting should become indistinguishable as dosing approaches zero. The specific scaling point was a 1% inhibiting treatment dose at time zero. Thus, a 1% reducing treatment at time zero was defined as the gain that produced the same change in neuron death as the 1% inhibiting treatment. Reducing gains were then varied between 1-1000%. Summarizing by continuing with our example with NMDA, the concentration-dependent dose that would be *subtracted* from Equation 2 to

reduce NMDA is represented by Equation 4, where S_{NMDA} is the applied scaling factor as described above.

$$NMDA_{\text{reduced}} = NMDA \cdot G_{total,_{NMDA}} \cdot S_{NMDA} \cdot dose \qquad \textbf{Equation 8.1.4}$$

Combination treatments

A factorial design was used to test single factor and multi-factor (simultaneously varying 2-5 factors) treatment combinations. The maximum of five was determined by a dimensionality analysis of the system (see (Mitchell and Lee 2007)).

Implementation

The model is implemented in MATLAB R2007a (The Mathworks, Inc.). Secondary injury simulations, sensitivity analyses, cross-correlation analysis for the landscape, and treatments were performed in MATLAB. Hierarchical clustering analysis for the sorting of the factors in the landscape was performed in Systat (Systat Software, Inc.). Pathology diagrams were created in SmartDraw (SmartDraw.com).

Results

Characterization of overall pathology

A key goal of this study was to examine the overall pathology of secondary injury at the system level, including the process dynamics. As a starting point, two generalized

mechanisms of secondary injury propagation were examined. The first is a rate-dependent process, similar to a burning forest fire, where damage is driven by *interactions* between factors. Using this analogy, a fire is critically dependent upon the interactions between fuel availability, wind speed, humidity, etc. and even small changes in any one of these can have dramatic effects on the fire's progression and the extent of its damage. The second mechanism is an accumulation-dependent process that is analogous to a rising flood, where damage is driven by the *accumulation* of factors. Using this analogy, the flood is dependent upon summation over time of flow rates, geographic contours, etc. and small changes in these factors generally result in only small effects on the overall flood and extent of its damage. The prevailing view of secondary injury would be akin to the fire analogy. Thus, our initial expectation was that the system would be driven by ongoing, rate-dependent interactions of factors.

We began our examination of the secondary injury pathology by investigating the time course of individual factors and neuron death. The primary model output used to signify the propagation of secondary injury is *neuron death* as a function of time. In actuality, "neuron death" represents the aggregation of all indicators of dead, dying and/or marked for death neurons. As such, it encompasses both the volume affected and the fraction of dying cells within that volume. In the first hour post-insult, the model predicts approximately a three-fold increase in neuron death. This first hour shows greatest activity in the excitotoxic factors (**Figure 2**) whose relationships were predominately based on in vitro literature. Subsequently, neuron death increases at a slower, but still substantial pace resulting in an additional three-fold increase over the next fifteen hours.

This sub-acute period shows substantial activity in the necro-apoptotic and inflammatory factors (Figure 2) and is based heavily on in vivo literature. The model was validated by comparing its output to experimental data (see Table 5), and especially, when possible, to experimental data not used as part of the model construction. Based on comparison to experimental data, the model appears to be valid out to 16 to 18 hours post-insult. However, the dearth of experimental data points between 12 and 24 hours make a precise determination difficult. Consequently, we limit our examination to the first 12 hours post-insult.

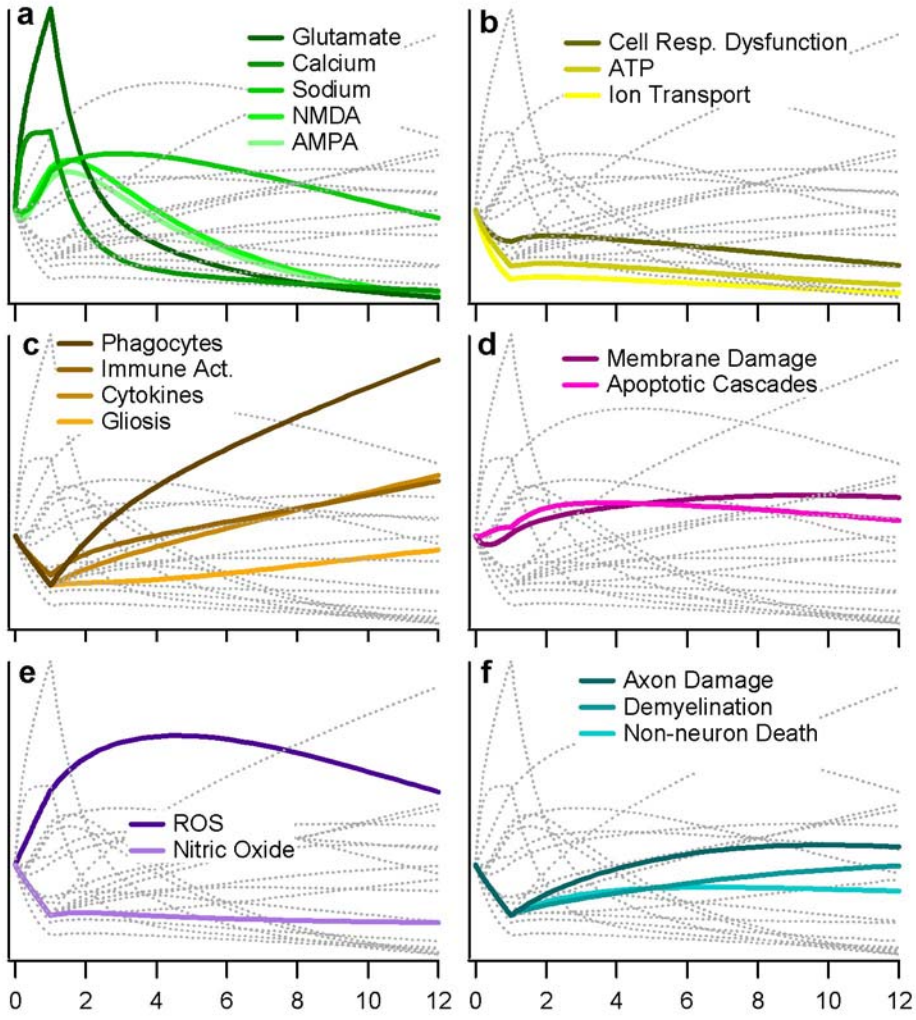

Figure 8.1.2. Progression of factors over time. For illustration purposes, the trajectories shown are relative to one another in that factors are scaled based on the average of all 19 factors. For comparison of specific factor *values* to experimental values at specified time points, see Table 5. Each category of factors is highlighted in an individual panel using a monochromatic color scheme that aligns with the category colors used in Figure 1a. Light gray lines in the background represent the non-highlighted factors in each respective panel and are shown for the purpose of comparing the different factor and factor category trajectories. (**a**) Excitotoxic factors (**b**) Energetic factors (**c**) Inflammatory factors (**d**) Necro-apoptotic factors (**e**) Free radical factors (**f**) Other factors.

Next, we assessed the simultaneous inter-relationships (i.e. correlations) among the nineteen factors and neuron death to obtain "snapshots" of the entire secondary injury process over time (Figure 3). By looking at how these snapshots change over time, we can visualize the dynamics of propagation. The landscapes (***left* Figure 3**) represent both a summary of the two-way, experimentally observed correlations, and the model's predictions regarding broader interactions among the factors. The corresponding pathology diagrams (***right* Figure 3**) indicate the relative flow and impact of factors, and thus represent the accumulation of factors over time. Initially, all factors are tightly coupled as denoted by the widespread, intense block of correlations in the landscape. This tight coupling results in a one-dimensional behavior that is indicative of a process that is dominated by interactions (i.e. the fire). However, with time, the system decouples as the effects of interactions diminish. Simultaneously, the effects of factor accumulation rise, eventually dominating the process as indicated in the pathology diagrams, and resulting in a pathology that behaves like multiple independent floods.

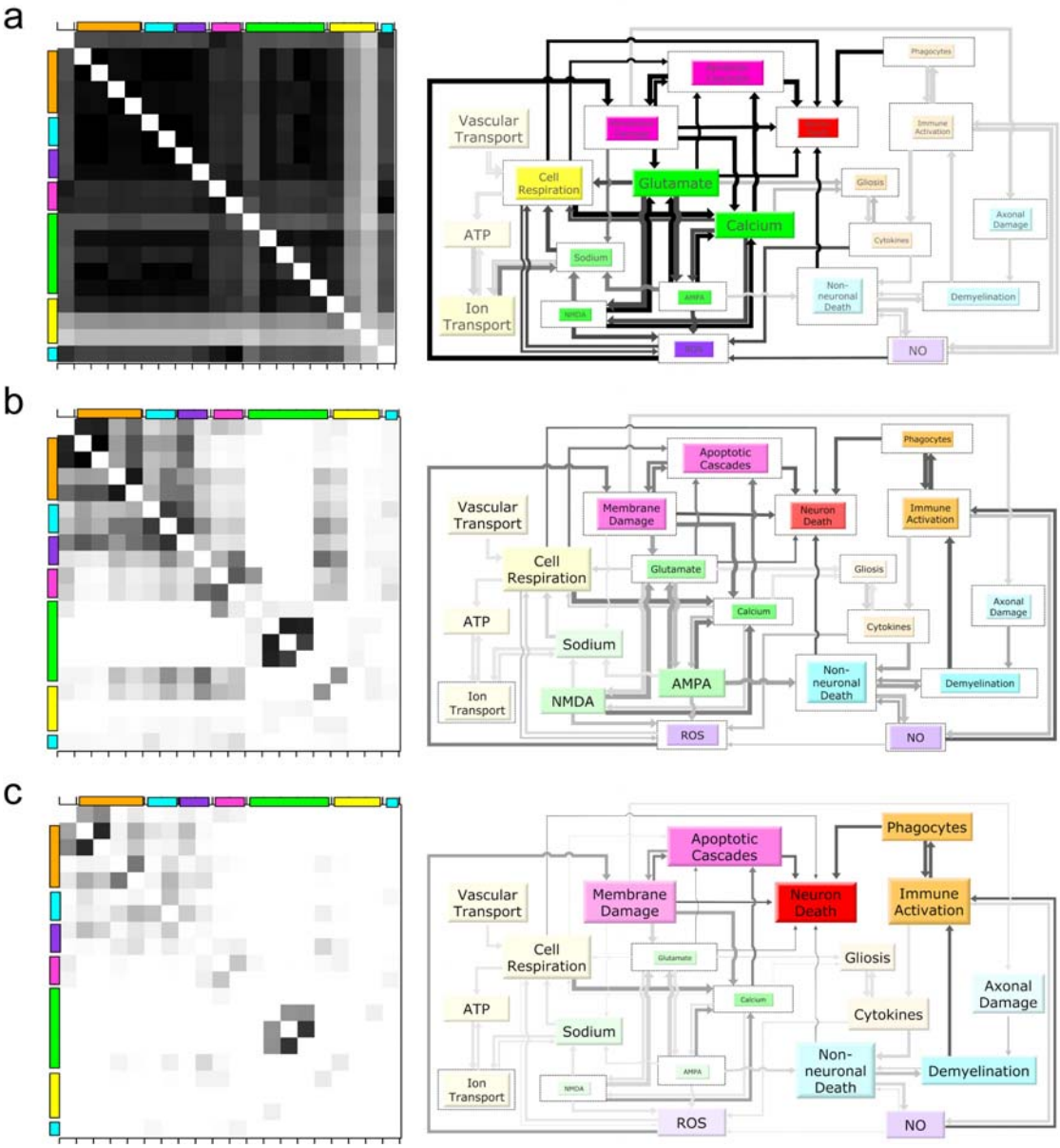

Figure 8.1.3. Analysis of the fire versus flood dynamics of secondary injury pathology. (*Left*) Landscape of correlations quantifying the strengths of the inter-relationships or interactions among the factors and neuron death. Correlation magnitudes are represented by the grayscale color, and range from zero (white, uncorrelated) to one (black, completely correlated), Colors on the axes represent the category to which the factor(s) belong as denoted in Figure 1. The matrix contains a diagonal line of unity, which has been removed for clarity. (*Right*) Pathology diagram signifying the "flow" versus accumulation of factors and their impact on neuron death. Arrow line thickness illustrates the effect of one factor on another while line darkness represents the impact of that effect on neuron death. The inner, colored box size illustrates "accumulation" of a factor and is scaled by the factor's maximum, represented by its outline. Box color saturation symbolizes the impact of the factor on neuron death. Continued on next page…

Figure 8.1.3 (continued). (**a**) One-hour snapshot. All factors in the landscape are highly correlated, indicative of the very large interactions associated with a fire, with only minimal factors showing substantial accumulation in the pathology diagram. (**b**) Two-hour snapshot. The system shows substantial decoupling in the landscape, and an increase in the number of accumulating factors in the diagram, indicating a mixed rate and accumulation-dependent pathology (i.e. fire and flood). (**c**) Eight-hour snapshot. The system is functionally decoupled, and accumulation clearly dominates, indicative of pathology consisting of several independent floods.

Our examination of secondary injury during the first 12 hours post-insult has revealed that while the commonly held view of the pathology as a propagating fire is consistent with the system behavior initially, it quickly transitions into "flood" dynamics where the accumulation of factors over time dominates neuron death (**Figure 4**). Notably, this transition occurs relatively early, as a substantial majority of neuron death occurs during the flood phase.

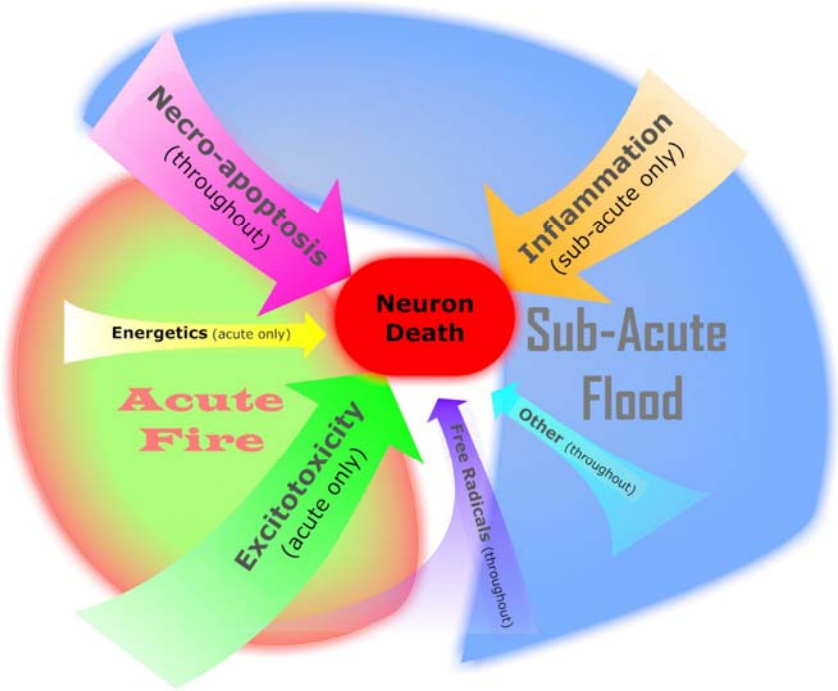

Figure 8.1.4. Summary of secondary injury pathology dynamics: acute fire versus the sub-acute flood. The pathology dynamics consist of an early, acute fire of interactions chiefly dominated by excitotoxic factors followed by a larger, sub-acute flood of accumulating factors chiefly dominated by necro-apoptotic and inflammatory factors. The relative size of the arrows indicates the relative impact of the corresponding factor category on neuron death. Excitotoxicity, necro-apoptosis, and inflammation all have a substantial impact on neuron death, while energetics, free radicals, and other factors have a still significant but smaller impact on neuron death. Time of impact is indicated in parentheses.

Single Factor Treatments.

With the above view of the overall pathology in mind, we began our examination of hypothetical treatments by inhibiting the growth of single factors by doses ranging from 10-95% inhibition (e.g. a 50% dose would be expected to reduce the growth of the factor by 50% if all else remained the same). To determine the maximum possible impact of each factor on neuron death, calculated single factor treatments were initiated at time zero

(i.e. simultaneous with the insult - **Figure 5A**). Based on a 50% inhibiting dose, the impact of these single factor treatments ranges from negligible to nearly a 20% decrease in neuron death. However, treatment efficacy drops rapidly with time post-insult (**Figure 5B**). Notably, while the impact of all factors decreased substantially with treatment time, several factors that had been highly effective when treatment was initiated at time zero drop precipitously, making them low prospects as the basis for clinical treatment. The net result is that the top 5 single factor treatments in the 2 to 8 hr treatment initiation window are: phagocytes (e.g. macrophages, neutrophils, etc), immune activation (e.g. microglia), apoptotic mediators (e.g. caspase, calpain, etc), membrane damage, and cytosolic calcium.

Combination Treatments.

To examine the supposition that multi-factor treatments would be more effective in treating secondary injury, we tested combinations of treating two to five factors. The maximum of five was based on a statistical analysis of significance based on the system dimensionality (for dimensionality assessment method, see Mitchell and Lee, 2007). The results indicate the effects of combination therapy during the first 12 hours post insult are substantially sublinear, rather than synergistic. That is, of the approximately 20,000 possible combinations, none performed better and most performed worse than what would be expected by adding the dose-proportional effects of single treatments together (**Figure 5C).** Although more effect is gained with each additional factor treated, the majority of the impact resides in treating three factors.

Inhibiting versus Reducing Treatments

Based on our analysis of the overall system behavior, we explored alternative treatments beyond those that simply inhibit factor growth. Most clinical therapies are aimed at decreasing neuron death by *inhibiting* the growth of a factor by acting via a specific mechanistic pathway. For example, a common experimental treatment is to inhibit NMDA activation using a receptor antagonist. These inhibiting treatments target interactions by preventing the rate-dependent growth of a factor and its subsequent interaction with other factors. In contrast to this inhibiting treatment paradigm, we also examined *reducing* treatment paradigms to decrease neuron death (**Figure 5C-D**). This paradigm targets the accumulation-dependent nature of the system by directly reducing a factor in a manner similar to adding a 'drain' to the flood analogy. An example of a reducing treatment is a free radical scavenger, which actively seeks to 'mop up' free radicals, rather than prevent their formation.

The switch from a rate-dependent propagation of secondary injury (i.e. the fire) to an accumulation-dependent process (i.e. the flood), is evident in the performance of the respective inhibiting and reducing treatment paradigms. During the acute period, inhibiting treatments outperform their reducing counterparts, particularly at less aggressive treatment doses. However, this difference becomes negligible by hour two for three-factor combination treatments and by hour four for two-factor combinations, (**Figure 5D**). By hour eight, reducing treatments outperform inhibiting treatments in all treatment scenarios.

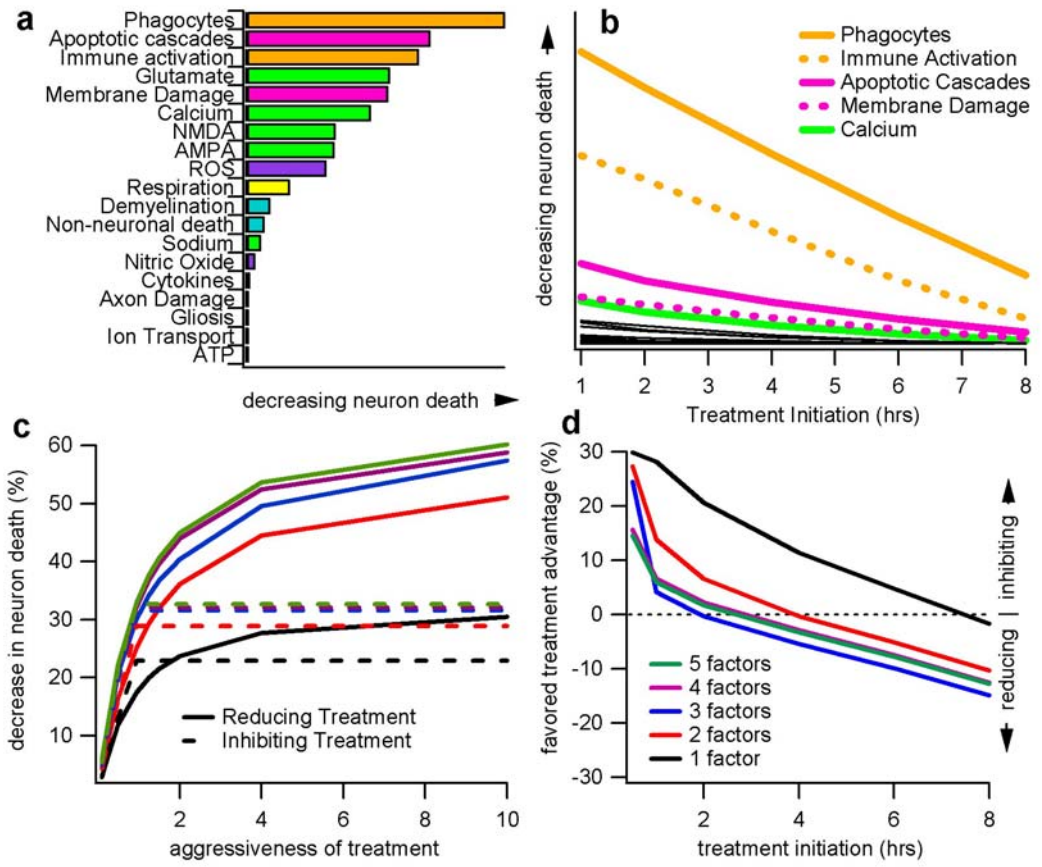

Figure 8.1.5. Evaluation and ranking of various hypothetical single, reducing, inhibiting, and combination treatments. (**a**) Impact ranking of individual secondary injury factors on neuron death as determined by immediate post-insult treatment initiation (zero hours) that inhibits single factors by 50%. (**b**) Impact of time of treatment initiation on neuron death over clinically relevant time frames. The factors relevant at later, clinically relevant time points contrast from those shown at time zero. The top five single factors are shown in their respective category color (from Figure 1): phagocytes, immune activation, apoptotic cascades, membrane damage, and calcium. The remaining factors are shown in black. (**c**) The effect of reducing and inhibiting single and combination treatments as a function of aggressiveness of treatment. The impact of treatment, especially combination treatments, is greatly increased by reducing paradigms (solid lines) which allow for much more aggressive treatment than inhibiting treatments (dashed lines). Aggressiveness of treatment measured relative to maximum (i.e. 100%) inhibiting treatment. Thus, inhibiting treatments max out at 1.0 while reducing treatments can be much more aggressive. (**d**) Quantified advantage of reducing versus inhibiting combination treatment paradigms. The order of factors for each *n*-factor combination shown in (c) and (d) are: phagocytes, immune activation, necro-apoptosis, membrane damage, and calcium. As shown in both (c) and (d), the majority of effective impact of combination treatments is contained within 3 factors.

Pathology-driven therapeutic strategies

Based on our results, the switch from the acute, highly interactive, rate-dependent pathology to a sub-acute lower interaction, accumulation-dependent pathology determines two critical aspects of secondary injury: 1) the strength of relationships governing a factor's impact on neuron death (**Figure 6**) and 2) the time frame over which factors are relevant, referred to as the factor "treatment window" (Figure 4). Since a truly effective treatment must take into account both of these components, ultimately only a few factors are highly influential at clinically relevant time frames. This would appear to explain the disconnect between promising experimental studies, which pre-treat or treat acute factors within minutes of insult (Blight and Tuszynski 2006; Faden and Stoica 2007; Tolias and Bullock 2004), and clinical studies where treatment time frames are typically 4-8 hours (Tator and Fehlings 1999) as the effective treatment window for acute factors has been surpassed. Furthermore, the lack of synergism predicted by the model for combination treatments is also a direct result of the early switch to a diverging, flood-like pathology since synergism is derived from the sustained presence of strong interactions.

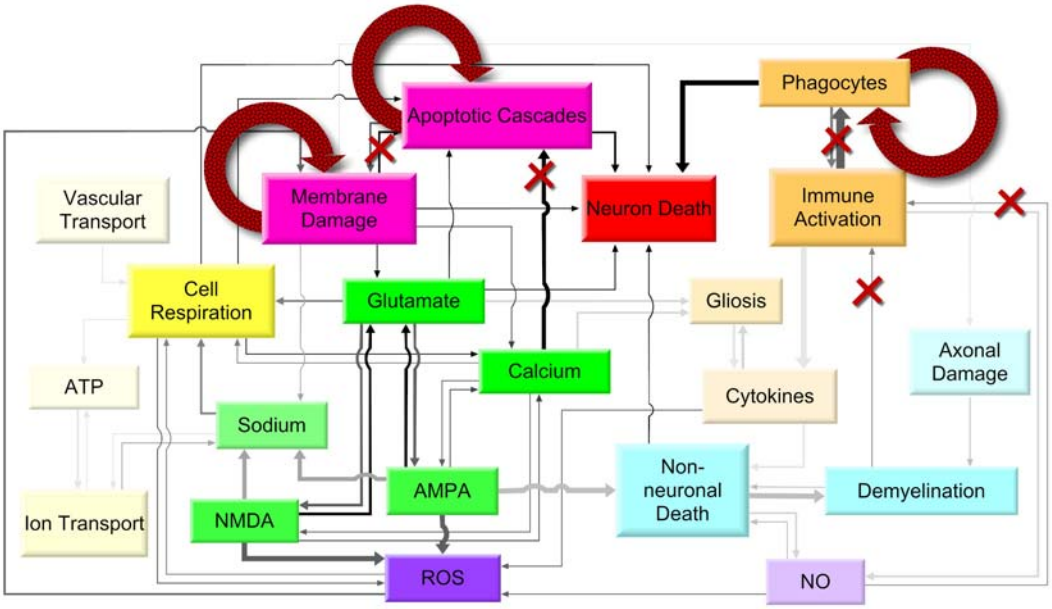

Figure 8.1.6. Summary of the secondary injury pathology dynamics and the top model-predicted therapeutic strategies at clinically relevant time frames. The diagram summarizes the flows and effects of factors on neuron death and the corresponding higher-impact inhibiting and reducing treatments over the 2-8 hr time frame. Circular arrows represent the best targets for reducing treatments: membrane damage, apoptotic cascades, and phagocytes. Inhibiting treatments are indicated by an "x" through the targeted interaction: interaction between NO and immune activation, non-neuronal death and immune activation, immune activation and phagocytes, calcium and apoptotic cascades, and membrane damage and apoptotic cascades. Arrow line thickness to and from factors represents relative "flow" and is indicative of the relative rates coming into and out of factor while line darkness represents the impact of "flow" on neuron death. Box color saturation symbolizes the impact of a factor on neuron death.

Summary of Predictions

As shown, the presented secondary injury relational model is able to transcribe literature-extracted relationships into a network of time-varying factors that reproduce a number of experimental results. However, an important aspect of any model is the ability to characterize previously unknown dynamics, mechanisms, or functions. In this work, we have made several predictions regarding the previously uncharacterized dynamics of secondary injury and its response to numerous hypothetical single and multi-factor combination treatment types. A summary of the model's testable predictions is given in **Table 6.**

Table 6. Summary of secondary injury dynamics and therapeutic predictions over the 0-12 hour simulated time period. Therapeutic predictions are continued on the next page.

Dynamical Predictions
• *Dynamical Time Course:* Hours 1-2 are dominated by an acute "fire" of rate-dependent interactions. Hours 2-6 exhibit a mixture of fire-like interactions and the flood-like accumulation of independent factors. Hours 6-12 reveal a nearly decoupled system analogous to a flood. • *Factor Category Time Course:* Excitotoxicity and energetics peak in hours 1-2. Free radical and necro-apoptosis peak during hours 2-6. Inflammation and "other" peak in the last hours of the sub-acute period (>6 hours). • *Factor Impact on Neuron Death:* Excitotoxicity and energetics impact neuron death in the acute periods. Impact of inflammation is in the sub-acute period. Impacts of necro-apoptosis, free radicals, and "other" can be seen throughout the entire time course.

Table 6 (continued).

Therapeutic Predictions
• Single Factor Treatments: Best treatments during clinically relevant time frames (hours 2-8) are phagocytes, immune activation, apoptotic cascades, membrane damage, and calcium. • Combination Treatments: Are additive rather than synergistic. Majority of treatment impact obtained with 3 factors. • Inhibiting Treatments: Target interactions; most effective 0-4 hrs post-insult. • Reducing Treatments: Target accumulation of factors; most effective >4 hours post-insult. Can have much higher doses compared to inhibiting treatments, making them the superior general clinical strategy.

Discussion

At first, it may seem that this characterization of the secondary injury pathology simply adds to the already disheartening picture painted by a host of failed clinical trials. However, our results may indicate quite the opposite. The pathology characterization presented here identifies positive current and future directions to pursue based on fundamental pathology dynamics. While multi-factor treatment combinations do not provide the much hoped-for synergistic effects, our results do suggest that some combinations would be functionally additive, namely factors with longer treatments windows, such as necro-apoptotic and inflammatory factors. Furthermore, the effects of combination treatments can be amplified with very aggressive reducing treatment paradigms. Such paradigms may be possible with careful selection of existing pharmaceuticals. Thus, multi-factor treatments may still play a role in treating SCI, but

expectations regarding their effectiveness should remain realistic with continued exploration being pragmatic.

More importantly, our results suggest that the way forward may lie in pursuing the detailed dynamics of how the secondary injury process propagates rather than just the factors involved in that propagation. For example, treatment of secondary injury based on a flood paradigm opens up therapeutic avenues not currently explored. There are three possible ways to 'treat' a flood: 1) 'wall off' the flood by building a containment dam; 2) repair the source; and 3) distribute the flooding over a larger area/volume thereby minimizing its impact. In the case of secondary injury, each has its pros and cons. The physiological mechanism seems to be to wall off the area via inflammation and glial scarring (Fawcett and Asher 1999). However, this approach sacrifices any surviving cells remaining within the walled area. Repairing the source, which could involve repairing the damaged cells, possibly through membrane re-sealing (Liu-Snyder et al. 2007), may have a limited feasible treatment window but may still result in long-term success. More radical would be attempting to distribute the flood in a regulated manner, possibly through controlled activation and inactivation of inflammatory factors over time to minimize overall damage. This last approach could potentially leverage the positive, mediating aspects of inflammation while minimizing the negative, sacrificial effects. A key challenge for many of these alternative approaches lies in the ability to experimentally characterize and analyze the changing spatial and temporal dynamics of the pathology, such as the ability to differentiate early rate-dependent damage from later, accumulation-dependent damage.

While this model does provide the first, preliminary systems-level view of the secondary injury process and possible hypothetical treatments as a whole based on the current state of the field, it is merely scratching the surface. Thus, admittedly, there are multiple factors, details, and mechanisms that will likely need to be added or modified in the future as new experimental findings allow us to hone in closer to the roots, inner-workings, and related systems, which specify the underlying pathology and ultimately the efficacy of very specific treatments. Specific examples of possible refinements include the addition of the mediating effects of inflammation and membrane re-sealing and a more detailed examination of underspecified factors, such axonal damage, where useable, available data is scarce. Finally, in addition to the excluded mediating and discordant direct factors stated in the justification for factor inclusion/exclusion section, this model does not account for secondary injury occurring at the level of the organism (hypoxia and hypotension) resulting from dysfunction of other organ systems. In the future, such aforementioned refinements will provide further confidence in our ability to predict clinical outcomes.

We foresee this and similar forms of modeling and analysis, perhaps better classified as "theoretical physiology", to be an invaluable complementary tool to the details and mechanisms identified and validated by spinal cord injury experimental and clinical studies by allowing a comprehensive, holistic view into the pathology dynamics and interactions. Ultimately, with continued refinement, modeling may provide a high-throughput screening process from which potential experiments, treatments, and detailed

protocols can be tested for feasibility and prioritization, thus speeding the time between therapeutic discovery and clinical success.

Acknowledgements

This work is supported by the National Science Foundation (NSF) via a Graduate Research Fellowship and an Integrative Graduate Education and Research Traineeship Fellowship (DGE-0333411) to C.S.M. Additional support was provided by the Human Brain Project (NINDS, NIMH and NIBIB NS046851) to R.H.L.

References

Agrawal, S.K., Fehlings, M.G. (1996) Mechanisms of secondary injury to spinal cord axons in vitro: Role of Na+,Na+-K+-ATPase, the N+-H+ exchanger, and the Na+-Ca2+ exchanger. Journal of Neuroscience 16, 545-552.

Agrawal, S.K., Fehlings, M.G. (1997) Role of NMDA and non-NMDA ionotropic glutamate receptors in traumatic spinal cord axonal injury. J Neurosci 17, 1055-1063.

Ahmed, S.M., Weber, J.T., Liang, S., Willoughby, K.A., Sitterding, H.A., Rzigalinski, B.A., Ellis, E.F. (2002) NMDA receptor activation contributes to a portion of the decreased mitochondrial membrane potential and elevated intracellular free calcium in strain-injured neurons. J Neurotrauma 19, 1619-1629.

Alano, C.C., Beutner, G., Dirksen, R.T., Gross, R.A., Sheu, S.S. (2002) Mitochondrial permeability transition and calcium dynamics in striatal neurons upon intense NMDA receptor activation. J Neurochem 80, 531-538.

Anderson, D.K., Means, E.D., Waters, T.R., Spears, C.J. (1980) Spinal cord energy metabolism following compression trauma to the feline spinal cord. J Neurosurg 53, 375-380.

Ankarcrona, M., Dypbukt, J.M., Bonfoco, E., Zhivotovsky, B., Orrenius, S., Lipton, S.A., Nicotera, P. (1995) Glutamate-Induced Neuronal Death - a Succession of

Necrosis or Apoptosis Depending on Mitochondrial-Function. Neuron 15, 961-973.

Ates, O., Cayli, S.R., Gurses, I., Turkoz, Y., Tarim, O., Cakir, C.O., Kocak, A. (2007) Comparative neuroprotective effect of sodium channel blockers after experimental spinal cord injury. Journal of Clinical Neuroscience 14, 658-665.

Azbill, R.D., Mu, X., Bruce-Keller, A.J., Mattson, M.P., Springer, J.E. (1997) Impaired mitochondrial function, oxidative stress and altered antioxidant enzyme activities following traumatic spinal cord injury. Brain Res 765, 283-290.

Bartholdi, D., Schwab, M.E. (1997) Expression of pro-inflammatory cytokine and chemokine mRNA upon experimental spinal cord injury in mouse: an in situ hybridization study. Eur J Neurosci 9, 1422-1438.

Barut, S., Unlu, Y.A., Karaoglan, A., Tuncdemir, M., Dagistanli, F.K., Ozturk, M., Colak, A. (2005) The neuroprotective effects of z-DEVD.fmk, a caspase-3 inhibitor, on traumatic spinal cord injury in rats. Surgical neurology 64, 213-220; discussion 220.

Beattie, M.S. (2004) Inflammation and apoptosis: linked therapeutic targets in spinal cord injury. Trends in molecular medicine 10, 580-583.

Blight, A.R. (1985) Delayed demyelination and macrophage invasion: a candidate for secondary cell damage in spinal cord injury. Cent Nerv Syst Trauma 2, 299-315.

Blight, A.R., Tuszynski, M.H. (2006) Clinical trials in spinal cord injury. J Neurotrauma 23, 586-593.

Carlson, S.L., Parrish, M.E., Springer, J.E., Doty, K., Dossett, L. (1998) Acute inflammatory response in spinal cord following impact injury. Experimental Neurology 151, 77-88.

Carriedo, S.G., Yin, H.Z., Sensi, S.L., Weiss, J.H. (1998) Rapid Ca2+ entry through Ca2+-permeable AMPA/kainate channels triggers marked intracellular Ca2+ rises and consequent oxygen radical production. Journal of Neuroscience 18, 7727-7738.

Choo, A.M., Liu, J., Lam, C.K., Dvorak, M., Tetzlaff, W., Oxland, T.R. (2007) Contusion, dislocation, and distraction: primary hemorrhage and membrane permeability in distinct mechanisms of spinal cord injury. J Neurosurg Spine 6, 255-266.

Churchwell, K.B., Wright, S.H., Emma, F., Rosenberg, P.A., Strange, K. (1996) NMDA receptor activation inhibits neuronal volume regulation after swelling induced by veratridine-stimulated Na+ influx in rat cortical cultures. J Neurosci 16, 7447-7457.

Crowe, M.J., Bresnahan, J.C., Shuman, S.L., Masters, J.N., Beattie, M.S. (1997) Apoptosis and delayed degeneration after spinal cord injury in rats and monkeys. Nat Med 3, 73-76.

Cullen, D.K., LaPlaca, M.C. (2006a) The Effects of Shear vs. Compressive Loading in 3-D Neuronal-Astrocytic Co-Cultures. In: Neurotrauma. St. Louis, MO.

Cullen, D.K., LaPlaca, M.C. (2006b) Neuronal response to high rate shear deformation depends on heterogeneity of the local strain field. J Neurotrauma 23, 1304-1319.

Dusart, I., Schwab, M.E. (1994) Secondary Cell-Death and the Inflammatory Reaction after Dorsal Hemisection of the Rat Spinal-Cord. European Journal of Neuroscience 6, 712-724.

Faden, A.I., Chan, P.H., Longar, S. (1987) Alterations in lipid metabolism, Na+,K+-ATPase activity, and tissue water content of spinal cord following experimental traumatic injury. J Neurochem 48, 1809-1816.

Faden, A.I., Stoica, B. (2007) Neuroprotection - Challenges and opportunities. Arch Neurol-Chicago 64, 794-800.

Farkas, O., Lifshitz, J., Povlishock, J.T. (2006) Mechanoporation induced by diffuse traumatic brain injury: An irreversible or reversible response to injury? Journal of Neuroscience 26, 3130-3140.

Fawcett, J.W., Asher, R.A. (1999) The glial scar and central nervous system repair. Brain Research Bulletin 49, 377-391.

Fehlings, M.G., Agrawal, S. (1995) Role of sodium in the pathophysiology of secondary spinal cord injury. Spine 20, 2187-2191.

Fleming, J.C., Norenberg, M.D., Ramsay, D.A., Dekaban, G.A., Marcillo, A.E., Saenz, A.D., Pasquale-Styles, M., Dietrich, W.D., Weaver, L.C. (2006) The cellular inflammatory response in human spinal cords after injury. Brain 129, 3249-3269.

Fujiki, M., Furukawa, Y., Kobayashi, H., Abe, T., Ishii, K., Uchida, S., Kamida, T. (2005) Geranylgeranylacetone limits secondary injury, neuronal death, and progressive necrosis and cavitation after spinal cord injury. Brain Res 1053, 175-184.

Gaviria, M., Bonny, J.M., Haton, H., Jean, B., Teigell, M., Renou, J.P., Privat, A. (2006) Time course of acute phase in mouse spinal cord injury monitored by ex vivo quantitative MRI. Neurobiol Dis 22, 694-701.

Giulian, D., Robertson, C. (1990) Inhibition of mononuclear phagocytes reduces ischemic injury in the spinal cord. Ann Neurol 27, 33-42.

Goforth, P.B., Ellis, E.F., Satin, L.S. (2004) Mechanical injury modulates AMPA receptor kinetics via an NMDA receptor-dependent pathway. Journal of Neurotrauma 21, 719-732.

Gomes-Leal, W., Corkill, D.J., Freire, M.A., Picanco-Diniz, C.W., Perry, V.H. (2004) Astrocytosis, microglia activation, oligodendrocyte degeneration, and pyknosis following acute spinal cord injury. Experimental Neurology 190, 456-467.

Green, D., Kroemer, G. (1998) The central executioners of apoptosis: caspases or mitochondria? Trends Cell Biol 8, 267-271.

Hall, E.D., Braughler, J.M. (1993) Free radicals in CNS injury. Res Publ Assoc Res Nerv Ment Dis 71, 81-105.

Hall, E.D., Springer, J.E. (2004) Neuroprotection and acute spinal cord injury: a reappraisal. NeuroRx 1, 80-100.

Hamada, Y., Ikata, T., Katoh, S., Tsuchiya, K., Niwa, M., Tsutsumishita, Y., Fukuzawa, K. (1996) Roles of nitric oxide in compression injury of rat spinal cord. Free Radic Biol Med 20, 1-9.

Hartmann, A., Hunot, S., Michel, P.P., Muriel, M.P., Vyas, S., Faucheux, B.A., Mouatt-Prigent, A., Turmel, H., Srinivasan, A., Ruberg, M., Evan, G.I., Agid, Y., Hirsch, E.C. (2000) Caspase-3: A vulnerability factor and final effector in apoptotic death of dopaminergic neurons in Parkinson's disease. Proc Natl Acad Sci U S A 97, 2875-2880.

Hu, S., Peterson, P.K., Chao, C.C. (1997) Cytokine-mediated neuronal apoptosis. Neurochem Int 30, 427-431.

Iwai, T., Tanonaka, K., Inoue, R., Kasahara, S., Motegi, K., Nagaya, S., Takeo, S. (2002) Sodium accumulation during ischemia induces mitochondrial damage in perfused rat hearts. Cardiovasc Res 55, 141-149.

Jurkowitzalexander, M.S., Altschuld, R.A., Hohl, C.M., Johnson, J.D., Mcdonald, J.S., Simmons, T.D., Horrocks, L.A. (1992) Cell Swelling, Blebbing, and Death Are Dependent on Atp Depletion and Independent of Calcium during Chemical Hypoxia in a Glial-Cell Line (Roc-1). Journal of Neurochemistry 59, 344-352.

Kandel, E.R., Schwartz, J.H., Jessell, T.M. (2000) Principles of Neural Science, Fourth Edition: McGraw-Hill.

Klusman, I., Schwab, M.E. (1997) Effects of pro-inflammatory cytokines in experimental spinal cord injury. Brain Research 762, 173-184.

Krajewski, S., Krajewska, M., Ellerby, L.M., Welsh, K., Xie, Z., Deveraux, Q.L., Salvesen, G.S., Bredesen, D.E., Rosenthal, R.E., Fiskum, G., Reed, J.C. (1999)

Release of caspase-9 from mitochondria during neuronal apoptosis and cerebral ischemia. Proc Natl Acad Sci U S A 96, 5752-5757.

LaPlaca, M.C., Thibault, L.E. (1998) Dynamic mechanical deformation of neurons triggers an acute calcium response and cell injury involving the N-methyl-D-aspartate glutamate receptor. Journal of neuroscience research 52, 220-229.

Lemke, M., Demediuk, P., McIntosh, T.K., Vink, R., Faden, A.I. (1987) Alterations in tissue Mg++, Na+ and spinal cord edema following impact trauma in rats. Biochem Biophys Res Commun 147, 1170-1175.

Li, S., Stys, P.K. (2001) Na+-K+-ATPase inhibition and depolarization induce glutamate release via reverse Na+-dependent transport in spinal cord white matter. Neuroscience 107, 675-683.

Liu, D., Xu, G.Y., Pan, E., McAdoo, D.J. (1999) Neurotoxicity of glutamate at the concentration released upon spinal cord injury. Neuroscience 93, 1383-1389.

Liu-Snyder, P., Logan, M.P., Shi, R., Smith, D.T., Borgens, R.B. (2007) Neuroprotection from secondary injury by polyethylene glycol requires its internalization. The Journal of experimental biology 210, 1455-1462.

Louis, J.C., Magal, E., Takayama, S., Varon, S. (1993) Cntf Protection of Oligodendrocytes against Natural and Tumor Necrosis Factor-Induced Death. Science 259, 689-692.

Lovas, G., Szilagyi, N., Majtenyi, K., Palkovits, M., Komoly, S. (2000) Axonal changes in chronic demyelinated cervical spinal cord plaques. Brain 123 (Pt 2), 308-317.

Lu, J., Ashwell, K.W., Waite, P. (2000) Advances in secondary spinal cord injury: role of apoptosis. Spine 25, 1859-1866.

Mattiasson, G. (2004) Analysis of mitochondrial generation and release of reactive oxygen species. Cytometry Part A 62A, 89-96.

Merrill, J.E., Ignarro, L.J., Sherman, M.P., Melinek, J., Lane, T.E. (1993) Microglial cell cytotoxicity of oligodendrocytes is mediated through nitric oxide. J Immunol 151, 2132-2141.

Mitchell, C.S., Feng, S.S., Lee, R.H. (2007) An analysis of glutamate spillover on the N-methyl-D-aspartate receptors at the cerebellar glomerulus. J Neural Eng 4, 276-282.

Mitchell, C.S., Lee, R.H. (2007) Output-based comparison of alternative kinetic schemes for the NMDA receptor within a glutamate spillover model. J Neural Eng 4, 380-389.

Nicholls, D.G., Budd, S.L. (2000) Mitochondria and neuronal survival. Physiological Reviews 80, 315-360.

O'Brien, M.F., Lenke, L.G., Lou, J., Bridwell, K.H., Joyce, M.E. (1994) Astrocyte response and transforming growth factor-beta localization in acute spinal cord injury. Spine 19, 2321-2329; discussion 2330.

Park, E., Velumian, A.A., Fehlings, M.G. (2004) The role of excitotoxicity in secondary mechanisms of spinal cord injury: A review with an emphasis on the implications for white matter degeneration. Journal of Neurotrauma 21, 754-774.

Pettus, E.H., Povlishock, J.T. (1996) Characterization of a distinct set of intra-axonal ultrastructural changes associated with traumatically induced alteration in axolemmal permeability. Brain Research 722, 1-11.

Pineau, I., Lacroix, S. (2007) Proinflammatory cytokine synthesis in the injured mouse spinal cord: multiphasic expression pattern and identification of the cell types involved. J Comp Neurol 500, 267-285.

PorteraCailliau, C., Price, D.L., Martin, L.J. (1997) Non-NMDA and NMDA receptor-mediated excitotoxic neuronal deaths in adult brain are morphologically distinct: Further evidence for an apoptosis-necrosis continuum. Journal of Comparative Neurology 378, 88-104.

Saftenku, E.E. (2005) Modeling of slow glutamate diffusion and AMPA receptor activation in the cerebellar glomerulus. Journal of theoretical biology 234, 363-382.

Schnell, L., Fearn, S., Klassen, H., Schwab, M.E., Perry, V.H. (1999) Acute inflammatory responses to mechanical lesions in the CNS: differences between brain and spinal cord. European Journal of Neuroscience 11, 3648-3658.

Schwab, M.E., Bartholdi, D. (1996) Degeneration and regeneration of axons in the lesioned spinal cord. Physiol Rev 76, 319-370.

Schwartz, G., Fehlings, M.G. (2001) Evaluation of the neuroprotective effects of sodium channel blockers after spinal cord injury: improved behavioral and neuroanatomical recovery with riluzole. Journal of Neurosurgery 94, 245-256.

Shi, R., Whitebone, J. (2006) Conduction deficits and membrane disruption of spinal cord axons as a function of magnitude and rate of strain. Journal of Neurophysiology 95, 3384-3390.

Springer, J.E., Azbill, R.D., Knapp, P.E. (1999) Activation of the caspase-3 apoptotic cascade in traumatic spinal cord injury. Nature Medicine 5, 943-946.

Sullivan, P.G., Krishnamurthy, S., Patel, S.P., Pandya, J.D., Rabchevsky, A.G. (2007) Temporal characterization of mitochondrial bioenergetics after spinal cord injury. J Neurotrauma 24, 991-999.

Tator, C.H., Fehlings, M.G. (1999) Review of clinical trials of neuroprotection in acute spinal cord injury. Neurosurgical focus 6, e8.

Tian, D.S., Yu, Z.Y., Xie, M.J., Bu, B.T., Witte, O.W., Wang, W. (2006) Suppression of astroglial scar formation and enhanced axonal regeneration associated with functional recovery in a spinal cord injury rat model by the cell cycle inhibitor olomoucine. Journal of neuroscience research 84, 1053-1063.

Tian, D.S., Xie, M.J., Yu, Z.Y., Zhang, Q., Wang, Y.H., Chen, B., Chen, C., Wang, W. (2007) Cell cycle inhibition attenuates microglia induced inflammatory response and alleviates neuronal cell death after spinal cord injury in rats. Brain Research 1135, 177-185.

Tolias, C.M., Bullock, M.R. (2004) Critical appraisal of neuroprotection trials in head injury: what have we learned? NeuroRx 1, 71-79.

Totoiu, M.O., Keirstead, H.S. (2005) Spinal cord injury is accompanied by chronic progressive demyelination. J Comp Neurol 486, 373-383.

Vela, J.M., Yanez, A., Gonzalez, B., Castellano, B. (2002) Time course of proliferation and, elimination of microglia/macrophages in different neurodegenerative conditions. Journal of Neurotrauma 19, 1503-1520.

Volterra, A., Trotti, D., Tromba, C., Floridi, S., Racagni, G. (1994) Glutamate uptake inhibition by oxygen free radicals in rat cortical astrocytes. J Neurosci 14, 2924-2932.

White, R.J., Reynolds, I.J. (1996) Mitochondrial depolarization in glutamate-stimulated neurons: an early signal specific to excitotoxin exposure. J Neurosci 16, 5688-5697.

Wingrave, J.M., Schaecher, K.E., Sribnick, E.A., Wilford, G.G., Ray, S.K., Hazen-Martin, D.J., Hogan, E.L., Banik, N.L. (2003) Early induction of secondary injury factors causing activation of calpain and mitochondria-mediated neuronal apoptosis following spinal cord injury in rats. Journal of neuroscience research 73, 95-104.

Xiong, Y., Rabchevsky, A.G., Hall, E.D. (2007) Role of peroxynitrite in secondary oxidative damage after spinal cord injury. J Neurochem 100, 639-649.

Xu, G.Y., Hughes, M.G., Ye, Z., Hulsebosch, C.E., McAdoo, D.J. (2004) Concentrations of glutamate released following spinal cord injury kill oligodendrocytes in the spinal cord. Exp Neurol 187, 329-336.

Yanase, M., Sakou, T., Fukuda, T. (1995) Role of N-Methyl-D-Aspartate Receptor in Acute Spinal-Cord Injury. Journal of Neurosurgery 83, 884-888.

Yoshioka, A., Bacskai, B., Pleasure, D. (1996) Pathophysiology of oligodendroglial excitotoxicity. Journal of neuroscience research 46, 427-437.

Zhang, L., Rzigalinski, B.A., Ellis, E.F., Satin, L.S. (1996) Reduction of voltage-dependent Mg2+ blockade of NMDA current in mechanically injured neurons. Science 274, 1921-1923.

Zhao, W., Xie, W., Le, W., Beers, D.R., He, Y., Henkel, J.S., Simpson, E.P., Yen, A.A., Xiao, Q., Appel, S.H. (2004) Activated microglia initiate motor neuron injury by a nitric oxide and glutamate-mediated mechanism. J Neuropathol Exp Neurol 63, 964-977.

CHAPTER 9

PHYSIOLOGICAL AXONAL TRANSPORT

Interest in axonal transport has spiked in the last decade as deficits and disruptions in axonal transport have been implicated in pathological and neurodegenerative motoneuron diseases such as Amyotrophic Lateral Sclerosis (ALS) (e.g. Kieran et al, 2005). However, many questions remain to be answered about physiological transport before pathological transport can be addressed. One such question is the role of multi-motor cooperativity in axonal transport. The published model (Mitchell and Lee, 2009) presented in this section addresses the role of cooperativity and provides the foundation for our work in ALS as presented in Chapter 10.

Because axonal transport is a highly interactive process and because of its small physiological scale over a longer time scale, it is a difficult process to fully characterize experimentally or theoretically. While it works well to study some aspects of axonal transport using a full-fledged, purely mechanistic model on individual motors and cargos in a system aimed to look at population mechanics and behavior, it would limit the types of questions we want to address. Additionally, many of the questions that we wanted to address would have been out of our reach if we were reliant on knowing detailed mechanisms. Thus, a purely traditional mechanistic model was not the best tool to simulate this system. Furthermore, because axonal transport has a large stochastic component and because it lacks the intricate feedback relationships that are seen with, for example, SCI, relational modeling is not an amenable methodology to this system either.

Instead, a hybrid mechanistic-conceptual approach is the method of choice as it provides the easiest means to implement and test higher level functional concepts, such as cooperativity, while maintaining the integrity of underlying mechanistic principles, such as motor kinetics, when possible and efficient.

Briefly, two questions were addressed: 1) What forces do motors experience when transporting a cargo and how do these forces impact their velocity profile(s)? and 2) How many motors of the same polarity (i.e. total number kinesins or total number of dyneins) is necessary to obtain velocity profiles that match those seen experimentally for either fast or slow axonal transport? To answer these questions we combined an adapted stochastic-mechanistic model of motor to microtubule kinetics and two conceptual models to represent the effects of drag force and multi-motor cooperativity on transport velocity. The paper as published in the *Journal of Theoretical Biology* 257(3): 430-437 (Mitchell and Lee, 2009).

Axonal Transport Background

Motoneurons can have extremely long axons, which can extend up to a meter in length (Kandel et al, 2000). Because axons are unable to manufacture their own proteins, axonal transport along the entire length of the axon, from the soma to the synapse and back, is essential to motoneuron function and survival (Goldstein and Yang, 2000). Axons contain microtubules that serve as a railroad for the transport of necessary constituents (including neurotransmitters, organelles, and proteins) needed for cellular

support from the soma to the synapse and the return of proteins destined for degradation from the synapse back to the soma (Figure 1). The transport carriers for this process are the molecular motors kinesin and dynein, which bind the cargos and take them to their destination. Just like the microtubules upon which they bind, kinesin and dynein are directionally polarized. Kinesin is responsible for anterograde transport of cargos from the soma to the synapse whereas dynein is responsible for the retrograde transport of cargos from the synapse back to the soma. Both kinesin and dynein utilize ATP to process along the microtubule. Multiple kinesins or dyneins can carry cargos independently, together, or work in a concerted fashion, the latter two being defined as cooperative transport (Kural et al, 2005).

There are different types of axonal transport, which are categorized based on the directionality and speed of cargo transport, with each type of transport having its preferential cargo types (Brown 2000): Fast anterograde or fast retrograde axonal transport (200-400 mm/day) is largely responsible for the movement of most organelles and larger proteins. Fast bi-directional transport (50-100 mm/day) is mainly responsible for the bi-directional movement of mitochondria throughout the axon, placing them where they are needed as a function of energy requirements and axonal growth. Slow anterograde or slow retrograde transport (0.3-8 mm/day) is typically used to transport cytoskeletal structures such as neurofilaments and some smaller proteins to where they are needed along the axon.

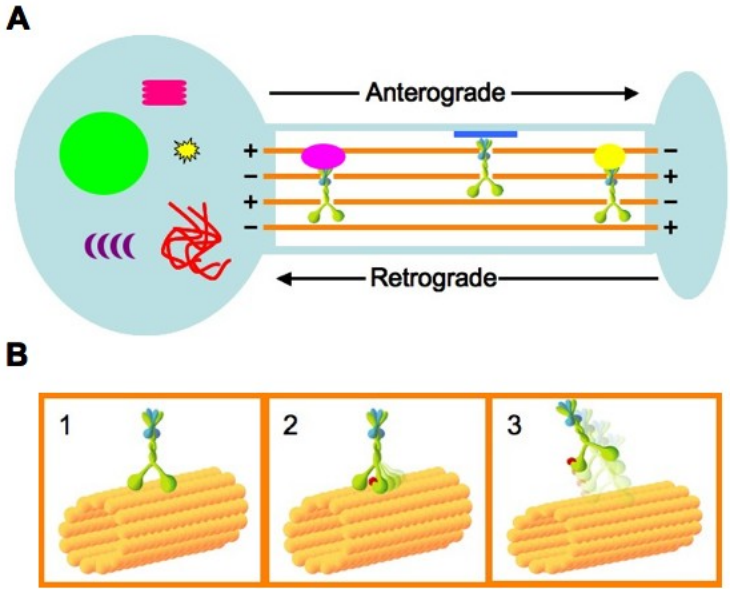

Figure 9.0.1. Overview of axonal transport. (A) Cargos such as proteins, neurofilaments, organelles, and neurotransmitters are transported along polarized microtubules across the entire length of axon via molecular motors kinsesin (anterograde, + end directed motor) and dynein (retrograde, - end directed motor). (B) As shown in (1), a molecular motor is bound to the microtubule track until it acquires a molecule of ATP as shown in (2). For every step, one molecule of ATP is utilized. Due to either a random event or a predetermined chemical signaling event, such as a patch of tau or a phosphorylation site which dictates motor binding events, the motor detaches from the microtubule as shown in (3). Figure 9.0B credit: Special thanks to Brock Wester for the motor binding/unbinding illustrations.

A quantitative examination of the role of cargo-exerted forces in axonal transport

Journal of Theoretical Biology 257(3): 430-437

doi:10.1016/j.jtbi.2008.12.011

http://www.sciencedirect.com/science/journal/00225193

Contributions of the authors

Cassie Mitchell developed the conceptual drag force and cooperativity sub-models, applied and implemented the sub-models and the overall motor-cargo model, performed the simulations and analysis, and wrote the manuscript. Dr. Robert Lee contributed to the drag force sub-model, assisted in the implementation of the event-based simulator, and co-edited the manuscript.

Abstract

Axonal transport, via molecular motors kinesin and dynein, is a critical process in supplying the necessary constituents to maintain normal neuronal function. In this study, we predict the role of cooperativity by motors of the same polarity across the entire spectrum of physiological axonal transport. That is, we examined how the number of motors, either kinesin or dynein, working together to move a cargo, results in the experimentally determined velocity profiles seen in fast and slow anterograde and

retrograde transport. We quantified the physiological forces exerted on a motor by a cargo as a function of cargo size, transport velocity, and transport type. Our results show that the force exerted by our base case neurofilament (D_{NF}=10nm, L_{NF}=1.6μm) is ~1.25pN at 600nm/s; additionally, the force exerted by our base case organelle (D_{Org}=1μm) at 1,000nm/s is ~5.7pN. Our results indicate that while a single motor can independently carry an average cargo, cooperativity is required to produce the experimental velocity profiles for fast transport. However, no cooperativity is required to produce the slow transport velocity profiles; thus, a single dynein or kinesin can carry the average neurofilament retrogradely or anterogradely, respectively. The potential role cooperativity may play in the hypothesized mechanisms of motoneuron transport diseases such as Amyotrophic Lateral Sclerosis (ALS) is discussed.

Keywords

neurofilament, axoplasm, microtubule, computational model, cooperative transport, drag force

Introduction

With axons being unable to manufacture their own proteins, axonal transport is a critical process responsible for providing essential cellular parts and materials throughout the entire axon and for returning molecules destined for degradation back to the lysosomes in the soma (Sabry et al. 1995). For a review of axonal transport, see (Goldstein and Yang 2000). With numerous recent experimental investigations pointing to the potential role of axonal transport in such devastating motoneuron diseases as Amyotrophic Lateral

Sclerosis (ALS) (Pantelidou et al. 2007; Rao and Nixon 2003; Zhang et al. 2007), Spinal Muscular Atrophy (Briese et al. 2005), and Charcot-Marie-Tooth disease (Brownlees et al. 2002; Lupski 2000), there is an ongoing effort to reveal the pathological mechanisms resulting in associated transport defects. However, many questions remain regarding the physiological mechanisms of axonal transport, and the answers to these questions lie in the path of our full understanding of transport-related diseases.

One such question has been the identification and subsequent characterization of cooperative movement of cargos by multiple motors, which equally share load force. That is, how many motors does it take to move a cargo, and if and how is cooperativity affected by cargo type/size and transport speed? Although it has been suggested that cooperativity does exist (Alano et al. 2002; Ashkin et al. 1990; Klumpp and Lipowsky 2005; Kural et al. 2005), experimental validation has proven difficult. Most work examining cooperativity has focused on the cooperative movement between motors of opposite polarity (Alano et al. 2002; Kural et al. 2005) (i.e. dynein and kinesin moving a cargo in a concerted fashion) rather than the cooperativity of multiple same polarity kinesins or dyneins working to move a cargo either anterogradely or retrogradely, respectively. While optical trap experiments have characterized the maximum forces a molecular motor can withstand (Alano et al. 2002; Ashkin et al. 1990; Coppin et al. 1995), little is known as to how these measured forces compare to what physiological forces a motor may experience when carrying cargos. Therefore, it has been difficult to determine the number of motors necessary to overcome the forces imposed by moving a given cargo.

In this study, we quantitatively examine the role of same polarity multi-motor cooperativity as a function of cargo type/size, transport velocity, and transport type. We determine the forces imposed on a molecular motor under a wide physiological range of parameters. Using these calculated forces in combination with an adapted version of an experimentally-derived kinetic model (Craciun et al. 2005), which accurately describes the appropriate states of the motor as it processes along the microtubule, we were able to quantify and characterize molecular motor cooperativity over established, experimentally determined, fast (200-400 mm/day) and slow transport (0.3-8 mm/day) ranges (Brown 2000; Brown et al. 2005; Kural et al. 2005; Shea and Flanagan 2001; Wang et al. 2000). Our results indicate under certain transport scenarios, cooperativity is necessary to achieve fast transport, but its role in slow transport is minimal. Furthermore, our results suggest the potential for a substantial impact of cooperativity in transport disease pathologies.

Methods

The two most characterized cargo types are the neurofilaments, which undergo slow transport, and mitochondria, which undergo fast bi-directional transport. Thus, we choose to focus the majority of our study on these two cargo populations. Table 1 lists the experimental velocity transport ranges for most common types of hypothesized and known cargo types.

Table 9.1.1. Experimentally determined transport ranges and known/hypothesized transport types (adapted from Brown (Brown 2000)).

Transport Type	Velocity (mm/day)	Velocity (mm/s)	Example Cargo Type(s)
Fast			
--Anterograde	200-400	2.31-4.63	Golgi-derived vesicles, tubules, neurotransmitters
--Retrograde	200-400	2.31-4.63	enodosomes, lysosomes
--Bidirectional	50-100	0.58-1.16	mitochondria
Slow			
--Component A	0.3-3	0.003-0.035	neurofilaments
--Component B	2-8	0.02-0.08	microfilaments, actin

The general strategy was to determine the force imposed by various cargo types and to use this information to determine the number of bound motors required to move a specific cargo type at transport velocity ranges that match those determined experimentally using optical traps (Coppin et al. 1995). This general strategy is based on: 1) determining the force imposed by the cargo by calculating the drag force as a function of velocity and cargo geometry; 2) assuming the drag force is equivalent to the maximum force exerted by the cargo on the molecular motor; and 3) determining the velocity distributions for various cargo sizes and types undergoing transport by a specified number of bound motors using the appropriate transport kinetics to describe the interaction of the molecular motors with the microtubule for each specific transport type.

Drag Force Calculation

The drag force imposed by a cargo was represented by simplified equations derived from the Stokes-Einstein equation for a particle at a low Reynolds number, $Re<<1$ (Berg 1993; Truskey et al. 2003). The relationship of drag force, (F_D), to velocity (V) for an arbitrarily shaped particle is described by Equation 1 where f is the frictional coefficient:

$$F_D = f \cdot v \qquad \textbf{Equation 9.1.1}$$

The geometry-specific frictional coefficient, f, for a cylindrical neurofilament is calculated using Equation 2 (Truskey et al. 2003) where L_{NF} is length, D_{NF} is diameter, and μ is viscosity of the surrounding cytoplasm (sometimes referred to as the axoplasm).

$$f = \frac{4\pi\mu L_{NF}}{\ln\left(L/(D_{NF}/2)\right) + 0.193} \qquad \textbf{Equation 9.1.2}$$

Organelles carried in fast transport, such as mitochondria, are known to have a spherical geometry and were modeled as simple spheres. The simplified geometry-specific frictional coefficient for a spherical organelle is given by Equation 3 (Berg 1993) where D_{org} is the diameter of the organelle.

$$f = 6\pi\mu\left(D_{org}/2\right) \qquad \textbf{Equation 9.1.3}$$

The maximum allowable drag force is calculated by multiplying the number of bound motors, N_B, by their maximum force, F_s, for the appropriate motor type (Equation 4). A motor's maximum force can be assumed to be its measured "stall" force. (The stall force

is the opposing force needed to slow a motor to zero velocity.) The stall force has been experimentally determined to be ~1.2 pN for dynein (Gao 2006; Schmitz et al. 2000) and ~5.65 pN for kinesin (Coppin et al. 1995; Kural et al. 2005) at physiological concentrations of available ATP; thus, we use these average experimental values of F_s in the this study.

$$F_{D_{MAX}} = F_s \cdot N_B \qquad \textbf{Equation 9.1.4}$$

The velocity of an individual cargo was determined by substituting the maximum drag force ($F_{D,MAX}$) in Equation 4 for the drag force (F_D) in Equation 1. Thus, the cargo velocity calculation is given by Equation 5.

$$V = F_{D_{MAX}} / f \qquad \textbf{Equation 9.1.5}$$

Determination of drag force parameters.

Much care was taken to obtain values for all four of the drag force calculation parameters over their physiological ranges (see Table 2). Three such aforementioned parameters describe cargo geometry: the diameter of either an organelle (D_{org}) or a neurofilament (D_{NF}) and the length of a neurofilament (L_{NF}). Neurofilaments have been determined to be approximately 10nm in diameter (Lupski 2000), but their lengths have not yet been precisely determined. Neurofilaments are thought to be transported in their polymerized form, which implies that they could reach great lengths, ~1-3μm (Brown 1998; Trivedi et al. 2007; Wagner et al. 2004), with an average around 1.8 μm. Neurofilaments contain "branches" or "side arms" due to the neurofilament medium and

heavy subunits (NF-M and NF-H, respectively), which provide the cross-linking and phosphorylation interaction and regulation sites (Marszalek et al. 1996). However, we chose to assume a simpler, plain cylindrical shape to model the neurofilament geometry. As shown in the results, increasing the diameter to include the side arms has a minimal impact on the calculated force. The size of fast transport particles can vary from the nanometer to micrometer scale. The average size of mitochrondria is about 1 μm. Note that 'reasonable' instantaneous velocities (i.e. velocities < ~3000 nm/s over a time period of ~ 5 seconds as shown by an invivo study slow transport of neurofilaments (Brown et al. 2005) and by an invivo study of quantum dot labeled fast transport (Yoo et al. 2008)) can only be attained with organelle diameters greater than approximately 200 nm. Diameters smaller than this are assumed to be kinetically limited, rather than force limited and thus are not included in this study.

The fourth drag force parameter is the viscosity of the surrounding cytoplasm (or axoplasm). Due to the anisotropic properties of the cytoplasm, a precise determination of viscosity is very difficult. Bulk cytoplasm contains ~20% protein, which contributes to physical properties that mimic a weakly viscoelastic gel (Hou et al. 1990). This gel is a result of the combined properties of the actin protein network, which provides cytoskeletal structure and support and the cytoplasmic fluid itself which is about 80% water (Hou et al. 1990). Cytoplasmic viscosity measurements that do not include the protein/ actin component can be as small as 0.06 Poise (Haak et al. 1976). However, viscosity measurements which look at the total cytoplasmic viscosity (actin + fluid) can

be orders of magnitude higher (Keller et al. 2003). Using data from (Keller et al. 2003), we estimate the viscosity to be about 6 Poise (or 0.6 Pa•s).

Table 9.1.2. Base parameter values, ranges, and references used for calculating drag force. Note that the higher end of the neurofilament diameter range includes side arms, and that viscosity is that of measurements which include the cytoplasmic protein network in addition to the cytoplasmic fluid itself.

Parameter Name	Base	Primary Physiological Range	Primary References
Viscosity, m (Poise)	6	unknown (see Methods)	(Keller et al. 2003)
Neurofilament length, L_{NF} (mm)	1.6	1-3	(Trivedi et al. 2007; Wagner et al. 2004)
Neurofilament diameter, D_{NF} (nm)	10	10-50	(Marszalek et al. 1996)
Organelle diameter, D_{Org} (nm)	1	200-2000	(Freitas 2003)
Velocity, v (mm /s)	1	0.25-3	(Brown et al. 2005; Klumpp and Lipowsky 2005; Kural et al. 2005; Visscher et al. 1999)

Motor to microtubule binding kinetics

We adapt transport kinetics described by Craciun et al. (2005) in order to obtain physiological average velocities that take into account different possible motor-

microtubule kinetic states. This scheme, as shown in Figure 1, describes both retrograde and anterograde transport using the following five states: S_O) off-track, paused; S_{KP}) kinesin, on-track, paused; S_{DP}) dynein, on-track, paused; S_{KM}) kinesin, on-track, moving anterogradely; S_{DM}) dynein, on-track, moving retrogradely. The scheme is such that a cargo must disengage from the track before switching directions, and it must pass through an on-track paused state before moving.

We implement the kinetic scheme using event-based simulation (Banks et al. 2005), a method that speeds simulation time by avoiding unnecessary repetitive calculations by predicting how long a cargo will remain in the same state. The expected duration of each possible state, t_{state}, is calculated by multiplying the inverse of the state's rate constant, k, by the natural log of a random number, *rand*, in the range 0-1 exclusive giving:

$$t_{state} = -1/k \cdot \ln(rand) \qquad \textbf{Equation 9.1.6}$$

The form of Equation 6 is chosen to fit the exponential first order process that is apparent in experimental data (Wang and Brown 2001) as published in Table 1 of (Brown et al. 2005). The state with the shortest duration becomes the next state for that cargo. Based on the duration of the cargo's current state and the current time in the simulation, a sorted list determines when each cargo should be re-evaluated so that not every cargo need be evaluated at every time step.

Rate constants for slow transport were adjusted from those originally published by (Craciun et al. 2005) (i.e. λ and γ and were varied while all other parameters were held constant) to fit our model implementation and still match the original outputs (for derivation details, see (Craciun et al. 2005)). Briefly, γ and λ were tuned such that the histogram of cargo velocities for a neurofilament matched those presented in Table 1 of (Brown et al. 2005) for an equivalent simulated period of 4.74 seconds, giving $\gamma = 2.5$ and $\lambda = 0.1$.

The same Craciun kinetic model, with different rate constants, was used to obtain fast transport kinetics. It has been shown that slow transport is 'slow' because of the long on- and off-track pauses that occur over a longer period, making the actual movement of slow transport fast, but asynchronous and intermittent (Brown 2000; Brown et al. 2005). Thus, the instantaneous velocity ranges during the moving states (S_{KM} and S_{DM}) for transient movement during slow transport are relatively similar to that of fast transport, but the amount of time spent in the paused and off-track states (λ and γ respectively; see figure 1) differs.

Another potential difference between slow and fast transport Craciun kinetics concerns the directionality of cargos. In the case of slow transport, the directionality of neurofilaments was found to be *net* anterograde with a ratio of anterograde to retrograde movement approximately 2:1, resulting in a kinetic rate coefficient specifying the directionality to be 69/31 as illustrated in Figure 1. In the case of fast transport of mitochondria, the net directionality is a function of axonal growth. During axonal growth

the direction of movement is net anterograde, and in non-growing periods the direction of movement is net retrograde (Morris and Hollenbeck 1993). Nonetheless, the directionality ratio was similar to that of slow transport for separate net anterograde and retrograde populations. That is, the rate of anterograde to retrograde movement is on average about 2:1 for a net anterograde population and approximately 1:2 for a net retrograde population (Morris and Hollenbeck 1993). To take into account this difference in directionality, *net* anterograde and *net* retrograde populations were modeled separately for fast axonal transport.

Given that the directionality rate coefficients for fast transport are known, the kinetics described by the Craciun model can be made fast by simply adjusting the rate constants governing how long a cargo spends in the paused or off-track states (λ and γ). To simulate fast transport, the rate parameters, λ and γ, were adjusted or 'tuned' (i.e. λ and γ and were varied while all other parameters were held constant) until the average velocity of a population of cargos with a single bound motor ($N_B = 1$) over the duration of the entire simulation matched that seen experimentally (Visscher et al. 1999). These adjustments ($\gamma = 0.2$ and $\lambda = 10$) increase the amount of total time spent in the moving states and decrease the amount of overall time spent in the paused and off-track states. Using these adjustments, the fast transport of net anterograde and net retrograde populations were modeled. This adjustment of kinetic parameters to match fast experimental transport data was based on neurofilament cargos undergoing net anterograde fast transport both for consistency and in an attempt to keep the cargo sizes small (neurofilament cargos produce forces that are equivalent to ~250 nm spherical or

organelle cargo). Keeping the cargo sizes on the smaller end of the physiological and force-limited range kept the analysis of kinetics to be independent from that of cooperativity. Rate constants were tuned such that the net anterograde population of cargos, each being carried by a single motor ($N_B = 1$), had an average velocity equal to that shown by analysis of single kinesin molecules undergoing fast transport as studied under molecular clamp (~ 1 μm/s) (Visscher et al. 1999).

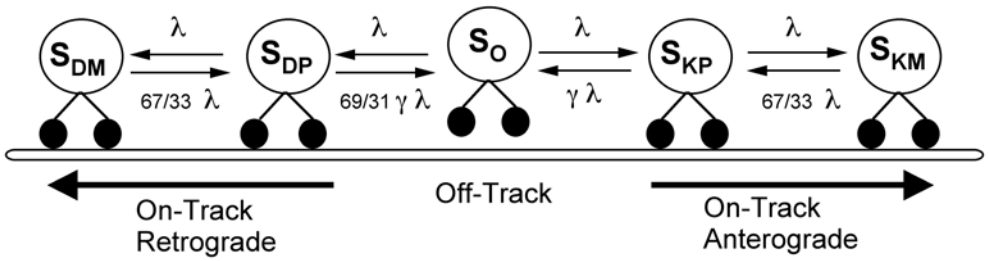

Figure 9.1.1. The motor-microtubule binding kinetics are adapted from Craciun et al (Craciun et al. 2005). The model contains five states, *S*, which are differentiated using the following subscript nomenclature: *P* represents a paused motor (i.e. $V = 0$), *M* represents a moving motor (i.e. $V > 0$), *K* represents the molecular motor kinesin, *D* represents the molecular motor dynein, and *O* represents an off-track motor. Using this nomenclature, we obtain the following states: S_O) off-track, paused; S_{KP}) kinesin, on-track, paused; S_{DP}) dynein, on-track, paused; S_{KM}) kinesin, on-track, moving anterogradely; S_{DM}) dynein, on-track, moving retrogradely. Rate constants are shown in parameter-form as given in Craciun et al (Craciun et al. 2005). The tuned slow transport rate parameters are $\gamma = 2.5$ and $\lambda = 0.1$. Fast transport rate parameters are $\gamma = 0.2$ and $\lambda = 10$. For details regarding the derivation of rate constants and equations, see Craciun et al (Craciun et al. 2005).

Model Implementation

The entire model, including the calculation of drag force and motor kinetics is implemented in MATLAB 2007a (The Mathworks, Inc.). Simulations were repeated for 1,000 cargos to obtain the histogram velocity profiles. For validation purposes, the

simulated time frame was 4.74 (or ~5) seconds, a time frame that is equivalent to the time frames and resolution of previous published experimental studies (Alano et al. 2002; Ashkin et al. 1990; Wang et al. 2000).

Results

Cargo imposed forces (i.e. drag force)

Geometry, viscosity, and velocity data taken from experimental studies were used to determine the average drag force for both neurofilaments (typical slow transport cargos) and organelles (typical fast transport cargos). Note that from here forward, we use "drag force" and "cargo imposed force" interchangeably (see assumptions in the Methods). The drag force exerted by the base case neurofilament (D_{NF}=10nm, L_{NF}=1.6μm) is ~1.25pN at 600nm/s; additionally, the drag force exerted by the base case organelle (D_{Org}=1μm) at 1,000nm/s is ~5.7pN. These values are functionally significant in that they align well with the experimentally determined maximum forces of kinesin and dynein (see Discussion).

Figure 2 shows the relationship between the drag force and each parameter over its physiological range based on Equation 2 for neurofilaments and Equation 3 for organelles. In general, the physiological range of calculated drag force is between 0.1-4 pN for a neurofilament and between and 0.3-10 pN for an organelle. Viscosity has a potentially wide range depending on how it is measured (see determination of drag force parameters in the Methods). However, viscosities lower than ~5 Poise or greater than ~7

Poise results in highly unrealistic velocity distributions (not shown). As for geometry, the spherical organelle diameter has the largest impact. Notably, increasing the diameter of the cylindrical neurofilament to include the side arms of NF-H subunits does not have a dramatic effect on the resulting drag force, increasing it by only ~25%, thereby justifying the simpler cylindrical geometry excluding side arms (see Methods). While the physiological range of transport is, for the most part, between 1,000-3,000 nm/s, speeds up to 12,000 nm/s for a peroxisome have been observed (Kural et al. 2005), a velocity that would result in a ~68 pN drag force.

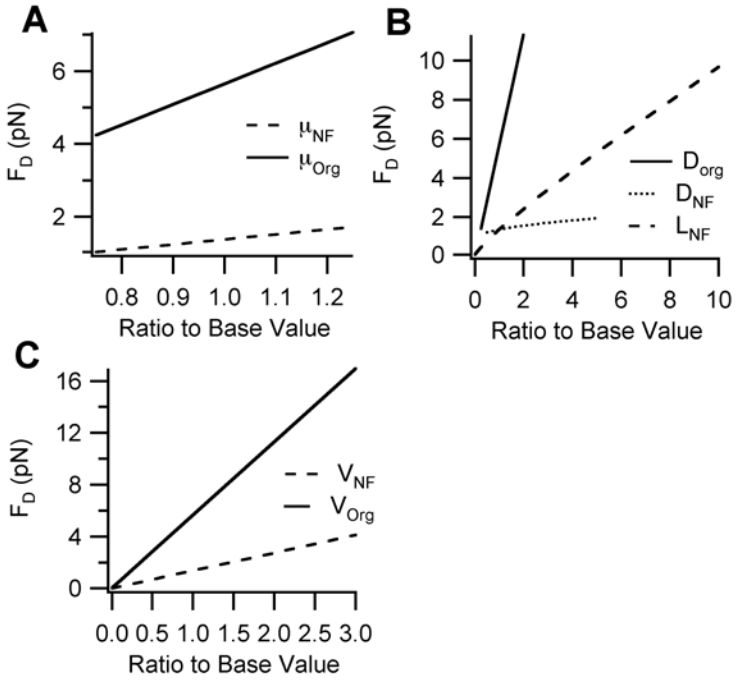

Figure 9.1.2. Range of drag force (F_D) over physiologically relevant parameter ranges for cytoplasmic viscosity (m), cargo geometry, and cargo transport velocity (*V*) as listed in Table 2 for both a neurofilament and an organelle. The x-axis 'ratio to base value' refers to the ratio of the base parameter value given in Table 2. A. Effect of cytoplasmic viscosity. B. Effect of cargo geometry: the diameter and length of a cylindrical neurofilament (D_{NF}) and the diameter of a spherical organelle (D_{Org}). C. Effect of cargo velocity.

Effect of Cooperativity

Using the force values calculated for organelles and neurofilament transport along with the appropriate fast or slow transport kinetics, the number of bound molecular motors required to achieve a velocity profile matching experimentally measured velocity ranges was determined for each transport type: fast anterograde and retrograde, 'bi-directional' anterograde and retrograde, and 'net anterograde' slow transport. The number of required bound motors to obtain the average velocity for each form of fast transport is illustrated in Figure 3 and summarized in Table 3.

Table 9.1.3. Number of bound motors (N_B) required for various experimentally determined fast transport speeds and cargo sizes. For experimental range categories, refer to Table 1.

Average Velocity (mm/day)	**Average Velocity (mm/s)**	**Cargo Diameter (nm)**	**N_B Retro-grade**	**N_B Antero-grade**
50-100	0.58-1.16	500	5-7	1-2
50-100	0.58-1.16	1000	11-14	2-3
200-400	2.31-4.63	200	9-12	2-3
200-400	2.31-4.63	300	12-15	3-4
200-400	2.31-4.63	500	26-30	6-8

Fast transport

For fast bidirectional anterograde transport of a 1 μm organelle (Figure 3A), 2 motors results in an average velocity of 0.68 μm/s (59 mm/day) with a standard deviation of 0.11 μm/s (9 mm/day). For 3 motors (not shown) the average velocity is 0.97 μm/s (80

mm/day) with a standard deviation of 0.15 μm/s (13 mm/day). Thus, both 2 and 3 motors result in profiles that could be classified as being within the experimentally observed range of 50 to 100 mm/day if the experimentally observed range is assumed to include at least the middle two standard deviations (i.e. +/- 1 standard deviation). Likewise, 11-14 motors result in profiles that could be classified as being within the experimentally observed range of 50 to 100 mm/day for fast bidirectional retrograde transport of a 1 μm organelle (see Figure 3B). For fast anterograde and retrograde transport (200-400 mm/day) of a 200 nm organelle, the number of motors required is 2-3 and 9-12, respectively (Figures 3C and 3D). Interestingly, the number of bound motors for an anterogradely moving 200 nm organelle is comparable to what has been suggested experimentally for amoeba mitochondria of approximately the same size (Ashkin et al. 1990). In general, the results in Table 3 illustrate that a substantially lesser amount of cooperativity is required for fast anterograde versus retrograde transport. That is, a higher degree of cooperativity is required to retrogradely move cargos, particularly larger cargos, at the top fast transport speeds. The large calculated values for retrograde cooperativity suggest a functional role for the lower stall force of dynein in sorting and maintaining proper transport directionality and give clues as to the types and characteristics of retrogradely-bound cargos (see Discussion).

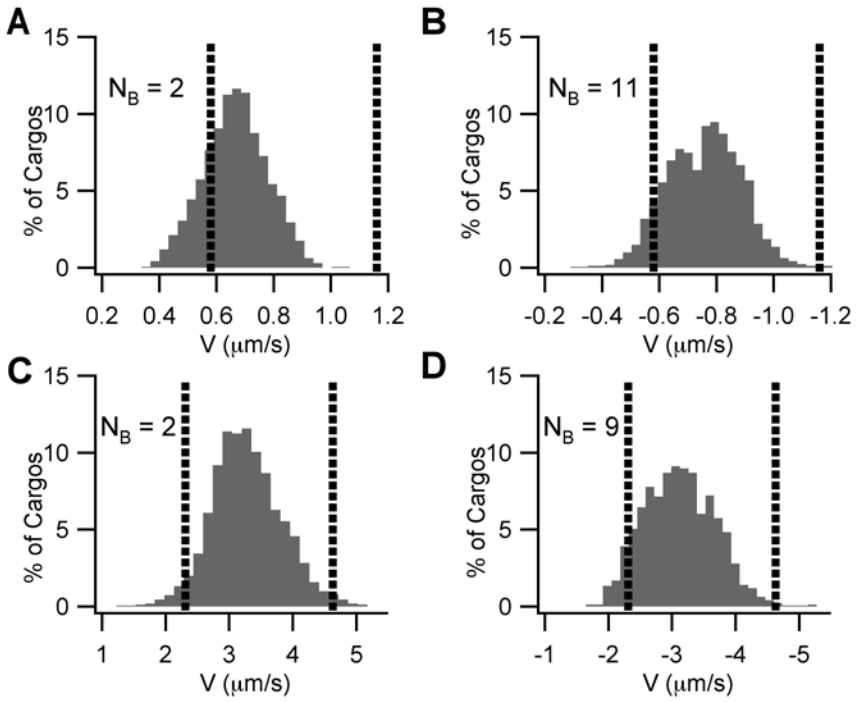

Figure 9.1.3. Velocity distributions over fast axonal transport ranges. Anterograde transport by kinesin is represented by a positive sign convention while retrograde transport by dynein is represented by a negative sign convention. The distributions represent the average velocity of a population of cargos over the 4.74 second simulated period. The figure represents the minimum number of bound motors (N_B) required to obtain a population of cargos whose average velocity is approximately centered at the average of the experimental ranges shown in Table 1. Vertical lines represent the edges of the experimental velocity ranges shown in Table 1. The ordinate indicated the normalized percentage of cargos which fall within each velocity bin. **A.** Anterograde populations of 1mm spherical cargos representative of the 'bi-directional' transport range of ~0.58-1.16 mm/s (e.g. 50-100 mm/day) require greater than 2 bound kinesin motors per cargo. **B.** Retrograde populations of 1mm spherical cargos representative of the 'bi-directional' transport range of 0.58-1.16 mm/s (e.g. 50-100 mm/day) require 11 bound dynein motors. **C.** Anterograde populations of 200 nm spherical cargos representative of the fast transport range of ~2.31-4.63 mm/s (e.g. 200-400 mm/day) is obtained by a minimum of 2 bound kinesin motors per cargo. **D**. Retrograde populations of 200 nm spherical cargos representative of the fast transport range of ~2.31-4.63 mm/s (e.g. 200-400 mm/day) is obtained by a minimum of 9 bound dynein motors per cargo.

Slow transport

Slow transport of neurofilaments is net anterograde, with movements being in the anterograde direction 69% of the time and in the retrograde direction 31% of the time (Brown et al. 2005; Craciun et al. 2005), but due to the amount of time spent paused and off-track, there is little to no distinction between 'retrograde' and 'anterograde' populations. The slow transport velocity profile for a population of neurofilaments (L_{NF}=1.6 μm and D_{NF} = 10nm) is equivalent the profiles published in (Brown et al. 2005), with 83% of the motors being paused over a simulated period of 4.74 seconds (Figure 4). Across the physiological range of neurofilament lengths (~1-3 μm), no cooperativity is required (i.e. within two standard deviations of experimental data). However, the best fit to experimental data is obtained when a fraction of neurofilaments have two motors bound, particularly for neurofilaments lengths ≥2 μm. For example, to duplicate the velocity distribution given in (Brown et al. 2005) for a population of 2 μm neurofilaments, transport is accomplished with a single motor ~67% of the time and two motors ~33% of the time.

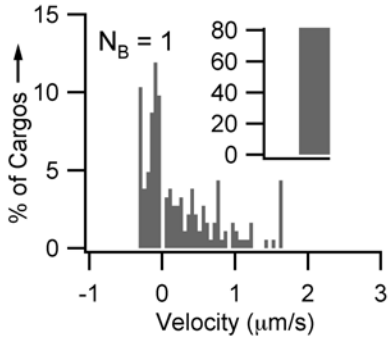

Figure 9.1.4. Slow transport of neurofilaments. To obtain an experimentally equivalent velocity profile for slow transport of neurofilaments, no cooperativity is required. That is, only one bound motor is needed per cargo. The figure shows the velocity histogram of a population of average-sized neurofilaments (L_{NF} =1.6 mm and D_{NF} = 10 nm). Note that for visual clarity the zero velocity bin (0 mm/s) as been moved to the inset. Thus, the inset shows the number of cargos that remained paused during the length of the simulation (i.e. ~83% of cargos had velocities equal to 0 mm/s over the 4.74 second simulated period, similar to the 85% seen experimentally (Brown et al. 2005)).

Summary of Predictions

As we have shown, using a computational model that includes kinetics and cooperativity, we are able to reproduce the experimentally determined velocity ranges for the various fast and slow transport types. However, an important aspect of any model is the ability to make specific predictions regarding previously uncharacterized dynamics or functions. Here we use our simulations to predict the following:

- The physiological range of values for both velocity and geometry have substantial impacts on the cargo drag force (Figure 2). While there is a large potential range for cytoplasmic viscosity, which in turn would drastically alter

the calculated drag forces, only the smaller simulated range (Figure 2) has an impact that mimics physiological forces that match experimental velocities.

- Cooperativity is required by motors of the same polarity to produce fast transport profiles (Figure 3). Thus, multiple motors are required for typical physiological fast transport.
- No cooperativity is required by motors of the same polarity to produce slow transport profiles (Figure 4). Neurofilaments are carried anterogradely or retrogradely by a single kinesin or dynein most of the time.

Discussion

In this study, we provide an initial quantitative characterization of cooperativity, including an assessment of the forces experienced by the molecular motors kinesin and dynein under physiological ranges of cargo type/size and transport velocity. Our results indicate that kinesin and dynein are ideally suited to transport the *average* cargo at the *average* speed for slow transport and *smaller* cargos at the *average* speed for fast transport without the need for cooperativity. However, cooperativity is crucial, particularly in fast transport, to obtain the full range of velocities observed experimentally. These results not only indicate possible functional outcomes of cooperativity in the regulation and maintenance of normal physiological transport, but also reveal its potential role in hypothesized pathological mechanisms of transport deficits associated with diseases such as ALS. The details and implications of these results are discussed below.

Physiological role of cooperativity

Our results show that the drag force exerted by our base case neurofilament and organelle are 1.25 pN and 5.7 pN, respectively. It is likely no coincidence that these forces are near the experimental stall forces for a single dynein and kinesin, 1.2 pN (Gao 2006) and 5-6 pN (Coppin et al. 1995), respectively. Thus, it would seem that the "stall" or maximum generated forces are such that a single motor is generally able to carry the average neurofilament load; a single kinesin can move an average organelle at speeds up to 1 μm/s while a single dynein reaches top speed with such an organelle cargo at ~200 nm/s. These results support the experimental evidence that slow transport of neurofilaments is accomplished by a single motor of each type (Howard et al. 1989), i.e. one kinesin for anterograde movement and one dynein for retrograde movement, and that larger organelle cargos undergoing fast transport require multiple motors (Kural et al. 2005), i.e. multiple kinesins or dyneins for anterograde or retrograde movement, respectively. This inherent ability of a single motor to be able to move a load is likely a key factor helping to maintain axonal traffic by preventing the pile-up of motors and/or cargos, which would occur if multiple motors would be required to move every single cargo. Though cooperativity is not required to simply move an average cargo, it is required to move cargos at higher rates of speed and larger cargo sizes, particularly in the retrograde direction. The ability of cooperativity to alter and organize the speeds of various cargo types traveling in a specific direction could be quite functional, serving as a potential 'pacing' mechanism to prioritize which cargos are moving when and how fast.

The approximately five-fold difference between the stall forces of dynein and kinesin accounts for the equivalent linear increase in cooperativity that is required for dynein compared to kinesin. This difference could have a functional purpose in that it helps the directionality and speeds of the transported cargos, aiding in transport kinetics. That is, a bigger cargo headed anterogradely will tend to remain headed anterogradely due to the larger number of bound dyneins that would be required for it to reverse direction (i.e. the availability of dynein and their probability of binding is rate-limiting to the reverse reaction). However, it could be that this difference simply indicates that, in general, retrogradely transported cargos are smaller. It seems rather unlikely, for example, that 14 dyneins would routinely bind to carry a larger cargo such as an organelle at top fast transport speeds of 400 mm/day. Such extreme necessity for cooperativity involving very high-order kinetics would likely become an energetic burden resulting in possible local ATP depletion and ultimately a motor-limited transport process that would be extremely erratic and slow. Having smaller retrograde cargos would seem to make intuitive sense given that most retrograde bound cargos are hypothesized to be destined to the lysosomes for degradation. Thus, these cargos may have already undergone some preliminary form of degradation into smaller subunits or pieces at the synapse or in the axon.

An interesting possibility is that the difference between fast and slow transport is not attributable to kinetics at all, but rather is based entirely on cooperativity. A simple calculation indicates that fast transport speeds can be attained with slow transport kinetics applied to multiple motors acting cooperatively. However, further investigation of the

interactions of multiple motors and their resulting kinetics will be necessary to decisively determine whether cooperativity can solely account for the differences seen in fast and slow transport.

Pathological role of cooperativity

The apparent role of cooperativity and its necessity, particularly in fast transport and in carrying larger cargos, increases the negative impact of potential hypothesized pathological mechanisms associated with disease-related transport deficits. For example, some experimental models of ALS have been linked to mutations in either dynein or kinesin (Brownlees et al. 2002; Hafezparast et al. 2003; Hurd and Saxton 1996; Teuchert et al. 2006), which render a subpopulation of the motors ineffective (Jiang et al. 2005; Pantelidou et al. 2007; Rao and Nixon 2003). A decrease in the number of functional motors available for transport would decrease the functional capability of cooperativity as transport became motor-limited, resulting in subsequent transport deficits. In fact, one hypothesis for the therapeutic action of the ALS therapeutic drug riluzole is that by decreasing the excitability of neurons (Kuo et al. 2006), riluzole decreases the demand for axonal transport of cargos such as mitochondria and synaptic vesicles. Such a pharmacological action would help to compensate in the disease-related increase in necessary cooperativity. Another hypothesized pathological mechanism for which there is some experimental evidence is protein aggregation (Kieran et al. 2005; Wood et al. 2003). Protein aggregation could potentially increase the cargo sizes, via pathways such as misfolding or in the formation of dimers (Elam et al. 2003). Additionally there is the possibility for aggregation of multiple cargos into a single ‘megacargo’ due to the pile-up

caused by slowed transport or a change in the inter-cargo distances, potentially due to changes in the stoichiometric composition of NF-H subunits (Meier et al. 1999), which normally regulates such spacing. Thus, protein aggregation would necessitate additional cooperativity, which would eventually lead to a constrained motor population unable to keep up with demand. Therefore, in summary, while cooperativity can potentially add more robustness and functionality to normal physiological transport, it can also amplify the impairments and deficits in pathological transport.

Model Limitations

Perhaps the biggest limitation of the model is that it assumes the velocity of a cargo is limited by the force imposed by the cargo (i.e. the drag force) and not by the kinetics, themselves. For example, despite the fact that the drag force is much smaller for smaller cargos (such as cargos < 200 nm diameter cargo), the kinetics could impose a limitation such that these smaller cargos travel at or about the same speed as larger cargos (i.e. there is a motor kinetically-determined maximum velocity). More generally stated, this assumption implies that the solution presented here could be non-unique in that different sets of force and kinetic contributions and/or parameters could result in the same experimentally observed velocity profiles and/or the same amount of calculated cooperativity.

Another limitation of the model is the chosen Craciun kinetic scheme, which requires that a cargo go off-track before switching directions. Very recent evidence has suggested that

perhaps the cargo does not have to fully disengage from the track in order to switch directions (Muller et al. 2008). It has been proposed that the effective cargo unbinding rate decreased exponentially with the number of bound motors (Klumpp and Lipowsky 2005). However, it is unclear if that applies only during motor over crowding or more generally. Consequently, we chose to keep the binding rate constant to maintain independent analysis of cooperativity from kinetics

Acknowledgements

This work is supported by the National Science Foundation (NSF) via a Graduate Research Fellowship and an Integrative Graduate Education and Research Traineeship Fellowship (DGE-0333411) to C.S.M. and by the Human Brain Project (NINDS, NIMH and NIBIB NS046851) to R.H.L.

References

Ashkin, A., Schutze, K., Dziedzic, J.M., Euteneuer, U., and Schliwa, M., 1990. Force generation of organelle transport measured in vivo by an infrared laser trap. Nature 348, 346-8.

Banks, J., Carson, J., Nelson, B., and Nicol, D., 2005. Discrete-event system simulation Pearson.

Berg, H., 1993. A Random Walk in Biology. Princeton.

Briese, M., Esmaeili, B., and Sattelle, D.B., 2005. Is spinal muscular atrophy the result of defects in motor neuron processes? Bioessays 27, 946-57.

Brown, A., 1998. Contiguous phosphorylated and non-phosphorylated domains along axonal neurofilaments. J Cell Sci 111 (Pt 4), 455-67.

Brown, A., 2000. Slow axonal transport: stop and go traffic in the axon. Nat Rev Mol Cell Biol 1, 153-6.

Brown, A., Wang, L., and Jung, P., 2005. Stochastic simulation of neurofilament transport in axons: the "stop-and-go" hypothesis. Mol Biol Cell 16, 4243-55.

Brownlees, J., Ackerley, S., Grierson, A.J., Jacobsen, N.J., Shea, K., Anderton, B.H., Leigh, P.N., Shaw, C.E., and Miller, C.C., 2002. Charcot-Marie-Tooth disease neurofilament mutations disrupt neurofilament assembly and axonal transport. Hum Mol Genet 11, 2837-44.

Coppin, C.M., Finer, J.T., Spudich, J.A., and Vale, R.D., 1995. Measurement of the isometric force exerted by a single kinesin molecule. Biophys J 68, 242S-244S.

Craciun, G., Brown, A., and Friedman, A., 2005. A dynamical system model of neurofilament transport in axons. J Theor Biol 237, 316-22.

Elam, J.S., Taylor, A.B., Strange, R., Antonyuk, S., Doucette, P.A., Rodriguez, J.A., Hasnain, S.S., Hayward, L.J., Valentine, J.S., Yeates, T.O., and Hart, P.J., 2003. Amyloid-like filaments and water-filled nanotubes formed by SOD1 mutant proteins linked to familial ALS. Nat Struct Biol 10, 461-7.

Freitas, R., 2003. Biocompatibility. Nanomedicine IIA.

Gao, Y.Q., 2006. A simple theoretical model explains dynein's response to load. Biophys J 90, 811-21.

Goldstein, L.S., and Yang, Z., 2000. Microtubule-based transport systems in neurons: the roles of kinesins and dyneins. Annu Rev Neurosci 23, 39-71.

Gross, S.P., Welte, M.A., Block, S.M., and Wieschaus, E.F., 2002. Coordination of opposite-polarity microtubule motors. J Cell Biol 156, 715-24.

Haak, R.A., Kleinhans, F.W., and Ochs, S., 1976. The viscosity of mammalian nerve axoplasm measured by electron spin resonance. J Physiol 263, 115-37.

Hafezparast, M., Klocke, R., Ruhrberg, C., Marquardt, A., Ahmad-Annuar, A., Bowen, S., Lalli, G., Witherden, A.S., Hummerich, H., Nicholson, S., Morgan, P.J., Oozageer, R., Priestley, J.V., Averill, S., King, V.R., Ball, S., Peters, J., Toda, T., Yamamoto, A., Hiraoka, Y., Augustin, M., Korthaus, D., Wattler, S., Wabnitz, P., Dickneite, C., Lampel, S., Boehme, F., Peraus, G., Popp, A., Rudelius, M., Schlegel, J., Fuchs, H., Hrabe de Angelis, M., Schiavo, G., Shima, D.T., Russ, A.P., Stumm, G., Martin, J.E., and Fisher, E.M., 2003. Mutations in dynein link motor neuron degeneration to defects in retrograde transport. Science 300, 808-12.

Hou, L., Lanni, F., and Luby-Phelps, K., 1990. Tracer diffusion in F-actin and Ficoll mixtures. Toward a model for cytoplasm. Biophys J 58, 31-43.

Howard, J., Hudspeth, A.J., and Vale, R.D., 1989. Movement of microtubules by single kinesin molecules. Nature 342, 154-8.

Hurd, D.D., and Saxton, W.M., 1996. Kinesin mutations cause motor neuron disease phenotypes by disrupting fast axonal transport in Drosophila. Genetics 144, 1075-1085.

Jiang, Y.M., Yamamoto, M., Kobayashi, Y., Yoshihara, T., Liang, Y.D., Terao, S., Takeuchi, H., Ishigaki, S., Katsuno, M., Adachi, H., Niwa, J., Tanaka, F., Doyu, M., Yoshida, M., Hashizume, Y., and Sobue, G., 2005. Gene expression profile of spinal motor neurons in sporadic amyotrophic lateral sclerosis. Annals of Neurology 57, 236-251.

Keller, M., Tharmann, R., Dichtl, M.A., Bausch, A.R., and Sackmann, E., 2003. Slow filament dynamics and viscoelasticity in entangled and active actin networks. Philos Transact A Math Phys Eng Sci 361, 699-711; discussion 711-2.

Kieran, D., Hafezparast, M., Bohnert, S., Dick, J.R., Martin, J., Schiavo, G., Fisher, E.M., and Greensmith, L., 2005. A mutation in dynein rescues axonal transport defects and extends the life span of ALS mice. J Cell Biol 169, 561-7.

Klumpp, S., and Lipowsky, R., 2005. Cooperative cargo transport by several molecular motors. Proc Natl Acad Sci U S A 102, 17284-9.

Kuo, J.J., Lee, R.H., Zhang, L., and Heckman, C.J., 2006. Essential role of the persistent sodium current in spike initiation during slowly rising inputs in mouse spinal neurones. J Physiol 574, 819-34.

Kural, C., Kim, H., Syed, S., Goshima, G., Gelfand, V.I., and Selvin, P.R., 2005. Kinesin and dynein move a peroxisome in vivo: a tug-of-war or coordinated movement? Science 308, 1469-72.

Lupski, J.R., 2000. Axonal Charcot-Marie-Tooth disease and the neurofilament light gene (NF-L). Am J Hum Genet 67, 8-10.

Marszalek, J.R., Williamson, T.L., Lee, M.K., Xu, Z., Hoffman, P.N., Becher, M.W., Crawford, T.O., and Cleveland, D.W., 1996. Neurofilament subunit NF-H modulates axonal diameter by selectively slowing neurofilament transport. J Cell Biol 135, 711-24.

Meier, J., Couillard-Despres, S., Jacomy, H., Gravel, C., and Julien, J.P., 1999. Extra neurofilament NF-L subunits rescue motor neuron disease caused by overexpression of the human NF-H gene in mice. J Neuropathol Exp Neurol 58, 1099-110.

Morris, R.L., and Hollenbeck, P.J., 1993. The regulation of bidirectional mitochondrial transport is coordinated with axonal outgrowth. J Cell Sci 104 (Pt 3), 917-27.

Muller, M.J., Klumpp, S., and Lipowsky, R., 2008. Tug-of-war as a cooperative mechanism for bidirectional cargo transport by molecular motors. Proc Natl Acad Sci U S A 105, 4609-14.

Pantelidou, M., Zographos, S.E., Lederer, C.W., Kyriakides, T., Pfaffl, M.W., and Santama, N., 2007. Differential expression of molecular motors in the motor cortex of sporadic ALS. Neurobiol Dis 26, 577-89.

Rao, M.V., and Nixon, R.A., 2003. Defective neurofilament transport in mouse models of amyotrophic lateral sclerosis: a review. Neurochem Res 28, 1041-7.

Sabry, J., O'Connor, T.P., and Kirschner, M.W., 1995. Axonal transport of tubulin in Ti1 pioneer neurons in situ. Neuron 14, 1247-56.

Schmitz, K.A., Holcomb-Wygle, D.L., Oberski, D.J., and Lindemann, C.B., 2000. Measurement of the force produced by an intact bull sperm flagellum in isometric arrest and estimation of the dynein stall force. Biophys J 79, 468-78.

Shea, T.B., and Flanagan, L.A., 2001. Kinesin, dynein and neurofilament transport. Trends Neurosci 24, 644-8.

Teuchert, M., Fischer, D., Schwalenstoecker, B., Habisch, H.J., Bockers, T.M., and Ludolph, A.C., 2006. A dynein mutation attenuates motor neuron degeneration in SOD1(G93A) mice. Exp Neurol 198, 271-4.

Trivedi, N., Jung, P., and Brown, A., 2007. Neurofilaments switch between distinct mobile and stationary states during their transport along axons. J Neurosci 27, 507-16.

Truskey, G., Yuan, F., and Katz, D., 2003. Transport Phenomena in Biological Systems. Prentice Hall.

Visscher, K., Schnitzer, M.J., and Block, S.M., 1999. Single kinesin molecules studied with a molecular force clamp. Nature 400, 184-9.

Wagner, O.I., Ascano, J., Tokito, M., Leterrier, J.F., Janmey, P.A., and Holzbaur, E.L., 2004. The interaction of neurofilaments with the microtubule motor cytoplasmic dynein. Mol Biol Cell 15, 5092-100.

Wang, L., and Brown, A., 2001. Rapid intermittent movement of axonal neurofilaments observed by fluorescence photobleaching. Mol Biol Cell 12, 3257-67.

Wang, L., Ho, C.L., Sun, D., Liem, R.K., and Brown, A., 2000. Rapid movement of axonal neurofilaments interrupted by prolonged pauses. Nat Cell Biol 2, 137-41.

Wood, J.D., Beaujeux, T.P., and Shaw, P.J., 2003. Protein aggregation in motor neurone disorders. Neuropathol Appl Neurobiol 29, 529-45.

Yoo, J., Kambara, T., Gonda, K., and Higuchi, H., 2008. Intracellular imaging of targeted proteins labeled with quantum dots. Exp Cell Res.

Zhang, F., Strom, A.L., Fukada, K., Lee, S., Hayward, L.J., and Zhu, H., 2007. Interaction between familial amyotrophic lateral sclerosis (ALS)-linked SOD1 mutants and the dynein complex. J Biol Chem 282, 16691-9.

CHAPTER 10

AMYOTROPHIC LATERAL SCLEROSIS

Amyotrophic Lateral Sclerosis (ALS), also known as Lou Gehrig's disease, is one of the most devastating and deadliest neural pathologies with a mean survival time of ~3-5 years from the initial onset of symptoms (Bruijn, 2004). It is a disease that affects especially the motoneurons, particularly the large motoneurons, causing them to retract from the neuromuscular junction and eventually die, resulting in the clinical presentation of muscle paralysis (Stieber, 2000). Histologically, it typically presents with filamentous lesions which occur in the axon and are hypothesized to be the result of impeded axonal transport. Additionally, it has many of the pathological characteristics of spinal cord injury, sharing such hallmark physiological dysfunctions as excitotoxicity, energetic failure, and inflammation (Bruijn, 2004). Thus, in addition to our general scientific and personal clinical interests, ALS was a natural fit to our research in axonal transport, motoneuron physiology, and spinal cord injury, making it an ideal test case for aggregating multiple viewpoints. Finally, because our exposure to ALS was only ancillary through related fields of research, we had no significant preconceived mechanistic hypotheses to ensure that our methodological development and evaluation process was unbiased.

ALS represents the last test case included in this work. However, this test case is different from the other test cases previously presented in that it is a work in progress.

Thus, while some aspects are more complete, such as our modeling work with ALS-disrupted axonal transport, others, such as our relational model of the comprehensive ALS pathology and our experimental motoneuron research, which focuses on how the properties of motoneurons change based on their size (an important viewpoint since ALS seems to preferentially affect large motoneurons), are less complete. The purpose of including this 'work in progress' chapter into this dissertation is to give the reader a real sense or 'snapshot' inside our methodological process and in particular the process of gathering and aggregating viewpoints.

The first study in this chapter highlights our work in ALS-disrupted axonal transport. This paper was originally submitted to the Journal of Neuroscience and is currently in revision. Inside this paper, a version of the model presented in the axonal transport test case is used as the 'base' or physiological model to study axonal transport. Conceptual modeling was the chosen technique to implement pathological transport within this physiological model. Three different ALS-induced pathologies were 'conceptualized' based on experimental literature: protein aggregation, mutations to the molecular motors kinesin and dynein that render the motors ineffective, and a constrained motor population due to either a genetic defect resulting in an inefficient production of molecular motors or a cargo population overload resulting in decreased availability of motors. Our relational analysis technique is used to differentiate these pathologies, based on their landscapes. This differentiation is a critical step forward for the field because, to date, traditional analytical techniques based on using only metric or output values cannot be used to

differentiate these pathologies due to the high degree of variability within the experimental data and among experimental preparations.

The second study in this chapter illustrates an early relational model of ALS. The relational modeling process snapshot shown is about 30% through the process. An ALS database has built with approximately 250 papers, categorized by factor. The model that is presented here is a 'category model' that shows the time course and impact of the presented categories, which were constructed based on experimental data. Already, even at the category level, this model has some interesting and significant findings.

While still a critical viewpoint of this ALS research, the work on motoneurons is not presented in this chapter but instead is presented under Component Analysis, Chapter 5, as a test case in how to use the technique to examine experimental data. Briefly summarized, our work with motoneurons examines the effects of motoneuron size on excitability and firing properties, both of which are known to markedly change in ALS (Kuo, 2004).

Neurofilament distributions differentiate ALS pathologies

Submitted to Journal of Neuroscience. Currently in revision.

Contributions of the authors

Cassie Mitchell developed the pathological and cooperativity sub-models, applied and implemented the sub-models and the overall motor-cargo model, performed the simulations and analysis, and wrote the manuscript. Dr. Robert Lee assisted with conceptualizations of the pathologies, assisted in the implementation of the event-based simulator, and co-edited the manuscript.

Abstract

Impaired axonal transport is thought to be a key component of Amyotrophic Lateral Sclerosis (ALS). Based on computer models of axonal transport of neurofilament cargos, we predict the "signatures" of three proposed categories of axonal transport impairment (protein aggregation, protein dysregulation, and molecular motor mutations) by analyzing their neurofilament distribution profiles. The ability to distinguish among these categories will aid in potential pathogenic mechanism identification and thus clinical treatments for ALS.

Introduction

Amyotrophic lateral sclerosis (ALS) is a devastating neurodegenerative disease characterized by loss of motoneurons in the spinal cord, brainstem, and motor cortex (Jiang et al. 2005). Initial muscle weakness ultimately progresses to complete paralysis, and 50% of patients die within 3 years after the onset of symptoms (Beers 2004). Several studies point to the involvement of axonal transport (a process by which the polarized molecular motors, dynein and kinesin provide retrograde and anterograde transport respectively in the axons motoneurons) (Elam et al. 2003; Jiang et al. 2005; Kieran et al. 2005; Pantelidou et al. 2007; Rao and Nixon 2003; Wood et al. 2003). Of the various types of axonal transport, ALS is thought to most affect the slow transport of neurofilaments (Rao and Nixon 2003; Zhang et al. 1997). Based on current experimental evidence from superoxide dismutase 1 (SOD1) and neurofilament heavy (NF-H) transgenic mouse models, three categories of axonal transport impairment mechanisms have been hypothesized: 1) protein aggregation/misfolding (Cluskey and Ramsden 2001; Elam et al. 2003; Valentine and Hart 2003; Wood et al. 2003); 2) dysregulation of motor proteins and/or cargo (Jiang et al. 2005; Pantelidou et al. 2007; Rao and Nixon 2003); and 3) molecular motor mutations (Hafezparast et al. 2003; Kieran et al. 2005; Teuchert et al. 2006; Warita et al. 1999; Zhang et al. 1997). However, little progress has been made in differentiating these pathologies, a critical step towards the development of ALS treatments.

In this work, we address the question: Can the mechanistic categories of ALS axonal transport impairment be differentiated based on the distribution of transported cargos?

Here we use a combination of published theoretical (Brown et al. 2005; Craciun et al. 2005; Gao 2006; Klumpp and Lipowsky 2005) and experimental data (Kural et al. 2005; Wang and Brown 2001) to implement a computational model of neurofilament cargo transport that compares the normal, non-diseased state population distribution of cargo position over time to the distributions resulting from the modeled ALS mechanisms. Based on our findings, we conclude that the three ALS mechanistic categories can be distinguished by the "signature" of the population distribution.

Methods

The transport of neurofilaments is bi-directional with a net movement that is anterograde and accompanied by on- and off-track pauses (Brown et al. 2005; Craciun et al. 2005; Wang and Brown 2001). Computational models have been used to validate pulse-labeling experiments, which show that the velocity of neurofilament cargos is dependent upon the ATP concentration (Gao 2006), multi-motor cooperativity (i.e. several motors binding to and carrying a single cargo) (Klumpp and Lipowsky 2005; Kural et al. 2005), cargo load size (Gao 2006; Klumpp and Lipowsky 2005), and "stop-and-go" kinetics (Brown et al. 2005; Craciun et al. 2005). Here we include all the aforementioned features collectively to examine the distribution of bi-directionally transported neurofilament cargos in both the normal and ALS disease states. The "normal" model was verified by comparison to the experimental data from Wang and Brown (2001) as given in Brown et al (2005) for a simulation time of 4.73 s (not shown). ALS pathology is modeled using a "black box" approach where ALS mechanisms are represented purely based on their

functional implication(s). The model is implemented in MATLAB R2006b. Simulations were run for 1,000 s for 10,000 neurofilament cargos.

Protein Aggregation/Misfolding

Various types of proteins are seen in aggregates with the most common being misfolded SOD1, intermediate filament, neurofilament, and peripherin (Cluskey and Ramsden 2001; Elam et al. 2003; Valentine and Hart 2003; Wood et al. 2003). These aggregates are of high molecular weight, and when the cell's ability to degrade them is exceeded, they are transported down the microtubules to the microtubule organizing center where they are incorporated into aggregsomes (Valentine and Hart 2003). Thus, we assert that protein folding and aggregation can be modeled as an increase in the typical cargo load size. For model implementation, see *Load*.

Protein Dysregulation

Gene expression profiling has been used to show a decrease in expression of motor proteins associated either with dynein or kinesin (e.g. Jiang et al. 2005; Pantelidou et al. 2007; Warita et al. 1999) and an overexpression of cargo-related proteins (Jiang et al. 2005). Whether this dysregulation of proteins results in less motors or more cargos, the implication of either is a constrained motor population (i.e. not enough motors). Thus, we assert that protein dysregulation can be modeled as a constrained motor population. For implementation of a constrained population, see *Specifying the Motor Population*.

Molecular Motor Mutations

Mutations can render the motors, whether retrograde (e.g. Hafezparast et al. 2003) or anterograde (e.g. Warita et al. 1999), to have limited or no functionality; the result is a population in which at least a portion of the motors are rendered ineffective thereby diluting the functioning motors. Thus, we assert that molecular motor mutations can be modeled as a dilute population where the number of functioning motors available is sufficient to meet the transport needs, but in which non-functioning motors are interspersed. For implementation of diluted populations, see *Specifying the Motor Population*.

Specifying the Motor Population

In the real cells, the total number of molecular motors and the percentage of which are ineffective depends on the type and degree of dysfunction resulting from protein dysregulation or mutations. We model the availability of motors for the "constrained" and "diluted" cases using conservation balances where the total number of motors and the percentage of motors deemed "functional" are specified. A constant factor, k_T, is used to scale the total number of motors in the population, M_{total}, with "just enough" motors defined as $k_T=1$ as described by Equation 1. The total number of cargos, C_{total}, is 10,000. The maximum allowable number of motors per cargo, N, is 12. (see *Cooperativity*).

$$M_{total} = C_{total} \cdot N \cdot k_T \qquad \textbf{Equation 10.1.1}$$

Similarly, a functional motor factor, k_F, is used to specify the percentage of total motors deemed "functional" (Equation 2) with 100% functionality described as k_F=1.

$$M_{F,total} = M_{total} \cdot k_F \qquad \textbf{Equation 10.1.2}$$

Conservation balances (Equations 3-5) are used to keep track of how many functional ($M_{F,avail}$), non-functional ($M_{NF,avail}$), and total motors ($M_{total,avail}$) are available to be assigned to a cargo.

$$M_{F,avail} = M_{F,total} - \sum_{i=1}^{i=C_{total}} M_{F,i} \qquad \textbf{Equation 10.1.3}$$

$$M_{NF,avail} = M_{NF,total} - \sum_{i=1}^{i=C_{total}} M_{NF,i} \qquad \textbf{Equation 10.1.4}$$

$$M_{total,avail} = M_{F,avail} + M_{NF,avail} \qquad \textbf{Equation 10.1.5}$$

Given availability, the maximum total number of motors that can be assigned to any one cargo is specified by *N* (see *Cooperativity*), and the number of functional and non-functional motors for each cargo is assigned randomly using k_F as the probability criterion (i.e. if a random number between 0-1 is less than or equal to k_F, the motor assigned is functional).

Kinetics

We use the slow transport kinetics described by Craciun et al. (2005). This scheme describes bidirectional transport of neurofilaments using the following five states: 0) off-track, paused; 1) kinesin, on-track, paused; 2) dynein, on-track, paused; 3) kinesin, on-track, moving anterogradely; 4) dynein, on-track, moving retrogradely. States must proceed in the following manner:

$$4 \Leftrightarrow 2 \Leftrightarrow 0 \Leftrightarrow 1 \Leftrightarrow 3 \qquad \textbf{Equation 10.1.6}$$

That is, a motor must disengage from the track before switching directions, and it must pass through an on-track paused state before moving. Since motors have been shown to work together in a concerted effort (Kural et al. 2005), all of a cargo's microtubule-bound motors are assumed to be in the same state (either in state 1, 2, 3, or 4). Similarly, in order to be "off-track" all of a cargo's motors must be disengaged (in state 0). All cargo states are initially set to state 0 at the beginning of the simulation.

We implement this kinetic scheme using event-based simulation (Banks et al. 2005; Robinson 2004), a method that speeds simulation time by avoiding unnecessary repetitive calculations by predicting how long a cargo will remain in the same state. The expected duration of each possible state, t_{state}, is calculated by multiplying the inverse of the state's rate constant, k, by the log of a random number, *rand*, between 0-1 giving:

$$t_{state} = -1/k \cdot \log(rand) \qquad \textbf{Equation 10.1.7}$$

The form of Equation 7 is chosen to fit the exponential first order process that is apparent in experimental data (Wang and Brown 2001). Rate constants and rate equations are given in (Craciun et al. 2005). The state with the shortest duration becomes the next state for that cargo. Based on the duration of the cargo's current state and the current time in the simulation, a sorted list determines when each cargo should be re-evaluated so that not every cargo need be evaluated at every time step.

ATP dependence

ATP dependence was modeled using a constant ATP concentration. The ATP-dependent stall force, F_s, of kinesin and dynein was adapted from Gao (2006). A constant physiological ATP concentration of 1,000 μM was used giving dynein an approximate 1 pN stall force and kinesin an approximate 5 pN stall force, comparable to experimental findings.

Cooperativity

The number of motors bound to the microtubule for each cargo is determined by the equation proposed by Klumpp and Lipowsky (2005) (Equation 8), which assumes dilute enough motor coverage that exclusion effects are negligible. The number of bound motors, N_b, is a function of the motor to microtubule binding (π_{AD}) and unbinding (ε) rates, the previous state's number of bound motors (n), the maximum allowable number of motors able to bind (N), the load (F), the detachment force, F_d = 3 pN (Klumpp and

Lipowsky 2005), and the stall force (F_s). The binding and unbinding rates are determined by the kinetic rates used to calculate the state duration. The maximum allowable number of bound motors is 12 per cargo, as determined by experimental evidence from Kural et al (2005).

$$N_b = \frac{(\pi_{ad}/\varepsilon)[1+(\pi_{ad}/\varepsilon)]^{N-1}}{[1+(\pi_{ad}/\varepsilon)]^{N}-1} N \qquad \textbf{Equation 10.1.8}$$

Load

Each cargo's size (F) was randomly determined over a set range starting at a minimum of 0.1 pN (Gao 2006); using the experimental data from Wang and Brown (2001) as given in Brown et al. (2005) as the target output to tune the model, the maximum cargo size for "normal" transport was set to 4 pN. To model the effect of an increased load due to protein aggregation and/or misfolding, we expand the range to 10 pN. This approximation was based on the formation of dimers (Elam et al. 2003). The effect of load on the unbinding rate is calculated as described by Klumpp and Lipowsky (2005):

$$\varepsilon(F) = n\varepsilon \cdot \exp\left(\frac{F}{nF_d}\right) \qquad \textbf{Equation 10.1.9}$$

Velocity

Based on the approximate linear proportional relationship of the number of bound motors to velocity as illustrated in the experimental data of (Kural et al. 2005), we obtain

the velocity for a cargo, i , as a function of the number of motors bound, load, and the ATP-dependent stall force. v_{const} is the average uncorrected constant velocity of kinesin and dynein , 1,000 μm/s (Klumpp and Lipowsky 2005).

$$V_i = v_{const} \cdot \left[1 - \frac{F_i}{N_{b,i} F_{s,i}} \right] \cdot N_{b,i} \qquad \textbf{Equation 10.1.10}$$

Distributions

The main output of the model consists of a distribution of final cargo positions at the end of the simulated time. The bin size of each distribution is scaled to the distribution's range (the minimum and maximum cargo position).

Results

Based on stacked histograms of position versus load (Figure 1), we find that each of the three categories of mechanisms shows a clearly recognizable pattern that is a "signature" of the mechanism. The functional impact of the mechanistic categories can therefore be distinguished based on the distribution shape, height, and range as described below:

Normal Physiology

The shape of the "normal" transport distribution is bimodal with distributions lying on either side of 0 μm (see Figure 1a; note that the zero position bin has been moved to inset

for clarity). That is, at the simulated time of 1,000 s, the normal case's distribution has already separated into distinct anterograde and retrograde populations. Note that we use the traditional sign convention to distinguish transport direction, positive (+) for anterograde and negative (-) for retrograde. The position range is about twice as large for the anterograde population compared to the retrograde population; this is due to the kinetics imposed on the system based on experimental data showing that the ratio of anterograde to retrograde movement is approximately 2:1 (Brown et al. 2005; Craciun et al. 2005). Under physiological conditions, the number of cargos that do not move is only about 5% (inset Figure 1a).The number of motors in the normal case is considered to be "just enough". That is, there are enough motors for every cargo to bind 12 motors, the maximum set by *N*, and all of the motors are "functional". We define this as being the "base population" with k_T=1 and k_F=1. Note that since our model assumes an equal dispersion of motors, specifying more motors than necessary (k_T>1) does not change the normal case result since all motors are assumed to be functional under normal physiology.

Protein aggregation/misfolding

Protein aggregation/misfolding is modeled as an increase in the maximum load size from 0.1-4 pN to 0.1-10 pN. Protein aggregation/misfolding results in changing the shape of the distribution (Figure 1b). At the simulated time of 1,000 s, protein aggregation results in a single, unimodal distribution centered at 0 μm (Figure 1b) compared to the bimodal normal case. Thus, in an ALS model where cargo load size is affected, the splitting of the population into retrograde and anterograde populations has a

definite delay in onset. Consequently, even when the protein aggregated case has had enough time to become separated, the normal case will still have a larger gap between the anterograde and retrograde populations (not shown). The overall scaled height of the distribution remains similar to the normal case except for the bins close to 0 μm due to the change of shape from bimodal to unimodal; for a load distribution between 0.1-10 pN, this results in a 25% increase in the number of cargos in the zero position bin (inset Figure 1b). The range of the distribution (i.e. the minimum and maximum position as shown on the x-axes) for the protein aggregation case remains relatively unchanged compared to the normal case. For simple protein aggregation (Figure 1b), the motor population defined to be equal to the base population.

Protein Dysregulation

Protein dysregulation is modeled as a constrained population. That is, the scaling factor k_T is used to specify the percentage of motors in the population in comparison to the normal case. Protein dysregulation results in changing the height of the distribution over the simulated time (Figure 1c). The heights of the non-zero bins decrease (i.e. fewer cargos per non-zero position bin) while the number of cargos in the zero bin increases to almost 80% in this example. However, again, the range of the distribution does not vary substantially from the normal case. That is, protein dysregulation results in a substantial increase in the number of total cargos that are not moving compared to the normal case, but the positions of cargos that are moving remains similar to the normal case. While the constrained cases shown in Figure 1c and 1d represent a motor population that is 10% of

the normal population (k_T=0.1, k_F=1), the effect was noticeable with percentages as high as 70% over the 1,000 seconds of simulated time.

Molecular Motor Mutations

Molecular motor mutations are represented by diluting the motor population. Diluting the number of motors results in decreasing the heights of the non-zero bins and the range of the distribution. In fact, in this example, the height of the distribution non-zero positions bins is approximately 10% of that of the normal case, and the position range is less than half of the normal range. That is, there are fewer total cargos that are moving (only 5%) compared to both the normal and constrained cases; additionally, those cargos that are moving are doing so at a slower velocity, resulting in the substantial decrease in the distribution position range. Thus, having an ample number of motors, of which a large portion are ineffective, results in a much more severe axonal transport impairment compared to simply constraining the motors (see *Discussion*). We define this phenomenon as "population dilution". For example, the diluted populations shown in Figures 1e and 1f have a motor population that is ten times larger (k_T=10) than the normal case with 90% of this population being ineffective (k_F=0.1) resulting in an equivalent number of functional motors. When looking at a diluted population over 1,000 s, the effects of dilution becomes quite noticeable when the ratio of total motors to effective motors is as low as 3:1 and increases proportionally as the number of total motors is increased and the number of effective motors is held constant.

Multi-factorial Pathology

Some experimental evidence suggests that ALS is multi-factorial (Cluskey and Ramsden 2001). For example, what if there is protein dysregulation and protein aggregation? The cargos would be both more numerous and heavy, resulting in a constrained distribution that would resemble Figure 1d. Similarly, what if there was both protein aggregation and molecular motor mutations? In that case, the cargos would be heavier and the motor population would be diluted as shown in Figure 1f. As can be seen in these examples, the traits which distinguish a certain pathology are still evident even in mixed pathologies.

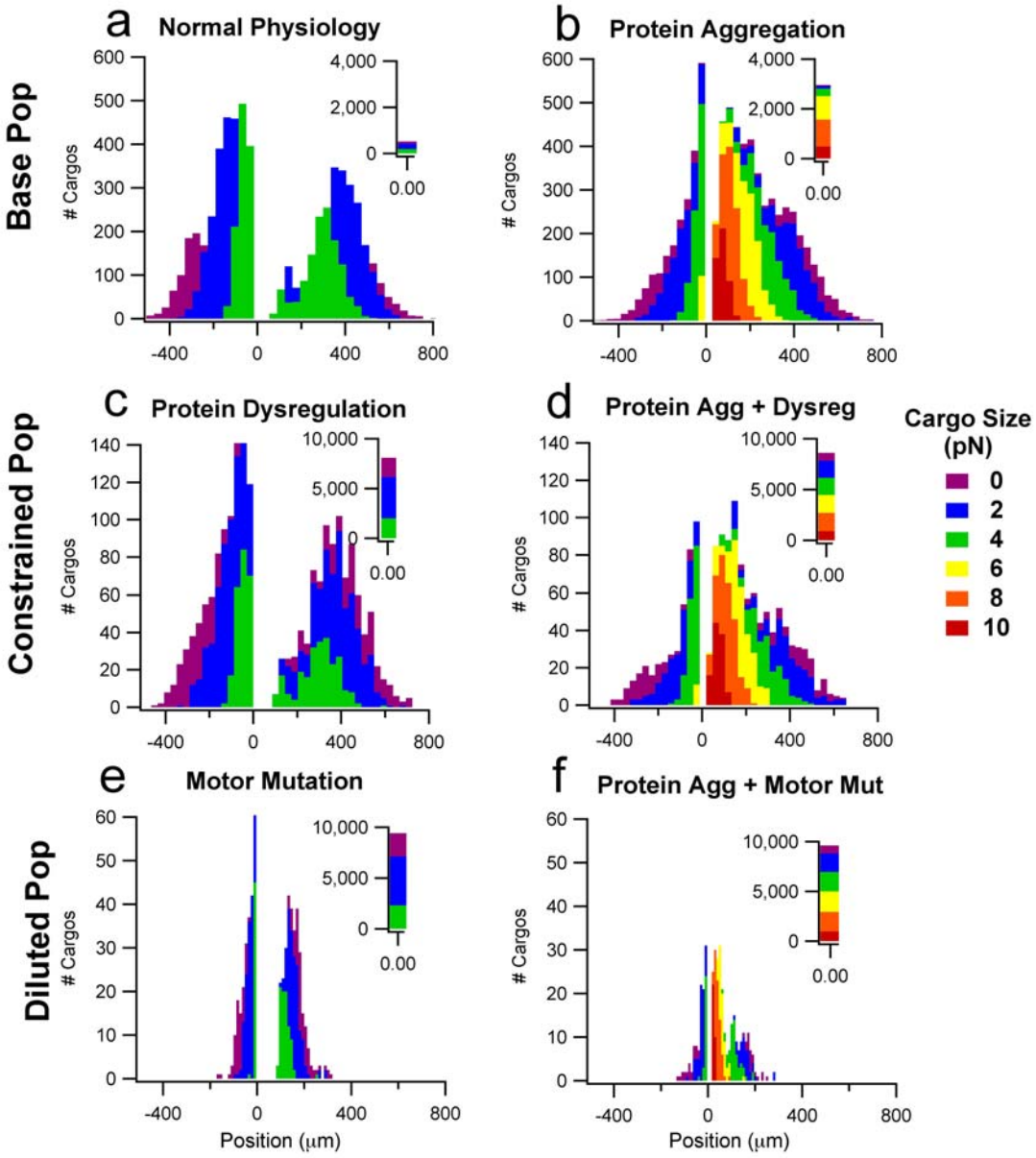

Figure 10.1.1. Distributions of neurofilaments. The figure illustrates the position distribution as a function of cargo size. Negative (-) position represents retrograde movement via dynein whereas positive (+) position represent anterograde movement via kinesin. The 0 μm bin has been removed and is illustrated in the *inset*. The *left* column depicts normal size cargo distributions and the *right* column depicts heavier cargo size distributions.

Mapping the Pathologies

One critical obstacle in the investigation of axonal transport, whether normal or pathological transport, is that there is great variability in the intrinsic properties and in velocity profiles among different experimental preparations. For example, in vitro molecular motor studies may record velocities that are an order of magnitude larger or smaller than in vivo preparations. Another issue with pathological transport is that transport deficits can be to a large degree a function of the type and severity of the mutation involved. Thus, comparison using quantitative outputs alone can be misleading and confusing. An analysis-based solution that allows different pathologies to be compared and contrasted is to look at the data sets relative to one another by viewing the relationships among the metrics or outputs using our relational analysis technique instead of comparing the exact quantitative values. Additionally, this approach can be used to compare experimental data sets to model output data sets. Using relational analysis, the different pathological versions of axonal transport can each be individually visualized in a map of cross-correlations called a 'landscape'.

The landscape of the 'base case' (Figure 2A) or normal physiology (Figure 2B-G) is illustrated with the landscapes of each of the pathological versions of transport. The major highlighted differences between the physiology and pathology landscapes are marked on the pathology landscapes. The metrics used to create the landscape are shown to the right of Figure 2. When comparing the landscapes, there are some definite generalized patterns that are attributable to the specific pathologies. One particular pattern that is of interest is the conserved highly positively correlated block of velocity

correlations (large red block in the middle the normal physiology (Figure 2A). This block is affected in all of the pathologies. However, in particular, this block is telling for the pathologies in which both motor types are affected. For example, the velocity correlations for the neurofilaments at the upper end of the velocity distributions are nearly insignificant when both motor populations are affected (Figure 2D and 2G). If either motor population is constrained or diluted (Figure 2B-C and E-F), the effects of the pathology are most apparent in the correlations that contain the separated average velocities of dynein and kinesin. However, even these 4 pathologies, which are more similar, can still be differentiated. The constrained populations have a very strong block of positive correlations among the correlations containing the number of bound motors that is not present in the mutated pathologies. Finally, the type of motor population affected, whether kinesin or dynein, can be predicted based on the correlations containing the separated average velocities of dynein and kinesin. If kinesin is mutated or constrained, both the dynein and kinesin velocity correlations are affected whereas if dynein is mutated or constrained, only the dynein velocity correlations show significant changes.

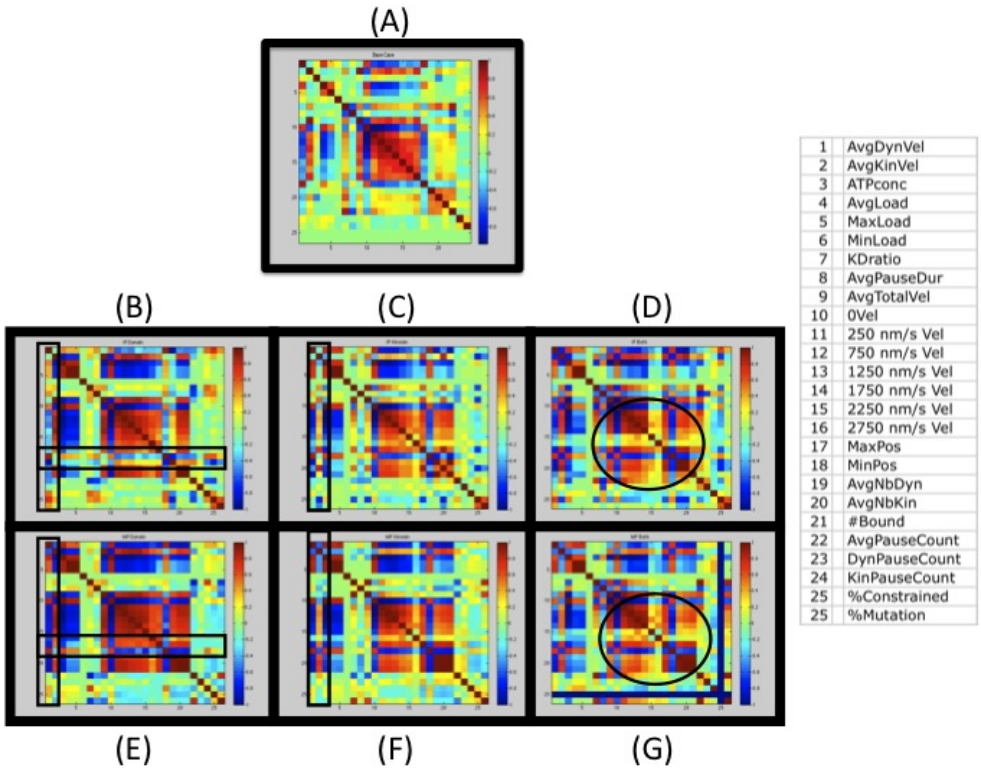

Figure 10.1.2. Landscapes comparing the different pathology cases to the 'normal' case. Note that cargo size (protein aggregation) is excluded from these landscapes since there are no experimental correlations to have a basis of comparison. (A) Normal physiology (B) Dynein Mutation (C) Kinesin Mutation (D) Kinesin and Dynein Mutations (E) Dynein Constrained Population (F) Kinesin Constrained Population (G) Kinesin and Dynein Constrained Population.

Discussion

Our modeling results predict that the three proposed categories of impaired axonal transport mechanisms (and their respective combinations) can be distinguished by comparing distributions of cargo versus position over a specified time interval. Protein aggregation/misfolding affects the distribution shape; protein dysregulation changes the distribution height, and molecular motor mutations alter the distribution height and range.

Thus, given the normal density of motors in a particular motoneuron type, histograms of cargo position versus time are a potential indicator of ALS pathology. The predicted "signatures" provided by these modeled mechanisms will help plan and interpret future experimental data comparing ALS axonal transport to normal axonal transport, and thus take us one step closer in pinpointing a mechanism for which clinical treatments could be designed.

Currently, the only treatment for ALS is the drug riluzole (Kuo et al. 2006; Wood et al. 2003). It is not known precisely how this drug slows ALS, but it is thought to 1) decrease the excitability of the motoneurons (Kuo et al. 2006), thus decreasing excitotoxicity and 2) decrease protein aggregation (Wood et al. 2003), thus reducing the effect of increased cargo size in axonal transport. However, it is possible that excitotoxicity and impaired axonal transport are linked. It is known that electrical activity cannot change the actual speed of transport (Jankowska et al. 1969) (i.e. the distribution range), but it could change the volume of cargos being shipped. A motoneuron with a higher firing rate would require more energy via mitochondria (Kong and Xu 1998), more neurotransmitter, ionic channel parts, and "maintenance" proteins all of which are moved via axonal transport. Attempts to "ship" the required demand could speed the process of clogging the axonal microtubule tracks on which the molecular motors carry their cargo. Thus, we would expect to see a distribution that is similar to the motor-constrained case.

It would seem that the overall impact of the ALS mechanism is largely a function of cooperativity. Cooperativity specifies the number of motors that are simultaneously

moving a cargo and, thus, helps to set the attainable velocity range and, by extension, the attainable position range. Cooperativity relates to ALS pathology in that the number of motors bound is a function of load size and the number of available motors. The impact of cooperativity is apparent in every ALS case model here, but has a particularly strong impact on the diluted case and the retrograde subpopulations.

For the diluted case, the chances of a cargo being assigned an ineffective motor is higher when there are more motors than when there are "just enough" or "not enough". This produces less effective transport overall, because the chance of multiple functional motors being bound to a cargo is greatly reduced. Thus, in this case, it is almost beneficial for there to be fewer motors. Where does the ample supply come from? It could be caused by a positive feedback loop telling the cells to produce more motors (of which a percentage are always ineffective) in an attempt to compensate for the impaired transport.

As is seen experimentally in ALS, retrograde transport is more affected than anterograde transport (Kieran et al. 2005). This holds true for all three categories of modeled mechanisms. This is likely due to the stall force of dynein, which is approximately 1 pN (Gao 2006) compared to the approximate 5 pN (Klumpp and Lipowsky 2005) stall force of kinesin in physiological ATP concentrations (≥1,000 μM). Because of its lower stall force, dynein is more dependent upon motor cooperativity than kinesin. Hence, having a larger cargo or simply not having enough effective motors that can work together cooperatively has a much greater impact on retrograde transport.

Acknowledgements

This work is supported by the National Science Foundation (NSF) Graduate Research Fellowship Program, the NSF IGERT Program (DGE 0333411), the Human Brain Project (NINDS, NIMH and NIBIB NS046851), and NINDS (NS045199).

References

Banks J, Carson J, Nelson B, Nicol D (2005) Discrete-event system simulation 4th Edition: Pearson.

Beers M (2004) The Merck Manual of Medical Information, 2nd Edition: Simon & Schuster, Inc.

Brown A, Wang L, Jung P (2005) Stochastic simulation of neurofilament transport in axons: the "stop-and-go" hypothesis. Mol Biol Cell 16:4243-4255.

Cluskey S, Ramsden DB (2001) Mechanisms of neurodegeneration in amyotrophic lateral sclerosis. Mol Pathol 54:386-392.

Craciun G, Brown A, Friedman A (2005) A dynamical system model of neurofilament transport in axons. J Theor Biol 237:316-322.

Elam JS, Taylor AB, Strange R, Antonyuk S, Doucette PA, Rodriguez JA, Hasnain SS, Hayward LJ, Valentine JS, Yeates TO, Hart PJ (2003) Amyloid-like filaments and water-filled nanotubes formed by SOD1 mutant proteins linked to familial ALS. Nat Struct Biol 10:461-467.

Gao YQ (2006) A simple theoretical model explains dynein's response to load. Biophys J 90:811-821.

Hafezparast M, Klocke R, Ruhrberg C, Marquardt A, Ahmad-Annuar A, Bowen S, Lalli G, Witherden AS, Hummerich H, Nicholson S, Morgan PJ, Oozageer R, Priestley JV, Averill S, King VR, Ball S, Peters J, Toda T, Yamamoto A, Hiraoka Y, Augustin M, Korthaus D, Wattler S, Wabnitz P, Dickneite C, Lampel S, Boehme F, Peraus G, Popp A, Rudelius M, Schlegel J, Fuchs H, Hrabe de Angelis M, Schiavo G, Shima DT, Russ AP, Stumm G, Martin JE, Fisher EM (2003) Mutations in dynein link motor neuron degeneration to defects in retrograde transport. Science 300:808-812.

Jankowska E, Lubinska L, Niemierko S (1969) Translocation of AChE-containing particles in the axoplasm during nerve activity. Comp Biochem Physiol 28:907-913.

Jiang YM, Yamamoto M, Kobayashi Y, Yoshihara T, Liang YD, Terao S, Takeuchi H, Ishigaki S, Katsuno M, Adachi H, Niwa J, Tanaka F, Doyu M, Yoshida M, Hashizume Y, Sobue G (2005) Gene expression profile of spinal motor neurons in sporadic amyotrophic lateral sclerosis. Annals of Neurology 57:236-251.

Kieran D, Hafezparast M, Bohnert S, Dick JR, Martin J, Schiavo G, Fisher EM, Greensmith L (2005) A mutation in dynein rescues axonal transport defects and extends the life span of ALS mice. J Cell Biol 169:561-567.

Klumpp S, Lipowsky R (2005) Cooperative cargo transport by several molecular motors. Proc Natl Acad Sci U S A 102:17284-17289.

Kong J, Xu Z (1998) Massive mitochondrial degeneration in motor neurons triggers the onset of amyotrophic lateral sclerosis in mice expressing a mutant SOD1. J Neurosci 18:3241-3250.

Kuo JJ, Lee RH, Zhang L, Heckman CJ (2006) Essential role of the persistent sodium current in spike initiation during slowly rising inputs in mouse spinal neurones. J Physiol 574:819-834.

Kural C, Kim H, Syed S, Goshima G, Gelfand VI, Selvin PR (2005) Kinesin and dynein move a peroxisome in vivo: a tug-of-war or coordinated movement? Science 308:1469-1472.

Pantelidou M, Zographos SE, Lederer CW, Kyriakides T, Pfaffl MW, Santama N (2007) Differential expression of molecular motors in the motor cortex of sporadic ALS. Neurobiol Dis 26:577-589.

Rao MV, Nixon RA (2003) Defective neurofilament transport in mouse models of amyotrophic lateral sclerosis: a review. Neurochem Res 28:1041-1047.

Robinson S (2004) The practice of model development and use.: Wiley.

Teuchert M, Fischer D, Schwalenstoecker B, Habisch HJ, Bockers TM, Ludolph AC (2006) A dynein mutation attenuates motor neuron degeneration in SOD1(G93A) mice. Exp Neurol 198:271-274.

Valentine JS, Hart PJ (2003) Misfolded CuZnSOD and amyotrophic lateral sclerosis. Proc Natl Acad Sci U S A 100:3617-3622.

Wang L, Brown A (2001) Rapid intermittent movement of axonal neurofilaments observed by fluorescence photobleaching. Mol Biol Cell 12:3257-3267.

Warita H, Itoyama Y, Abe K (1999) Selective impairment of fast anterograde axonal transport in the peripheral nerves of asymptomatic transgenic mice with a G93A mutant SOD1 gene. Brain Res 819:120-131.

Wood JD, Beaujeux TP, Shaw PJ (2003) Protein aggregation in motor neurone disorders. Neuropathol Appl Neurobiol 29:529-545.

Zhang B, Tu P, Abtahian F, Trojanowski JQ, Lee VM (1997) Neurofilaments and orthograde transport are reduced in ventral root axons of transgenic mice that express human SOD1 with a G93A mutation. J Cell Biol 139:1307-1315.

Relational Modeling Approach to ALS

As was alluded to in the introduction, ALS is a disease that includes many factors. In fact, there are so many factors and interactions, that scientists have yet to come up with a single comprehensive theory. ALS is typically divided into two types—sporadic and familial. Familial or inherited forms only make up about 10% of the documented cases. However, this is not to say that sporadic cases do not have a genetic component as many sporadic ALS patients have been found to have one or more genetic mutations which are thought to either cause or contribute to their diagnosis. The confusion as to how exactly ALS 'works' is not helped by the fact that there are literally hundreds of different documented genetic mutations, protein defects, aberrant chemistries and misfunctions which have been associated with several different variants of ALS. With so many variants of ALS and so many involved factors, scientists and clinicans are left grasping to find a comprehensive theory, which would explain the strikingly common clinical presentation that results from what are very often seemingly different underlying pathological causes. Given the number of factors present, the extent the field understands the diesease's mechanisms, and the absence of solid conceptual theories describing the ALS process, relational modeling is the analytical method of choice for developing an initial system-level view of ALS.

Upon performing the intial literature review of ALS, it became very apparent that the commonalities among the different forms of ALS were not just in the clinical or symptomatic presentation, but also at the physiological presentation. Whether familial or sporadic, mutation or no mutation, there were ten very general commonalities that were

present. The ten commonalities became the ten categories of the ALS model, and they essentially represent different paths or misfunctions that are present in ALS, any one of which could potentially be an underlying cause: axonal transport (AT), energetics (EN), excitotoxicity (EX), inflammation (IN), necro-apoptosis (NA), free radicals (FR), genetic mutations (GM), aberrant chemistry (CH), proteomics (PR), and systemic defects (SY). Based on this first literature review, it was at this point when we first hypothesized that perhaps ALS results not from a single mechanism but rather it emerges from the complex interactions and relationships of multiple mechanisms. Thus, if this hypothesis is correct, ALS is in fact an emergent property that can be obtained from different possible mechanisms or combinations of different mechanisms. If we think of each of these categories as a 'knob' that provides feedback to help control the signal(s) of the system (the motoneuron and surrounding environment), then turning any one mechanistic knob severely in the wrong direction or turning multiple knobs just slightly in the wrong direction could potentially cause a 'loss in control' of the physiological system that results in the ALS pathology.

The literature review was expanded to include ~250 papers, but this expansion only resulted in an increase in the number of individual factors and not the number of categories. From this second expansion it appeared that there would need to be at least 40-50 factors in the 'final' factor-based relational model based on factors. Thus, to help guide our research efforts, we decided to build a category model at this stage. The resulting category 'map' or network of ALS categories and their interactions is presented in Figure 1.

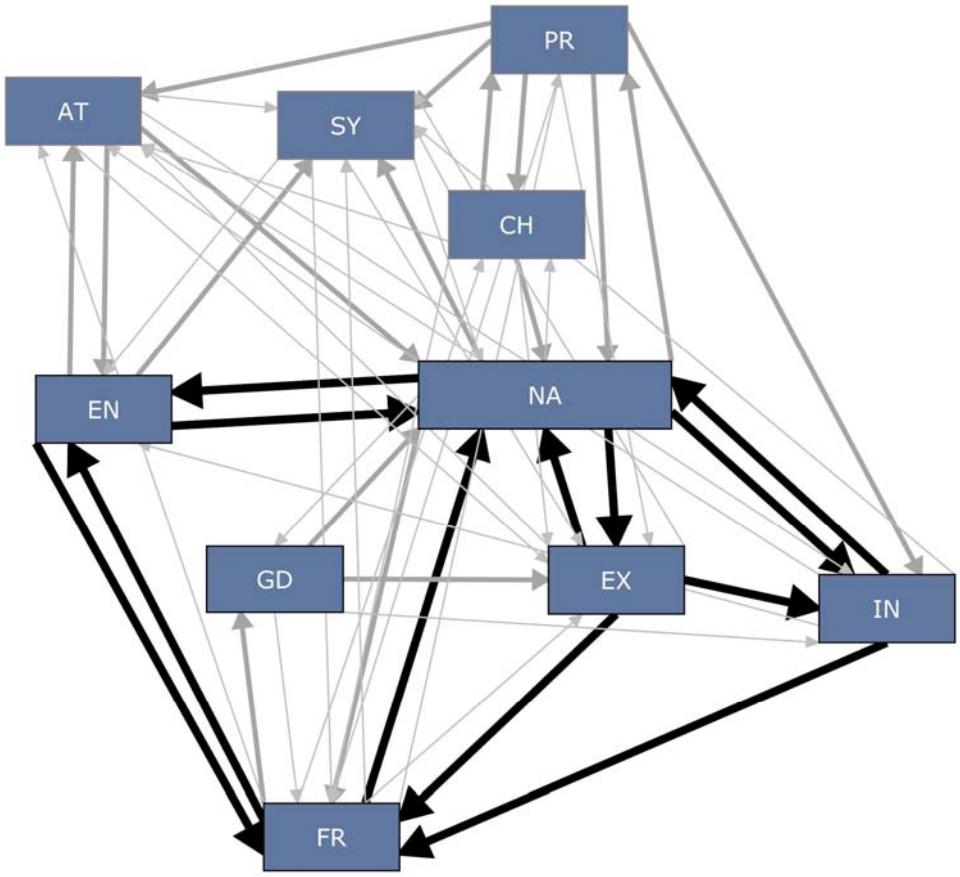

Figure 10.2.1. Category relational model of ALS. The different size and hues of arrows represent the relative size of the hypothesized interaction. The thick black arrow represents a 'large' interaction; the thick grey arrow represents a 'medium' interaction, and the thin grey arrow represents a 'small' interaction.

In order to computationally model the interactions of the categories, category gains and time constants were estimated from the literature. The extracted quantitative relationships or 'gains' and time constants represent the effects of ALS from the G93A (SOD1 mutation) in the mouse. Table 1 illustrates the hypothesized size of the one-way interactions and their sign. Note that the interaction is read in the "from to" direction.

For example, the sign of the interaction of free radicals to or 'on' excitotoxicity is listed as '+S', a small positively correlated interaction.

Table 10.2.1. Magnitudes and signs of the one-way category interactive gains as estimated from experimental literature.

From \ To	Axonn Trans	Chemistry	Excitotox	Energetics	Free Rads	Gene Dmg	Inflam	Necro-Apop	Proteomics	Systemic
Axon Trans (AT)	-M		+S	-M			-S	-M		-S
Chemistry (CH)	-S		+S		+S			+M	+M	+S
Excitotox (EX)	-S		-M	-L	+L		+L	+L		+S
Energetics (EN)	+M		+L	+M	+L		+M	+L		+M
Free Rads (FR)	-S	+S	+S	+L	+M	+M	+M	+L	+S	+S
Gene Dmg (GD)			+M		S'+	-M	-S	+M		
Inflam (IN)	-S		+M	-S	+L		-M	+L		+S
Necro-Apop (NA)	+S	-S	+L	-L	+M	+S	+L	-L	+M	+M
Proteomics (PR)	-M	+M	+S		+S		+M	+M	-S	+M
Systemic (SY)			+S	-S	+S			+S		-S

The quantitative values representing the small, medium, and large gains were varied using a sensitivity analysis and were found to not have a major impact on the time course of the category effects as long as their ratios were kept relatively constant. However, for reference, the 'base case' category gains were selected to be 0.5, 1, and 1.5 to represent small, medium, and large respectively. Since at this stage, our main interest is simply view the 'shape' and main characteristics/features of the category time courses and their relative magnitudes to each other, the quantitative values of these categories themselves were irrelevant. Time constants were chosen to reflect the life cycle and appearance of

ALS symptoms in the G93A mouse, with fast, medium, and slow representing 60, 90, and 120 days.

To initiate 'ALS' one or more factors must be moved from their base values to start the simulation. The simulation below is a case in which energetics was the initiator. However, a very rough sensitivity analysis indicates that the patterns of model behavior are very similar regardless of what category is used as the initiator. Interestingly, the results of the category simulations already exhibit some findings which are also reflected in the experimental data. For example, most of the factors do not move significantly from baseline until about 80 days out (see Figure 2), which is within the range that clinical presentation is exhibited in the G93A mouse. Additionally, axonal transport (highlighted in red) and energetics (shown in yellow) have a very different looking pattern compared to the other categories. Finally, a major change happens at around day 150, as all of the factors seem to 'explode', a trait of an unstable system. Not coincidentally, day 150 is within the experimental range of when symptoms become very severe and marks the beginning of the sudden and severe decline seen in end-stage ALS mice.

The results of this very preliminary relational model have generated a few hypotheses that we will test as we continue with our model development. For example, one hypothesis is that the emergence of the sudden decline seen in end-stage ALS is a result of a system instability. Using the rules of control theory, if enough feedback could be apportioned correctly, the propagation of ALS would stop. Thus, one potential

therapeutic concept is to add self-feedback to each category to investigate whether the system can be made stable. As was the case in the spinal cord injury model, testing such theoretical ideas can potentially give way to hypothetical treatments, which can be examined for positive therapeutic effects.

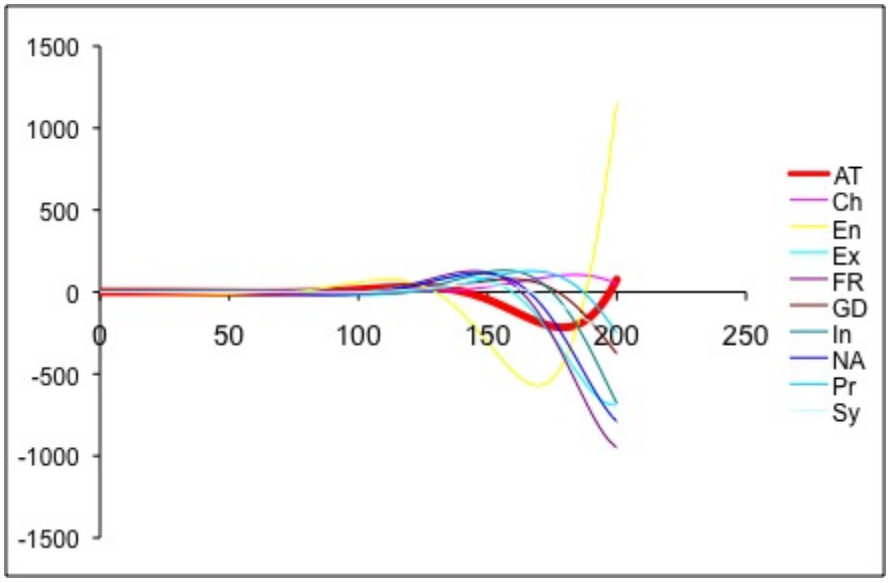

Figure 10.2.2. Time course of categories in a preliminary category model of ALS. The y-axis represents the magnitude of the category's impact and the x-axis represents time in days. Note that only relative category magnitudes are meaningful and not the actual quantitative values, themselves. However, the quantitative values on the x-axis are meaningful as they represent the pathological time course of the G93A ALS mouse.

Aggregating views

These viewpoints (ALS-disrupted axonal transport model, motoneuron data, and the relational model) have and will continue to be used together to obtain a complete and comprehensive view of ALS. For example, the correlations obtained from the velocity profiles of the ALS-disrupted axonal transport model were used to approximate gains and

time constants for the relational model as such gains and time constants were difficult if not impossible to obtain from the current pathological experimental data. In fact, the lack of experimental data and our inability to properly characterize available data was precisely the motivation for the initial development of the conceptual-mechanistic model. Similarly, the identification of size related firing property relationships, which were not explicitly published in the ALS literature, influenced the selection of potential factors to include in the excitotoxicity component of the ALS model. Thus, these more detailed 'category' modeling viewpoints were able to 'fill in' the experimental gaps to construct an initial working relational model.

Once a full relational model with individuated factors is complete, relational analysis will be used to indentify the key factors and their dynamic relationships and interactions. This system-level analysis will be used to distinguish areas that need further refinement and to replace high-impact categories with more detailed models, such as mechanistic or conceptual models. Thus, further down the road, the relational model will feed back into the refinement of the axonal transport and motoneuron models and aid in the planning of future motoneuron experiments. Other areas necessitating more detail are liable to warrant their own modeling viewpoints as well, and these will be identified and implemented as needed. Therefore, in conclusion, the process will iterate with each addition and refinement, bringing a new and necessary perspective to complete our desired multi-dimensional view of ALS.

CHAPTER 11

CONCLUSIONS

In the Introduction, it was stated that the overall purpose of this work was to provide the foundational research that enables comprehensive views of complex physiological and pathological systems to be obtained. In this chapter, we return to this purpose, discussing and evaluating the progress that was made through the development of methodologies to assist in the construction and analysis of computational models that provide unique viewpoints into the system. The chapter concludes by presenting a new form of scientific inquiry, viewpoint aggregation, which is based upon the findings of this work and provides a new and exciting possibility for the future exploration and analysis of complex biological systems.

Conclusions about a relational approach to modeling and analysis

Using the philosophy of complex systems, namely the 'bowtie effect' theory of biological systems, we have developed novel methods to deduce complex multi-scale interactions and dynamics that occur at the critical 'pinch point' by either identifying and/or utilizing the inner relationships of a system, which result in its emergent properties. Relational analysis, using the search-survey-and summarize technique (S3 -Mitchell and Lee 2007) to identify the complex relationships within a system, enables the characterization of both model and experimental data, permitting exploration and direct comparison of

mechanistic function, and generation of testable experimental and clinical hypotheses and predictions. Relational modeling, using the review-relate-refine technique (R3-Mitchell and Lee 2009) to utilize complex system relationships identified within the experimental data, enables foundational models to be quickly and efficiently built that connect disparate pockets of detailed experimental data and provide a comprehensive view into the system as a whole and a preliminary basis upon which detailed bottom-up mechanisms and top-down theories can then be implemented and refined.

Thus, in summary, relational analysis fulfills specific aim one by providing the analytical tools to tease out and explain the underlying mechanisms, organizing principles, and/or dynamics of emergent, complex adaptive behavior within computational models, and relational modeling fulfills specific aim two by providing a methodology that enables initial, system-level "scaffolding" models to be quickly built and assessed based on available literature or experimental data without the need for unknown detailed properties. Together, these two additions to the repertoire of traditional modeling methodologies and data analysis tools provide the foundation necessary to help move the model from a confirmatory to an exploratory research tool.

Conclusions regarding different viewpoints

Using a variety of modeling techniques, we have traversed several different complex physiological and pathological systems, including synaptic neurotransmitter spillover (Mitchell et al. 2007; Mitchell and Lee 2007), normal and pathological axonal transport (Mitchell and Lee, 2009), secondary injury SCI (Mitchell and Lee, 2008), motoneurons

(Mitchell and Lee, 2009c *in preparation*) and most recently we have entered into Amyotrophic Lateral Sclerosis (Mitchell and Lee, 2009b *in revision*). Along the way, we have come to appreciate the value multiple perspectives have when modeling a system. In this project, the differing perspectives are 1) "bottom-up" mechanism-centric approaches that seek to have higher-level function emerge; 2) "top-down" theory-centric approaches that seek to explain higher-level function in terms of lower-level mechanisms; and 3) "middle-out" data-centric approaches that seek to recapitulate and predict experimental and clinical findings. In conjunction with our relational analysis techniques, which enabled the construction of models that produced the desired emergent properties and the construction of landscape that revealed the underlying system dynamics, we found that each of these viewpoints gave us a unique, necessary and often even a new perspective into each of the studied test case systems.

Although experimental and clinical research was not physically performed as part of this dissertation, actual data representing each view was analyzed from studies performed inside (motoneuron experimental data shown in Chapter 5) and outside our lab (not shown) utilizing our relational analysis techniques. Using our developed relational analysis techniques to look through each system's pinch point to either utilize or uncover the relationships that result in the system's emergent properties and complex dynamics, we were able to produce different viewpoints into a system. Below is a brief review of our experience with the three modeling viewpoints and with their experimental and clinical viewpoint counterparts.

Bottom-up Model View

In our experience with a bottom-up synaptic neurotransmitter spillover model (Mitchell et al. 2007b; Mitchell and Lee 2007c), we found that there was substantial non-uniqueness in the parameters values (i.e. multiple parameter value sets could achieve the same target output goals). Similarly, we found that in our mechanistic models of axonal transport, a few different degenerate models, each representing a different transport mechanism, could result in experimentally valid velocity profiles. Thus, though we were able to successfully and efficiently reach our target output goals, we did not know *why* we had achieved them.

Top-down Model View

We explored the use of top-down models, which use a hierarchical tree of hypotheses whose ramifications determined either the mechanism parameter values or the mechanisms themselves, to compare different hypotheses and conceptualizations. Our conceptual models of ALS-disrupted axonal transport were able to differentiate between different pathological causes, such as protein aggregation and mutations, a feat that would not be possible in a mechanistic model. Additionally, using a top-down motoneuron model (not presented in this dissertation) we were able to make explicit predictions regarding previously little understood functions, such as the role of the after hyper-polarization potential (AHP) in determining the motoneurons frequency-current gain (FI gain). The top-down conceptualizations explicitly provided the "why" that was missing from the true bottom-up model. However, the top-down model, while possible

for the study of smaller systems with a fewer number of factors, such as in axonal transport, or for larger but more well-characterized systems such as motoneuron neurophysiology, is not a good candidate for modeling comprehensive clinical pathologies (e.g. ALS and SCI)—systems that are both enormously large, containing multiple factors across several different categories, and for which few, if any, over-arching theories are available.

Relational or "Middle Out" Model View

In the case of pathologies, such as spinal cord injury, starting with either a bottom-up or top-down model was essentially impossible without copious speculation due to the numerous gaps between detailed pockets of experimental data. Consequently, a new modeling technique was developed in order to build the "scaffolding" that would be necessary to connect disparate sets of experimental data together before being able to look at mechanisms and high-level theories. The chosen strategy was to build a "relational model" based exclusively on the relationships or correlations between various identified important factors within the substantial experimental data. This relational model was able to predict previously uncharacterized system dynamics, providing the ***first*** system-level view into a large and complicated pathology. Although the relational model is an excellent starting point to quickly obtain a holistic view of the system and make fundamental predictions early in the research process, it alone cannot provide the detailed, component-level insight of a mechanistic model or the explicit predictions of a top-down model.

Experimental View

To date, experimental viewpoints have been and will continue to be an important aspect of systems physiology. In fact, it is experimental data that provides the parameters, inputs, outputs, mechanisms and even the validation criteria of our models. However, experimental data alone, outside the confines of a computational model, has its own unique viewpoint. Our work with experimental viewpoints, nominally with motoneurons and spinal cord injury data, has been helpful in providing the necessary viewpoint of 'how' relationships result in the emerging dynamics seen within a system. For example, it was through our experimental data that we were able to hypothesize how motoneuron size results in distinct firing properties, a task that was not possible through modeling alone.

Clinical View

Clinical viewpoints, in many ways, serve as the 'final stamp of approval' as to the correctness of our understanding and perhaps more importantly, the impact of our research, in terms of therapeutics to treat pathological conditions. Only within the human, where all of the real complex system properties and characteristics are present, can the system function and behavior be fully analyzed. However, due to safety and ethical concerns, clinical studies are limited to the extent they can 'alter the system', whether through drugs, stimulation or other modalities, in order to evaluate the system's robust behavior over multiple operating points. We learned through the analysis of clinical spinal cord injury data, that the clinical viewpoint contributes the 'what' of

systems physiology (what is affected, what is the impact, what is the time course). In fact, based on our work in SCI, it is our assertion that it is the difference between the 'what' of experimental and clinical studies, which likely results in the failure of clinical trials that seemed promising at the experimental stage.

Aggregating viewpoints

While each of the viewpoints above gave us a necessary view into the studied system, none produced the full multi-scalar, integrative and comprehensive view that we as biomedical engineers desired—the type of complete and profound comprehensive view described in the Introduction, which is necessary in order to have the vast understanding and impact of physiologies and pathologies that is desired in order to completely change the lives of patients. However, our experience with each of these viewpoints has lead us to what we believe is an approach, which is capable of producing the complete, multi-scalar and comprehensive view that is needed. We contend that the best approach to study a complex biological system is not contained within any one method or viewpoint, but rather the best approach is to aggregate and reconcile these differing points of view into a unified, but not necessarily monolithic whole. This unification process can be accomplished using our developed set of relational analysis techniques. Because relational analysis focuses on the intrinsic relationships between system measures rather than on the quantitative values themselves, it provides an equivalent means to compare and contrast differing viewpoints through their system landscapes. We refer to this unification process as viewpoint aggregation (see Figure 1). Using relational analysis as the centerpiece, this truly comprehensive approach aggregates the viewpoints produced

from relational ‘middle-out’ scaffolding, top-down conceptualizations, bottom-up mechanisms, and experimental and clinical observations in an iterative loop of continual model refinement and subsequent experimental and clinical prediction and prioritization.

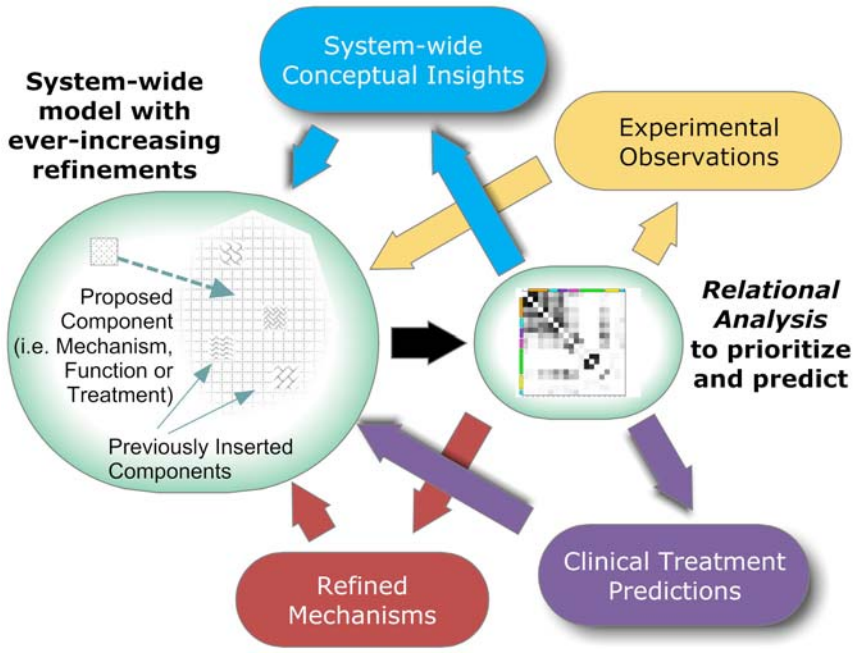

Figure 11.1: Overview of viewpoint aggregation process. Using relational analysis as the centerpiece, we have developed a comprehensive approach, that aggregates the viewpoints produced from relational scaffolding, top-down conceptualizations, bottom-up mechanisms, and experimental and clinical observations in an iterative loop of continual model refinement and subsequent experimental and clinical prediction and prioritization. This loop brings the system into ever-greater focus with each iteration.

A new approach to systems physiology

In summary, we conclude that the developed relationship-based analytical and modeling methods, in combination with multiple viewpoints, encompasses a new approach to systems physiology that will provide the multi-scalar, truly comprehensive views that we as engineers, scientists, and clinicians desire. One of the key benefits of viewpoint aggregation by utilizing relationships is that it incorporates not just the modeling viewpoints discussed in the previous section, but also experimental and clinical viewpoints. This iterative loop is driven by the continuous act of comparing and contrasting theoretical, conceptual, experimental, and clinical viewpoints as each new or revised viewpoint becomes available. As such, with each iteration viewpoint aggregation brings the system into ever-greater focus.

In essence, viewpoint aggregation represents a new, integrative approach to systems physiology that focuses on the process of research exploration rather than the actual product. This viewpoint aggregation process does not fit the typical research mold of hypothesis-driven inquiry, in that it is instead hypothesis challenging and generating inquiry, with hypothesis testing coming later in the process. However, we believe this exploratory approach to be the key to obtaining truly multi-scalar, comprehensive views into the complex physiological and pathological systems that we as biomedical engineers need in order to accomplish our ultimate goal of helping patients.

APPENDIX A

SCI RELATIONAL MODEL LITERATURE DATABASE

Category 1	Category 2	Author	Year	Title	Journal	Invitro	Invivo	TBI	SCI	Description
Clinical		Baptiste, D. C. and M. G. Fehlings	2006	Pharmacological approaches to repair the injured spinal cord	J Neurotrauma 23(3-4): 318-34.		x		x	review of clinical pharma-cological approaches
Clinical		Blight, A. R. and M. H. Tuszyns	2006	Clinical trials in spinal cord injury	J Neurotrauma 23(3-4): 586-93.		x		x	preclinical translation to clinical trials
Clinical		Bracken, M. B., M. J. Shepard, et al.	1990	A randomized, controlled trial of methylprednisolone or naloxone in the treatment of acute spinal-cord injury. Results of the Second National Acute Spinal Cord Injury Study	N Engl J Med 322		x		x	methylpredni solone (NASCIS)
Clinical		Bracken, M. B., M. J. Shepard, et al.	1992	Methylprednisolone or naloxone treatment after acute spinal cord injury: 1-year follow-up data. Results of the second National Acute Spinal Cord Injury Study	J Neurosurg 76(1): 23-31.		x		x	methylpredni solone and naloxone
Clinical		Bracken, M. B., M. J. Shepard, et al.	1997	Administration of methylprednisolone for 24 or 48 hours or tirilazad mesylate for 48 hours in the treatment of acute spinal cord injury. Results of the Third National Acute Spinal Cord Injury Randomized Controlled Trial. National Acute Spinal Cord Injury Study	JAMA 277		x		x	methylpredni solone or tirilazad (NASCIS 3)
Clinical		Cayli, S. R., O. Ates, et al.	2006	Neuroprotective effect of etomidate on functional recovery in experimental spinal cord injury	Int J Dev Neurosci 24(4): 233-9.		x		x	etomidate
Clinical		Chen, H. Y., J. M. Lin, et al.	1998	Raffinee, a free radical scavenger, in the treatment of subacute stage brain and spinal cord lesions: A case report	American Journal of Chinese Medicine 26(1): 97-108.		x	x	x	free radical scavenger raffinee

Category 1	Category 2	Author	Year	Title	Journal	Invitro	Invivo	TBI	SCI	Description
Clinical		Courtine, G., B. Song, et al.	2008	Recovery of supraspinal control of stepping via indirect propriospinal relay connections after spinal cord injury	Nat Med 14(1): 69-74.		x		x	supraspinal control of stepping
Clinical		Faden, A. I. and S. Salzman	1992	Pharmacological Strategies in Cns Trauma	Trends in Pharmacological Sciences 13(1): 29-35.		x			pharma-cological strategies: corticosteroids, free radical scavengers, opioid antagonsists
Clinical		Faden, A. I. and B. Stoica	2007	Neuroprotection - Challenges and opportunities	Archives of Neurology 64(6): 794-800.		x		x	pharma-cological strategies, multi-potential drugs
Clinical		Fearnside, S. M.	2006	Managing acute spinal cord injury - Examining the controversy	Australian Veterinary Practitioner 36(4): 148-+.		x		x	methylprednisolone controversy/side effects
Clinical		Fu, E. S. and R. P. Tummala	2005	Neuroprotection in brain and spinal cord trauma	Curr Opin Anaesthesiol 18(2): 181-7.		x	x	x	neuro-protection strategies
Clinical		Hulsebosch, C. E.	2002	Recent advances in pathophysiology and treatment of spinal cord injury	Advances in Physiology Education 26(4): 238-255.		x		x	patho-physiology and treatment strategies
Clinical		Jin, Y., M. L. McEwen, et al.	2004	The mitochondrial uncoupling agent 2,4-dinitrophenol improves mitochondrial function, attenuates oxidative damage, and increases white matter sparing in the contused spinal cord	J Neurotrauma 21(10): 1396-404.		x		x	mitochon-drial uncoupling agent 2,4-dinitrophenol
Clinical		Kaneko, S., A. Iwanami, et al.	2006	A selective Sema3A inhibitor enhances regenerative responses and functional recovery of the injured spinal cord	Nat Med 12(12): 1380-9.		x		x	(rat) Sema3A inhibitor

Category 1	Category 2	Author	Year	Title	Journal	Invitro	Invivo	TBI	SCI	Description
Clinical		Kwon, B. K., W. Tetzlaff, et al.	2004	Pathophysiology and pharmacologic treatment of acute spinal cord injury	Spine J 4(4): 451-64.		x		x	patho-physiology and treatment strategies
Clinical		Lim, P. A. C. and A. M. Tow	2007	Recovery and regeneration after spinal cord injury: A review and summary of recent literature	Annals Academy of Medicine Singapore 36(1): 49-57.		x		x	regeneration
Clinical		Lipton, S. A.	2004	Failures and successes of NMDA receptor antagonists: molecular basis for the use of open-channel blockers like memantine in the treatment of acute and chronic neurologic insults	NeuroRx 1(1): 101-10.		x	x	x	NMDA receptor antagonsists
Clinical		Maas, A. I., G. Murray, et al.	2006	Efficacy and safety of dexanabinol in severe traumatic brain injury: results of a phase III randomised, placebo-controlled, clinical trial	Lancet Neurol 5(1): 38-45.		x	x		dexanabinol
Clinical		Muizelaar, J. P., A. Marmarou, et al.	1993	Improving the outcome of severe head injury with the oxygen radical scavenger polyethylene glycol-conjugated superoxide dismutase: a phase II trial	J Neurosurg 78(3): 375-82.		x	x		ROS scavenger polyethylene glycol-conjugated superoxide dismutase phase II clinical trial
Clinical		Nockels, R. and W. Young	1992	Pharmacological Strategies in the Treatment of Experimental Spinal-Cord Injury	Journal of Neurotrauma 9: S211-S217.		x		x	pharma-cological strategies: NMDA & excitotoxic blockers, gangliosides
Clinical		Oudega, M.	2007	Schwann cell and olfactory ensheathing cell implantation for repair of the contused spinal cord	Acta Physiologica 189(2): 181-189.		x		x	Schwann cell and olfactory ensheathing cell implantation

Category 1	Category 2	Author	Year	Title	Journal	Invitro	Invivo	TBI	SCI	Description
Clinical		Ribotta, M. G., M. Gaviria, et al.	2002	Strategies for regeneration and repair in spinal cord traumatic injury	Spinal Cord Trauma: Regeneration, Neural Repair and Functional Recovery 137: 191-212.		x		x	strategies for regeneration and repair
Clinical		Stirling, D. P., K. Khodarahmi, et al.	2004	Minocycline treatment reduces delayed oligodendrocyte death, attenuates axonal dieback, and improves functional outcome after spinal cord injury	J Neurosci 24(9): 2182-90.		x		x	minocycline
Clinical		Tator, C. H. and M. G. Fehlings	1999	Review of clinical trials of neuroprotection in acute spinal cord injury	Neurosurg Focus 6(1): e8.		x		x	review of clinical trials of neuroprotection
Clinical		Tolias, C. M. and M. R. Bullock	2004	Critical appraisal of neuroprotection trials in head injury: what have we learned?" NeuroRx 1(1): 71-9.			x	x		neuroprotection trials in head injury
Clinical		Young, W.	1993	Secondary injury mechanisms in acute spinal cord injury	J Emerg Med 11 Suppl 1: 13-22.		x		x	NASCIS 2 analysis: dose, iniation time
Energetics		Agrawal, S. K. and M. G. Fehlings	1996	Mechanisms of secondary injury to spinal cord axons in vitro: Role of Na+,Na+-K+-ATPase, the N+-H+ exchanger, and the Na+-Ca2+ exchanger		x			x	(axon) sodium and Na-K-ATPase
Energetics		Ahmed, S. M., J. T. Weber, et al.	2002	NMDA receptor activation contributes to a portion of the decreased mitochondrial membrane potential and elevated intracellular free calcium in strain-injured neurons	J Neurotrauma 19(12): 1619-29.	x		x		decreased mito-chondrial potential
Energetics		Alano, C. C., G. Beutner, et al.	2002	Mitochondrial permeability transition and calcium dynamics in striatal neurons upon intense NMDA receptor activation	J Neurochem 80(3): 531-8.	x		x		(striatal) NMDA induced mitochondrial calcium

Category 1	Category 2	Author	Year	Title	Journal	Invitro	Invivo	TBI	SCI	Description
Energetics		Anderson, D. K., E. D. Means, et al.	1980	Spinal cord energy metabolism following compression trauma to the feline spinal cord	J Neurosurg 53(3): 375-80.		x		x	(cat) glucose, ATP time course
Energetics		Anderson, D. K., L. D. Prockop, et al.	1976	Cerebrospinal fluid lactate and electrolyte levels following experimental spinal cord injury	J Neurosurg 44(6): 715-22.		x		x	(cat) ions and lactate sub-acute
Energetics		Ankarcrona, M., J. M. Dypbukt, et al.	1995	Glutamate-Induced Neuronal Death - a Succession of Necrosis or Apoptosis Depending on Mitochondrial-Function	Neuron 15(4): 961-973.	x		x		(granule) mitochondria and ca induced apoptosis
Energetics		Faden, A. I., P. H. Chan, et al.	1987	Alterations in lipid metabolism, Na+,K+-ATPase activity, and tissue water content of spinal cord following experimental traumatic injury	J Neurochem 48(6): 1809-16.		x		x	(cat) Na-K-ATPase
Energetics		Ferreira, I. L., C. B. Duarte, et al.	1997	'Chemical ischemia' in cultured retina cells: the role of excitatory amino acid receptors and of energy levels on cell death	Brain Res 768(1-2): 157-66.	x				(retina) mito-chondrial function, ATP
Energetics		Fiskum, G.	2000	Mitochondrial participation in ischemic and traumatic neural cell death	Journal of Neurotrauma 17(10): 843-855.			x		mitochondria & cell death
Energetics		Hovda, D. A., D. P. Becker, et al.	1992	Secondary injury and acidosis	J Neurotrauma 9 Suppl 1: S47-60.			x		glucose
Energetics		Iwai, T., K. Tanonaka, et al.	2002	Sodium accumulation during ischemia induces mitochondrial damage in perfused rat hearts	Cardiovasc Res 55(1): 141-9.	x				Na-induced mitochondral damage
Energetics		Jacobs, T. P., O. Kempski, et al.	1992	Blood-Flow and Vascular-Permeability during Motor Dysfunction in a Rabbit Model of Spinal-Cord Ischemia	Stroke 23(3): 367-373.		x		x	(rabbit) blood flow & ischemia

Category 1	Category 2	Author	Year	Title	Journal	Invitro	Invivo	TBI	SCI	Description
Energetics		Jolivet, R. and P. Magistretti	2007	Spike-frequency adaptation is modulated by interacting currents: Role of the Na, K-ATPase	Journal of Neurophysiology.					Na-K-ATPase mechanics
Energetics		Jurkowitz alexander, M. S., R. A. Altschuld, et al.	1992	Cell Swelling, Blebbing, and Death Are Dependent on Atp Depletion and Independent of Calcium during Chemical Hypoxia in a Glial-Cell Line (Roc-1)	Journal of Neurochemistry 59(1): 344-352.	x				(glial) ATP & calcium
Energetics		Kadekaro, M., A. M. Crane, et al.	1985	Differential-Effects of Electrical-Stimulation of Sciatic-Nerve on Metabolic-Activity in Spinal-Cord and Dorsal-Root Ganglion in the Rat	Proceedings of the National Academy of Sciences of the United States of America 82(17): 6010-6013.		x		x	(rat) metabolism vs. activity
Energetics		Kandel, E. R., J. H. Schwartz, et al.	2000	Principles of Neural Science	McGraw-Hill.					Na-K-ATPase mechanisms
Energetics		Kong, B. Y. and R. J. Clarke	2004	Identification of potential regulatory sites of the Na+,K+-ATPase by kinetic analysis	Biochemistry 43(8): 2241-50.	x				function of Na-K-ATPase pump
Energetics	Necro-Apoptosis	Krajewski, S., M. Krajewska, et al.	1999	Release of caspase-9 from mitochondria during neuronal apoptosis and cerebral ischemia	Proc Natl Acad Sci U S A 96(10): 5752-7.		x	x		caspase-9 from mitochondria
Energetics		Li, S. and P. K. Stys	2001	Na+-K+-ATPase inhibition and depolarization induce glutamate release via reverse Na+-dependent transport in spinal cord white matter	Neuroscience 107(4): 675-683.	x			x	Na-K-ATPase
Energetics	Free Radicals	Mattiasson, G.	2004	Analysis of mitochondrial generation and release of reactive oxygen species	Cytometry Part A 62A(2): 89-96.	x				ROS vs mitochondrial generation

Category 1	Category 2	Author	Year	Title	Journal	Invitro	Invivo	TBI	SCI	Description
Energetics		Nicholls, D. G. and S. L. Budd	2000	Mitochondria and neuronal survival	Physiological Reviews 80(1): 315-360.			x	x	mitochondria & neuronal survival
Energetics	Free Radicals	Opii, W. O., V. N. Nukala, et al.	2007	Proteomic identification of oxidized mitochondrial proteins following experimental traumatic brain injury	Journal of Neurotrauma 24(5): 772-789.		x	x		(rat) oxidized mitochondrial proteins
Energetics		Robertson, C. S., J. C. Goodman, et al.	1992	Blood flow and metabolic therapy in CNS injury	J Neurotrauma 9 Suppl 2: S579-94.			x		hyper-rmetabolism
Energetics		Sullivan, P. G., S. Krishnamurthy, et al.	2007	Temporal characterization of mitochondrial Energetic after spinal cord injury	J Neurotrauma 24(6): 991-9.		x		x	temporal mitochondrial energetics
Energetics	Necro-Apoptosis	Sullivan, P. G., A. G. Rabchevsky, et al.	2005	Mitochondrial permeability transition in CNS trauma: Cause or effect of neuronal cell death?" Journal of Neuroscience Research 79(1-2): 231-239.			x	x		mitochondria & cell death
Energetics		Sullivan, P. G., J. E. Springer, et al.	2004	Mitochondrial uncoupling as a therapeutic target following neuronal injury	Journal of Energetic and Biomembranes 36(4): 353-356.			x	x	mito-chondrial uncoupling
Energetics	Necro-Apoptosis	Tator, C. H. and M. G. Fehlings	1991	Review of the secondary injury theory of acute spinal cord trauma with emphasis on vascular mechanisms	J Neurosurg 75(1): 15-26.				x	vascular mechanisms
Energetics		Tator, C. H. and I. Koyanagi	1997	Vascular mechanisms in the pathophysiology of human spinal cord injury	J Neurosurg 86(3): 483-92.		x			(human) vascular permability, swelling
Energetics		White, R. J. and I. J. Reynolds	1996	Mitochondrial depolarization in glutamate-stimulated neurons: an early signal specific to excitotoxin exposure	J Neurosci 16(18): 5688-97.	x		x		mitochondria and calcium
Energetics		Young, W.	1992	Role of Calcium in Central-Nervous-System Injuries	Journal of Neurotrauma 9: S9-S25.			x	x	calcium

Category 1	Category 2	Author	Year	Title	Journal	Invitro	Invivo	TBI	SCI	Description
Excitotoxicity		Allen, J. W., S. Vicini, et al.	2001	Exacerbation of neuronal cell death by activation of group 1 metabotropic glutamate receptors: Role of NMDA receptors and arachidonic acid release	Experimental Neurology 169(2): 449-460.	x		x	x	NMDA
Excitotoxicity		Ankarcrona, M., J. M. Dypbukt, et al.	1995	Glutamate-Induced Neuronal Death - a Succession of Necrosis or Apoptosis Depending on Mitochondrial-Function	Neuron 15(4): 961-973.	x		x		necrosis or apoptosis via glutamate
Excitotoxicity		Arundine, M. and M. Tymianski	2004	Molecular mechanisms of glutamate-dependent neurodegeneration in ischemia and traumatic brain injury	Cellular and Molecular Life Sciences 61(6): 657-668.		x	x		NMDA activation mechanisms
Excitotoxicity		Arundine, M., G. K. Chopra, et al.	2003	Enhanced vulnerability to NMDA toxicity in sublethal traumatic neuronal injury in vitro	Journal of Neurotrauma 20(12): 1377-1395.	x		x		NMDA
Excitotoxicity		Ates, O., S. R. Cayli, et al.	2007	Comparative neuroprotective effect of sodium channel blockers after experimental spinal cord injury	Journal of Clinical Neuroscience 14(7): 658-665.		x		x	(rat) sodium/effects channel blockers
Excitotoxicity		Bakiri, Y., N. B. Hamilton, et al.	2008	Testing NMDA receptor block as a therapeutic strategy for reducing ischaemic damage to CNS white matter	Glia 56(2): 233-40.	x		x	x	oligodendroglial excitotoxicity
Excitotoxicity		Carbonell, W. S. and M. S. Grady	1999	Evidence disputing the importance of excitotoxicity in hippocampal neuron death after experimental traumatic brain injury	Neuroprotective Agents: Fourth International Conference 890: 287-298.	x		x		contribution of excitotoxicity to neuronal death
Excitotoxicity		Carriedo, S. G., H. Z. Yin, et al.	1998	Rapid Ca2+ entry through Ca2+-permeable AMPA/kainate channels triggers marked intracellular Ca2+ rises and consequent oxygen radical production	Journal of Neuroscience 18	x		x		calcium via AMPA

Category 1	Category 2	Author	Year	Title	Journal	Invitro	Invivo	TBI	SCI	Description
Excitotoxicity		Choi, D. W.	1992	Excitotoxic cell death	J Neurobiol 23(9): 1261-76.			x	x	excitotoxic mechanisms
Excitotoxicity		Choi, D. W. and S. M. Rothman	1990	The Role of Glutamate Neurotoxicity in Hypoxic-Ischemic Neuronal Death	Annual Review of Neuroscience 13: 171-182.			x	x	glu neurotoxicity
Excitotoxicity		Fehlings, M. G. and S. Agrawal	1995	Role of sodium in the pathophysiology of secondary spinal cord injury	Spine 20	x			x	role of sodium
Excitotoxicity		Goforth, P. B., E. F. Ellis, et al.	2004	Mechanical injury modulates AMPA receptor kinetics via an NMDA receptor-dependent pathway	Journal of Neurotrauma 21(6): 719-732.	x		x		AMPA-R activation via NMDA-R
Excitotoxicity		Hilton, G. D., J. L. Nunez, et al.	2006	Glutamate-mediated excitotoxicity in neonatal hippocampal neurons is mediated by mGluR-induced release of Ca++ from intracellular stores and is prevented by estradiol	European Journal of Neuroscience 24(11): 3008-3016.	x		x		glutamate via metabotropic-R
Excitotoxicity		Kaptanoglu, E., I. Solaroglu, et al.	2005	Blockade of sodium channels by phenytoin protects ultrastructure and attenuates lipid peroxidation in experimental spinal cord injury	Acta Neurochirurgica 147(4): 405-412.		x		x	(rat) sodium/effects channel blockers
Excitotoxicity		Kimura, M., K. Katayama, et al.	1999	Role of glutamate receptors and voltage-dependent calcium channels in glutamate toxicity in energy-compromised cortical neurons	Japanese Journal of Pharmacology 80(4): 351-358.	x		x		relationship of glu, ca, & energy
Excitotoxicity		LaPlaca, M. C. and L. E. Thibault	1998	Dynamic mechanical deformation of neurons triggers an acute calcium response and cell injury involving the N-methyl-D-aspartate glutamate receptor	Journal of Neuroscience Research 52(2): 220-229.	x		x		calcium via NMDA

Category 1	Category 2	Author	Year	Title	Journal	Invitro	Invivo	TBI	SCI	Description
Excito-toxicity		LaPlaca, M. C., V. M. Y. Lee, et al.	1997	An in vitro model of traumatic neuronal injury: Loading rate-dependent changes in acute cytosolic calcium and lactate dehydrogenase release	Journal of Neurotrauma 14(6): 355-368.	x		x		calcium vs LDH
Excito-toxicity		Lemke, M., P. Demediuk, et al.	1987	Alterations in tissue Mg++, Na+ and spinal cord edema following impact trauma in rats	Biochem Biophys Res Commun 147(3): 1170-5.		x		x	sodium, magnesium, water content
Excito-toxicity	Inflam-mation	Lima, R. R., J. Guimaraes-Silva, et al.	2007	Diffuse Axonal Damage, Myelin Impairment, Astrocytosis and Inflammatory Response Following Microinjections of NMDA into The Rat Striatum	Inflammation.		x	x		(rat) inflammation in response to NMDA-R activation
Excito-toxicity		Liu, D., G. Y. Xu, et al.	1999	Neurotoxicity of glutamate at the concentration released upon spinal cord injury	Neuroscience 93(4): 1383-1389.		x		x	glutamate concentration
Excito-toxicity		Lusardi, T. A., J. A. Wolf, et al.	2004	Effect of acute calcium influx after mechanical stretch injury in vitro on the viability of hippocampal neurons	Journal of Neurotrauma 21(1): 61-72.	x		x		calcium influx via stretch or NMDA
Excito-toxicity		Matute, C., E. Alberdi, et al.	2001	The link between excitotoxic oligodendroglial death and demyelinating diseases	Trends in Neuro-sciences 24(4): 224-230.					oligodendroglial excitotoxicity
Excito-toxicity		McBurney, R. N., D. Daly, et al.	1992	New CNS-specific calcium antagonists	J Neurotrauma 9 Suppl 2: S531-43.	x		x		role of ca & ca antagonists
Excito-toxicity		Nesic, O., N. M. Svrakic, et al.	2002	DNA microarray analysis of the contused spinal cord: effect of NMDA receptor inhibition	J Neurosci Res 68(4): 406-23.				x	effects of NMDA using DNA microarray
Excito-toxicity	Necro-Apop-tosis	Park, E., Y. Liu, et al.	2003	Changes in glial cell white matter AMPA receptor expression after spinal cord injury and relationship to apoptotic cell death	Experi-mental Neurology 182(1): 35-48.				x	white matter excitotoxicity-mediated death

Category 1	Category 2	Author	Year	Title	Journal	Invitro	Invivo	TBI	SCI	Description
Excito-toxicity	Free Radicals	Park, E., A. A. Velumian, et al.	2004	The role of excitotoxicity in secondary mechanisms of spinal cord injury: A review with an emphasis on the implications for white matter degeneration	Journal of Neurotrauma 21(6): 754-774.				x	white matter excitotoxicity free radical induced cell death
Excito-toxicity	Free Radicals	Piani, D., K. Frei, et al.	1993	Glutamate Uptake by Astrocytes Is Inhibited by Reactive Oxygen Intermediates but Not by Other Macrophage-Derived Molecules Including Cytokines, Leukotrienes or Platelet-Activating-Factor	Journal of Neuro-immunology 48(1): 99-104.	x		x	x	decreased glutamate & ROS uptake
Excito-toxicity	Necro-Apop-tosis	PorteraCailliau, C., D. L. Price, et al.	1997	Non-NMDA and NMDA receptor-mediated excitotoxic neuronal deaths in adult brain are morphologically distinct: Further evidence for an apoptosis-necrosis continuum	Journal of Comparative Neurology 378(1): 88-104.			x		(rat) apoptosis vs necrosis/ role of NMDA vs non-NMDA
Excito-toxicity		Regan, R. F. and D. W. Choi	1991	Glutamate Neurotoxicity in Spinal-Cord Cell-Culture	Neuropscience 43(2-3): 585-591.	x			x	glu neurotoxicity
Excito-toxicity		Runnerstam, M., F. Bao, et al.	2001	A new model for diffuse brain injury by rotational acceleration: II. Effects on extracellular glutamate, intracranial pressure, and neuronal apoptosis	Journal of Neurotrauma 18(3): 259-273.		x	x		(rabbit) glutamate and apoptosis
Excito-toxicity		Sattler, R., Z. G. Xiong, et al.	2000	Distinct roles of synaptic and extrasynaptic NMDA receptors in excitotoxicity	Journal of Neuro-science 20(1): 22-33.	x		x	x	NMDA
Excito-toxicity		Schwart, G. and M. G. Fehlings	2001	Evaluation of the neuroprotective effects of sodium channel blockers after spinal cord injury: improved behavioral and neuroanatomical recovery with riluzole	Journal of Neuro-surgery 94(2): 245-256.	x			x	sodium/effects channel blockers

Category 1	Category 2	Author	Year	Title	Journal	Invitro	Invivo	TBI	SCI	Description
Excitotoxicity	Free Radicals	Springer, J. E., R. D. Azbill, et al.	1999	Activation of the caspase-3 apoptotic cascade in traumatic spinal cord injury	Nature Medicine 5(8): 943-946.		x		x	lipid peroxidation inhibits glu uptake
Excitotoxicity		Takahashi, S., M. Shibata, et al.	1999	Role of sodium ion influx in depolarization-induced neuronal cell death by high KCl or veratridine	European Journal of Pharmacology 372(3): 297-304.	x				role of sodium influx
Excitotoxicity		Tenneti, L. and S. A. Lipton	2000	Involvement of activated caspase-3-like proteases in N-methyl-D-aspartate-induced apoptosis in cerebrocortical neurons	J Neurochem 74(1): 134-42.	x				caspase-3 in NMDA induced apoptosis
Excitotoxicity		Uhler, T. A., D. M. Frim, et al.	1994	The Effects of Megadose Methylprednisolone and U-78517f on Toxicity Mediated by Glutamate Receptors in the Rat Neostriatum	Neurosurgery 34(1): 122-128.		x	x		(rat) methylprednisolone glu-R neurotoxicity
Excitotoxicity	Free Radicals	Volterra, A., D. Trotti, et al.	1994	Glutamate uptake inhibition by oxygen free radicals in rat cortical astrocytes	J Neurosci 14(5 Pt 1): 2924-32.	x		x		ROS mediated decreased glutamate uptake
Excitotoxicity		Wrathall, J. R., Y. D. Teng, et al.	1997	Delayed antagonism of AMPA/kainate receptors reduces long-term functional deficits resulting from spinal cord trauma	Exp Neurol 145(2 Pt 1): 565-73.		x		x	AMPA-R
Excitotoxicity		Xin, W. K., X. H. Zhao, et al.	2005	The removal of extracellular calcium: a novel mechanism underlying the recruitment of N-methyl-D-aspartate (NMDA) receptors in neurotoxicity	European Journal of Neuroscience 21(3): 622-636.	x		x		calcium/ sodium impact on NMDA
Excitotoxicity		Xu, G. Y., M. G. Hughes, et al.	2004	Concentrations of glutamate released following spinal cord injury kill oligodendrocytes in the spinal cord	Exp Neurol 187(2): 329-36		x		x	(rat) oligodendroglial excitotoxicity

Category 1	Category 2	Author	Year	Title	Journal	Invitro	Invivo	TBI	SCI	Description
Excitotoxicity		Xu, G. Y., M. G. Hughes, et al.	2005	Administration of glutamate into the spinal cord at extracellular concentrations reached post-injury causes functional impairments	Neuroscience Letters 384(3): 271-276.		x		x	glutamate concentration
Excitotoxicity	Other	Yanase, M., T. Sakou, et al.	1995	Role of N-Methyl-D-Aspartate Receptor in Acute Spinal-Cord Injury	Journal of Neurosurgery 83(5): 884-888.		x		x	(rabbit) NMDA-R
Excitotoxicity		Yoshioka, A., B. Bacskai, et al.	1996	Pathophysiology of oligodendroglial excitotoxicity	J Neurosci Res 46(4): 427-37.	x		x	x	oligodendroglial excitotoxicity
Excitotoxicity		Young, W.	1987	The post-injury responses in trauma and ischemia: secondary injury or protective mechanisms	Cent Nerv Syst Trauma 4(1): 27-51.				x	emphasis on calcium
Excitotoxicity		Yum, S. W. and A. I. Faden	1990	Comparison of the neuroprotective effects of the N-methyl-D-aspartate antagonist MK-801 and the opiate-receptor antagonist nalmefene in experimental spinal cord ischemia	Arch Neurol 47(3): 277-81.		x		x	role of NMDA vs opiate receptors
Excitotoxicity		Zhang, L., B. A. Rzigalinski, et al.	1996	Reduction of voltage-dependent Mg2+ blockade of NMDA current in mechanically injured neurons	Science 274(5294): 1921-3.	x		x		NMDA
Free Radicals								x	x	lipid peroxidation/ oxygen radicals
Free Radicals	Inflammation	Chalimoniuk, M., K. King-Pospisil, et al.	2006	Macrophage migration inhibitory factor induces cell death and decreases neuronal nitric oxide expression in spinal cord neurons	Neuroscience 139(3): 1117-1128.	x			x	macrophage and nitric oxide
Free Radicals		Dawson, T. M., V. L. Dawson, et al.	1994	Molecular mechanisms of nitric oxide actions in the brain	Ann N Y Acad Sci 738: 76-85.			x		nitric oxide

Category 1	Category 2	Author	Year	Title	Journal	Invitro	Invivo	TBI	SCI	Description
Free Radicals		Dawson, T. M., J. Zhang, et al.	1994	Nitric oxide: cellular regulation and neuronal injury	Prog Brain Res 103: 365-9.			x	x	nitric oxide
Free Radicals		Dohi, K., K. Satoh, et al.	2007	Does edaravone (MCI-186) act as an antioxidant and a neuroprotector in experimental traumatic brain injury?" Antioxid Redox Signal 9(2): 281-7.			x		x	(rat) free radical scavenger, edaravone
Free Radicals		Genoves e, T., E. Mazzon, et al.	2007	Role of endogenous glutathione in the secondary damage in experimental spinal cord injury in mice	Neurosci Lett 423(1): 41-6.		x		x	(mouse) free radical scavenger, glutathione
Free Radicals		Hall, E. D.	1992	The Neuroprotective Pharmacology of Methylprednisolone	Journal of Neurosurgery 76(1): 13-22.				x	free radical neuro-protection with methyl-prednisolone
Free Radicals		Hall, E. D. and J. M. Braugh-ler	1993	Free radicals in CNS injury	Res Publ Assoc Res Nerv Ment Dis 71: 81-105.			x	x	
Free Radicals		Hall, E. D., J. M. Braugh-ler, et al.	1992	Antioxidant Effects in Brain and Spinal-Cord Injury	Journal of Neurotrauma 9: S165-S172.			x	x	antioxidants
Free Radicals		Hall, E. D., P. A. Yonkers, et al.	1992	Biochemistry and Pharmacology of Lipid Antioxidants in Acute Brain and Spinal-Cord Injury	Journal of Neurotrauma 9: S425-S442.			x	x	lipid antioxidants
Free Radicals		Hamada, Y., T. Ikata, et al.	1996	Roles of nitric oxide in compression injury of rat spinal cord	Free Radic Biol Med 20(1): 1-9.		x		x	(rat) nitric oxide
Free Radicals		Huang, Z., P. L. Huang, et al.	1994	Effects of cerebral ischemia in mice deficient in neuronal nitric oxide synthase	Science 265(5180): 1883-5.		x			(rat) effects of NOS on ischemia
Free Radicals		Khaldi, A., C. C. Chiueh, et al.	2002	The significance of nitric oxide production in the brain after injury	Nitric Oxide: Novel Actions, Deleterious Effects and Clinical Potential 962: 53-59.	x	x	x		nitric oxide

Category 1	Category 2	Author	Year	Title	Journal	Invitro	Invivo	TBI	SCI	Description
Free Radicals		Kirsch, J. R., M. A. Helfaer, et al.	1992	Evidence for Free-Radical Mechanisms of Brain Injury Resulting from Ischemia Reperfusion-Induced Events	Journal of Neurotrauma 9: S157-S163.			x		free radical mechanisms
Free Radicals		Kwak, E. K., J. W. Kim, et al.	2005	The role of inducible nitric oxide synthase following spinal cord injury in rat	J Korean Med Sci 20(4): 663-9.		x		x	(rat) inducible nitrix oxide, I-NOS
Free Radicals		Merrill, J. E., L. J. Ignarro, et al.	1993	Microglial cell cytotoxicity of oligodendrocytes is mediated through nitric oxide	J Immunol 151(4): 2132-41.	x		x		microglia, oligodendrocytes, nitric oxide
Free Radicals		Ohta, S., Y. Iwashita, et al.	2005	Neuroprotection and enhanced recovery with edaravone after acute spinal cord injury in rats	Spine 30(10): 1154-1158.		x		x	(rat) free radical scavenger, edaravone
Free Radicals		Schreiberova, A., M. Lackova, et al.	2006	Neuronal nitric oxide synthase immunopositivity in motoneurons of the rabbit's spinal cord after transient ischemia/reperfusion injury	Cellular and Molecular Neurobiology 26(7-8): 1483-1494.		x			(rabbit) nitrix oxide synthase (NOS)
Free Radicals		Sharma, H. S., J. Westman, et al.	1996	Involvement of nitric oxide in acute spinal cord injury: an immunocytochemical study using light and electron microscopy in the rat	Neurosci Res 24(4): 373-84.		x		x	(rat) nitric oxide
Free Radicals		Topsakal, C., N. Kilic, et al.	2003	Effects of prostaglandin E1, melatonin, and oxytetracycline on lipid peroxidation, antioxidant defense system, paraoxonase (PON1) activities, and homocysteine levels in an animal model of spinal cord injury	Spine 28(15): 1643-52.		x		x	(rat) lipid peroxidation, prostaglandin, melatonin
Free Radicals		Xiong, Y., A. G. Rabchevsky, et al.	2007	Role of peroxynitrite in secondary oxidative damage after spinal cord injury	J Neurochem 100(3): 639-49.		x		x	(rat) nitric oxide synthase radical, peroxynitrite

Category 1	Category 2	Author	Year	Title	Journal	Invitro	Invivo	TBI	SCI	Description
Free Radicals	Inflammation	Zhao, W., W. Xie, et al.	2004	Activated microglia initiate motor neuron injury by a nitric oxide and glutamate-mediated mechanism	J Neuropathol Exp Neurol 63(9): 964-77.	x			x	microglia activation via nitric oxide
Inflammation		Bartholdi, D. and M. E. Schwab	1997	Expression of pro-inflammatory cytokine and chemokine mRNA upon experimental spinal cord injury in mouse: an in situ hybridization study	Eur J Neurosci 9(7): 1422-38.		x		x	(rat) cytokines and chemokines
Inflammation		Blight, A. R.	1985	Delayed demyelination and macrophage invasion: a candidate for secondary cell damage in spinal cord injury	Cent Nerv Syst Trauma 2(4): 299-315.		x		x	macrophage and demyelination time line
Inflammation		Blight, A. R.	1992	Macrophages and inflammatory damage in spinal cord injury	J Neurotrauma 9 Suppl 1: S83-91.		x	x		(rat) mononuclear phagocytes, astrogliosis
Inflammation		Carlson, S. L., M. E. Parrish, et al.	1998	Acute inflammatory response in spinal cord following impact injury	Experimental Neurology 151(1): 77-88.		x		x	(rat) macrophages, microglia & neutrophils; time line
Inflammation		Conrad, S., H. J. Schluesener, et al.	2005	Spinal cord injury induction of lesional expression of profibrotic and angiogenic connective tissue growth factor confined to reactive astrocytes, invading fibroblasts and endothelial cells	Journal of Neurosurgery-Spine 2(3): 319-326.		x		x	(rat) astrocytosis and glial scar formation
Inflammation		de Leme, R. J. and G. Chadi	2001	Distant microglial and astroglial activation secondary to experimental spinal cord lesion	Arquivos De Neuro-Psiquiatria 59(3A): 483-492.		x		x	(rat) microglia & astrocyte activation
Inflammation		Dusart, I. and M. E. Schwab	1994	Secondary Cell-Death and the Inflammatory Reaction after Dorsal Hemisection of the Rat Spinal-Cord	European Journal of Neuroscience 6(5): 712-724.		x		x	(rat) inflammation. Macrophages, microglia; lesion size

Category 1	Category 2	Author	Year	Title	Journal	Invitro	Invivo	TBI	SCI	Description
Inflammation		Fleming, J. C., M. D. Norenberg, et al.	2006	The cellular inflammatory response in human spinal cords after injury	Brain 129(Pt 12): 3249-69.		x		x	(human) microglia, macrophage, neutrophil, & lymphocyte timcourse
Inflammation	Other	Frei, E., I. Klusman, et al.	2000	Reactions of oligodendrocytes to spinal cord injury: Cell survival and myelin repair	Experimental Neurology 163(2): 373-380.		x		x	(rat)relationship between oligo-dendrocyte death & inflammation; myelination
Inflammation		Giulian, D. and C. Robertson	1990	Inhibition of mononuclear phagocytes reduces ischemic injury in the spinal cord	Ann Neurol 27(1): 33-42.		x		x	(rabbit) mononumclear phagocytes
Inflammation		Giulian, D., J. Woodward, et al.	1988	Interleukin-1 Injected into Mammalian Brain Stimulates Astrogliosis and Neovascularization	Journal of Neuroscience 8(7): 2485-2490.		x	x		astrogliosis
Inflammation		Gomes-Leal, W., D. J. Corkill, et al.	2004	Astrocytosis, microglia activation, oligodendrocyte degeneration, and pyknosis following acute spinal cord injury	Experimental Neurology 190(2): 456-467.		x		x	(rat) astrocytes, microglia, oligodendrocytes
Inflammation		Gonzalez, R., J. Glaser, et al.	2003	Reducing inflammation decreases secondary degeneration and functional deficit after spinal cord injury	Experimental Neurology 184(1): 456-463.		x		x	(rat) lymphocytes and lesion evolution
Inflammation		Kigerl, K. A., V. M. McGaughy, et al.	2006	Comparative analysis of lesion development and intraspinal inflammation in four strains of mice following spinal contusion injury	J Comp Neurol 494(4): 578-94.		x		x	(mouse) comparing genetic and inflammatory factors to lesion size
Inflammation		Kimelberg, H. K.	1992	Astrocytic edema in CNS trauma	J Neurotrauma 9 Suppl 1: S71-81.			x	x	astrocytic edema
Inflammation		Klusman, I. and M. E. Schwab	1997	Effects of pro-inflammatory cytokines in experimental spinal cord injury	Brain Research 762(1-2): 173-184.		x		x	(mice) cytokines

Category 1	Category 2	Author	Year	Title	Journal	Invitro	Invivo	TBI	SCI	Description
Inflammation		Lee, Y. L., K. Shih, et al.	2000	Cytokine chemokine expression in contused rat spinal cord	Neurochem Int 36(4-5): 417-25.		x		x	(rat) cytokines and chemokines
Inflammation		Louis, J. C., E. Magal, et al.	1993	Cntf Protection of Oligodendrocytes against Natural and Tumor Necrosis Factor-Induced Death	Science 259(5095): 689-692.	x				TNF-induced oligo-dendrocyte death
Inflammation	Other	MacFarlane, S. N. and H. Sontheimer	1997	Electrophysiological changes that accompany reactive gliosis in vitro	J Neurosci 17	x			x	electro-physiological changes with reactive gliosis
Inflammation		McKay, S. M., D. J. Brooks, et al.	2007	microglial activation in white and grey matter of rat lumbosacral cord after mid-thoracic spinal transection	J Neuropathol Exp Neurol 66(8): 698-710.		x		x	(rat) white vs grey matter microglial activation
Inflammation	Other	Mills, L. R., A. A. Velumian, et al.	2004	Confocal imaging of changes in glial calcium dynamics and homeostasis after mechanical injury in rat spinal cord white matter	Neuroimage 21(3): 1069-1082.		x		x	(rat) glial calcium dynamics
Inflammation		Nakamura, M., R. A. Houghtling, et al.	2003	Differences in cytokine gene expression profile between acute and secondary injury in adult rat spinal cord	Exp Neurol 184(1): 313-25.		x		x	(rat) cytokines and chemokines
Inflammation		O'Brien, M. F., L. G. Lenke, et al.	1994	Astrocyte response and transforming growth factor-beta localization in acute spinal cord injury	Spine 19(20): 2321-9		x		x	(rat) astrocyte activation
Inflammation		Perry, V. H., P. B. Andersson, et al.	1993	Macrophages and Inflammation in the Central-Nervous-System	Trends in Neurosciences 16(7): 268-273.					macrophage, inflammation
Inflammation		Piani, D., K. Frei, et al.	1993	Astrocytes Is Inhibited by Reactive Oxygen Intermediates but Not by Other Macrophage-Derived Molecules Including Cytokines, Leukotrienes or Platelet-Activating-	Journal of Neuroimmunology 48(1): 99-104.	x		x	x	role of macrophages /cytokines in glutamate uptake
Inflammation		Pineau, I. and S. Lacroix	2007	Proinflammatory cytokine synthesis in the injured mouse spinal cord: multiphasic expression pattern and identification of the cell	J Comp Neurol 500(2): 267-85.		x		x	(mouse) cytokines

Category 1	Category 2	Author	Year	Title	Journal	Invitro	Invivo	TBI	SCI	Description
Inflammation		D. K., S. H. Graham, et al.	1998	Role of cyclooxygenase 2 in acute spinal cord injury	J Neurotrauma 15(12): 1005-13.		x		x	(rat) prostaglandins
Inflammation		Rosenberg, L. J., L. J. Zai, et al.	2005	Chronic alterations in the cellular composition of spinal cord white matter following contusion injury	Glia 49(1): 107-20.		x		x	density of oligodendrocytes, astrocytes, microglia, and macrophage
Inflammation		Schnell, L., S. Fearn, et al.	1999	Acute inflammatory responses to mechanical lesions in the CNS: differences between brain and spinal cord	European Journal of Neuroscience 11(10): 3648-3658.		x	x	x	(rat) comparing TBI and SCI inflammatory response
Inflammation		Skaper, S. D.	2003	Poly(ADP-ribose) polymerase-1 in acute neuronal death and inflammation - A strategy for neuroprotection	Neuroprotective Agents 993: 217-228.			x	x	Poly(ADP-ribose) polymerase-1 in acute neuronal death and inflammation
Inflammation		hi, S., M. Shibata, et al.	2000	Astroglial cell death induced by excessive influx of sodium ions	Journal of Pharmacology 408(2): 127-	x		x	x	astroglial death via sodium
Inflammation		Takuma, K., A. Baba, et al	2004	Astrocyte apoptosis: implications for neuroprotection	Progress in Neurobiology 72(2): 111-127.	x		x		astrocyte apoptosis
Inflammation		Taoka, Y., K. Okajima, et al.	1997	Role of neutrophils in spinal cord injury in the rat	Neuroscience 79(4): 1177-82.		x		x	(rat) neutrophils
Inflammation		Vela, J. M., A. Yanez, et al.	2002	Time course of proliferation and, elimination of microglia/macrophages in different neurodegenerative conditions	Journal of Neurotrauma 19(11): 1503-1520.		x	x		microglia/macrophage time course
Necr-Apoptosis		Green, D. and G. Kroemer	1998	The central executioners of apoptosis: caspases or mitochondria?	Trends Cell Biol 8(7): 267-71.			x	x	mitochondria and caspases in apoptosis
Necr-Apoptosis		Bartus, R. T.	1997	The calpain hypothesis of neurodegeneration: Evidence for a common cytotoxic pathway	Neuroscientist 3(5): 314-327.			x	x	role of calpain

Category 1	Category 2	Author	Year	Title	Journal	Invitro	Invivo	TBI	SCI	Description
Necr-Apop-tosis	Free Radicals	Barut, S., A. Canbolat, et al.	1993	Lipid-Peroxidation in Experimental Spinal-Cord Injury - Time-Level Relationship	Neurosurgical Review 16(1): 53-59.		x		x	(rat) lipid peroxidation & treatment window
Necr-Apop-tosis		Barut, S., Y. A. Unlu, et al.	2005	The neuroprotective effects of z-DEVD.fmk, a caspase-3 inhibitor, on traumatic spinal cord injury in rats	Surg Neurol 64(3): 213-20		x		x	(rat) lipid peroxidation/ time course
Necr-Apop-tosis		Beattie, M. S.	2004	Inflammation and apoptosis: linked therapeutic targets in spinal cord injury	Trends Mol Med 10(12): 580-3.				x	inflammation & apoptosis/ treatments
Necr-Apop-tosis		Beattie, M. S., G. E. Her-mann, et al.	2002	Cell death in models of spinal cord injury	Spinal Cord Trauma: Regeneration, Neural Repair and Functional Recovery 137: 37-47.				x	cell death models: apoptosis & necrosis
Necr-Apop-tosis		Bendel, O., I. A. Langmoen, et al.	2004	Crush injury induces NMDA-receptor-dependent delayed nerve cell death in rat entorhinal-hippocampal slice cultures	Brain Res 1025(1-2): 35-42.	x		x		NMDA-induced early & late cell death
Necr-Apop-tosis		Braughler, J. M. and E. D. Hall	1992	Involvement of Lipid-Peroxidation in Cns Injury	Journal of Neurotrauma 9: S1-S7.			x	x	lipid peroxidation/ oxygen radicals
Necr-Apop-tosis		Byrnes, K. R., B. A. Stoica, et al.	2007	Cell cycle activation contributes to post-mitotic cell death and secondary damage after spinal cord injury	Brain 130: 2977-2992.		x		x	(rat) cell cycle activation, neuronal & oligodendroglial apoptosis, glial scar, microglia
Necr-Apop-tosis	Free Radicals	Clausen, F., H. Lundqvist, et al.	2004	Oxygen free radical-dependent activation of extracellular signal-regulated kinase mediates apoptosis-like cell death after traumatic brain injury	Journal of Neurotrauma 21(9): 1168-1182.		x	x		(rat) apoptosis via free radicals
Necr-Apop-tosis		Crowe, M. J., J. C. Bresnahan, et al.	1997	Apoptosis and delayed degeneration after spinal cord injury in rats and monkeys	Nat Med 3(1): 73-6.		x		x	(rat, monkey) apoptosis, oligodendrocytes, and demyelination

Category 1	Category 2	Author	Year	Title	Journal	Invitro	Invivo	TBI	SCI	Description
Necr-Apoptosis		Cullen, D. K. and M. C. LaPlaca	2006	Neuronal response to high rate shear deformation depends on heterogeneity of the local strain field	J Neurotrauma 23(9): 1304-19.	x		x		cell viability vs shear deformation
Necr-Apoptosis		Cullen, D. K. and M. C. LaPlaca	2006	The Effects of Shear vs. Compressive Loading in 3-D Neuronal-Astrocytic Co-Cultures	Neurotrauma, St. Louis, MO.	x		x		permeability vs death
Necr-Apoptosis		Di Giovanni, S., V. Movsesyan, et al.	2005	Cell cycle inhibition provides neuroprotection and reduces glial proliferation and scar formation after traumatic brain injury	Proc Natl Acad Sci U S A 102(23): 8333-8.		x	x		(rat) caspase & apoptosis & glial scar
Necr-Apoptosis		Emery, E., P. Aldana, et al.	1998	Apoptosis after traumatic human spinal cord injury	Journal of Neurosurgery 89(6): 911-920.		x		x	(human) apoptosis, oligodendrocytes, caspase-3
Necr-Apoptosis		Farkas, O., J. Lifshitz, et al.	2006	Mechanoporation induced by diffuse traumatic brain injury: An irreversible or reversible response to injury?" Journal of Neuroscience 26(12): 3130-3140.			x	x		(rat) mechanoporation/ membrane permeability
Necr-Apoptosis		Farkas, O., R. Singleton, et al.	2004	Traumatic neuronal plasmalemmal disruption can lead to cell death not necessarily associated with concomitant calpain activation	Journal of Neurotrauma 21(9): 1291-1291.			x		membrane permeablity in cell death
Necr-Apoptosis		Fujiki, M., Y. Furukawa, et al.	2005	Geranylgeranylacetone limits secondary injury, neuronal death, and progressive necrosis and cavitation after spinal cord injury	Brain Res 1053(1-2): 175-84.		x		x	(rat) neutrophils; lesion size/ volume
Necr-Apoptosis		Galle, B., H. Ouyang, et al.	2007	Correlations between tissue-level stresses and strains and cellular damage within the guinea pig spinal cord white matter	Journal of Biomechanics 40(13): 3029-3033.		x		x	(guinea pig) cellular damage/permeability

Category 1	Category 2	Author	Year	Title	Journal	Invitro	Invivo	TBI	SCI	Description
Necr-Apoptosis		Goetz, P., A. Blamire, et al.	2004	Increase in apparent diffusion coefficient in normal appearing white matter following human traumatic brain injury correlates with injury severity	Journal of Neurotrauma 21(6): 645-654.		x	x		(human) vascular permeability
Necr-Apoptosis	Free Radicals	Hall, E. D.	1991	Inhibition of lipid peroxidation in CNS trauma	J Neurotrauma 8 Suppl 1: S31-40				x	lipid peroxidation & treatment window
Necr-Apoptosis		Hartmann, A., S. Hunot, et al.	2000	Caspase-3: A vulnerability factor and final effector in apoptotic death of dopaminergic neurons in Parkinson's disease	Proc Natl Acad Sci U S A 97(6): 2875-80.		x			(human) caspase-3 and apoptosis
Necr-Apoptosis	Inflammation	Hu, S., P. K. Peterson, et al.	1997	Cytokine-mediated neuronal apoptosis	Neurochem Int 30(4-5): 427-31.	x			x	(human) cytokines and nitric oxide
Necr-Apoptosis	Inflammation	Kang, S. K., J. E. Yeo, et al.	2007	Cytoplasmic extracts from adipose tissue stromal cells alleviates secondary damage by modulating apoptosis and promotes functional recovery following spinal cord injury	Brain Pathol 17(3): 263-75.	x			x	apoptosis inhibition
Necr-Apoptosis		Katoh, K., T. Ikata, et al.	1996	Induction and its spread of apoptosis in rat spinal cord after mechanical trauma	Neuroscience Letters 216(1): 9-12.		x		x	(rat) induction of apoptosis
Necr-Apoptosis		Keane, R. W., A. R. Davis, et al.	2006	Inflammatory and apoptotic signaling after spinal cord injury	J Neurotrauma 23(3-4): 335-44.				x	TNF, inflammation & apoptotic signaling
Necr-Apoptosis	Other	Li, G. L., G. Brodin, et al.	1996	Apoptosis and expression of Bcl-2 after compression trauma to rat spinal cord	Journal of Neuropathology and Experimental Neurology 55(3): 280-289.		x		x	(rat) oligodendrocyte apoptosis/ Bcl-2
Necr-Apoptosis		Ling, X. and D. Liu	2007	Temporal and spatial profiles of cell loss after spinal cord injury: Reduction by a metalloporphyrin	J Neurosci Res 85(10): 2175-85.		x		x	temporal & spatial profiles of cell loss

Category 1	Category 2	Author	Year	Title	Journal	Invitro	Invivo	TBI	SCI	Description
Necr-Apop-tosis		Liu-Snyder, P., M. P. Logan, et al.	2007	Neuroprotection from secondary injury by polyethylene glycol requires its internalization	J Exp Biol 210(Pt 8): 1455-62.		x		x	membrane permeability/ repair by polyethylene glycol
Necr-Apop-tosis		Liu, N. K., Y. P. Zhang, et al.	2006	A novel role of phospholipase A2 in mediating spinal cord secondary injury	Ann Neurol 59(4): 606-19.	x	x		x	role of phospholipase (PLA2)
Necr-Apop-tosis		Lu, J., K. W. Ashwell, et al.	2000	Advances in secondary spinal cord injury: role of apoptosis	Spine 25(14): 1859-66.				x	role of apoptosis
Necr-Apop-tosis		Ray, S. K., S. Karmakar, et al.	2006	Inhibition of calpain and caspase-3 prevented apoptosis and preserved electrophysiological properties of voltage-gated and ligand-gated ion channels in rat primary cortical neurons exposed to glutamate	Neuroscience 139(2): 577-595.	x		x		caspase-3 & apoptosis in glutamate toxicity
Necr-Apop-tosis		Ray, S. K., G. G. Wilford, et al.	1999	Calpeptin and methylprednisolone inhibit apoptosis in rat spinal cord injury	Ann N Y Acad Sci 890: 261-9.		x		x	(rat) role of calpain/ treatments
Necr-Apop-tosis	Free Radicals	Scholpp, J., J. K. Schubert, et al.	2004	Lipid peroxidation early after brain injury	Journal of Neurotrauma 21(6): 667-677.		x	x		(human) lipid peroxidation
Necr-Apop-tosis	Other	Shi, R. and J. Whitebone	2006	Conduction deficits and membrane disruption of spinal cord axons as a function of magnitude and rate of strain	Journal of Neurophysiology 95(6): 3384-3390.				x	(guinea pig) membrane permeability; axonal damage
Necr-Apop-tosis	Other	Shi, R. Y.	2004	The dynamics of axolemmal disruption in guinea pig spinal cord following compression	Journal of Neurocytology 33(2): 203-211.		x		x	(guinea pig) membrane permeability and conduction deficits
Necr-Apop-tosis	Other	Shuman, S. L., J. C. Bresnahan, et al.	1997	Apoptosis of microglia and oligodendrocytes after spinal cord contusion in rats	Journal of Neuroscience Research 50(5): 798-808.		x		x	(rat) apoptosis of oligodendrocytes/role of demyelin-ation

Category 1	Category 2	Author	Year	Title	Journal	Invitro	Invivo	TBI	SCI	Description
Necr-Apoptosis		Srinivasan, A., K. A. Roth, et al.	1998	In situ immunodetection of activated caspase-3 in apoptotic neurons in the developing nervous system	Cell Death Differ 5(12): 1004-16.	x				caspase-3 and apoptosis
Necr-Apoptosis		Sullivan, P. G., A. J. Bruce-Keller, et al.	1999	Exacerbation of damage and altered NF-kappaB activation in mice lacking tumor necrosis factor receptors after traumatic brain injury	J Neurosci 19(15): 6248-56.		x	x		TNFalpha neuro-protection
Necr-Apoptosis		Sullivan, P. G., J. N. Keller, et al.	2002	Cytochrome c release and caspase activation after traumatic brain injury	Brain Research 949(1-2): 88-96.		x	x		cytochrome-c and caspase-3; time line
Necr-Apoptosis		Tarabal, O., J. Caldero, et al.	2005	Protein retention in the endoplasmic reticulum, blockade of programmed cell death and autophagy selectively occur in spinal cord motoneurons after glutamate receptor-mediated injury	Molecular and Cellular Neuroscience 29(2): 283-298.	x			x	(chick embryo) NMDA and cell death
Necr-Apoptosis	Inflammation	Tian, D. S., M. J. Xie, et al.	2007	Cell cycle inhibition attenuates microglia induced inflammatory response and alleviates neuronal cell death after spinal cord injury in rats	Brain Research 1135(1): 177-185.		x		x	(rat) cell cycle & apoptosis; astroglial scar
Necr-Apoptosis	Inflammation	Tian, D. S., Z. Y. Yu, et al.	2006	Suppression of astroglial scar formation and enhanced axonal regeneration associated with functional recovery in a spinal cord injury rat model by the cell cycle inhibitor olomoucine	Journal of Neuro-science Research 84(5): 1053-1063.		x		x	(rat) astroglial scar relationship to cell cycle; treatment with olomoucine
Necr-Apoptosis		Vaquero, J., M. Zurita, et al.	2006	Early administration of methylprednisolone decreases apoptotic cell death after spinal cord injury	Histology and Histopathology 21(10): 1091-1102.		x		x	(rat) apoptosis & methylprednisolone

Category 1	Category 2	Author	Year	Title	Journal	Invitro	Invivo	TBI	SCI	Description
Necr-Apoptosis		Villapol, S., L. Acarin, et al.	2007	Distinct spatial and temporal activation of caspase pathways in neurons and glial cells after excitotoxic damage to the immature rat brain	J Neurosci Res 85(16): 3545-56.		x	x		(rat) spatial & temporal caspase activation
Necr-Apoptosis	Excito-toxicity	Wingrave, J. M., K. E. Schaecher, et al.	2003	Early induction of secondary injury factors causing activation of calpain and mitochondria-mediated neuronal apoptosis following spinal cord injury in rats	J Neurosci Res 73(1): 95-104.		x		x	(rats) relationship between calpain, calcium & mito-chondrial damage
Necr-Apoptosis		Yakovlev, A. G. and A. I. Faden	2004	Mechanisms of neural cell death: implications for development of neuroprotective treatment strategies	NeuroRx 1(1): 5-16.					cell death mechanisms/ neuroprotection
Other		Azanchi, R., G. Bernal, et al.	2004	Combined demyelination plus Schwann cell transplantation therapy increases spread of cells and axonal regeneration following contusion injury	Journal of Neurotrauma 21(6): 775-788.		x	x	x	demyelination and Schwann cell transplantation
Other		Churchwell, K. B., S. H. Wright, et al.	1996	NMDA receptor activation inhibits neuronal volume regulation after swelling induced by veratridine-stimulated Na+ influx in rat cortical cultures	J Neurosci 16(23): 7447-57.		x	x		cell volume regulation
Other		Fawcett, J. W. and R. A. Asher	1999	The glial scar and central nervous system repair	Brain Research Bulletin 49(6): 377-391.				x	glial scar
Other		Fitch, M. T., C. Doller, et al.	1999	Cellular and molecular mechanisms of glial scarring and progressive cavitation: In vivo and in vitro analysis of inflammation-induced secondary injury after CNS trauma	Journal of Neuro-science 19	x			x	glial scarring, cavitation & inflammation

Category 1	Category 2	Author	Year	Title	Journal	Invitro	Invivo	TBI	SCI	Description
Other		Fuller, M. L., A. K. DeChant, et al.	2007	Bone morphogenetic proteins promote gliosis in demyelinating spinal cord lesions	Ann Neurol 62(3): 288-300.		x		x	(rat) gliosis and bone morphogenetic proteins
Other		Gaviria, M., J. M. Bonny, et al.	2006	Time course of acute phase in mouse spinal cord injury monitored by ex vivo quantitative MRI	Neurobiol Dis 22(3): 694-701.		x		x	(mouse) time course acute phase sci via MRI
Other		Guest, J. D., E. D. Hiester, et al.	2005	Demyelination and Schwann cell responses adjacent to injury epicenter cavities following chronic human spinal cord injury	Exp Neurol 192(2): 384-93.		x		x	(human) demyelination
Other		Gupta, A. K., D. A. Zygun, et al.	2004	Extracellular brain pH and outcome following severe traumatic brain injury	Journal of Neurotrauma 21(6): 678-684.		x	x		(human) extracellular pH
Other		Hagg, T. and M. Oudega	2006	Degenerative and spontaneous regenerative processes after spinal cord injury	Journal of Neurotrauma 23(3-4): 264-280.				x	axonal degeneration and regeneration
Other		Lovas, G., N. Szilagyi, et al.	2000	Axonal changes in chronic demyelinated cervical spinal cord plaques	Brain 123 (Pt 2): 308-17.		x			(human) axonal damage
Other		McDonald, J. W. and V. Belegu	2006	Demyelination and remyelination after spinal cord injury	J Neurotrauma 23(3-4): 345-59.				x	demyelin-ation and remyelin-ation
Other		McGavern, D. B., P. D. Murray, et al.	1999	Quantitation of spinal cord demyelination, remyelination, atrophy, and axonal loss in a model of progressive neurologic injury	J Neurosci Res 58(4): 492-504.	x			x	demyelination, remyelination & axonal loss
Other		Mitchell, C. S., S. S. Feng, et al.	2007	An analysis of glutamate spillover on the N-methyl-D-aspartate receptors at the cerebellar glomerulus	J Neural Eng 4(3): 276-82.					NMDA and glutamate relationships

Category 1	Category 2	Author	Year	Title	Journal	Invitro	Invivo	TBI	SCI	Description
Other		Park, E., A. A. Velumian, et al.	2004	The role of excitotoxicity in secondary mechanisms of spinal cord injury: A review with an emphasis on the implications for white matter degeneration	Journal of Neurotrauma 21(6): 754-774.				x	demyelination
Other		Pettus, E. H. and J. T. Povlishock	1996	Characterization of a distinct set of intra-axonal ultrastructural changes associated with traumatically induced alteration in axolemmal permeability	Brain Research 722(1-2): 1-11.		x	x		(cat) axonal damage
Other		Saftenku, E. E.	2005	Modeling of slow glutamate diffusion and AMPA receptor activation in the cerebellar glomerulus	J Theor Biol 234(3): 363-82.					AMPA and glutamate relationships
Other		Schwab, M. E. and D. Bartholdi	1996	Degeneration and regeneration of axons in the lesioned spinal cord	Physiol Rev 76(2): 319-70.				x	regeneration of axons
Other		Totoiu, M. O. and H. S. Keirstead	2005	Spinal cord injury is accompanied by chronic progressive demyelination	J Comp Neurol 486(4): 373-83.		x		x	(rat) demyelination
Other		Vick, R. S., T. J. Neuberger, et al.	1992	Role of adult oligodendrocytes in remyelination after neural injury	J Neurotrauma 9 Suppl 1: S93-103.			x	x	remyelination by oligodendrocytes
Other		Waxman, S. G.	1992	Demyelination in spinal cord injury and multiple sclerosis: what can we do to enhance functional recovery?	J Neurotrauma 9 Suppl 1: S105-17.				x	demyelination
Other		Waxman, S. G., B. R. Ransom, et al.	1991	Nonsynaptic Mechanisms of Ca2+-Mediated Injury in Cns White Matter	Trends in Neurosciences 14(10): 461-468.				x	conduction of CNS white matter
Other		Xu, R. and C. Luo	2001	Relationship between changes of N-methyl-D-aspartate receptor activity and brain edema after brain injury in rats	Chin J Traumatol 4(3): 135-8.			x	x	volume regulation/ edema

Category 1	Category 2	Author	Year	Title	Journal	Invitro	Invivo	TBI	SCI	Description
Other		Zhang, S. X., J. W. Geddes, et al.	2005	X-irradiation reduces lesion scarring at the contusion site of adult rat spinal cord	Histology and Histopathology 20(2): 519-530.		x		x	(rat) lesion scarring

APPENDIX B

ALS RELATIONAL MODEL LITERATURE DATABASE

Category 1	Category 2	Author	Year	Title	Journal	ALS type	Exp Type	Model	SOD	R/O	Factor Description
Axon Transport	Energetic	Hollenbeck, P. J., D. Bray, et al	1985	Effects of the uncoupling agents FCCP and CCCP on the saltatory movements of cytoplasmic organelles	Cell Biol Int Rep 9(2): 193-9					x	transport correlation to mitochondrial potential and/or ATP
Axon Transport	Energetic	Miller, K. E. and M. P. Sheetz	2004	Axon mitochondrial transport and potential are correlated	J Cell Sci 117(Pt 13): 2791-804					x	mitochondrial transport and its role in potential, apoptosis
Axon Transport	Excitotoxicity	Ilieva, H. S., K. Yamanaka, et al	2008	Mutant dynein (Loa) triggers proprioceptive axon loss that extends survival only in the SOD1 ALS model with highest motor neuron death	Proc Natl Acad Sci U S A 105(34): 12599-604	F		Loa			Loa dynein and their paradoxical effect on ALS
Axon Transport	Excitotoxicity	Kanai, A. J., L. L. Pearce, et al	2001	Identification of a neuronal nitric oxide synthase in isolated cardiac mitochondria using electrochemical detection.						x	inhibition of transport by calcium
Axon Transport	Excitotoxicity	Kato, S., M. Kato, et al	2005	Redox system expression in the motor neurons in amyotrophic lateral sclerosis (ALS): immunohistochemical studies on sporadic ALS, superoxide dismutase 1 (SOD1)-mutated familial ALS, and SOD1-mutated ALS animal models	Acta Neuropathol 110(2): 101-12	F/S	invivo	human			expression of redox genes

Category 1	Category 2	Author	Year	Title	Journal	ALS type	Exp Type	Model	SOD	R/O	Factor Description
Axon Transport	Excitotoxicity	Kendal, W. S., Z. J. Koles, et al	1983	Oscillatory motion of intra-Axon organelles of Xenopus laevis following inhibition of their rapid transport	J Physiol 345: 501-13					x	inhibition of transport by calcium
Axon Transport	Genetic	Meyer, M. A. and N. T. Potter	1995	Sporadic ALS and chromosome 22: evidence for a possible neurofilament gene defect	Muscle Nerve 18(5): 536-9	S	invivo	human			defect in NF-H causes SALS
Axon Transport	Genetic	Pantelidou, M., S. E. Zographos, et al	2007	Differential expression of molecular motors in the motor cortex of sporadic ALS."	Neurobiol Dis 26(3): 577-89	S	invivo	human	x		reduction of KIF3Abeta protein levels
Axon Transport	Multiple	Gonatas, N. K., A. Stieber, et al	2006	Fragmentation of the Golgi apparatus in neurodegenerative diseases and cell death	J Neurol Sci 246(1-2): 21-30	F	invivo	G93A	x		fragmentation associated w/ Axon transport defects & other signs of neurodegener
Axon Transport	Necro-Apoptosis	Xue, L., G. C. Fletcher, et al.	2001	Mitochondria are selectively eliminated from eukaryotic cells after blockade of caspases during apoptosis	Curr Biol 11(5): 361-5					x	correlation between transport and apoptosis
Axon Transport	None	Kieran, D., M. Hafezparast, et al	2005	A mutation in dynein rescues Axon transport defects and extends the life span of ALS mice	J Cell Biol 169(4): 561-7	F	invivo	Loa	x		impaired Axon transport
Axon Transport	None	Tateno, M., S. Kato, et al	2008	Mutant SOD1 impairs Axon transport of choline acetyltransferase and acetylcholine release by sequestering KAP3	Hum Mol Genet	F	invivo	G93A	x		choline acetyltransferase transport impairment, KAP3

Category 1	Category 2	Author	Year	Title	Journal	ALS type	Exp Type	Model	SOD	R/O	Factor Description
Axon Transport	None	Teuchert, M., D. Fischer, et al	2006	A dynein mutation attenuates motor neuron degeneration in SOD1(G93A) mice	Exp Neurol 198(1): 271-4	F	invivo	G93A/Loa	x		role of retrograde transport in ALS
Axon Transport	None	Zhang, F., A. L. Strom, et al	2007	between familial amyotrophic lateral sclerosis (ALS)-linked SOD1 mutants and the dynein complex	J Biol Chem 282(22): 16691-9	F	invitro	G93A & G85R	x		dynein, retrograde transport
Axon Transport	Proteomic	Wong, N. K., B. P. He, et al	2000	Characterization of neuronal intermediate filament protein expression in cervical spinal motor neurons in sporadic amyotrophic lateral sclerosis (ALS)	J Neuropathol Exp Neurol 59(11): 972-82	S	invivo	human			NF-M, NF-H, tubuliln, aggregates
Chemistry	?	Ludolph, A. C.	2006	Matrix metalloproteinases--a conceptional alternative for disease-modifying strategies in ALS/MND?	Exp Neurol 201(2): 277-80	?	?	?			metalloproteinases
Chemistry	Free Radical	Bredesen, D. E., M. Wiedau-Pazos, et al.	1996	Cell death mechanisms in ALS." Neurology 47(4 Suppl 2): S36-8		F	invitro	G93A	x		copper chelators, diethyldithiocarbamate and penicillamine, inhibited the mutants' peroxidase activity,
Chemistry	Free Radical	Carroll, M. C., C. E. Outten, et al	2006	The effects of glutaredoxin and copper activation pathways on the disulfide and stability of Cu,Zn superoxide dismutase	J Biol Chem 281(39): 28648-56	F	both	A4V	x		balance b/w cellular reductant glutaredoxin and copper activation pathways

Category 1	Category 2	Author	Year	Title	Journal	ALS type	Exp Type	Model	SOD	R/O	Factor Description
Chemistry	Free Radical	Tokuda, E., S. Ono, et al	2008	Ammonium tetrathiomolybdate delays onset, prolongs survival, and slows progression of disease in a mouse model for amyotrophic lateral sclerosis	Exp Neurol 213(1): 122-8	F	invivo	G93A	x		aberrant chemisty, lipid peroxidation
Chemistry	Genetic	Banci, L., I. Bertini, et al	2008	SOD1 and amyotrophic lateral sclerosis: mutations and oligomerization	PLoS ONE 3(2): e1677	F	invivo	mult	x		SOD1 mutant oligomerization
Chemistry	Genetic	Banci, L., I. Bertini, et al	2007	Metal-free superoxide dismutase forms soluble oligomers under physiological conditions: a possible general mechanism for familial ALS	Proc Natl Acad Sci U S A 104(27): 11263-7	F	invivo	mult/human	x		cysteine role in ollgomerization in SOD1 aggregation
Chemistry	None	Tiwari, A., Z. Xu, et al	2005	Aberrantly increased hydrophobicity shared by mutants of Cu,Zn-superoxide dismutase in familial amyotrophic lateral sclerosis	J Biol Chem 280(33): 29771-9	F	invivo	mult	x		cellular disulfide reducing environment and zinc loss converts/destabilizes SOD1
Chemistry	None	Watanabe, S., S. Nagano, et al	2007	Increased affinity for copper mediated by cysteine 111 in forms of mutant superoxide dismutase 1 linked to amyotrophic lateral sclerosis	Free Radic Biol Med 42(10): 1534-42	F	invivo	A4V	x		stability of SOD1

Category 1	Category 2	Author	Year	Title	Journal	ALS type	Exp Type	Model	SOD	R/O	Factor Description
Chemistry	Proteomic	Furukawa, Y. and T. V. O'Halloran	2006	Posttranslational modifications in Cu,Zn-superoxide dismutase and mutations associated with amyotrophic lateral sclerosis	Antioxid Redox Signal 8(5-6): 847-67		F	invivo	?	x	role of SOD1 in aggregates
Chemistry	Proteomic	Nordlund, A. and M. Oliveberg	2006	Folding of Cu/Zn superoxide dismutase suggests structural hotspots for gain of neurotoxic function in ALS: parallels to precursors in amyloid disease	Proc Natl Acad Sci U S A 103(27): 10218-23	F	invivo	?	x		misfolding of SOD w/ and w/ aggregation
Energetic	None	Niessen, H. G., G. Debska-Vielhaber, et al	2007	Metabolic progression markers of neurodegeneration in the transgenic G93A-SOD1 mouse model of amyotrophic lateral sclerosis	Eur J Neurosci 25(6): 1669-77	F	invivo	G93A	x		N-acetyl aspartate, glutamine, GABA; metabolic markers
Energetic	Inflammation	Cassina, P., A. Cassina, et al	2008	Mitochondrial dysfunction in SOD1G93A-bearing astrocytes promotes motor neuron degeneration: prevention by mitochondrial-targeted antioxidants	J Neurosci 28(16): 4115-22.	F	invivo	G93A	x		mitochondrial dysfunction in astrocytes; help w/ anti-oxidants
Energetic	Excitotoxicity	Beal, M. F.	1992	Does impairment of energy metabolism result in excitotoxic neuronal death in neurodegenerative illnesses?	Ann Neurol 31(2): 119-30	F/S				x	mitochondrial energy metabolism & glutamate

Category 1	Category 2	Author	Year	Title	Journal	ALS type	Exp Type	Model	SOD	R/O	Factor Description
Energetic	Excitotoxicity	Nicholls, D. G., S. Vesce, et al	2003	Interactions between mitochondrial bioEnergetic and cytoplasmic calcium in cultured cerebellar granule cells	Cell Calcium 34(4-5): 407-24		invitro			x	Ca, AMPA, NMDA, & mitochondrial function
Energetic	Free Radical	Krishnan, J., K. Vannuvel, et al	2008	Over-expression of Hsp27 does not influence disease in the mutant SOD1(G93A) mouse model of amyotrophic lateral sclerosis	J Neurochem 106(5): 2170-83		invivo	G93A	x		single transgenic hHsp27 were protected f/ ischemia but SOD1 were not
Energetic	Free Radical	Lev, N., D. Ickowicz, et al	2008	DJ-1 Changes in G93A-SOD1 Transgenic Mice: Implications for Oxidative Stress in ALS	J Mol Neurosci.	F	invivo	G93A	x		correlation b/w oxidative stress and mitochondrial dysfunction
Energetic	Free Radical	Mattiazzi, M., M. D'Aurelio, et al	2002	Mutated human SOD1 causes dysfunction of oxidative phosphorylation in mitochondria of transgenic mice	J Biol Chem 277(33): 29626-33	F	invivo	G93A	x		Mitochondrial respiration, electron transfer chain, ATP, lipid/protein oxidation
Energetic	Genetic	Ferraiuolo, L., P. R. Heath, et al	2007	Microarray analysis of the cellular pathways involved in the adaptation to and progression of motor neuron injury in the SOD1 G93A mouse model of familial ALS	J Neurosci 27(34): 9201-19	F	invivo	G93A	x		downregulation of metabolic function
Energetic	Inflammation	Ellis, D. Z., J. Rabe, et al	2003	Global loss of Na,K-ATPase and its nitric oxide-mediated regulation in a transgenic mouse model of amyotrophic lateral sclerosis	J Neurosci 23(1): 43-51	F	invivo	G93A	x		losses and dysfunction of Na-K-ATP pump

Category 1	Category 2	Author	Year	Title	Journal	ALS type	Exp Type	Model	SOD	R/O	Factor Description
Energetic	Multiple	Kaal, E. C., A. S. Vlug, et al	2000	Chronic mitochondrial inhibition induces selective motoneuron death in vitro: a new model for amyotrophic lateral sclerosis	J Neurochem 74(3): 1158-65		invitro			x	Free Radical, AMPA, ATP; malonate-induced MN death
Energetic	Multiple	Mattson, M. P., W. A. Pedersen, et al	1999	Cellular and molecular mechanisms underlying perturbed energy metabolism and neuronal degeneration in Alzheimer's and Parkinson's diseases	Ann N Y Acad Sci 893: 154-75					x	oxidative stress disrupts energy metabolism, glu transport
Energetic	Necro-Apoptosis	Fornai, F., P. Longone, et al	2008	Lithium delays progression of amyotrophic lateral sclerosis	Proc Natl Acad Sci U S A 105(6): 2052-7	F	invivo	G93A	x		lithium reduced the slow necrosis by mitochondrial vacuolization
Energetic	Necro-Apoptosis	Kirkinezos, I. G., S. R. Bacman, et al	2005	Cytochrome c association with the inner mitochondrial membrane is impaired in the CNS of G93A-SOD1 mice	J Neurosci 25(1): 164-72	F	invivo	G93A	x		role of cytochrome c
Energetic	Necro-Apoptosis	Kong, J. and Z. Xu	1998	Massive mitochondrial degeneration in motor neurons triggers the onset of amyotrophic lateral sclerosis in mice expressing a mutant SOD1	J Neurosci 18(9): 3241-50	F	invivo	G93A	x		mitochondrial vacuolization occurs before MN death

Category 1	Category 2	Author	Year	Title	Journal	ALS type	Exp Type	Model	SOD	R/O	Factor Description
Energetic	None	Browne, S. E., L. Yang, et al	2006	Bioenergetic abnormalities in discrete cerebral motor pathways presage spinal cord pathology in the G93A SOD1 mouse model of ALS	Neurobiol Dis 22(3): 599-610	F	invivo	G93A	x		glucose impairment; brain degeneration primary to spinal cord
Energetic	None	Mali, Y. and N. Zisapels	2008	Gain of interaction of ALS-linked G93A superoxide dismutase with cytosolic malate dehydrogenase	Neurobiol Dis 32(1): 133-41	F	?	G93A	x		Mitochondrial NADH/NAD+ ratio is also elevated; higher lactate levels
Energetic	None	Wendt, S., A. Dedeoglu, et al	2002	Reduced creatine kinase activity in transgenic amyotrophic lateral sclerosis mice	Free Radic Biol Med 32(9): 920-6	F	invivo	G93A	x		CK activity decreased to 49% and in mitochondrial fractions to 67%
Energetic	None	Wiedeman n, F. R., G. Manfredi, et al	2002	Mitochondrial DNA and respiratory chain function in spinal cords of ALS patients." J Neurochem 80(4): 616-25.		F/S	invivo	human	x		respiratory chain, mitochondrial decrease, DNA
Energetic	Proteomic	Higgins, C. M., C. Jung, et al	2003	ALS-associated mutant SOD1G93A causes mitochondrial vacuolation by expansion of the intermembrane space and by involvement of SOD1 aggregation and peroxisomes	BMC Neurosci 4: 16						mitochondrial vacuolization, degeneration, leakeate, and aggregation
Energetic	Proteomic	Xu, Z., C. Jung, et al	2004	Mitochondrial degeneration in amyotrophic lateral sclerosis	J Bioenerg Biomembr 36(4): 395-9	F	invivo	?	x		lysosomes, peroxisomes, mitochondria, vacuolization

Category 1	Category 2	Author	Year	Title	Journal	ALS type	Exp Type	Model	SOD	R/O	Factor Description
Energetic	Systemic	Dupuis, L., J. L. Gonzalez de Aguilar, et al	2004	Mitochondria in amyotrophic lateral sclerosis: a trigger and a target	Neurodegener Dis 1(6): 245-54	F				x	mitochdondrial dysfunction in motoneurons & systemic
Energetic	Systemic	Echaniz-Laguna, A., J. Zoll, et al	2002	Mitochondrial respiratory chain function in skeletal muscle of ALS patients	Ann Neurol 52(5): 623-7	S		human			mitochdondrial dysfunction in motoneurons but not systemic in SALS
Energetic	Clinical	Bucher, S., K. E. Braunstein, et al	2007	Vacuolization correlates with spin-spin relaxation time in motor brainstem nuclei and behavioural tests in the transgenic G93A-SOD1 mouse model of ALS	Eur J Neurosci 26(7): 1895-901	F	invivo	G93A	x		mitochondrial vacuolization
Energetic	Clinical	Pena-Altamira, E., C. Crochemore, et al	2005	Neurochemical correlates of differential neuroprotection by long-term dietary creatine supplementation	Brain Res 1058(1-2): 183-8	F	invivo	G93A	x		creatine supplementation increased the activity of the GABAergic enzyme, glutamate decarboxylase,
Energetic	Genetic	Fukada, K., F. Zhang, et al	2004	Mitochondrial proteomic analysis of a cell line model of familial amyotrophic lateral sclerosis	Mol Cell Proteomic 3(12): 1211-23	F	invitro	G93A	x		role of mitochondrial proteins, such as VDAC2
Excitotoxicity	Axon Transport	Deitch, J. S., G. M. Alexander, et al	2002	GLT-1 glutamate transporter levels are unchanged in mice expressing G93A human mutant SOD1	J Neurol Sci 193(2): 117-26	F	invivo	G93A	x		GLT-1 glutamate transporters; change in mobility/distribution

Category 1	Category 2	Author	Year	Title	Journal	ALS type	Exp Type	Model	SOD	R/O	Factor Description
Excitotoxicity	Energetic	Andries, M., P. Van Damme, et al.	2007	Ivermectin inhibits AMPA receptor-mediated excitotoxicity in cultured motor neurons and extends the life span of a transgenic mouse model of amyotrophic lateral sclerosis	Neurobiol Dis 25(1): 8-16	F	invivo	G93A	x		excitotoxic protection f/ AMPA by ATP, P2X4 receptor
Excitotoxicity	Energetic	Bittigau, P. and C. Ikonomidou	1997	Glutamate in neurologic diseases	J Child Neurol 12(8): 471-85					x	impaired metabolism relationship to glutamate
Excitotoxicity	Energetic	Ikonomidou, C. and L. Turski	1996	Neurodegenerative disorders: clues from glutamate and energy metabolism	Crit Rev Neurobiol 10(2): 239-63	F/S				x	loss of Mg block on NMDA, glutamate uptake impairment by loss of energy
Excitotoxicity	Energetic	Jabaudon, D., M. Scanziani, et al	2000	Acute decrease in net glutamate uptake during energy deprivation	Proc Natl Acad Sci U S A 97(10): 5610-5					x	correlation between decreased energy and glutamate uptake
Excitotoxicity	Energetic	Jekabsons, M. B. and D. G. Nicholls	2004	In situ respiration and bioenergetic status of mitochondria in primary cerebellar granule neuronal cultures exposed continuously to glutamate	J Biol Chem 279(31): 32989-3000					x	correlations of ATP, glutamate, respiration capacity, NMDA

Category 1	Category 2	Author	Year	Title	Journal	ALS type	Exp Type	Model	SOD	R/O	Factor Description
Excitotoxicity	Free Radical	Sala, G., S. Beretta, et al	2005	Impairment of glutamate transport and increased vulnerability to oxidative stress in neuroblastoma SH-SY5Y cells expressing a Cu,Zn superoxide dismutase typical of familial amyotrophic lateral sclerosis	Neuroc hem Int 46(3): 227-34	F	invitro	human	x		EAAT, glutmate transport, antioxidants
Excitotoxicity	Genetic	Kawahara, Y., K. Ito, et al	2004	Glutamate receptors: RNA editing and death of motor neurons	Nature 427(6977): 801	S	?	?	?		mRNA editing of th AMPA subunit GluR2
Excitotoxicity	Genetic	Lipton, S. A.	2004	Sporadic ALS: blame it on the editor	Nat Med 10(4): 347	S				x	mRNA editing of th AMPA subunit GluR2
Excitotoxicity	Inflammation	Dunlop, J., H. Beal McIlvain, et al	2003	Impaired spinal cord glutamate transport capacity and reduced sensitivity to riluzole in a transgenic superoxide dismutase mutant rat model of amyotrophic lateral sclerosis	J Neurosci 23(5): 1688-96	F	invivo	G93A	x		glutatmate transport by GLT-1 and EAAC-1
Excitotoxicity	Inflammation	Sasabe, J., T. Chiba, et al	2007	D-serine is a key determinant of glutamate toxicity in amyotrophic lateral sclerosis	EMBO J 26(18): 4149-59	F/S	both	mult	x		D-serine, glutamate, microglia, glia
Excitotoxicity	Inflammation	Yin, H. Z., D. T. Tang, et al	2007	Intrathecal infusion of a Ca(2+)-permeable AMPA channel blocker slows loss of both motor neurons and of the astrocyte glutamate transporter, GLT-1 in a mutant SOD1 rat model of ALS	Exp Neurol 207(2): 177-85	F	invivo	G93A	x		Ca, AMPA, glutamate transporter, astrocytes

Category 1	Category 2	Author	Year	Title	Journal	ALS type	Exp Type	Model	SOD	R/O	Factor Description
Excitotoxicity	Multiple	Gibb, S. L., W. Boston-Howes, et al	2007	A caspase-3-cleaved fragment of the glial glutamate transporter EAAT2 is sumoylated and targeted to promyelocytic leukemia nuclear bodies in mutant SOD1-linked amyotrophic lateral sclerosis	J Biol Chem 282(44): 32480-90	F	both	G93A	x		inhibit EAAT2 by triggering caspase-3 cleavage of EAAT2; targeted to promyelocytic leukemia nuclear bodies invovled w/ gene transcription
Excitotoxicity	Necro-Apoptosis	Guo, H., L. Lai, et al	2003	Increased expression of the glial glutamate transporter EAAT2 modulates excitotoxicity and delays the onset but not the outcome of ALS in mice	Hum Mol Genet 12(19): 2519-32	F	both	G93A	x		EAAT overexpression by 2-fold delays caspase activation
Excitotoxicity	None	Arundine, M. and M. Tymianski	2003	Molecular mechanisms of calcium-dependent neurodegeneration in excitotoxicity	Cell Calcium 34(4-5): 325-37					x	calcium influx, saturatio, glutamate receptor-mediated excitotoxicity
Excitotoxicity	None	Carunchio, I., C. Mollinari, et al	2008	GAB(A) receptors present higher affinity and modified subunit composition in spinal motor neurons from a genetic model of amyotrophic lateral sclerosis	Eur J Neurosci 28(7): 1275-85	F	invivo	G93A	x		functionality and expression of GABA(A) receptors are altered
Excitotoxicity	None	Corona, J. C., L. B. Tovar-y-Romo	2007	Glutamate excitotoxicity and Clinical targets for amyotrophic lateral sclerosis	Expert Opin Ther Targets 11(11): 1415-28	F/S				x	excitotoxicity and clinical treatmetns

Category 1	Category 2	Author	Year	Title	Journal	ALS type	Exp Type	Model	SOD	R/O	Factor Description
Excitotoxicity	None	Guatteo, E., I. Carunchio, et al	2007	Altered calcium homeostasis in motor neurons following AMPA receptor but not voltage-dependent calcium channels' activation in a genetic model of amyotrophic lateral sclerosis	Neurobiol Dis 28(1): 90-100	F	invitro	G93A	x		calclium dynamics altered by AMPA
Excitotoxicity	None	Ikonomidou, C., Y. Qin Qin, et al	1996	Motor neuron degeneration induced by excitotoxin agonists has features in common with those seen in the SOD-1 transgenic mouse model of amyotrophic lateral sclerosis	J Neuropathol Exp Neurol 55(2): 211-24	F	invivo	G93A	x	x	effects of NMDA and AMPA in ALS and neurodegeneration
Excitotoxicity	None	Kuner, R., A. J. Groom, et al	2005	Mechanisms of disease: motoneuron disease aggravated by transgenic expression of a functionally modified AMPA receptor subunit	Ann N Y Acad Sci 1053: 269-86	F	invivo	G93A	x		elevated Ca influx via glutamate AMPA channels causes degeneration
Excitotoxicity	None	Kuo, J. J., M. Schonewille, et al	2004	Hyperexcitability of cultured spinal motoneurons from presymptomatic ALS mice	J Neurophysiol 91(1): 571-5	F	invivo	G93A	x		electrophysiological properties/hyperexcitability
Excitotoxicity	None	Pieri, M., I. Carunchio, et al	2008	Increased persistent sodium current determines cortical hyperexcitability in a genetic model of amyotrophic lateral sclerosis	Exp Neurol.	F	invitro	G93A	x		firing properties, PIC, sodium, riluzole, hyperexcitability

Category 1	Category 2	Author	Year	Title	Journal	ALS type	Exp Type	Model	SOD	R/O	Factor Description
Excitotoxicity	None	Sandyk, R.	2006	Serotonergic mechanisms in amyotrophic lateral sclerosis	Int J Neurosci 116(7): 775-826	F/S	invivo	human/G93A	x		glutamate, 5-HT, serotonin
Excitotoxicity	None	Turner, M. R., E. A. Rabiner, et al	2007	Cortical 5-HT1A receptor binding in patients with homozygous D90A SOD1 vs sporadic ALS	Neurology 68(15): 1233-5.	F/S	invivo	D90A	x		5-HT, serotonin
Excitotoxicity	None	Van Damme, P., M. Leyssen, et al	2003	The AMPA receptor antagonist NBQX prolongs survival in a transgenic mouse model of amyotrophic lateral sclerosis	Neurosci Lett 343(2): 81-4	F	invitro	G93A	x		effect of AMPA; intracellular Ca
Excitotoxicity	None	von Lewinski, F., J. Fuchs, et al	2008	Low Ca2+ buffering in hypoglossal motoneurons of mutant SOD1 (G93A) mice	Neurosci Lett 445(3): 224-8	F	invivo	G93A	x		Ca buffering effects
Excitotoxicity	None	Vucic, S., G. A. Nicholson, et al	2008	Cortical hyperexcitability may precede the onset of familial amyotrophic lateral sclerosis	Brain 131(Pt 6): 1540-50	F/S	invivo	human	x		cortical hyperexcitability precedes the development of clinical symptoms
Excitotoxicity	None	Zona, C., M. Pieri, et al	2006	Voltage-dependent sodium channels in spinal cord motor neurons display rapid recovery from fast inactivation in a mouse model of amyotrophic lateral sclerosis	J Neurophysiol 96(6): 3314-22	F	invitro	G93A	x		Na channel properties

Category 1	Category 2	Author	Year	Title	Journal	ALS type	Exp Type	Model	SOD	R/O	Factor Description
Excitotoxicity	Proteomic	Avossa, D., M. Grandolfo, et al.	2006	Early signs of motoneuron vulnerability in a disease model system: Characterization of transverse slice cultures of spinal cord isolated from embryonic ALS mice	Neuroscience 138(4): 1179-94	F	invivo	G93A	x		AMPA, glia and myelin, mitochondrial vacuolization, protein aggregation
Excitotoxicity	Clinical	Boston-Howes, W., E. O. Williams, et al	2008	Nordihydroguaiaretic acid increases glutamate uptake in vitro and in vivo: Clinical implications for amyotrophic lateral sclerosis	Exp Neurol 213(1): 229-37	F	invivo	G93A	x		(NDGA), an anti-inflammatory drug that inhibits lipoxygensases; drug resistance
Excitotoxicity	Clinical	Turner, M. R., E. A. Rabiner, et al	2005	[11C]-WAY100635 PET demonstrates marked 5-HT1A receptor changes in sporadic ALS	Brain 128(Pt 4): 896-905	F/S	invivo	?	x		5-HT, serotonin
Excitotoxicity	Clinical	Vogels, O. J., W. J. Oyen, et al	1999	Decreased striatal dopamine-receptor binding in sporadic ALS: glutamate hyperactivity?	Neurology 52(6): 1275-7	S	invivo	human	x		dopamine effects on glutamate hyperactivity
Free Radical	Energetic	Ahtoniemi, T., M. Jaronen, et al.	2008	Mutant SOD1 from spinal cord of G93A rats is destabilized and binds to inner mitochondrial membrane	Neurobiol Dis 32(3): 479-85	F	invivo	G93A	x		IMS binding and increased ROS production by destabilized SOD1
Free Radical	Energetic	Liu, R., B. Li, et al	2002	Increased mitochondrial antioxidative activity or decreased oxygen free radical propagation prevent mutant SOD1-mediated motor neuron cell death and increase amyotrophic lateral sclerosis-like transgenic mouse survival	J Neurochem 80(3): 488-500	F	invitro	G93A	x		cellular oxidative stress, mitochondrial dysfunction, cytochrome c release

Category 1	Category 2	Author	Year	Title	Journal	ALS type	Exp Type	Model	SOD	R/O	Factor Description
Free Radical	Energetic	Muller, F. L., Y. Liu, et al	2008	MnSOD deficiency has a differential effect on disease progression in two different ALS mutant mouse models	Muscle Nerve 38(3): 1173-83	F	invivo	G93A and H46R/H48Q	x		comparison to defficient mitochondrial anti-oxidants
Free Radical	Genetic	Aguirre, N., M. F. Beal, et al.	2005	Increased oxidative damage to DNA in an animal model of amyotrophic lateral sclerosis	Free Radic Res 39(4): 383-8	F	invivo	G93A	x		8-Hydroxy-2'-deoxyguanosine (8OH2'dG) in the nuclear DNA
Free Radical	Genetic	Ignacio, S., D. H. Moore, et al	2005	Effect of neuroprotective drugs on gene expression in G93A/SOD1 mice	Ann N Y Acad Sci 1053: 121-36	F	invivo	G93A	x		Clinical effects on genetic markers for methallothionein, EAAT2, NOS
Free Radical	Genetic	Mitsumoto, H., R. M. Santella, et al	2008	Oxidative stress biomarkers in sporadic ALS	Amyotroph Lateral Scler 9(3): 177-83	S	invivo	human			genetic measures of oxidative stress
Free Radical	Inflammation	Hozumi, I., M. Yamada, et al	2008	The expression of metallothioneins is diminished in the spinal cords of patients with sporadic ALS	Amyotroph Lateral Scler 9(5): 294-8	S	invivo	human			metallothioneins (free rad scavengers) decreased in SALS
Free Radical	Inflammation	Wu, D. C., D. B. Re, et al	2006	The inflammatory NADPH oxidase enzyme modulates motor neuron degeneration in amyotrophic lateral sclerosis mice	Proc Natl Acad Sci U S A 103(32): 12132-7	F	both	?	x		NADPH, IGF-1,oxidative stress
Free Radical	Necro-Apoptosis	Pehar, M., M. R. Vargas, et al	2007	Mitochondrial superoxide production and nuclear factor erythroid 2-related factor 2 activation in p75 neurotrophin receptor-induced motor neuron apoptosis	J Neurosci 27(29): 7777-85	F	?	G93A	x		NGF, p75, NO, mitochondrial superoxide

Category 1	Category 2	Author	Year	Title	Journal	ALS type	Exp Type	Model	SOD	R/O	Factor Description
Free Radical	Necro-Apop-tosis	Raoul, C., E. Buhler, et al	2006	Chronic activation in presymptomatic amyotrophic lateral sclerosis (ALS) mice of a feedback loop involving Fas, Daxx, and FasL	Proc Natl Acad Sci U S A 103(15): 6007-12	F	invivo	G93A & G85R			NO , FAS
Free Radical	None	Pierce, A., H. Mirzaei, et al	2008	GAPDH is conformationally and functionally altered in association with oxidative stress in mouse models of amyotrophic lateral sclerosis	J Mol Biol 382(5): 1195-210			G93A or H46R/H48Q			creatine, GADPH, oxidative stress
Free Radical	None	Yamashita, H., J. Kawamata, et al	2007	Heat-shock protein 105 interacts with and suppresses aggregation of mutant Cu/Zn superoxide dismutase: clues to a possible strategy for treating ALS	J Neurochem 102(5): 1497-505	F	invivo	G93A	x		Hsp70 and Hsp27, aggregates
Free Radical	Proteom ic	Schonhoff, C. M., M. Matsuoka, et al	2006	S-nitrosothiol depletion in amyotrophic lateral sclerosis	Proc Natl Acad Sci U S A 103(7): 2404-9	?	?	?	x		S-nitrosothiol, SNOS, GADPH, NO, protein aggregation
Free Radical	Clinical	Boll, M. C., M. Alcaraz-Zubeldia, et al	2003	Raised nitrate concentration and low SOD activity in the CSF of sporadic ALS patients	Neuroc hem Res 28(5): 699-703	S	invivo	hu-man	x		degeneration increases with increased NO production
Genetic	Chem-istry	Alexander, M. D., B. J. Traynor, et al	2002	"True" sporadic ALS associated with a novel SOD-1 mutation	Ann Neurol 52(5): 680-3	S	invivo	hu-man	x		mutation (H80A) is believed to alter zinc ligand binding

Category 1	Category 2	Author	Year	Title	Journal	ALS type	Exp Type	Model	SOD	R/O	Factor Description
Genetic	Excito-toxicity	Kawahara, Y., H. Sun, et al.	2006	Underediting of GluR2 mRNA, a neuronal death inducing molecular change in sporadic ALS, does not occur in motor neurons in ALS1 or SBMA	Neurosci Res 54(1): 11-4	F/S				x	mRNA editing of th AMPA subunit GluR2
Genetic	Free Radical	Chou, C. M., C. J. Huang, et al	2005	Identification of three mutations in the Cu,Zn-superoxide dismutase (Cu,Zn-SOD) gene with familial amyotrophic lateral sclerosis: transduction of human Cu,Zn-SOD into PC12 cells by HIV-1 TAT protein basic domain	Ann N Y Acad Sci 1042: 303-13	F	invivo	G93A	x		active Tat-SOD protects against oxidative stress.
Genetic	Multiple	Vargas, M. R., M. Pehar, et al	2008	Transcriptional profile of primary astrocytes expressing ALS-linked mutant SOD1	J Neurosci Res 86(16): 3515-25	F	invivo	G93A	x		transcription, signaling, cell proliferation, extracellular matrix synthesis, response to stress, and steroid and lipid metabolism, IGF
Genetic	None	Lindberg, M. J., L. Tibell, et al	2002	Common denominator of Cu/Zn superoxide dismutase mutants associated with amyotrophic lateral sclerosis: decreased stability of the apo state	Proc Natl Acad Sci U S A 99(26): 16607-12	F	invivo	mult	x		higher the stability loss, the lower the mean survival time
Genetic	None	Luquin, N., B. Yu, et al	2008	An analysis of the entire SOD1 gene in sporadic ALS	Neuromuscul Disord 18(7): 545-52	S	invivo	human	x		genetic analysis of complete SOD1 gene in SALS

Category 1	Category 2	Author	Year	Title	Journal	ALS type	Exp Type	Model	SOD	R/O	Factor Description
Genetic	None	Meyer, T., B. Alber, et al	2003	High rate of constitutional chromosomal rearrangements in apparently sporadic ALS	Neurology 60(8): 1348-50.\	S	invivo	human			genetic aberration is SALS
Genetic	None	Watanabe, M., M. Jackson, et al	2006	Genetic analysis of the cystatin C gene in familial and sporadic ALS patients	Brain Res 1073-1074: 20-4	S	invivo	human	x		biomarker for ALS
Genetic	None	Zetterstrom, P., H. G. Stewart, et al	2007	Soluble misfolded subfractions of mutant superoxide dismutase-1s are enriched in spinal cords throughout life in murine ALS models	Proc Natl Acad Sci U S A 104(35): 14157-62.	F	invivo	mult	x		SOD1 aggregates over entire life span of model
Genetic	Proteomic	Martin, I., P. Vourc'h, et al	2008	Association study of the ubiquitin conjugating enzyme gene UBE2H in sporadic ALS	Amyotroph Lateral Scler: 1-4	S	invivo	?			analysis of ubiquitin gene, specific one not implicated in SALS
Genetic	Proteomic	Offen, D., Y. Barhum, et al	2008	Spinal Cord mRNA Profile in Patients with ALS: Comparison with Transgenic Mice Expressing the Human SOD-1 Mutant	J Mol Neurosci	S	invivo	human & G93A			cathepsin, apolipoprotein E, EGF , ferritin, lysosomal trafficking marker
Genetic	Clinical	Andersen, P. M.	2001	Genetic of sporadic ALS	Amyotroph Lateral Scler Other Motor Neuron Disord 2 Suppl 1: S37-41	S	invivo	human	x		D90A and the I113T; inheritance & penetrance

Category 1	Category 2	Author	Year	Title	Journal	ALS type	Exp Type	Model	SOD	R/O	Factor Description
Genetic	Clinical	Aoki, M., S. Kato, et al	2005	Development of a rat model of amyotrophic lateral sclerosis expressing a human SOD1 transgene	Neuropathology 25(4): 365-70	F	invivo	G93A/H46R	x		SOD1 properties comparable to human SOD1
Genetic	Clinical	Armon, C	2005	Acquired nucleic acid changes may trigger sporadic amyotrophic lateral sclerosis	Muscle Nerve 32(3): 373-7	S	invivo	human			effects of DNA alkylation
Genetic	Clinical	Broom, W. J., M. J. Parton, et al	2004	No association of the SOD1 locus and disease susceptibility or phenotype in sporadic ALS	Neurology 63(12): 2419-22	F/S	invivo	human	x		effects of mutations at the SOD1 locus
Inflammation	Excitotoxicity	Rossi, D., L. Brambilla, et al	2008	Focal degeneration of astrocytes in amyotrophic lateral sclerosis	Cell Death Differ 15(11): 1691-700	F	invivo	G93A	x		gl receptor and astrocyte degeneration
Inflammation	Free Radical	Liang, X., Q. Wang, et al	2008	The prostaglandin E2 EP2 receptor accelerates disease progression and inflammation in a model of amyotrophic lateral sclerosis	Ann Neurol 64(3): 304-14	F	invivo	G93A	x		activation of pro-inflammatory paths via E2 receptor
Inflammation	Free Radical	Liu, Y., W. Hao, et al	2008	Expression of ALS-linked SOD1 mutant increases the neurotoxic potential of microglia via TLR2	J Biol Chem	F	invitro	multiple	x		NADPH oxidase-dependent ROS production, TLR-2, microglia
Inflammation	Free Radical	Pehar, M., M. R. Vargas, et al	2005	Complexity of astrocyte-motor neuron interactions in amyotrophic lateral sclerosis	Neurodegener Dis 2(3-4): 139-46	F	invivo	?	x		FGF, NGF, astrocytes, NO

Category 1	Category 2	Author	Year	Title	Journal	ALS type	Exp Type	Model	SOD	R/O	Factor Description
Inflammation	Free Radical	Pehar, M., P. Cassina, et al	2004	Astrocytic production of nerve growth factor in motor neuron apoptosis: implications for amyotrophic lateral sclerosis	J Neurochem 89(2): 464-73	F	invitro	G93A	x		astrocytes, NGF, NO, p75
Inflammation	Inflammation	Nagai, M., D. B. Re, et al	2007	Astrocytes expressing ALS-linked mutated SOD1 release factors selectively toxic to motor neurons.Nat Neurosci 10(5): 615-22		F	invivo	?	x		role of astrocytes and factors they express
Inflammation	Multiple	Barbeito, L. H., M. Pehar, et al	2004	A role for astrocytes in motor neuron loss in amyotrophic lateral sclerosis	Brain Res Brain Res Rev 47(1-3): 263-74	F/S				x	reactive astrocytes: ROS/NO prod, EAAT downreg, & apoptosis mediation
Inflammation	Necro-Apoptosis	Di Giorgio, F. P., M. A. Carrasco, et al	2007	Non-cell autonomous effect of glia on motor neurons in an embryonic stem cell-based ALS model	Nat Neurosci 10(5): 608-14	F	invitro	G93A	x		SOD1 glia cells affect motoneuron cell death in culture
Inflammation	Necro-Apoptosis	Kadoyama, K., H. Funakoshi, et al	2007	Hepatocyte growth factor (HGF) attenuates gliosis and motoneuronal degeneration in the brainstem motor nuclei of a transgenic mouse model of ALS	Neurosci Res 59(4): 446-56	F	invivo	G93A	x		HGF reduces microglial accumulation; pro-apoptotic protein inhibition
Inflammation	Necro-Apoptosis	Li, L., X. Zhang, et al	2008	Altered macroautophagy in the spinal cord of SOD1 mutant mice	Autophagy 4(3): 290-3	F	invivo	G93A	x		role of autophagy

Category 1	Category 2	Author	Year	Title	Journal	ALS type	Exp Type	Model	SOD	R/O	Factor Description
Inflammation	None	Chung, Y. H., K. M. Joo, et al	2008	Immunohistochemical study on the distribution of glycogen synthase kinase 3alpha in the central nervous system of SOD1(G93A) transgenic mice	Neurol Res 30(9): 926-31	F	invivo	G93A	x		GSK3alpha-immunoreactive astrocytes
Inflammation	None	Fendrick, S. E., Q. S. Xue, et al	2007	Formation of multinucleated giant cells and microglial degeneration in rats expressing a mutant Cu/Zn superoxide dismutase gene	J Neuroinflammation 4: 9	F	invivo	G93A	x		microglia aggregation & abnormalities
Inflammation	None	Gowing, G., T. Philips, et al	2008	Ablation of proliferating microglia does not affect motor neuron degeneration in amyotrophic lateral sclerosis caused by mutant superoxide dismutase	J Neurosci 28(41): 10234-44	F	invivo	G93A	x		50% reduction in reactive microglia did not reduce neurodegeneration
Inflammation	None	Hall, E. D., J. A. Oostveen, et al	1998	Relationship of microglial and astrocytic activation to disease onset and progression in a transgenic model of familial ALS	Glia 23(3): 249-56	F	invivo	G93A	x		timecourse of microglia and astrocytic activation
Inflammation	None	Hensley, K., H. Abdel-Moaty, et al	2006	Primary glia expressing the G93A-SOD1 mutation present a neuroinflammatory phenotype and provide a cellular system for studies of glial inflammation	J Neuroinflammation 3: 2	F	both	G93A	x		glial inflammation of microglia and astrocytes

Category 1	Category 2	Author	Year	Title	Journal	ALS type	Exp Type	Model	SOD	R/O	Factor Description
Inflammation	None	Kiaei, M., K. Kipiani, et al	2005	Peroxisome proliferator-activated receptor-gamma agonist extends survival in transgenic mouse model of amyotrophic lateral sclerosis	Exp Neurol 191(2): 331-6	F	invivo	G93A	x		PPARs role in inflammation
Inflammation	None	Lepore, A. C., C. Dejea, et al	2008	Selective ablation of proliferating astrocytes does not affect disease outcome in either acute or chronic models of motor neuron degeneration	Exp Neurol 211(2): 423-32	F	invivo	G93A	x		astrogliosis
Inflammation	None	Shibata, N., M. Kawaguchi-Niida, et al	2008	Effects of the PPARgamma activator pioglitazone on p38 MAP kinase and IkappaBalpha in the spinal cord of a transgenic mouse model of amyotrophic lateral sclerosis	Neuropathology 28(4): 387-98	F	invivo	G93A	x		PPAR gamma, p38, neuron and glial inflammation
Multiple	Excitotoxicity	Bruijn, L. I., T. M. Miller, et al	2004	Unraveling the mechanisms involved in motor neuron degeneration in ALS	Annu Rev Neurosci 27: 723-49					x	excitoxicity & nonneuronal support cells
Multiple	None	Bromberg, M. B.	1999	Pathogenesis of amyotrophic lateral sclerosis: a critical review	Curr Opin Neurol 12(5): 581-8					x	review of ALS pathogenesis
Multiple	Clinical	de Belleroche, J., R. Orrell, et al	1995	Familial amyotrophic lateral sclerosis/motor neurone disease (FALS): a review of current developments." J Med Genet 32(11): 841-7		F				x	FALS review

Category 1	Category 2	Author	Year	Title	Journal	ALS type	Exp Type	Model	SOD	R/O	Factor Description
Multiple	None	Martin, L. J., A. C. Price, et al	2000	Mechanisms for neuronal degeneration in amyotrophic lateral sclerosis and in models of motor neuron death (Review)	Int J Mol Med 5(1): 3-13	F/S				x	review of ALS mechanisms
Necro-Apoptosis	Energetic	Benchoua, A., C. Guegan, et al	2001	Specific caspase pathways are activated in the two stages of cerebral infarction	J Neurosci 21(18): 7127-34					x	means of caspase activation: mitochondria indep & dependent paths
Necro-Apoptosis	Energetic	Guegan, C., M. Vila, et al	2001	Recruitment of the mitochondrial-dependent apoptotic pathway in amyotrophic lateral sclerosis	J Neurosci 21(17): 6569-76	F	invivo	?	x		Bax, cytochrome c, caspase in apoptosis
Necro-Apoptosis	Energetic	Ilzecka, J	2007	Decreased cerebrospinal fluid cytochrome c levels in patients with amyotrophic lateral sclerosis	Scand J Clin Lab Invest 67(3): 264-9	F/S	invivo	human			cytochrome c measurements
Necro-Apoptosis	Energetic	Murakami, T., M. Nagai, et al	2007	Early decrease of mitochondrial DNA repair enzymes in spinal motor neurons of presymptomatic transgenic mice carrying a mutant SOD1 gene	Brain Res 1150: 182-9	F	invivo	?	x		expressions of DNA repair enzymes, dowregulated at mitochondria
Necro-Apoptosis	Excitotoxicity	Mattson, M. P. and W. Duan	1999	"Apoptotic" biochemical cascades in synaptic compartments: roles in adaptive plasticity and neurodegenerative disorders	J Neurosci Res 58(1): 152-66					x	caspase, proteolysis of Glu-R subunits, Ca effects on glutamate

Category 1	Category 2	Author	Year	Title	Journal	ALS type	Exp Type	Model	SOD	R/O	Factor Description
Necro-Apoptosis	Free Radical	Beere, H. M.	2004	"The stress of dying": the role of heat shock proteins in the regulation of apoptosis."	J Cell Sci 117(Pt 13): 2641-51					x	role of Hsp in apoptosis
Necro-Apoptosis	Free Radical	Gifondorwa, D. J., M. B. Robinson, et al	2007	Exogenous delivery of heat shock protein 70 increases lifespan in a mouse model of amyotrophic lateral sclerosis	J Neurosci 27(48): 13173-80	F	invivo	G93A	x		role of HSP70
Necro-Apoptosis	Free Radical	Kruman, II and M. P. Mattson	1999	Pivotal role of mitochondrial calcium uptake in neural cell apoptosis and necrosis	J Neurochem 72(2): 529-40		invitro			x	time course of Ca, ROS production, caspase activation
Necro-Apoptosis	Free Radical	Kruman, II, W. A. Pedersen, et al	1999	ALS-linked Cu/Zn-SOD mutation increases vulnerability of motor neurons to excitotoxicity by a mechanism involving increased oxidative stress and perturbed calcium homeostasis	Exp Neurol 160(1): 28-39	F	invitro	?	x		overexpression of Bcl-2 blocked Ca; blocking of Ca prevented apoptosis
Necro-Apoptosis	Free Radical	Malaspina, A., N. Jokic, et al	2008	Comparative analysis of the time-dependent functional and molecular changes in spinal cord degeneration induced by the G93A SOD1 gene mutation and by mechanical compression	BMC Genomics 9: 500	F	invivo	G93A	x	x	cytoskeletal protein metabolism is central to SCI & ALS

Category 1	Category 2	Author	Year	Title	Journal	ALS type	Exp Type	Model	SOD	R/O	Factor Description
Necro-Apoptosis	Free Radical	Nagata, T., H. Ilieva, et al	2007	Increased ER stress during motor neuron degeneration in a transgenic mouse model of amyotrophic lateral sclerosis	Neurol Res 29(8): 767-71	F	invivo	G93A	x		ER, caspase, oxidative stress
Necro-Apoptosis	Inflam-mation	Luo, Y., H. Xue, et al	2007	Impaired SDF1/CXCR4 signaling in glial progenitors derived from SOD1(G93A) mice	J Neurosci Res 85(11): 2422-32	F	invitro	G93A	x		ERTK 1/2 and CREB paths
Necro-Apoptosis	Inflam-mation	Wootz, H., E. Weber, et al	2006	Altered distribution and levels of cathepsinD and cystatins in amyotrophic lateral sclerosis transgenic mice: possible roles in motor neuron survival	Neurosc ience 143(2): 419-30	F	invivo	?	x		caspases, astrocytes
Necro-Apoptosis	None	Dewil, M., V. F. dela Cruz, et al	2007	Inhibition of p38 mitogen activated protein kinase activation and mutant SOD1(G93A)-induced motor neuron death	Neurobi ol Dis 26(2): 332-41	F	invivo	?	x		abnormal activation of p38 MAPK in mutant SOD1 mice
Necro-Apoptosis	None	Gonzalez de Aguilar, J. L., J. W. Gordon, et al	2000	Alteration of the Bcl-x/Bax ratio in a transgenic mouse model of amyotrophic lateral sclerosis: evidence for the implication of the p53 signaling pathway	Neurobi ol Dis 7(4): 406-15	F	invivo	G86R	x		p53, Bax/Bcl in apoptosis
Necro-Apoptosis	None	Guegan, C. and S. Przed-borski		Programmed cell death in amyotrophic lateral sclerosis	J Clin Invest 111(2): 153-61.	F/S	invitro				

Category 1	Category 2	Author	Year	Title	Journal	ALS type	Exp Type	Model	SOD	R/O	Factor Description
Necro-Apoptosis	None	Gajewski, C. D., M. T. Lin, et al.	2003	Mitochondrial DNA from platelets of sporadic ALS patients restores normal respiratory functions in rho(0) cells.	Exp Neurol 179(2): 229-35	F/S				x	
Necro-Apoptosis	None	He, B. P. and M. J. Strong	2000	Motor neuronal death in sporadic amyotrophic lateral sclerosis (ALS) is not apoptotic. A comparative study of ALS and chronic aluminium chloride neurotoxicity in New Zealand white rabbits	Neuropathol Appl Neurobiol 26(2): 150-60	F	invivo	?	?		lack of apoptosis; TUNEL hybridization; DNA laddering
Necro-Apoptosis	None	Kiaei, M., K. Kipiani, et al	2007	Matrix metalloproteinase-9 regulates TNF-alpha and FasL expression in neuronal, glial cells and its absence extends life in a transgenic mouse model of amyotrophic lateral sclerosis	Exp Neurol 205(1): 74-81	F	invivo	G93A	x		TNF-alpha and Fas activation by metalloproteinase

Category 1	Category 2	Author	Year	Title	Journal	ALS type	Exp Type	Model	SOD	R/O	Factor Description
Necro-Apoptosis	None	Lee, J. K., J. H. Shin, et al	2008	Tissue inhibitor of metalloproteinases-3 (TIMP-3) expression is increased during serum deprivation-induced neuronal apoptosis in vitro and in the G93A mouse model of amyotrophic lateral sclerosis: a potential modulator of Fas-mediated apoptosis	Neurobiol Dis 30(2): 174-85	F	invivo	G93A	x		metalloproteinases, caspases, Fas in necro-apoptosis
Necro-Apoptosis	None	Locatelli, F., S. Corti, et al	2007	Fas small interfering RNA reduces motoneuron death in amyotrophic lateral sclerosis mice	Ann Neurol 62(1): 81-92.	F	invivo	G93A	x		Fas-linked death, caspase, and cytochrome c
Necro-Apoptosis	None	Martin, L. J.	1999	Neuronal death in amyotrophic lateral sclerosis is apoptosis: possible contribution of a programmed cell death mechanism.	J Neuropathol Exp Neurol 58(5): 459-71	F/	invivo	?	?		Bax and Bak are elevate; Bcl-2 decreased
Necro-Apoptosis	None	Pasinelli, P., D. R. Borchelt, et al	1998	Caspase-1 is activated in neural cells and tissue with amyotrophic lateral sclerosis-associated mutations in copper-zinc superoxide dismutase	Proc Natl Acad Sci U S A 95(26): 15763-8	F	invitro	?	x		caspase, xanthine/xanthine oxidase which triggers cleavage and secretion pro-interleukin 1beta, and induces apoptosis.

Category 1	Category 2	Author	Year	Title	Journal	ALS type	Exp Type	Model	SOD	R/O	Factor Description
Necro-Apoptosis	None	Pasinelli, P., M. K. Housewear t, et al	2000	Caspase-1 and -3 are sequentially activated in motor neuron death in Cu,Zn superoxide dismutase-mediated familial amyotrophic lateral sclerosis	Proc Natl Acad Sci U S A 97(25): 13901-6	F	?	?	x		caspase
Necro-Apoptosis	None	Sathasivam , S. and P. J. Shaw	2005	Apoptosis in amyotrophic lateral sclerosis--what is the evidence	Lancet Neurol 4(8): 500-9.	F/S				x	apoptosis, caspase, Bcl-2, p53
Necro-Apoptosis	None	Sathasivam , S., P. G. Ince, et al	2001	Apoptosis in amyotrophic lateral sclerosis: a review of the evidence	Neurop athol Appl Neurobi ol 27(4): 257-74	F/S				x	apoptosis, caspase, Bcl-2, p53
Necro-Apoptosis	None	Tokuda, E., S. Ono, et al	2007	Dysequilibrium between caspases and their inhibitors in a mouse model for amyotrophic lateral sclerosis	Brain Res 1148: 234-42	F	invivo	G93A	x		caspase
Necro-Apoptosis	None	Vukosavic, S., M. Dubois-Dauphin, et al	1999	Bax and Bcl-2 interaction in a transgenic mouse model of familial amyotrophic lateral sclerosis	J Neuroch em 73(6): 2460-8	F	invivo	G93A	x		Bax & Bcl interaction; Bcl-2, Bcl-XL, Bad, and Bax
Necro-Apoptosis	None	Wengenack , T. M., S. S. Holasek, et al	2004	Activation of programmed cell death markers in ventral horn motor neurons during early presymptomatic stages of amyotrophic lateral sclerosis in a transgenic mouse model	Brain Res 1027(1-2): 73-86	F	invivo	G93A	x		MAP kinase, caspase

Category 1	Category 2	Author	Year	Title	Journal	ALS type	Exp Type	Model	SOD	R/O	Factor Description
Necro-Apoptosis	None	Yamazaki, M., E. Esumi, et al	2005	Is motoneuronal cell death in amyotrophic lateral sclerosis apoptosis?	Neuropathology 25(4): 381-7	F/S	invivo	human	x		caspase, DNA fragmentation
Necro-Apoptosis	Proteomic	Gould, T. W., R. R. Buss, et al	2006	Complete dissociation of motor neuron death from motor dysfunction by Bax deletion in a mouse model of ALS	J Neurosci 26(34): 8774-86	F	invivo	G93A	x		Bax acts via a mechanism distinct from cell death activation; mitochondrial vacuolization & denervation
Necro-Apoptosis	Proteomic	Oh, Y. K., K. S. Shin, et al	2008	Superoxide dismutase 1 mutants related to amyotrophic lateral sclerosis induce endoplasmic stress in neuro2a cells	J Neurochem 104(4): 993-1005.	F	invivo	G93A & G85R			ER, DNA nick labeling, apoptosis. Bcl
Necro-Apoptosis	Clinical	Li, M., V. O. Ona, et al	2000	Functional role of caspase-1 and caspase-3 in an ALS transgenic mouse model	Science 288(5464): 335-9	F	invivo	G93A	x		correlations and expression of caspase(s)
Necro-Apoptosis	Clinical	Zhu, S., I. G. Stavrovskaya, et al	2002	Minocycline inhibits cytochrome c release and delays progression of amyotrophic lateral sclerosis in mice	Nature 417(6884): 74-8	F	invivo	?			cytochrome c, MAPK
Inflammation	Energetic	Bilsland, L. G., N. Nirmalananthan, et al	2008	Expression of mutant SOD1 in astrocytes induces functional deficits in motoneuron mitochondria	J Neurochem 107(5): 1271-83	F	invivo	G93A	x		SOD1 in astrocytes: mito function did not correlate with Ca

Category 1	Category 2	Author	Year	Title	Journal	ALS type	Exp Type	Model	SOD	R/O	Factor Description
Proteomic	Chemistry	Bergemalm, D., P. A. Jonsson, et al	2006	Overloading of stable and exclusion of unstable human superoxide dismutase-1 variants in mitochondria of murine amyotrophic lateral sclerosis models	J Neurosci 26(16): 4147-54	F	invivo	G85R and G127insTGGG	x		loading of G85R and G127insTGGG in mitochondria
Proteomic	Energetic	Deng, H. X., Y. Shi, et al	2006	Conversion to the amyotrophic lateral sclerosis phenotype is associated with intermolecular linked insoluble aggregates of SOD1 in mitochondria	Proc Natl Acad Sci U S A 103(18): 7142-7	F	invivo	?	x		oxidation, protein aggregation, mitochondrial damage, and SOD1-mediated ALS
Proteomic	Energetic	Liu, J., C. Lillo, et al	2004	Toxicity of familial ALS-linked SOD1 mutants from selective recruitment to spinal mitochondria	Neuron 43(1): 5-17	F	invivo	?	x		protein aggregation in mitochondria
Proteomic	Energetic	Lukas, T. J., W. W. Luo, et al	2006	Informatics-assisted protein profiling in a transgenic mouse model of amyotrophic lateral sclerosis	Mol Cell Proteomic 5(7): 1233-44	F	invivo	G93A	x		expression: protein kinase signaling systems, ATP-driven ion transport, and neurotransmission
Proteomic	Energetic	Raimondi, A., A. Mangolini, et al	2006	Cell culture models to investigate the selective vulnerability of motoneuronal mitochondria to familial ALS-linked G93ASOD1	Eur J Neurosci 24(2): 387-99	F	invitro	G93A	x		swelling & cristae remodeling of mitochondria

Category 1	Category 2	Author	Year	Title	Journal	ALS type	Exp Type	Model	SOD	R/O	Factor Description
Proteomic	Free Radical	Aquilano, K., G. Rotilio, et al	2003	Proteasome activation and nNOS down-regulation in neuroblastoma cells expressing a Cu,Zn superoxide dismutase mutant involved in familial ALS	J Neurochem 85(5): 1324-35	F	invivo	G93A	x		ROS/NO interactions; proteasome inhbition
Proteomic	Free Radical	Kikuchi, H., G. Almer, et al	2006	Spinal cord endoplasmic reticulum stress associated with a microsomal accumulation of mutant superoxide dismutase-1 in an ALS model	Proc Natl Acad Sci U S A 103(15): 6025-30	F	invivo	?	x		protein aggregation in ER
Proteomic	Free Radical	Urushitani, M., J. Kurisu, et al	2002	Proteasomal inhibition by misfolded mutant superoxide dismutase 1 induces selective motor neuron death in familial amyotrophic lateral sclerosis	J Neurochem 83(5): 1030-42	F	invivo	mult	x		proteasome inhibition, oxidative stress
Proteomic	Genetic	Gal, J., A. L. Strom, et al	2007	p62 accumulates and enhances aggregate formation in model systems of familial amyotrophic lateral sclerosis	J Biol Chem 282(15): 11068-77	F	invivo	?	x		p62 nuclear pore protein role in aggregate formation/ RNA trafficking

Category 1	Category 2	Author	Year	Title	Journal	ALS type	Exp Type	Model	SOD	R/O	Factor Description
Proteomic	Genetic	Nakamura, M., H. Ito, et al	2008	Phosphorylated Smad2/3 immunoreactivity in sporadic and familial amyotropc lateral sclerosis and its mouse model	Acta Neuropathol 115(3): 327-34	F/S	invivo	human & G93A	x		lewi bodies, tau occlusions; effects of SMAD transcriptors
Proteomic	Genetic	Rakhit, R., J. Robertson, et al	2007	An immunological epitope selective for pathological monomer-misfolded SOD1 in ALS	Nat Med 13(6): 754-9	F	?	G93A, G85R, G37R	x		quantification of SOD1 with an epitope
Proteomic	Genetic	Robertson, J., T. Sanelli, et al	2007	Lack of TDP-43 abnormalities in mutant SOD1 transgenic mice shows disparity with ALS	Neurosci Lett 420(2): 128-32	F	invivo	?	x		mislocationalization of TAR-DNA binding protein
Proteomic	Genetic	Sau, D., S. De Biasi, et al	2007	Mutation of SOD1 in ALS: a gain of a loss of function	Hum Mol Genet 16(13): 1604-18	F	both				proteasome, oxidative stress

Category 1	Category 2	Author	Year	Title	Journal	ALS type	Exp Type	Model	SOD	R/O	Factor Description
Proteomic	Inflammation	Puttaparthi, K. and J. L. Elliot	2005	Non-neuronal induction of immunoproteasome subunits in an ALS model: possible mediation by cytokines	Exp Neurol 196(2): 441-51	F	invivo	G93A	x		proteasome, TNF alpha, cytokines, aggregation
Proteomic	Inflammation	Puttaparthi, K., L. Van Kaer, et al	2007	Assessing the role of immuno-proteasomes in a mouse model of familial ALS.	Exp Neurol 206(1): 53-8	F	invivo	G93A	x		proteasome
Proteomic	Necro-Apoptosis	Atkin, J. D., M. A. Farg, et al	2006	Induction of the unfolded protein response in familial amyotrophic lateral sclerosis and association of protein-disulfide isomerase with superoxide dismutase 1	J Biol Chem 281(40): 30152-65	F	invivo	G93A	x		unfolded protein response and ER stress-induced apoptosis
Proteomic	None	Cheroni, C., M. Marino, et al	2009	Functional alterations of the ubiquitin-proteasome system in motor neurons of a mouse model of familial amyotrophic lateral sclerosis	Hum Mol Genet 18(1): 82-96	F	invivo	G93A	x		ubiquitin-proteasome system

Category 1	Category 2	Author	Year	Title	Journal	ALS type	Exp Type	Model	SOD	R/O	Factor Description
Proteomic	None	Gomes, C., S. Keller, et al	2007	Evidence for secretion of Cu,Zn superoxide dismutase via exosomes from a cell model of amyotrophic lateral sclerosis	Neurosci Lett 428(1): 43-6	F	invitro	G93A	x		p115 and calnexin; endosomal transferance of toxicity
Proteomic	None	Ratnaparkhi, A., G. M. Lawless, et al	2008	A Drosophila model of ALS: human ALS-associated mutation in VAP33A suggests a dominant negative mechanism	PLoS ONE 3(6): e2334	F	invivo	ALS8	?		VAPB, aggregates
Proteomic	None	Rumfeldt, J. A., J. R. Lepock, et al	2009	Unfolding and folding kinetics of amyotrophic lateral sclerosis-associated mutant Cu,Zn superoxide dismutases	J Mol Biol 385(1): 278-98	F	invivo	mult	x		measures of protein aggregation
Proteomic	None	Rumfeldt, J. A., P. B. Stathopulos, et al	2006	Mechanism and thermodynamics of guanidinium chloride-induced denaturation of ALS-associated mutant Cu,Zn superoxide dismutases	J Mol Biol 355(1): 106-23	F	invivo	mult	x		protein aggregation, stability

Category 1	Category 2	Author	Year	Title	Journal	ALS type	Exp Type	Model	SOD	R/O	Factor Description
Proteomic	None	Shaw, B. F., H. L. Lelie, et al	2008	Detergent-insoluble aggregates associated with amyotrophic lateral sclerosis in transgenic mice contain primarily full-length, unmodified superoxide dismutase-1	J Biol Chem 283(13): 8340-50	F	invivo	mult	x		protein aggregate analysis
Proteomic	None	Teuling, E., S. Ahmed, et al	2007	Motor neuron disease-associated mutant vesicle-associated membrane protein-associated protein (VAP) B recruits wild-type VAPs into endoplasmic reticulum-derived tubular aggregates	J Neurosci 27(36): 9801-15	F	invivo	G93A	x		vesicle-associated membrane protein (VAP), aggregation
Proteomic	None	Vlug, A. S. and D. Jaarsma	2004	Long term proteasome inhibition does not preferentially afflict motor neurons in organotypical spinal cord cultures	Amyotroph Lateral Scler Other Motor Neuron Disord 5(1): 16-21	F	invitro	G93A	x		ubiquitin, proteasome, aggregation
Proteomic	None	Zhai, J., H. Lin, et al	2005	HoxB2 binds mutant SOD1 and is altered in transgenic model of ALS	Hum Mol Genet 14(18): 2629-40	F	invivo	G93A	x		HoxB2 in aggregates

Category 1	Category 2	Author	Year	Title	Journal	ALS type	Exp Type	Model	SOD	R/O	Factor Description
Systemic	Energetic	Gajewski, C. D., M. T. Lin, et al	2003	Mitochondrial DNA from platelets of sporadic ALS patients restores normal respiratory functions in rho(0) cells	Exp Neurol 179(2): 229-35	S	invivo	human			platelets relieve respiratory dysfunction
Systemic	Energetic	Wiedemann, F. R., K. Winkler, et al	1998	Impairment of mitochondrial function in skeletal muscle of patients with amyotrophic lateral sclerosis	J Neurol Sci 156(1): 65-72	S	invivo	human			NADH, NADPH in muscles
Systemic	Multiple	Cova, E., C. Cereda, et al	2006	Modified expression of Bcl-2 and SOD1 proteins in lymphocytes from sporadic ALS patients	Neurosci Lett 399(3): 186-90	S	invivo	human			mitochondria & Ca regulation dysfunction & Bcl-2 in peripheral lymphocytes
Systemic	None	Banerjee, R., R. L. Mosley, et al	2008	Adaptive immune neuroprotection in G93A-SOD1 amyotrophic lateral sclerosis mice	PLoS ONE 3(7): e2740	F	invivo	G93A	x		T-cell dysfunction

Category 1	Category 2	Author	Year	Title	Journal	ALS type	Exp Type	Model	SOD	R/O	Factor Description
Systemic	None	Hegedus, J., C. T. Putman, et al	2008	Preferential motor unit loss in the SOD1 G93A transgenic mouse model of amyotrophic lateral sclerosis	J Physiol 586(14): 3337-51	F	invivo	G93A	x		FF motor units die first
Systemic	Clinical	Chung, M. J. and Y. L. Suh	2002	Ultrastructural changes of mitochondria in the skeletal muscle of patients with amyotrophic lateral sclerosis	Ultrastruct Pathol 26(1): 3-7	F/S	invivo	human			changes in muscle mitochondria
Clinical	Genetic	Gamez, J., M. Corbera-Bellalta, et al	2006	Mutational analysis of the Cu/Zn superoxide dismutase gene in a Catalan ALS population: should all sporadic ALS cases also be screened for SOD1	J Neurol Sci 247(1): 21-8	S				x	prevalence of SOD1 mutations in SALS
Clinical	Genetic	Han-Xiang, D., J. Hujun, et al	2008	Molecular dissection of ALS-associated toxicity of SOD1 in transgenic mice using an exon-fusion approach	Hum Mol Genet 17(15): 2310-9	F	both	T116X	x		Genetic 'sufficient' to cause ALS
Clinical	Genetic	Urushitani, M., S. A. Ezzi, et al	2007	Clinical effects of immunization with mutant superoxide dismutase in mice models of amyotrophic lateral sclerosis	Proc Natl Acad Sci U S A 104(7): 2495-500	F	invivo	G93A & G37R	x		SOD1 immunization as a therapy

Category 1	Category 2	Author	Year	Title	Journal	ALS type	Exp Type	Model	SOD	R/O	Factor Description
Clinical	Inflammation	Nagano, I., H. Ilieva, et al	2005	Clinical benefit of intrathecal injection of insulin-like growth factor-1 in a mouse model of Amyotrophic Lateral Sclerosis	J Neurol Sci 235(1-2): 61-8.	F	invivo	G93A	x		IGF-1 intrathecallly improved motor scores, disease onset
Clinical	Inflammation	Narai, H., I. Nagano, et al	2005	Prevention of spinal motor neuron death by insulin-like growth factor-1 associating with the signal transduction systems in SODG93A transgenic mice	J Neurosci Res 82(4): 452-7	F	invivo	G93A	x		effects of IGF-1 treatment
Clinical	Inflammation	Schutz, B., J. Reimann, et al	2005	The oral antidiabetic pioglitazone protects from neurodegeneration and amyotrophic lateral sclerosis-like symptoms in superoxide dismutase-G93A transgenic mice	J Neurosci 25(34): 7805-12	F	invivo	G93A	x		microglia, NO
Clinical	Inflammation	Wang, L. J., Y. Y. Lu, et al	2002	Neuroprotective effects of glial cell line-derived neurotrophic factor mediated by an adeno-associated virus vector in a transgenic animal model of amyotrophic lateral sclerosis	J Neurosci 22(16): 6920-8	F	invivo	G93A	x		GDNF as a therapy
Clinical	Multiple	Benatar, M	2007	Lost in translation: treatment trials in the SOD1 mouse and in human ALS	Neurobiol Dis 26(1): 1-13	F/S				x	prioritization of favorable clinical therapies: oxidation, anti-inflammatory

Category 1	Category 2	Author	Year	Title	Journal	ALS type	Exp Type	Model	SOD	R/O	Factor Description
Clinical	Multiple	Del Signore, S. J., D. J. Amante, et al	2008	Combined riluzole and sodium phenylbutyrate therapy in transgenic amyotrophic lateral sclerosis mice	Amyotroph Lateral Scler: 1-10	F	invivo	G93A	x		combination therapy impact on apoptosis & astrogliosis
Clinical	Multiple	Nicaise, C., J. Coupier, et al	2008	Gemals, a new drug candidate, extends lifespan and improves electromyographic parameters in a rat model of amyotrophic lateral sclerosis	Amyotroph Lateral Scler 9(2): 85-90	F	invivo	G93A	x		combination therapy
Clinical	Necro-Apop-tosis	Ohta, Y., T. Kamiya, et al	2008	Clinical benefits of intrathecal protein therapy in a mouse model of amyotrophic lateral sclerosis	J Neurosci Res 86(13): 3028-37.						TAT-modified Bcl-X(L) therapy, caspase
Clinical	None	Andersen, P. M., G. D. Borasio, et al	2007	Good practice in the management of amyotrophic lateral sclerosis: clinical guidelines. An evidence-based review with good practice points. EALSC Working Group.	Amyotroph Lateral Scler 8(4): 195-213	F/S				x	clinical approaches
Clinical	None	Boucherie, C., A. S. Caumont, et al	2008	In vitro evidence for impaired neuroprotective capacities of adult mesenchymal stem cells derived from a rat model of familial amyotrophic lateral sclerosis (hSOD1(G93A))	Exp Neurol 212(2): 557-61	F	both	G93A	x		clinical use of stem cells
Clinical	None	Chandran, J., J. Ding, et al	2007	Alsin and the molecular pathways of amyotrophic lateral sclerosis	Mol Neurobiol 36(3): 224-31	F	invivo	ALS2		x	relationship between alsin and motor dysfunction

Category 1	Category 2	Author	Year	Title	Journal	ALS type	Exp Type	Model	SOD	R/O	Factor Description
Clinical	None	Corti, S., F. Locatelli, et al	2007	Neural stem cells LewisX+ CXCR4+ modify disease progression in an amyotrophic lateral sclerosis model	Brain 130(Pt 5): 1289-305	F	invivo	G93A	x		stem cell protections, VEGF/IGF paths helped
Clinical	None	Feng, H. L., Y. Leng, et al	2008	Combined lithium and valproate treatment delays disease onset, reduces neurological deficits and prolongs survival in an amyotrophic lateral sclerosis mouse model	Neuroscience 155(3): 567-72	F	invivo	G93A	x		synergistic combination therapy with lithium and valpoic acid
Clinical	None	Garbuzova-Davis, S., C. D. Sanberg, et al	2008	Human umbilical cord blood treatment in a mouse model of ALS: optimization of cell dose	PLoS ONE 3(6): e2494	F	invivo	G93A	x		anti-infammatory effect of transplanted cells
Clinical	None	Lai, E. C.	1999	Clinical developments in amyotrophic lateral sclerosis	Expert Opin Investig Drugs 8(4): 347-61	F/S				x	clincal therapies
Clinical	None	Matias-Guiu, J., J. A. Barcia, et al	2008	[Cellular therapy in amyotrophic lateral sclerosis]	Neurologia 23(4): 226-37	F	invivo	G93A	x	x	evaluation of stem cell transplantation
Clinical	None	Miller, R., W. Bradley, et al	2007	Phase II/III randomized trial of TCH346 in patients with ALS	Neurology 69(8): 776-84	F/S	invivo	human			therapy had no effect
Clinical	None	Shefner, J. M., M. Cudkowicz, et al	2006	Motor unit number estimation predicts disease onset and survival in a transgenic mouse model of amyotrophic lateral sclerosis	Muscle Nerve 34(5): 603-7	F	invivo	G93A	x		motor unit number estimation

Category 1	Category 2	Author	Year	Title	Journal	ALS type	Exp Type	Model	SOD	R/O	Factor Description
Clinical	None	Tang, W., U. Tasch, et al	2009	Measuring early pre-symptomatic changes in locomotion of SOD1-G93A rats-A rodent model of amyotrophic lateral sclerosis	J Neurosci Methods 176(2): 254-62	F	invivo	G93A	x		8 parameters to measure ALS
Clinical	None	Weiss, M. D., J. M. Ravits, et al	2006	A4V superoxide dismutase mutation in apparently sporadic ALS resembling neuralgic amyotrophy	Amyotroph Lateral Scler 7(1): 61-3	S	invivo	human	x		clinical presentation
Clinical	None	Zhao, Z., D. J. Lange, et al	2008	Vgf is a novel biomarker associated with muscle weakness in amyotrophic lateral sclerosis (ALS), with a potential role in disease pathogenesis	Int J Med Sci 5(2): 92-9	F/S	invivo	human			Vgf as a muscle weakness marker
Clinical	None	Zhou, C., C. P. Zhao, et al	2007	A method comparison in monitoring disease progression of G93A mouse model of ALS	Amyotroph Lateral Scler 8(6): 366-72	F	invivo	?	x		motor unit number estimation
Clinical	Proteomic	Watanabe, M., M. Dykes-Hoberg, et al	2001	Histological evidence of protein aggregation in mutant SOD1 transgenic mice and in amyotrophic lateral sclerosis neural tissues	Neurobiol Dis 8(6): 933-41	F	invivo	G93A	x		GDNF as a therapy; AAV; protein aggreation
Clinical	Proteomic	Kalmar, B., S. Novoselov, et al	2008	Late stage treatment with arimoclomol delays disease progression and prevents protein aggregation in the SOD1 mouse model of ALS	J Neurochem 107(2): 339-50	F	invivo	G93A	x		upregulation of HSP decreases protein aggregates

Category 1	Category 2	Author	Year	Title	Journal	ALS type	Exp Type	Model	SOD	R/O	Factor Description
Clinical	Proteomic	Kanje, M., A. Edstrom, et al	1981	Inhibition of rapid Axon transport in vitro by the ionophores X-537 A and A 23187	Brain Res 204(1): 43-50					x	inhibition of transport by calcium
Clinical	Systemic	Hegedus, J., C. T. Putman, et al	2007	Time course of preferential motor unit loss in the SOD1 G93A mouse model of amyotrophic lateral sclerosis	Neurobiol Dis 28(2): 154-64	F	invivo	G93A	x		time course of G93A ALS: MN axon length, size, motor unit pool size as outcome measures

APPENDIX C

LIST OF PUBLICATIONS

This appendix contains a list of current and planned publications which contain research and/or results from this dissertation.

Current Publications

Journal Articles

Mitchell CS, Feng SS, and Lee RH. An analysis of glutamate spillover on the N-methyl-D-aspartate receptors at the cerebellar glomerulus. J Neural Eng 4: 276-282, 2007.

Mitchell CS, and Lee RH. Output-based comparison of alternative kinetic schemes for the NMDA receptor within a glutamate spillover model. J Neural Eng 4(4):380-389, 2007.

Mitchell CS, and Lee RH. Output-based comparison of alternative kinetic schemes for the NMDA receptor within a glutamate spillover model. J Neural Eng 4: 380-389, 2007.

Mitchell CS, and Lee RH. Pathology dynamics predict spinal cord injury therapeutic success. J Neurotrauma 25(12) :1483-1497, 2008.

Proceedings and Abstracts

Comprehensive examination of secondary spinal cord injury and potential single and combinatorial neuroprotective therapeutic strategies (2008). 26th Annual National Neurotrauma Symposium, National Neurotrauma Society, Orlando, FL.

Mitchell CS, Lee RH. A Reconceptualization of the relationship between spike afterhypolarization and firing rate in lumbar motoneurons of the adult cat (2008). Society for Neuroscience, Washington DC.

Mitchell CS, Lee RH. A Quantitative Assessment of Secondary Injury Dynamics and Potential Multi-faceted Neuroprotective Therapeutics (2008). Society for Neuroscience, Washington DC.

Mitchell CS, Simon CM, Lee RH, LaPlaca ML. A Comprehensive Approach to Understanding SCI (2008). Christopher Reeves Foundation Research Symposium. Atlanta, GA.

Mitchell CS, Lee RH. A Re-examination of the AHP: Is it diffusion limited? Mechanisms of Plasticity and Disease in Motoneurons (2008). Seattle, WA.

Mitchell CS, Lee RH. A Computational Model of Secondary Traumatic Injury (2007). Society for Neuroscience, San Diego, CA. Society for Neuroscience, San Diego, CA.

Mitchell CS, Lee RH. A Comparison of Degenerate NMDA Receptor Models within the Context of a Larger Model (2007). Society for Neuroscience, San Diego, CA. Society for Neuroscience, San Diego, CA.

Mitchell CS, Lee RH. Biological Model Analysis: What does complexity theory have to offer? (2007). Integrative Systems Biology Meeting, Georgia Institute of Technology, Atlanta, GA.

Mitchell CS, Feng SJ, Lee RH. A model of glutamate spillover on the N-methyl-D-aspartate receptors of the cerebellar glomerulus (2006). Society for Neuroscience, Atlanta, GA.

Publications In Preparation

Mitchell CS, and Lee RH. Axonal transport cargo distributions differentiate ALS pathologies.

Mitchell CS, and Lee RH. Cooperativity determines axonal transport type.

Mitchell CS, and Lee RH. Firing properties of in vivo cat spinal cord motoneurons.

Mitchell CS, and Lee RH. Pathology dynamics predict ALS mechanisms.

APPENDIX D

ABSTRACTS AND POSTERS

A Comprehensive Approach to Understanding Spinal Cord Injury

2009 Christopher Reeves Foundation Symposium, Atlanta, GA,

C.S. Mitchell, C.M. Simon, M.C. LaPlaca, R.H. Lee

The Wallace H. Coulter Department of Biomedical Engineering at Georgia Tech and Emory University, Laboratory for Neuroengineering, 313 Ferst Dr., Atlanta, GA

Trauma to the spinal cord launches a complex cascade of events that leads to progressive damage and loss of function. Ultimately, spinal cord injury (SCI) outcome depends on the extent of secondary damage and the interactions among them, yet these mechanisms remain poorly understood. Several experimental studies have targeted certain hypothesized components of secondary damage such as excitotoxicity, energetics, free radical damage, inflammatory responses, and necroptosis. However, the combined effects of these factors as well as their interactions have yet to be examined in a holistic fashion. We have developed a comprehensive mathematical model of secondary injury based on the results of over 300 published studies, permitting quantitative examination of the interactions among the key factors. Results of the model indicate that relatively few factors are likely to be highly influential in early treatment. One of the factors having a significant impact on outcome is plasma membrane damage in the acute post-SCI period. In parallel, we examined membrane damage as a function of time in a rodent model of SCI. Fluorescent cell-impermeant dyes were injected into the cerebrospinal fluid of adult male rats prior to contusion injury, and the anatomical

location of cell bodies and axons taking up the dye SCI was quantified acutely (10 min), subacutely (24 hrs), and at chronically (3 days and 5 weeks). Asymmetrical rostral-caudal patterns of cell body permeability were observed at 10 minutes, but cell body damage was not extensive at other time points. Axonal uptake, however, was seen at all time points in a symmetric distribution. These data indicate that early non-specific damage is a key component of SCI pathology and persists in axons, possibly contributing to poor outcome and providing targets for developing novel treatment strategies. This two-pronged–modeling and experimental–approach will permit us to delve into the mechanisms and interactions underlying key factors such as membrane damage and then to use the experimental results to iteratively improve the accuracy and predictive power of the model. Ultimately, we expect this method to be a robust tool for designing pre-clinical studies to test effectiveness of mechanistically-driven treatment(s). Work supported by NIH NS045199 and NSF EEC-9731643.

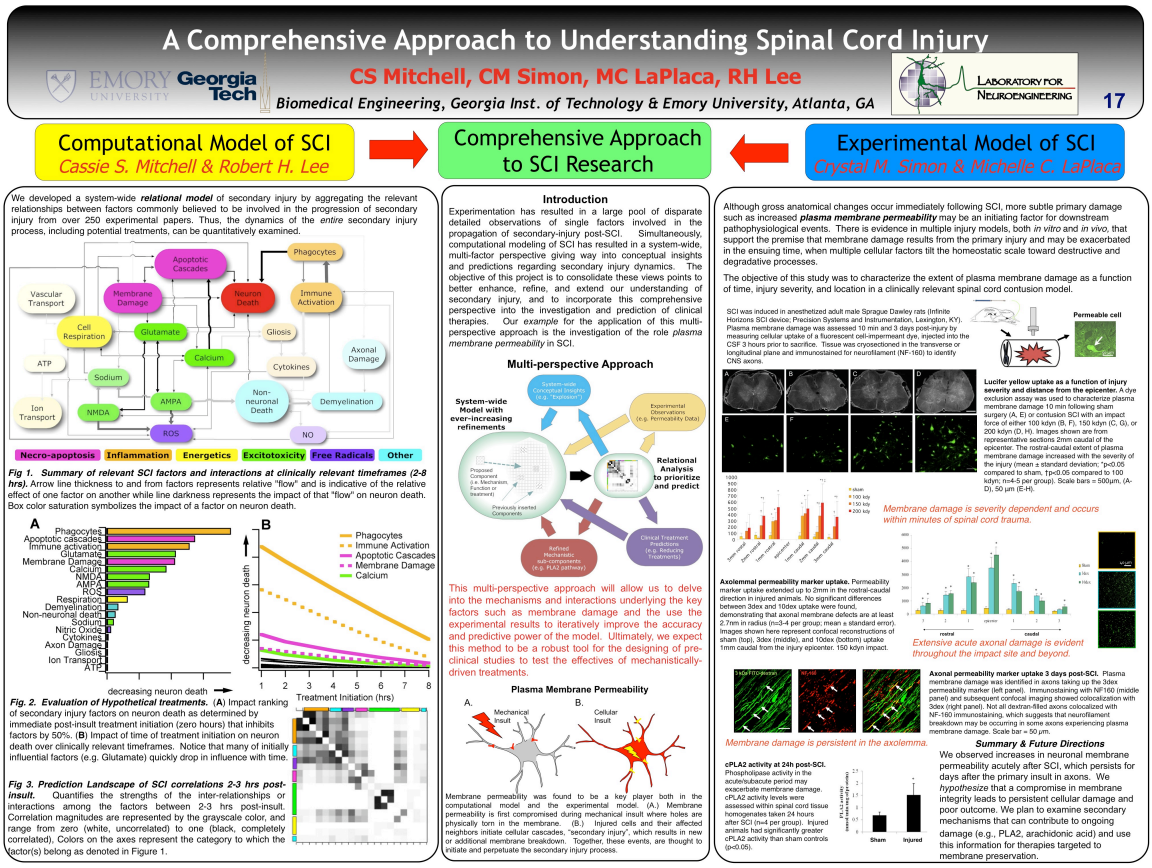

Figure D.1. A Comprehensive Approach to Understanding Spinal Cord Injury

Comprehensive examination of secondary spinal cord injury and potential single and combinatorial neuroprotective therapeutic strategies

2008 26th Annual National Neurotrauma Symposium, Orlando, FL.

C.S. Mitchell and R.H. Lee

The Wallace H. Coulter Department of Biomedical Engineering at Georgia Tech and Emory University, Laboratory for Neuroengineering, 313 Ferst Dr., Atlanta, GA

Secondary injury, a complex cascade of cellular events, which results in post-insult lesion expansion, is a major source of neuron death following spinal cord injury (SCI). Unfortunately, despite decades of research and several promising experimental findings, highly effective and repeatable clinical treatments have yet to emerge. Experimental investigation of individual secondary injury factors (such as excitotoxic, necrotic-apoptotic, free radical, inflammatory, and energetic factors) has resulted in a substantial, yet disparate pool of single factor data, making the interpretation of multi-factor effects and interactions difficult. We hypothesize that a lack of understanding of how the secondary injury process functions as a whole results in the disconnect that is seen between primary research and clinical outcomes. We developed methodology that greatly facilitates pooling disparate data, enabling a novel, comprehensive view into the pathology of secondary injury across time points, preparations, and protocols. Using this methodology, we developed a system-wide "relational model" of secondary injury by aggregating the relevant relationships between factors commonly believed to be involved in the progression of secondary injury from over 250 experimental papers. This relational

model represents a comprehensive view of the progression of neuron death following mechanical insult by directly incorporating the literature-derived experimental relationships (for example, the relationship between free radicals and membrane damage) into a network of time-varying factors. Using this model, we quantitatively examined the entire secondary injury process, including the interactions and dynamics of ~20 of the most commonly studied secondary injury factors and the effects of ~20,000 different single and combination therapies in reducing secondary injury related neuron death. Our results, which illustrate the impact-ranking of individual factors on neuron death over time, reveal that relatively few factors are highly influential at clinically relevant timeframes (4-8 hours post-insult). Furthermore, our results suggest the importance of process dynamics in determining the success of specific therapeutic intervention types. We expect further model refinement to lead to a high-throughput screening process where potential experimental mechanisms and clinical therapeutics can be pre-tested and prioritized.

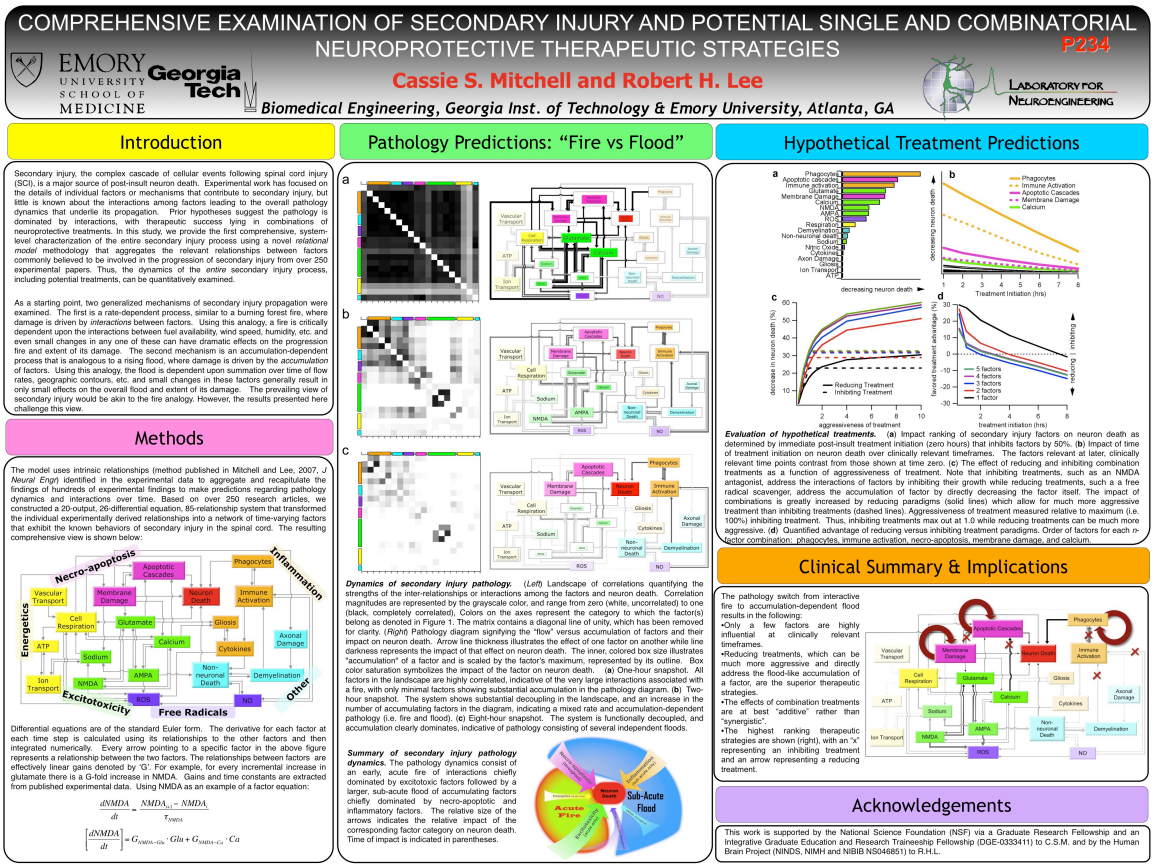

Figure D.2. Comprehensive examination of secondary spinal cord injury and potential single and combinatorial neuroprotective therapeutic strategies

A Re-examination of the AHP: Is it diffusion limited?

2008 Mechanisms of Plasticity and Disease in Motoneurons, Seattle, WA.

C.S. Mitchell and R.H. Lee

The Wallace H. Coulter Department of Biomedical Engineering at Georgia Tech and Emory University, Laboratory for Neuroengineering, 313 Ferst Dr., Atlanta, GA

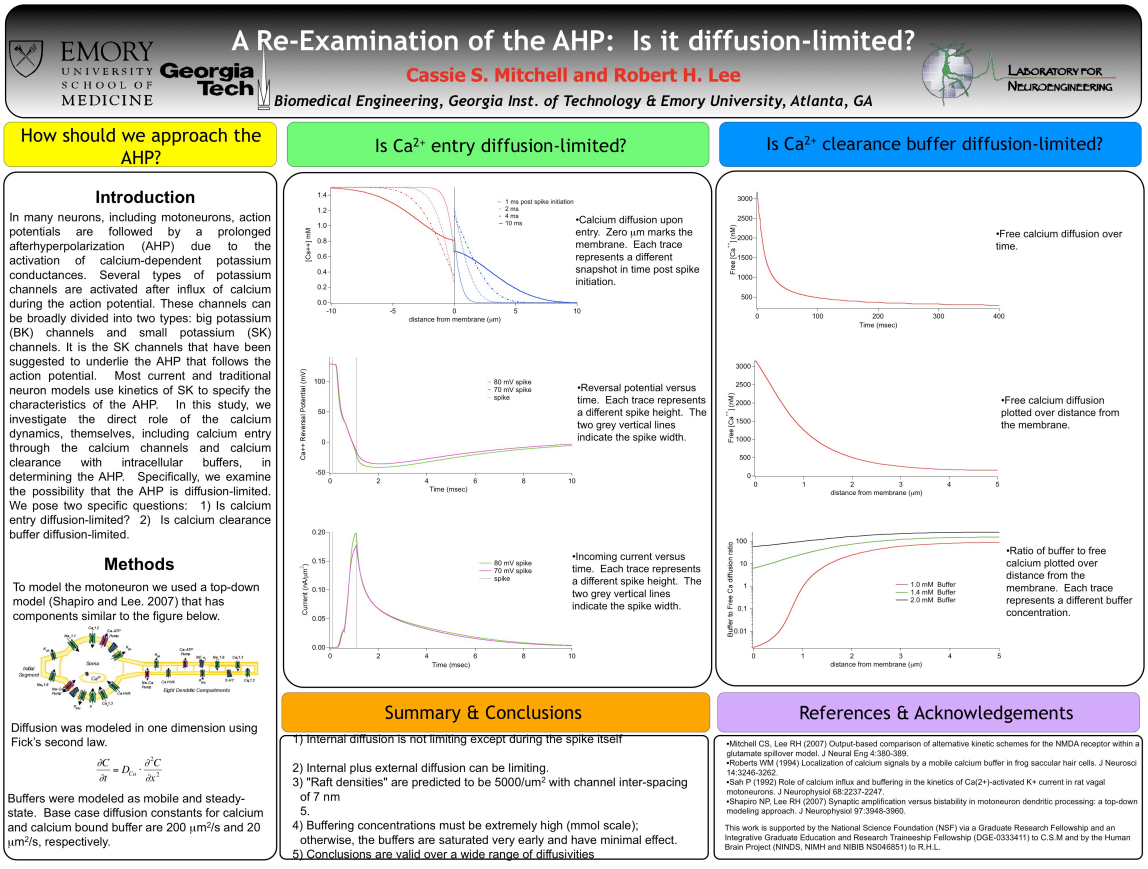

Figure D.3. A Re-examination of the AHP: Is it diffusion limited?

A quantitative assessment of secondary injury dynamics and potential multi-faceted neuroprotective therapeutics

2008 Society for Neuroscience, Washington DC

C.S. Mitchell and R.H. Lee

The Wallace H. Coulter Department of Biomedical Engineering at Georgia Tech and Emory University, Laboratory for Neuroengineering

Secondary injury, a complex cascade of cellular events, which results in post-insult lesion expansion, is a major source of neuron death following spinal cord injury (SCI). Experimentation has resulted in the detailed investigation of multiple individual secondary injury factors (such as excitotoxic, necrotic-apoptotic, free radical, inflammatory, and energetic factors), but little is known about their interactions and the overall process dynamics of secondary injury, which result in its propagation. Using our relational modeling and analysis techniques, we were able aggregate these detailed pockets of experimental findings into a relational model that recapitulates the findings of ~250 experimental papers, allowing the first comprehensive view into the secondary injury dynamics, which result in the progression of neuron death following mechanical insult. Using this model, we quantitatively examined the entire secondary injury process, including the interactions and temporal dynamics of multiple secondary injury factors and the effects of thousands of various single and combination neuroprotective therapies. Our results reveal the large contribution of overall process dynamics and the critical importance of treatment window (i.e. time of treatment initiation) in determining the success of various single and multi-faceted treatments and intervention types. Our preliminary analysis of the overall process dynamics provides new experimental and

clinical research directions to pursue and novel conceptualizations for potential therapeutic strategies.

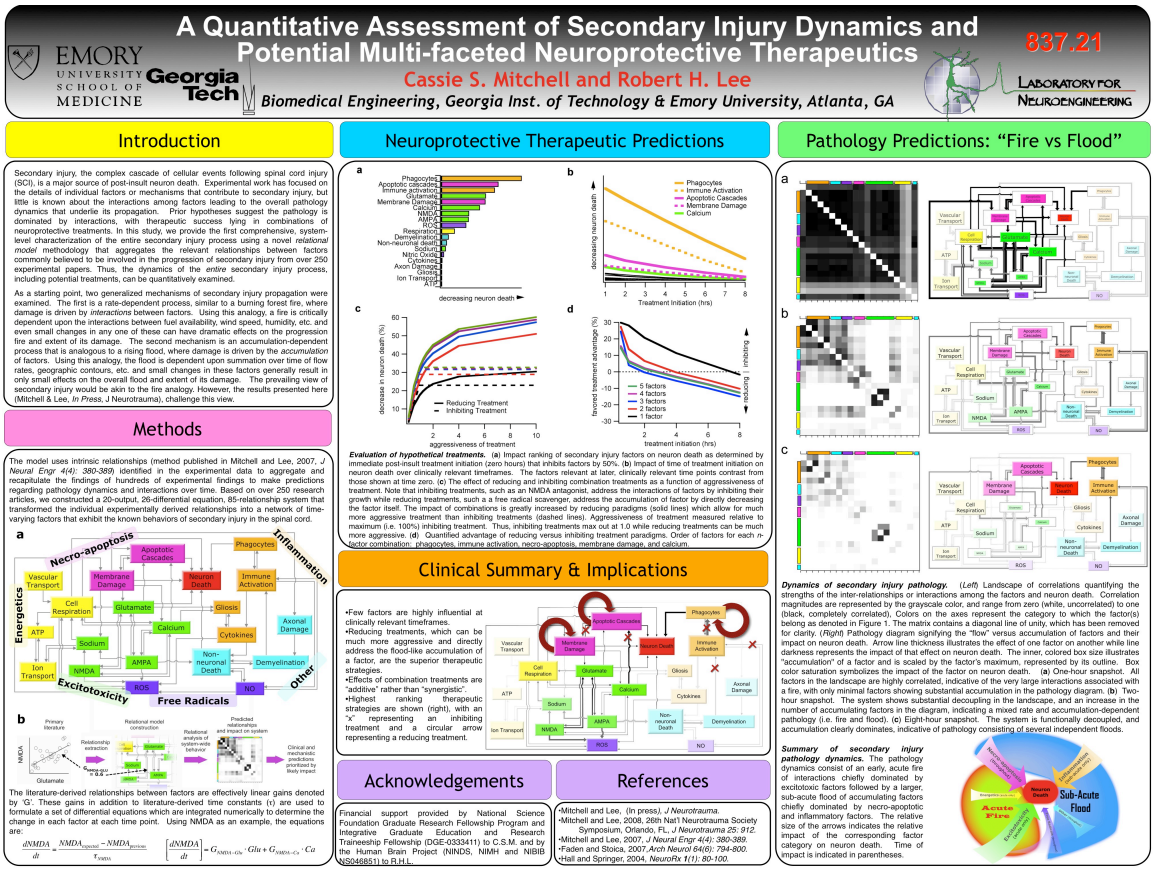

Figure D.4. A quantitative assessment of secondary injury dynamics and potential multi-faceted neuroprotective therapeutics

A Reconceptualization of the relationship between spike afterhypolarization and firing rate in lumbar motoneurons of the adult cat

2008 Society for Neuroscience, Washington DC

C.S. Mitchell and R.H. Lee

The Wallace H. Coulter Department of Biomedical Engineering at Georgia Tech and Emory University, Laboratory for Neuroengineering, 313 Ferst Dr., Atlanta, GA

While it is known that the afterhyperpolarization (AHP) following an action potential is generated by the calcium-dependent potassium channel SK, the relationship between dynamics of the action potential and the dynamics of the AHP remain unknown. The traditional view is that AHP's summate and thereby slow firing. However, recent evidence from the Bennett lab, suggests that two populations of SK are present in motoneurons and that they are associated with differing calcium channels (N and L respectively). What effect do these two populations have on the relationship between action potentials/firing rate and the AHP itself? We use relational analysis (Mitchell and Lee, 2007) to examine the effect of alternative conceptualizations of how calcium and SK combine to form the AHP and what impact those conceptualizations have on other motoneuron properties. Significantly, we conclude that the standard conceptualization of "AHP summation" results in a negative correlation between persistent sodium currents involved in spike initiation and the primary range slope of the injected current-firing rate relationship (i.e. F-I gain). However, experimental data suggests just the opposite. We explore several alternative conceptualizations of the link between the action potential waveform, calcium dynamics and SK channel dynamics resulting in an AHP.

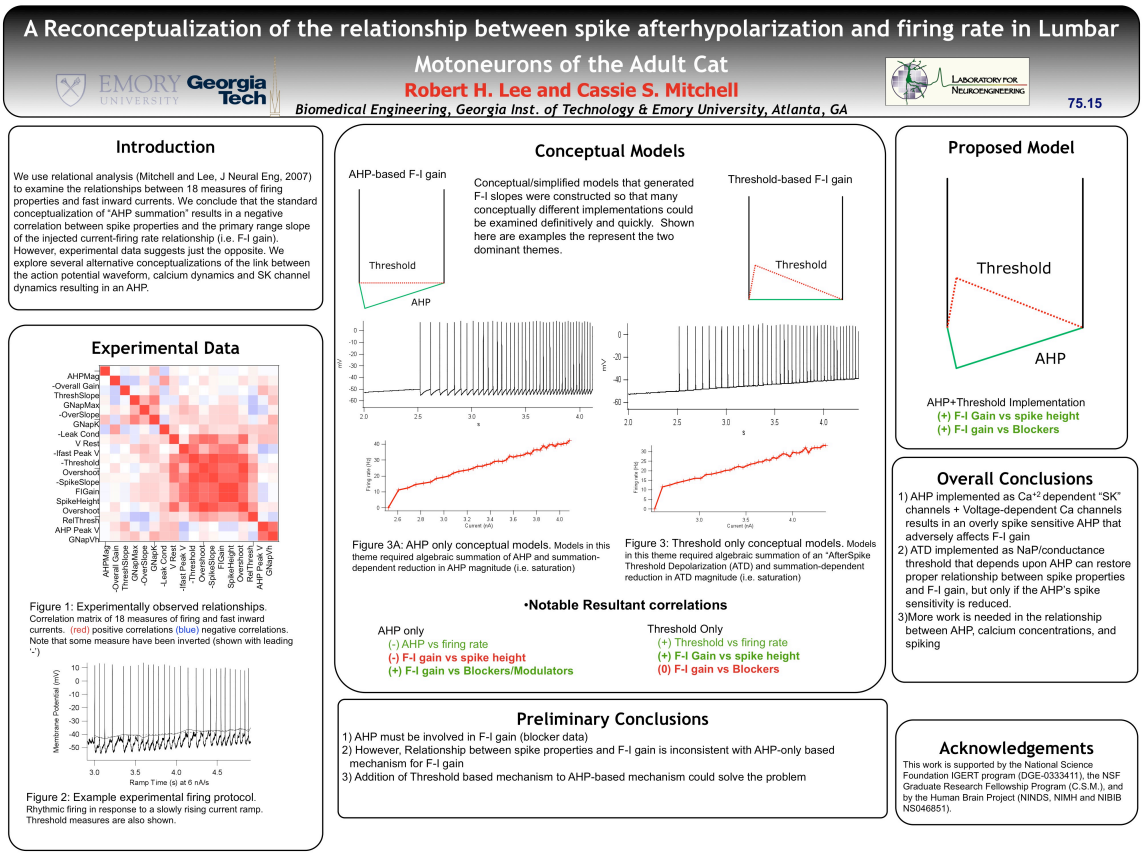

Figure D.5. A Reconceptualization of the relationship between spike afterhypolarization and firing rate in lumbar motoneurons of the adult cat

Comparison of degenerate NMDA-receptor models in the context of a larger model.

2007 Society for Neuroscience, San Diego, CA.

C.S. Mitchell and R.H. Lee

The Wallace H. Coulter Department of Biomedical Engineering at Georgia Tech and Emory University, Laboratory for Neuroengineering, 313 Ferst Dr., Atlanta, GA

One critical task each neural modeler must face, regardless of the system being studied, is balancing the level of physiological detail represented by the model with the computational load required by the model. The judgment call for "appropriate level of detail" typically centers on the ability of the model to produce desired outputs. This is based on the assumption that output is a good measure of model validity. However, is matching output sufficient to declare that mechanistic differences imparted by differences in level of detail result in models that are the "same" (i.e. "degenerate")? We investigate this question by comparing two different NMDA receptor models within the context of a glutamate spillover model. Using automated parameter searches and sensitivity profiles, we compare the cross-correlation matrices of the output metrics to establish a "model fingerprint". Based on the results presented here, the two receptor models, in the context of the larger spillover model, can result in the same overall model output but yield differing sensitivities and therefore different cross-correlations of outputs. Thus, our results indicate that the model fingerprint can reveal differences in models whose outputs would otherwise be considered the same. This opens the door to higher level analysis as a means to differentiate between model implementations and non-unique parameter sets.

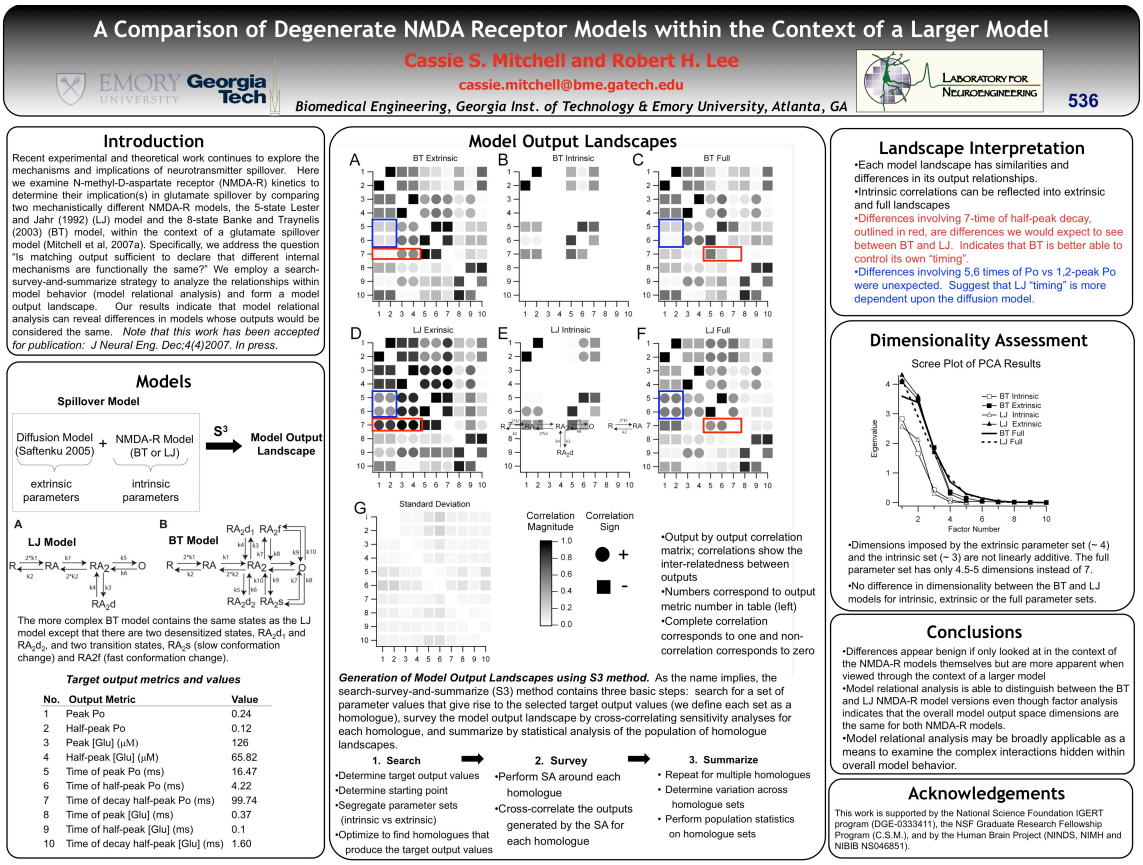

Figure D.6. Comparison of degenerate NMDA-receptor models in the context of a larger model.

A computational model of secondary traumatic injury

2007 Society for Neuroscience, San Diego, CA

C.S. Mitchell and R.H. Lee

The Wallace H. Coulter Department of Biomedical Engineering at Georgia Tech and Emory University, Laboratory for Neuroengineering, 313 Ferst Dr., Atlanta, GA

The outcome of traumatic brain or spinal cord injury depends on the extent of secondary damage, often referred to as "secondary injury", produced by a series of cellular and molecular events, which are initiated after the primary trauma. To date, these secondary injury mechanisms and particularly their interactions remain poorly understood. Several experimental studies have targeted certain hypothesized components of secondary damage such as excitotoxicity, free radical damage, decreased metabolism from mitochondrial damage, and inflammatory responses, to name a few. However, no study has been able to analyze these hypothesized cascades of events as a whole and determine each mechanism's contribution individually on the end result of secondary injury, cell death. We implement a computational model of secondary injury, which includes the aforementioned players and the interactions which result from their feedback. Preliminary results suggest that the hypothesized mechanisms have relatively similar sensitivities. Thus, the secondary injury process is not completely driven by any one particular mechanism but rather by the combined effects of them all. The significance of the model itself is that it allows various mechanisms to be tested theoretically and based on the results, can suggest future experimental avenues worthy of further investigation.

This worked is supported by the National Science Foundation IGERT #DGE-0333411.

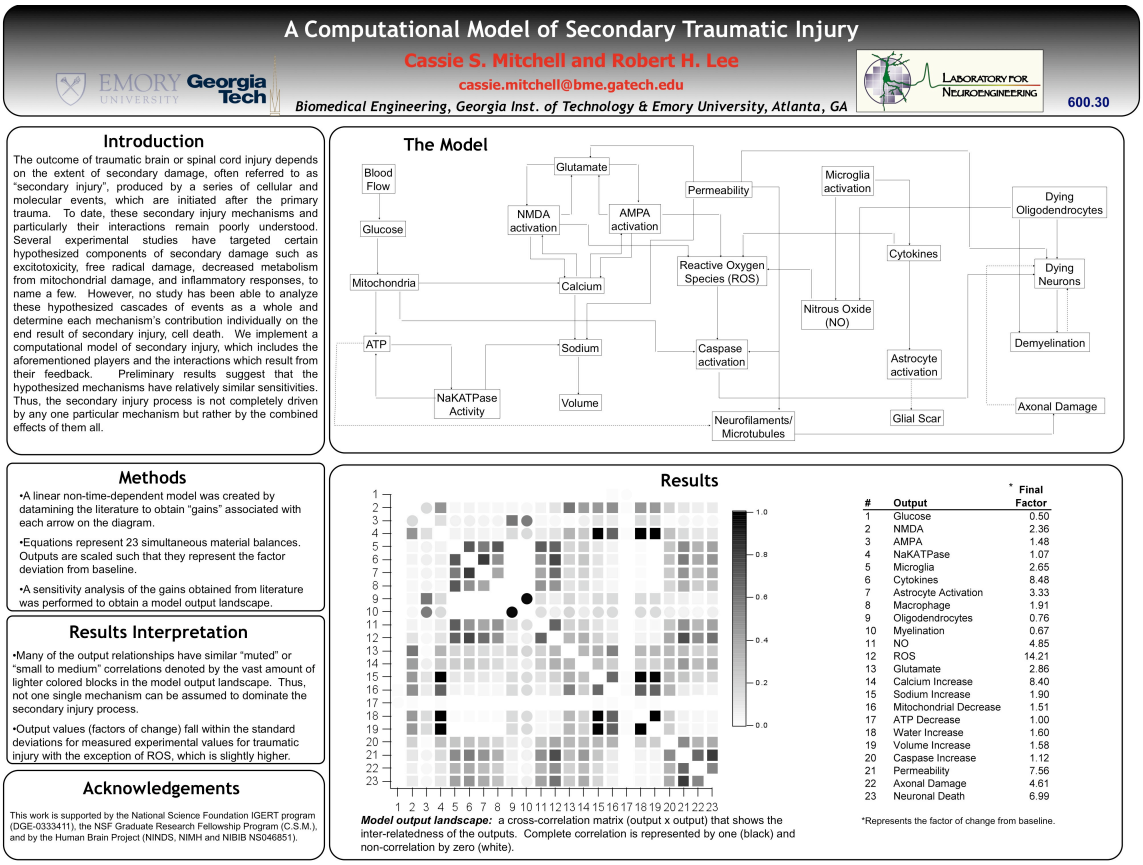

Figure D.7. A computational model of secondary traumatic injury

Biological Model Analysis: What Does Complexity Theory have to Offer?

2007 Integrative Systems Biology Meeting, Georgia Institute of Technology, Atlanta, GA.

C.S. Mitchell and R.H. Lee

The Wallace H. Coulter Department of Biomedical Engineering at Georgia Tech and Emory University, Laboratory for Neuroengineering, 313 Ferst Dr., Atlanta, GA

In the world of biomedical engineering, and especially neural engineering, models can give great insight into very dynamic, complex systems. As the complexity of these models increases, it becomes more to difficult to know how much detail to include, how to determine parameter values, and how to analyze the model results. Recent work has focused on the use of complexity to help analyze neurons and neural networks with a particular focus on degeneracy as it relates to parameter non-uniqueness. This work uses two very different models, a model of glutamate spillover model at the cerebellar glomerulus and a model of axonal transport via molecular motors, to 1.) determine if parameter non-uniqueness, as seen in neuron models, is ubiquitous among different model types and to 2.) determine if a combination of standard methods including parameter searches, sensitivity analysis, factor analysis, and other complexity methods can be used to characterize and analyze model mechanisms, parameters, and outputs.

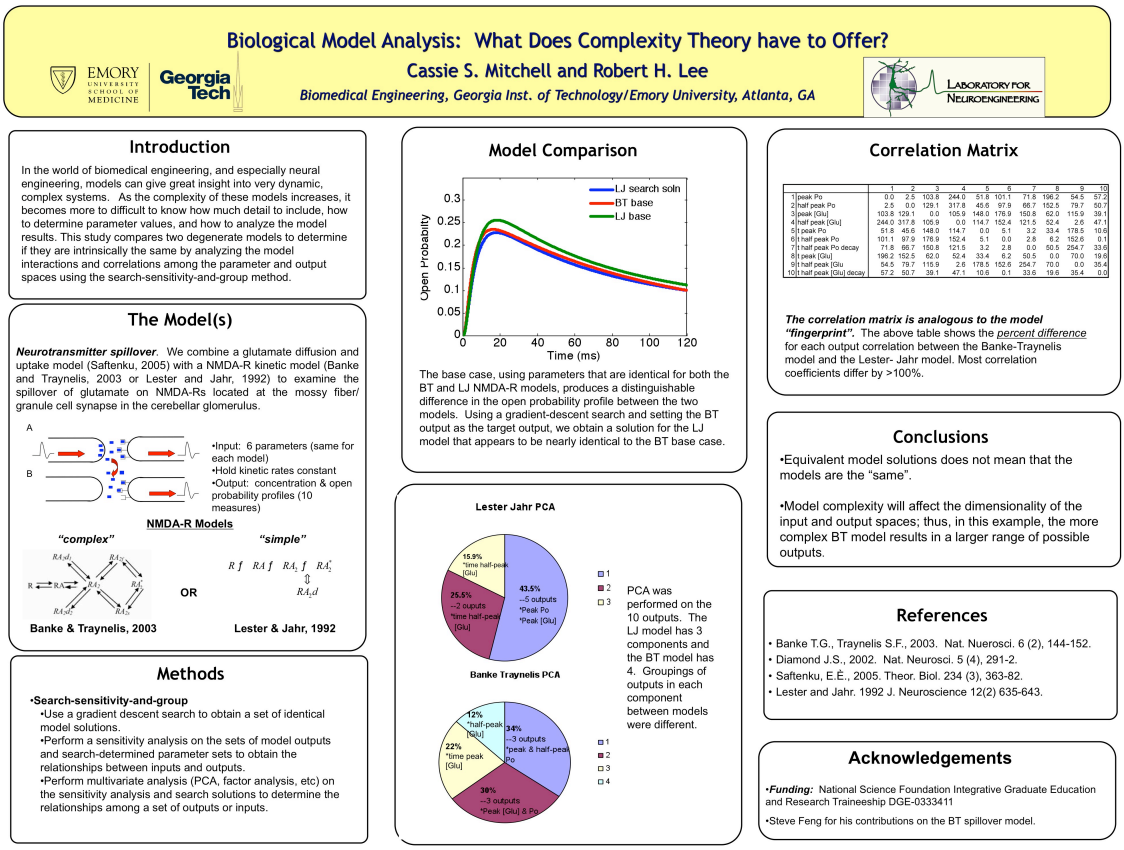

		1	2	3	4	5	6	7	8	9	10
1	peak Po	0.0	2.5	103.8	244.0	51.8	101.1	71.8	196.2	54.5	57.2
2	half peak Po	2.5	0.0	129.1	317.8	45.6	97.9	66.7	152.5	79.7	50.7
3	peak [Glu]	103.8	129.1	0.0	105.9	148.0	176.9	150.8	62.0	115.9	39.1
4	half peak [Glu]	244.0	317.8	105.9	0.0	114.7	152.4	121.5	52.4	2.6	47.1
5	t peak Po	51.8	45.6	148.0	114.7	0.0	5.1	3.2	33.4	178.5	10.6
6	t half peak Po	101.1	97.9	176.9	152.4	5.1	0.0	2.8	6.2	152.6	0.1
7	t half peak Po decay	71.8	66.7	150.8	121.5	3.2	2.8	0.0	50.5	254.7	33.6
8	t peak [Glu]	196.2	152.5	62.0	52.4	33.4	6.2	50.5	0.0	70.0	19.6
9	t half peak [Glu	54.5	79.7	115.9	2.6	178.5	152.6	254.7	70.0	0.0	35.4
10	t half peak [Glu] decay	57.2	50.7	39.1	47.1	10.6	0.1	33.6	19.6	35.4	0.0

Figure D.8. Biological Model Analysis: What Does Complexity Theory have to Offer?

A model of glutamate spillover on the N-methyl-D-aspartate receptors of the cerebellar glomerulus

2006 Society for Neuroscience, Atlanta, GA

C.S. Mitchell, S.S. Feng, and R.H. Lee

The Wallace H. Coulter Department of Biomedical Engineering at Georgia Tech and Emory University, Laboratory for Neuroengineering, 313 Ferst Dr., Atlanta, GA

Neurotransmitter spillover, defined as the escape of neurotransmitter from the synapse into which it is released to neighboring, quiescent synapses thereby activating receptors, remains a topic of experimental and theoretical debate. Spillover, if significantly present, would shatter the conventional wisdom behind independent synaptic transmission and plasticity. Given the difficulty of assessing spillover experimentally, modeling remains the most feasible method of investigation. The overall approach of this project is a broad-based assessment of all the factors governing spillover. We present a representative model of spillover using the mossy fiber of the cerebellar glomerulus by combining recent models of glutamate diffusion and N-methyl-D-aspartate receptor (NMDA-R) binding to determine the open probabilities of NMDA-Rs over time at a neighbor synapse. Simulation results from a baseline set of physiologically realistic parameters show that glutamate spillover onto a single neighbor synapse, created by glutamate that diffuses from a point source into a restricted fractional 2D-3D space and the glutamate concentration created by neighboring glutamate release sites, is sufficient to elicit an NMDA-R peak open probability of 0.23. However, simulations of limiting cases with parameter sets outside what is thought to be the physiological range did

produce peak open probabilities as low as 0.03 and as high as 0.28. The parameters that impact the degree of spillover the most when simulated with values inside the physiological range include the effective diffusion coefficient of glutamate in the extracellular space, the number of glutamate release sites in the cerebellar glomerulus, and the initial concentration of glutamate released. We conclude that glutamate spillover cannot be simply dismissed or assumed to be insignificant, and that further exploration of this issue is necessary.

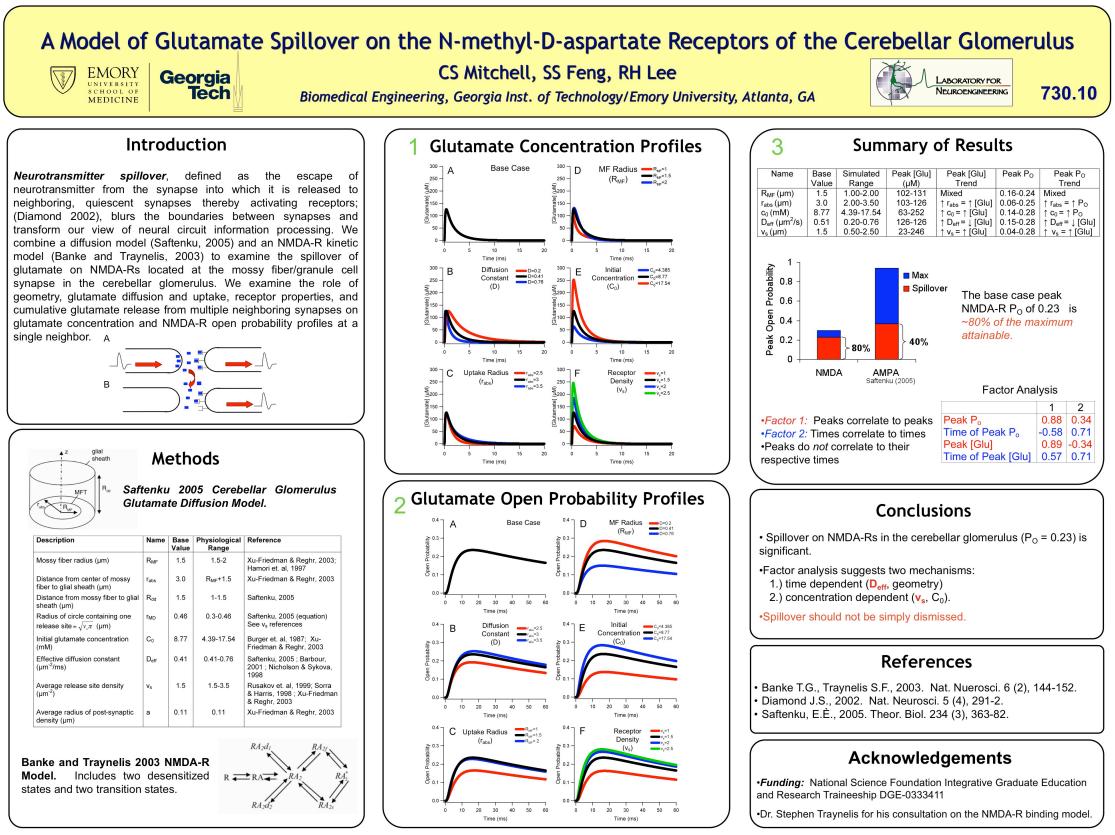

Figure D.9. A model of glutamate spillover on the N-methyl-D-aspartate receptors of the cerebellar glomerulus

REFERENCES

Achard P, and De Schutter E. Complex parameter landscape for a complex neuron model. PLoS Comput Biol 2: e94, 2006.

Agrawal SK, and Fehlings MG. Mechanisms of secondary injury to spinal cord axons in vitro: Role of Na+,Na+-K+-ATPase, the N+-H+ exchanger, and the Na+-Ca2+ exchanger. Journal of Neuroscience 16: 545-552, 1996.

Agrawal SK, and Fehlings MG. Role of NMDA and non-NMDA ionotropic glutamate receptors in traumatic spinal cord axonal injury. J Neurosci 17: 1055-1063, 1997.

Ahmed SM, Weber JT, Liang S, Willoughby KA, Sitterding HA, Rzigalinski BA, and Ellis EF. NMDA receptor activation contributes to a portion of the decreased mitochondrial membrane potential and elevated intracellular free calcium in strain-injured neurons. J Neurotrauma 19: 1619-1629, 2002.

Alano CC, Beutner G, Dirksen RT, Gross RA, and Sheu SS. Mitochondrial permeability transition and calcium dynamics in striatal neurons upon intense NMDA receptor activation. J Neurochem 80: 531-538, 2002.

Anderson DK, Means ED, Waters TR, and Spears CJ. Spinal cord energy metabolism following compression trauma to the feline spinal cord. J Neurosurg 53: 375-380, 1980.

Anderson NL, and Anderson NG. Proteome and proteomics: new technologies, new concepts, and new words. Electrophoresis 19: 1853-1861, 1998.

Ankarcrona M, Dypbukt JM, Bonfoco E, Zhivotovsky B, Orrenius S, Lipton SA, and Nicotera P. Glutamate-Induced Neuronal Death - a Succession of Necrosis or Apoptosis Depending on Mitochondrial-Function. Neuron 15: 961-973, 1995.

Arnold RJ, and Reilly JP. Fingerprint matching of E. coli strains with matrix-assisted laser desorption/ionization time-of-flight mass spectrometry of whole cells using a modified correlation approach. Rapid Commun Mass Spectrom 12: 630-636, 1998.

Ashkin A, Schutze K, Dziedzic JM, Euteneuer U, and Schliwa M. Force generation of organelle transport measured in vivo by an infrared laser trap. Nature 348: 346-348, 1990.

Ates O, Cayli SR, Gurses I, Turkoz Y, Tarim O, Cakir CO, and Kocak A. Comparative neuroprotective effect of sodium channel blockers after experimental spinal cord injury. Journal of Clinical Neuroscience 14: 658-665, 2007.

Azbill RD, Mu X, Bruce-Keller AJ, Mattson MP, and Springer JE. Impaired mitochondrial function, oxidative stress and altered antioxidant enzyme activities following traumatic spinal cord injury. Brain Res 765: 283-290, 1997.

Bak P. How nature works: The science of self-organized criticality. New York: Copernicus, 1996.

Baldi P, Vanier MC, and Bower JM. On the use of Bayesian methods for evaluating compartmental neural models. Journal of Computational Neuroscience 5: 285-314, 1998.

Banke TG, and Traynelis SF. Activation of NR1/NR2B NMDA receptors. Nature neuroscience 6: 144-152, 2003.

Banks J, Carson J, Nelson B, and Nicol D. Discrete-event system simulation Pearson, 2005.

Barbour B. An evaluation of synapse independence. J Neurosci 21: 7969-7984, 2001.

Bartholdi D, and Schwab ME. Expression of pro-inflammatory cytokine and chemokine mRNA upon experimental spinal cord injury in mouse: an in situ hybridization study. Eur J Neurosci 9: 1422-1438, 1997.

Barut S, Unlu YA, Karaoglan A, Tuncdemir M, Dagistanli FK, Ozturk M, and Colak A. The neuroprotective effects of z-DEVD.fmk, a caspase-3 inhibitor, on traumatic spinal cord injury in rats. Surgical neurology 64: 213-220; discussion 220, 2005.

Beattie MS. Inflammation and apoptosis: linked therapeutic targets in spinal cord injury. Trends in molecular medicine 10: 580-583, 2004.

Beers M. The Merck Manual of Medical Information. Simon & Schuster, Inc., 2004.

Berg H. A Random Walk in Biology. Princeton, 1993.

Blight AR. Delayed demyelination and macrophage invasion: a candidate for secondary cell damage in spinal cord injury. Cent Nerv Syst Trauma 2: 299-315, 1985.

Blight AR, and Tuszynski MH. Clinical trials in spinal cord injury. J Neurotrauma 23: 586-593, 2006.

Bower J, and Beeman D. The book of GENESIS: exploring realistic neural models with the GEneral NEural SImulation System. New York, NY: TELOS, 1998.

Briese M, Esmaeili B, and Sattelle DB. Is spinal muscular atrophy the result of defects in motor neuron processes? Bioessays 27: 946-957, 2005.

Brown A. Contiguous phosphorylated and non-phosphorylated domains along axonal neurofilaments. J Cell Sci 111 (Pt 4): 455-467, 1998.

Brown A. Slow axonal transport: stop and go traffic in the axon. Nat Rev Mol Cell Biol 1: 153-156, 2000.

Brown A, Wang L, and Jung P. Stochastic simulation of neurofilament transport in axons: the "stop-and-go" hypothesis. Molecular biology of the cell 16: 4243-4255, 2005.

Brownlees J, Ackerley S, Grierson AJ, Jacobsen NJ, Shea K, Anderton BH, Leigh PN, Shaw CE, and Miller CC. Charcot-Marie-Tooth disease neurofilament mutations disrupt neurofilament assembly and axonal transport. Hum Mol Genet 11: 2837-2844, 2002.

Bruijn, L. I., T. M. Miller, et al. Unraveling the mechanisms involved in motor neuron degeneration in ALS. Annu Rev Neurosci 27: 723-49, 2004.

Brunel N, and van Rossum MC. Lapicque's 1907 paper: from frogs to integrate-and-fire. Biol Cybern 97: 337-339, 2007.

Buchanan M. Ubiquity: Why catastrophes hapen. New York: Three River Press, 2000.

Cangelosi R, and Goriely A. Component retention in principal component analysis with application to cDNA microarray data. Biology direct 2: 2, 2007.

Carlson SL, Parrish ME, Springer JE, Doty K, and Dossett L. Acute inflammatory response in spinal cord following impact injury. Experimental Neurology 151: 77-88, 1998.

Carnevale N, and Hines M. The Neuron book. Cambridge, UK: Cambridge University Press, 2005.

Carriedo SG, Yin HZ, Sensi SL, and Weiss JH. Rapid Ca2+ entry through Ca2+-permeable AMPA/kainate channels triggers marked intracellular Ca2+ rises and consequent oxygen radical production. Journal of Neuroscience 18: 7727-7738, 1998.

Cathala L, Brickley S, Cull-Candy S, and Farrant M. Maturation of EPSCs and intrinsic membrane properties enhances precision at a cerebellar synapse. J Neurosci 23: 6074-6085, 2003.

Choo AM, Liu J, Lam CK, Dvorak M, Tetzlaff W, and Oxland TR. Contusion, dislocation, and distraction: primary hemorrhage and membrane permeability in distinct mechanisms of spinal cord injury. J Neurosurg Spine 6: 255-266, 2007.

Churchwell KB, Wright SH, Emma F, Rosenberg PA, and Strange K. NMDA receptor activation inhibits neuronal volume regulation after swelling induced by veratridine-stimulated Na+ influx in rat cortical cultures. J Neurosci 16: 7447-7457, 1996.

Cilliers P. Complexity and postermodernism: Understanding complex systems. London: Routledge, 1998.

Cluskey S, and Ramsden DB. Mechanisms of neurodegeneration in amyotrophic lateral sclerosis. Mol Pathol 54: 386-392, 2001.

Collins FS, Patrinos A, Jordan E, Chakravarti A, Gesteland R, and Walters L. New goals for the U.S. Human Genome Project: 1998-2003. Science 282: 682-689, 1998.

Coppin CM, Finer JT, Spudich JA, and Vale RD. Measurement of the isometric force exerted by a single kinesin molecule. Biophys J 68: 242S-244S, 1995.

Coveney PV, and Fowler PW. Modelling biological complexity: a physical scientist's perspective. Journal of the Royal Society, Interface / the Royal Society 2: 267-280, 2005.

Craciun G, Brown A, and Friedman A. A dynamical system model of neurofilament transport in axons. J Theor Biol 237: 316-322, 2005.

Crowe MJ, Bresnahan JC, Shuman SL, Masters JN, and Beattie MS. Apoptosis and delayed degeneration after spinal cord injury in rats and monkeys. Nat Med 3: 73-76, 1997.

Csete M, and Doyle J. Bow ties, metabolism and disease. Trends in Biotechnology 22: 446-450, 2004.

Csete ME, and Doyle JC. Reverse engineering of biological complexity. Science 295: 1664-1669, 2002.

Cullen DK, and LaPlaca MC. The Effects of Shear vs. Compressive Loading in 3-D Neuronal-Astrocytic Co-Cultures. In: Neurotrauma. St. Louis, MO: 2006a.

Cullen DK, and LaPlaca MC. Neuronal response to high rate shear deformation depends on heterogeneity of the local strain field. J Neurotrauma 23: 1304-1319, 2006b.

Dayan P, and Abbott L. Theoretical neuroscience. Cambridge, MA: MIT Press, 2001.

Diamond JS. A broad view of glutamate spillover. Nature neuroscience 5: 291-292, 2002.

Diamond JS. Neuronal glutamate transporters limit activation of NMDA receptors by neurotransmitter spillover on CA1 pyramidal cells. J Neurosci 21: 8328-8338, 2001.

DiGregorio DA, Nusser Z, and Silver RA. Spillover of glutamate onto synaptic AMPA receptors enhances fast transmission at a cerebellar synapse. Neuron 35: 521-533, 2002.

DiGregorio DA, Rothman JS, Nielsen TA, and Silver RA. Desensitization properties of AMPA receptors at the cerebellar mossy fiber granule cell synapse. J Neurosci 27: 8344-8357, 2007.

Dusart I, and Schwab ME. Secondary Cell-Death and the Inflammatory Reaction after Dorsal Hemisection of the Rat Spinal-Cord. European Journal of Neuroscience 6: 712-724, 1994.

Efron B. 1977 Rietz Lecture - Bootstrap Methods - Another Look at the Jackknife. Annals of Statistics 7: 1-26, 1979.

Elam JS, Taylor AB, Strange R, Antonyuk S, Doucette PA, Rodriguez JA, Hasnain SS, Hayward LJ, Valentine JS, Yeates TO, and Hart PJ. Amyloid-like filaments and water-filled nanotubes formed by SOD1 mutant proteins linked to familial ALS. Nat Struct Biol 10: 461-467, 2003.

Faden AI, Chan PH, and Longar S. Alterations in lipid metabolism, Na+,K+-ATPase activity, and tissue water content of spinal cord following experimental traumatic injury. J Neurochem 48: 1809-1816, 1987.

Faden AI, and Stoica B. Neuroprotection - Challenges and opportunities. Arch Neurol-Chicago 64: 794-800, 2007.

Farkas O, Lifshitz J, and Povlishock JT. Mechanoporation induced by diffuse traumatic brain injury: An irreversible or reversible response to injury? Journal of Neuroscience 26: 3130-3140, 2006.

Fawcett JW, and Asher RA. The glial scar and central nervous system repair. Brain Research Bulletin 49: 377-391, 1999.

Fehlings MG, and Agrawal S. Role of sodium in the pathophysiology of secondary spinal cord injury. Spine 20: 2187-2191, 1995.

Fleming JC, Norenberg MD, Ramsay DA, Dekaban GA, Marcillo AE, Saenz AD, Pasquale-Styles M, Dietrich WD, and Weaver LC. The cellular inflammatory response in human spinal cords after injury. Brain 129: 3249-3269, 2006.

Freitas R. Biocompatibility. Nanomedicine IIA: 2003.

Fujiki M, Furukawa Y, Kobayashi H, Abe T, Ishii K, Uchida S, and Kamida T. Geranylgeranylacetone limits secondary injury, neuronal death, and progressive necrosis and cavitation after spinal cord injury. Brain Res 1053: 175-184, 2005.

Gallagher R, and Appenzeller T. Beyond Reductionism. Science 284: 1999.

Gao YQ. A simple theoretical model explains dynein's response to load. Biophys J 90: 811-821, 2006.

Gaviria M, Bonny JM, Haton H, Jean B, Teigell M, Renou JP, and Privat A. Time course of acute phase in mouse spinal cord injury monitored by ex vivo quantitative MRI. Neurobiol Dis 22: 694-701, 2006.

Giulian D, and Robertson C. Inhibition of mononuclear phagocytes reduces ischemic injury in the spinal cord. Ann Neurol 27: 33-42, 1990.

Goforth PB, Ellis EF, and Satin LS. Mechanical injury modulates AMPA receptor kinetics via an NMDA receptor-dependent pathway. Journal of Neurotrauma 21: 719-732, 2004.

Goldman MS, Golowasch J, Marder E, and Abbott LF. Global structure, robustness, and modulation of neuronal models. J Neurosci 21: 5229-5238, 2001.

Goldstein LS, and Yang Z. Microtubule-based transport systems in neurons: the roles of kinesins and dyneins. Annu Rev Neurosci 23: 39-71, 2000.

Gomes-Leal W, Corkill DJ, Freire MA, Picanco-Diniz CW, and Perry VH. Astrocytosis, microglia activation, oligodendrocyte degeneration, and pyknosis following acute spinal cord injury. Experimental Neurology 190: 456-467, 2004.

Graas EL, Brown EA, and Lee RH. An FPGA-based approach to high-speed simulation of conductance-based neuron models. Neuroinformatics 2: 417-436, 2004.

Green D, and Kroemer G. The central executioners of apoptosis: caspases or mitochondria? Trends Cell Biol 8: 267-271, 1998.

Haak RA, Kleinhans FW, and Ochs S. The viscosity of mammalian nerve axoplasm measured by electron spin resonance. J Physiol 263: 115-137, 1976.

Hafezparast M, Klocke R, Ruhrberg C, Marquardt A, Ahmad-Annuar A, Bowen S, Lalli G, Witherden AS, Hummerich H, Nicholson S, Morgan PJ, Oozageer R, Priestley JV, Averill S, King VR, Ball S, Peters J, Toda T, Yamamoto A, Hiraoka Y,

Augustin M, Korthaus D, Wattler S, Wabnitz P, Dickneite C, Lampel S, Boehme F, Peraus G, Popp A, Rudelius M, Schlegel J, Fuchs H, Hrabe de Angelis M, Schiavo G, Shima DT, Russ AP, Stumm G, Martin JE, and Fisher EM. Mutations in dynein link motor neuron degeneration to defects in retrograde transport. Science (New York, NY 300: 808-812, 2003.

Hair J, Black W, Babbin B, Anderson R, and Tatham R. Multivariate Data Analysis. Pearson Prentice Hall, 2006.

Hall ED, and Braughler JM. Free radicals in CNS injury. Res Publ Assoc Res Nerv Ment Dis 71: 81-105, 1993.

Hall ED, and Springer JE. Neuroprotection and acute spinal cord injury: a reappraisal. NeuroRx 1: 80-100, 2004.

Hamada Y, Ikata T, Katoh S, Tsuchiya K, Niwa M, Tsutsumishita Y, and Fukuzawa K. Roles of nitric oxide in compression injury of rat spinal cord. Free Radic Biol Med 20: 1-9, 1996.

Hamori J, Jakab RL, and Takacs J. Morphogenetic plasticity of neuronal elements in cerebellar glomeruli during deafferentation-induced synaptic reorganization. Journal of neural transplantation & plasticity 6: 11-20, 1997.

Hartmann A, Hunot S, Michel PP, Muriel MP, Vyas S, Faucheux BA, Mouatt-Prigent A, Turmel H, Srinivasan A, Ruberg M, Evan GI, Agid Y, and Hirsch EC. Caspase-3: A vulnerability factor and final effector in apoptotic death of dopaminergic neurons in Parkinson's disease. Proc Natl Acad Sci U S A 97: 2875-2880, 2000.

Heppner DB, and Plonsey R. Simulation of electrical interaction of cardiac cells. Biophys J 10: 1057-1075, 1970.

Hodgkin AL, and Huxley AF. A quantitative description of membrane current and its application to conduction and excitation in nerve. J Physiol 117: 500-544, 1952.

Hooper SL. Multiple routes to similar network output. Nature neuroscience 7: 1287-1288, 2004.

Hou L, Lanni F, and Luby-Phelps K. Tracer diffusion in F-actin and Ficoll mixtures. Toward a model for cytoplasm. Biophys J 58: 31-43, 1990.

Howard J, Hudspeth AJ, and Vale RD. Movement of microtubules by single kinesin molecules. Nature 342: 154-158, 1989.

Hu S, Peterson PK, and Chao CC. Cytokine-mediated neuronal apoptosis. Neurochem Int 30: 427-431, 1997.

Hurd DD, and Saxton WM. Kinesin mutations cause motor neuron disease phenotypes by disrupting fast axonal transport in Drosophila. Genetics 144: 1075-1085, 1996.

Iwai T, Tanonaka K, Inoue R, Kasahara S, Motegi K, Nagaya S, and Takeo S. Sodium accumulation during ischemia induces mitochondrial damage in perfused rat hearts. Cardiovasc Res 55: 141-149, 2002.

Jankowska E, Lubinska L, and Niemierko S. Translocation of AChE-containing particles in the axoplasm during nerve activity. Comparative biochemistry and physiology 28: 907-913, 1969.

Jiang YM, Yamamoto M, Kobayashi Y, Yoshihara T, Liang YD, Terao S, Takeuchi H, Ishigaki S, Katsuno M, Adachi H, Niwa J, Tanaka F, Doyu M, Yoshida M, Hashizume Y, and Sobue G. Gene expression profile of spinal motor neurons in sporadic amyotrophic lateral sclerosis. Annals of Neurology 57: 236-251, 2005.

Judd K, and Nakamura T. Degeneracy of time series models: the best model is not always the correct model. Chaos (Woodbury, NY 16: 033105, 2006.

Jurkowitzalexander MS, Altschuld RA, Hohl CM, Johnson JD, Mcdonald JS, Simmons TD, and Horrocks LA. Cell Swelling, Blebbing, and Death Are Dependent on Atp Depletion and Independent of Calcium during Chemical Hypoxia in a Glial-Cell Line (Roc-1). Journal of Neurochemistry 59: 344-352, 1992.

Kandel ER, Schwartz JH, and Jessell TM. Principles of Neural Science. McGraw-Hill, 2000.

Keller M, Tharmann R, Dichtl MA, Bausch AR, and Sackmann E. Slow filament dynamics and viscoelasticity in entangled and active actin networks. Philos Transact A Math Phys Eng Sci 361: 699-711; discussion 711-692, 2003.

Kieran D, Hafezparast M, Bohnert S, Dick JR, Martin J, Schiavo G, Fisher EM, and Greensmith L. A mutation in dynein rescues axonal transport defects and extends the life span of ALS mice. J Cell Biol 169: 561-567, 2005.

Klumpp S, and Lipowsky R. Cooperative cargo transport by several molecular motors. Proceedings of the National Academy of Sciences of the United States of America 102: 17284-17289, 2005.

Klusman I, and Schwab ME. Effects of pro-inflammatory cytokines in experimental spinal cord injury. Brain Research 762: 173-184, 1997.

Kong J, and Xu Z. Massive mitochondrial degeneration in motor neurons triggers the onset of amyotrophic lateral sclerosis in mice expressing a mutant SOD1. J Neurosci 18: 3241-3250, 1998.

Krajewski S, Krajewska M, Ellerby LM, Welsh K, Xie Z, Deveraux QL, Salvesen GS, Bredesen DE, Rosenthal RE, Fiskum G, and Reed JC. Release of caspase-9 from mitochondria during neuronal apoptosis and cerebral ischemia. Proc Natl Acad Sci U S A 96: 5752-5757, 1999.

Kuiken TA, Marasco PD, Lock BA, Harden RN, and Dewald JP. Redirection of cutaneous sensation from the hand to the chest skin of human amputees with targeted reinnervation. Proc Natl Acad Sci U S A 104: 20061-20066, 2007.

Kuo CC, and Bean BP. Na+ channels must deactivate to recover from inactivation. Neuron 12: 819-829, 1994.

Kuo JJ, Lee RH, Zhang L, and Heckman CJ. Essential role of the persistent sodium current in spike initiation during slowly rising inputs in mouse spinal neurones. J Physiol 574: 819-834, 2006.

Kural C, Kim H, Syed S, Goshima G, Gelfand VI, and Selvin PR. Kinesin and dynein move a peroxisome in vivo: a tug-of-war or coordinated movement? Science (New York, NY 308: 1469-1472, 2005.

Lapicque L. Recherches quantitatives sur l'excitabilite´'e´lectrique des nerfs traite´e comme une polarisation. J Physiol Pathol Gen 9: 620–635, 1907.

LaPlaca MC, and Thibault LE. Dynamic mechanical deformation of neurons triggers an acute calcium response and cell injury involving the N-methyl-D-aspartate glutamate receptor. Journal of neuroscience research 52: 220-229, 1998.

Lashkari DA, DeRisi JL, McCusker JH, Namath AF, Gentile C, Hwang SY, Brown PO, and Davis RW. Yeast microarrays for genome wide parallel genetic and gene expression analysis. Proceedings of the National Academy of Sciences of the United States of America 94: 13057-13062, 1997.

Lee EK. Large-scale optimization-based classification models in medicine and biology. Annals of biomedical engineering 35: 1095-1109, 2007.

Lemke M, Demediuk P, McIntosh TK, Vink R, and Faden AI. Alterations in tissue Mg++, Na+ and spinal cord edema following impact trauma in rats. Biochem Biophys Res Commun 147: 1170-1175, 1987.

Lester RA, and Jahr CE. NMDA channel behavior depends on agonist affinity. J Neurosci 12: 635-643, 1992.

Li S, and Stys PK. Na+-K+-ATPase inhibition and depolarization induce glutamate release via reverse Na+-dependent transport in spinal cord white matter. Neuroscience 107: 675-683, 2001.

Lin FH, McIntosh AR, Agnew JA, Eden GF, Zeffiro TA, and Belliveau JW. Multivariate analysis of neuronal interactions in the generalized partial least squares framework: simulations and empirical studies. NeuroImage 20: 625-642, 2003.

Liu-Snyder P, Logan MP, Shi R, Smith DT, and Borgens RB. Neuroprotection from secondary injury by polyethylene glycol requires its internalization. The Journal of experimental biology 210: 1455-1462, 2007.

Liu D, Xu GY, Pan E, and McAdoo DJ. Neurotoxicity of glutamate at the concentration released upon spinal cord injury. Neuroscience 93: 1383-1389, 1999.

Logan SM, Partridge JG, Matta JA, Buonanno A, and Vicini S. Long-lasting NMDA receptor-mediated EPSCs in mouse striatal medium spiny neurons. J Neurophysiol 2007.

Lopreore CL, Bartol TM, Coggan JS, Keller DX, Sosinsky GE, Ellisman MH, and Sejnowski TJ. Computational modeling of three-dimensional electrodiffusion in biological systems: application to the node of Ranvier. Biophys J 95: 2624-2635, 2008.

Louis JC, Magal E, Takayama S, and Varon S. Cntf Protection of Oligodendrocytes against Natural and Tumor Necrosis Factor-Induced Death. Science 259: 689-692, 1993.

Lovas G, Szilagyi N, Majtenyi K, Palkovits M, and Komoly S. Axonal changes in chronic demyelinated cervical spinal cord plaques. Brain 123 (Pt 2): 308-317, 2000.

Lu J, Ashwell KW, and Waite P. Advances in secondary spinal cord injury: role of apoptosis. Spine 25: 1859-1866, 2000.

Lupski JR. Axonal Charcot-Marie-Tooth disease and the neurofilament light gene (NF-L). Am J Hum Genet 67: 8-10, 2000.

Ly C, and Tranchina D. Critical analysis of dimension reduction by a moment closure method in a population density approach to neural network modeling. Neural computation 19: 2032-2092, 2007.

Marcaggi P, and Attwell D. Short- and long-term depression of rat cerebellar parallel fibre synaptic transmission mediated by synaptic crosstalk. The Journal of physiology 578: 545-550, 2007.

Marder E, and Prinz AA. Modeling stability in neuron and network function: the role of activity in homeostasis. Bioessays 24: 1145-1154, 2002.

Marszalek JR, Williamson TL, Lee MK, Xu Z, Hoffman PN, Becher MW, Crawford TO, and Cleveland DW. Neurofilament subunit NF-H modulates axonal diameter by selectively slowing neurofilament transport. J Cell Biol 135: 711-724, 1996.

Mattiasson G. Analysis of mitochondrial generation and release of reactive oxygen species. Cytometry Part A 62A: 89-96, 2004.

Meier J, Couillard-Despres S, Jacomy H, Gravel C, and Julien JP. Extra neurofilament NF-L subunits rescue motor neuron disease caused by overexpression of the human NF-H gene in mice. J Neuropathol Exp Neurol 58: 1099-1110, 1999.

Meinhardt H, and Gierer A. Applications of a theory of biological pattern formation based on lateral inhibition. J Cell Sci 15: 321-346, 1974.

Melbin J, and Patterson DF. Computer simulation of cardiac cycle variables and arrhythmias. Comput Biomed Res 3: 182-199, 1970.

Merrill JE, Ignarro LJ, Sherman MP, Melinek J, and Lane TE. Microglial cell cytotoxicity of oligodendrocytes is mediated through nitric oxide. J Immunol 151: 2132-2141, 1993.

Mitchell CS, Feng SS, and Lee RH. An analysis of glutamate spillover on the N-methyl-D-aspartate receptors at the cerebellar glomerulus. J Neural Eng 4: 276-282, 2007.

Mitchell CS, and Lee RH. Output-based comparison of alternative kinetic schemes for the NMDA receptor within a glutamate spillover model. J Neural Eng 4(4):380-389, 2007.

Mitchell CS, and Lee RH. Output-based comparison of alternative kinetic schemes for the NMDA receptor within a glutamate spillover model. J Neural Eng 4: 380-389, 2007.

Mitchell CS, and Lee RH. Pathology dynamics predict spinal cord injury therapeutic success. J Neurotrauma 25(12) :1483-1497, 2008.

Morris RL, and Hollenbeck PJ. The regulation of bidirectional mitochondrial transport is coordinated with axonal outgrowth. J Cell Sci 104 (Pt 3): 917-927, 1993.

Muller MJ, Klumpp S, and Lipowsky R. Tug-of-war as a cooperative mechanism for bidirectional cargo transport by molecular motors. Proceedings of the National Academy of Sciences of the United States of America 105: 4609-4614, 2008.

Naundorf B, Wolf F, and Volgushev M. Unique features of action potential initiation in cortical neurons. Nature 440: 1060-1063, 2006.

Nicholls DG, and Budd SL. Mitochondria and neuronal survival. Physiological Reviews 80: 315-360, 2000.

Nicholson C, and Sykova E. Extracellular space structure revealed by diffusion analysis. Trends in neurosciences 21: 207-215, 1998.

Nielsen TA, DiGregorio DA, and Silver RA. Modulation of glutamate mobility reveals the mechanism underlying slow-rising AMPAR EPSCs and the diffusion coefficient in the synaptic cleft. Neuron 42: 757-771, 2004.

O'Brien MF, Lenke LG, Lou J, Bridwell KH, and Joyce ME. Astrocyte response and transforming growth factor-beta localization in acute spinal cord injury. Spine 19: 2321-2329; discussion 2330, 1994.

Okajima K. Binocular disparity encoding cells generated through an Infomax based learning algorithm. Neural Netw 17: 953-962, 2004.

Overstreet LS, Kinney GA, Liu YB, Billups D, and Slater NT. Glutamate transporters contribute to the time course of synaptic transmission in cerebellar granule cells. J Neurosci 19: 9663-9673, 1999.

Palay SL, and Chan-Palay V. Cortex: Cytology and Organization. New York: Springer-Verlag, 1974.

Pantelidou M, Zographos SE, Lederer CW, Kyriakides T, Pfaffl MW, and Santama N. Differential expression of molecular motors in the motor cortex of sporadic ALS. Neurobiol Dis 26: 577-589, 2007.

Park E, Velumian AA, and Fehlings MG. The role of excitotoxicity in secondary mechanisms of spinal cord injury: A review with an emphasis on the implications for white matter degeneration. Journal of Neurotrauma 21: 754-774, 2004.

Pearl J, and Russell S. Bayesian Networks. In: Handbook of Brain Theory and Neural Networks, edited by Arbib M. Cambrdige, MA: MIT Press, 2003.

Pettus EH, and Povlishock JT. Characterization of a distinct set of intra-axonal ultrastructural changes associated with traumatically induced alteration in axolemmal permeability. Brain Research 722: 1-11, 1996.

Pineau I, and Lacroix S. Proinflammatory cytokine synthesis in the injured mouse spinal cord: multiphasic expression pattern and identification of the cell types involved. J Comp Neurol 500: 267-285, 2007.

PorteraCailliau C, Price DL, and Martin LJ. Non-NMDA and NMDA receptor-mediated excitotoxic neuronal deaths in adult brain are morphologically distinct: Further evidence for an apoptosis-necrosis continuum. Journal of Comparative Neurology 378: 88-104, 1997.

Price CJ, and Friston KJ. Degeneracy and cognitive anatomy. Trends Cogn Sci 6: 416-421, 2002.

Prinz AA, Bucher D, and Marder E. Similar network activity from disparate circuit parameters. Nature neuroscience 7: 1345-1352, 2004.

Rall W. Branching dendritic trees and motoneuron membrane resistivity. Exp Neurol 1: 491-527, 1959.

Rall W. Theoretical significance of dendritic trees for neuronal input-output relations. In: Neuronal theory and modeling, edited by Reiss RStandford: Standford University Press, 1964, p. 73-97.

Rall W. Theory of physiological properties of dendrites. Ann N Y Acad Sci 96: 1071-1092, 1962.

Rao MV, and Nixon RA. Defective neurofilament transport in mouse models of amyotrophic lateral sclerosis: a review. Neurochem Res 28: 1041-1047, 2003.

Reklaitis G, Ravindran A, and Ragsdell K. Engineering Optimization: Methods and Applications. John Wiley & Sons, Inc., 1983.

Ricard J. Emergent collective properties, networks, and information in biology. Elsevier, 2006.

Rieke F, Warland D, Steveninck RdRv, and Bialek W. Spikes. Exploring the neural code. Cambridge, MA: The MIT Press, 1997.

Robinson S. The practice of model development and use. Wiley, 2004.

Rose PK, and Cushing S. Relationship between morphoelectrotonic properties of motoneuron dendrites and their trajectory. J Comp Neurol 473: 562-581, 2004.

Rossi P, Sola E, Taglietti V, Borchardt T, Steigerwald F, Utvik JK, Ottersen OP, Kohr G, and D'Angelo E. NMDA receptor 2 (NR2) C-terminal control of NR open probability regulates synaptic transmission and plasticity at a cerebellar synapse. J Neurosci 22: 9687-9697, 2002.

Rusakov DA, Kullmann DM, and Stewart MG. Hippocampal synapses: do they talk to their neighbours? Trends in neurosciences 22: 382-388, 1999.

Sabry J, O'Connor TP, and Kirschner MW. Axonal transport of tubulin in Ti1 pioneer neurons in situ. Neuron 14: 1247-1256, 1995.

Saftenku EE. Modeling of slow glutamate diffusion and AMPA receptor activation in the cerebellar glomerulus. Journal of theoretical biology 234: 363-382, 2005.

Sargent PB, Saviane C, Nielsen TA, DiGregorio DA, and Silver RA. Rapid vesicular release, quantal variability, and spillover contribute to the precision and reliability of transmission at a glomerular synapse. J Neurosci 25: 8173-8187, 2005.

Savageau MA. Biochemical systems analysis. II. The steady-state solutions for an n-pool system using a power-law approximation. Journal of theoretical biology 25: 370-379, 1969.

Schmitz KA, Holcomb-Wygle DL, Oberski DJ, and Lindemann CB. Measurement of the force produced by an intact bull sperm flagellum in isometric arrest and estimation of the dynein stall force. Biophys J 79: 468-478, 2000.

Schnell L, Fearn S, Klassen H, Schwab ME, and Perry VH. Acute inflammatory responses to mechanical lesions in the CNS: differences between brain and spinal cord. European Journal of Neuroscience 11: 3648-3658, 1999.

Schwab ME, and Bartholdi D. Degeneration and regeneration of axons in the lesioned spinal cord. Physiol Rev 76: 319-370, 1996.

Schwartz G, and Fehlings MG. Evaluation of the neuroprotective effects of sodium channel blockers after spinal cord injury: improved behavioral and

neuroanatomical recovery with riluzole. Journal of Neurosurgery 94: 245-256, 2001.

Sejnowski TJ, Koch C, and Churchland PS. Computational neuroscience. Science 241: 1299-1306, 1988.

Shapiro NP, and Lee RH. Synaptic amplification versus bistability in motoneuron dendritic processing: a top-down modeling approach. Journal of neurophysiology 97: 3948-3960, 2007.

Shea TB, and Flanagan LA. Kinesin, dynein and neurofilament transport. Trends Neurosci 24: 644-648, 2001.

Shi R, and Whitebone J. Conduction deficits and membrane disruption of spinal cord axons as a function of magnitude and rate of strain. Journal of Neurophysiology 95: 3384-3390, 2006.

Sorra KE, and Harris KM. Stability in synapse number and size at 2 hr after long-term potentiation in hippocampal area CA1. J Neurosci 18: 658-671, 1998.

Springer JE, Azbill RD, and Knapp PE. Activation of the caspase-3 apoptotic cascade in traumatic spinal cord injury. Nature Medicine 5: 943-946, 1999.

Stieber, A., J. O. Gonatas, et al. Aggregates of mutant protein appear progressively in dendrites, in periaxonal processes of oligodendrocytes, and in neuronal and astrocytic perikarya of mice expressing the SOD1(G93A) mutation of familial amyotrophic lateral sclerosis. J Neurol Sci 177(2): 114-23, 2000.

Strogatz SH. Exploring complex networks. Nature 410: 268-276, 2001.

Sullivan PG, Krishnamurthy S, Patel SP, Pandya JD, and Rabchevsky AG. Temporal characterization of mitochondrial bioenergetics after spinal cord injury. J Neurotrauma 24: 991-999, 2007.

Sun L, and June Liu S. Activation of extrasynaptic NMDA receptors induces a PKC-dependent switch in AMPA receptor subtypes in mouse cerebellar stellate cells. The Journal of physiology 583: 537-553, 2007.

Szapiro G, and Barbour B. Multiple climbing fibers signal to molecular layer interneurons exclusively via glutamate spillover. Nature neuroscience 10: 735-742, 2007.

Tator CH, and Fehlings MG. Review of clinical trials of neuroprotection in acute spinal cord injury. Neurosurgical focus 6: e8, 1999.

Teodoro ML, Phillips GN, Jr., and Kavraki LE. Understanding protein flexibility through dimensionality reduction. J Comput Biol 10: 617-634, 2003.

Teuchert M, Fischer D, Schwalenstoecker B, Habisch HJ, Bockers TM, and Ludolph AC. A dynein mutation attenuates motor neuron degeneration in SOD1(G93A) mice. Experimental neurology 198: 271-274, 2006.

Tian DS, Xie MJ, Yu ZY, Zhang Q, Wang YH, Chen B, Chen C, and Wang W. Cell cycle inhibition attenuates microglia induced inflammatory response and alleviates neuronal cell death after spinal cord injury in rats. Brain Research 1135: 177-185, 2007.

Tian DS, Yu ZY, Xie MJ, Bu BT, Witte OW, and Wang W. Suppression of astroglial scar formation and enhanced axonal regeneration associated with functional recovery in a spinal cord injury rat model by the cell cycle inhibitor olomoucine. Journal of neuroscience research 84: 1053-1063, 2006.

Tolias CM, and Bullock MR. Critical appraisal of neuroprotection trials in head injury: what have we learned? NeuroRx 1: 71-79, 2004.

Tononi, G., Sporns O, Edelman GM. A measure for brain complexity: relating functional segregation and integration in the nervous system. Proc Natl Acad Sci U S A 91(11): 5033-7, 1994.

Tononi G, Sporns O, and Edelman GM. Measures of degeneracy and redundancy in biological networks. Proc Natl Acad Sci U S A 96: 3257-3262, 1999.

Totoiu MO, and Keirstead HS. Spinal cord injury is accompanied by chronic progressive demyelination. J Comp Neurol 486: 373-383, 2005.

Trivedi N, Jung P, and Brown A. Neurofilaments switch between distinct mobile and stationary states during their transport along axons. J Neurosci 27: 507-516, 2007.

Trommershauser J, Marienhagen J, and Zippelius A. Stochastic model of central synapses: slow diffusion of transmitter interacting with spatially distributed receptors and transporters. Journal of theoretical biology 198: 101-120, 1999.

Truskey G, Yuan F, and Katz D. Transport Phenomena in Biological Systems. Prentice Hall, 2003.

Valentine JS, and Hart PJ. Misfolded CuZnSOD and amyotrophic lateral sclerosis. Proceedings of the National Academy of Sciences of the United States of America 100: 3617-3622, 2003.

Van Geit W, De Schutter E, and Achard P. Automated neuron model optimization techniques: a review. Biol Cybern 99: 241-251, 2008.

Vanier MC, and Bower JM. A comparative survey of automated parameter-search methods for compartmental neural models. Journal of Computational Neuroscience 7: 149-171, 1999.

Vela JM, Yanez A, Gonzalez B, and Castellano B. Time course of proliferation and, elimination of microglia/macrophages in different neurodegenerative conditions. Journal of Neurotrauma 19: 1503-1520, 2002.

Visscher K, Schnitzer MJ, and Block SM. Single kinesin molecules studied with a molecular force clamp. Nature 400: 184-189, 1999.

Volterra A, Trotti D, Tromba C, Floridi S, and Racagni G. Glutamate uptake inhibition by oxygen free radicals in rat cortical astrocytes. J Neurosci 14: 2924-2932, 1994.

von Bertalanffy L. General system theory: foundations, development, applications. New York: George Braziller, 1968.

von Bertalanffy L. An outline of general system theory. British Journal for the Philosophy of Science 1: 139-164, 1950.

Wagner OI, Ascano J, Tokito M, Leterrier JF, Janmey PA, and Holzbaur EL. The interaction of neurofilaments with the microtubule motor cytoplasmic dynein. Molecular biology of the cell 15: 5092-5100, 2004.

Wang L, and Brown A. Rapid intermittent movement of axonal neurofilaments observed by fluorescence photobleaching. Molecular biology of the cell 12: 3257-3267, 2001.

Wang L, Ho CL, Sun D, Liem RK, and Brown A. Rapid movement of axonal neurofilaments interrupted by prolonged pauses. Nat Cell Biol 2: 137-141, 2000.

Warita H, Itoyama Y, and Abe K. Selective impairment of fast anterograde axonal transport in the peripheral nerves of asymptomatic transgenic mice with a G93A mutant SOD1 gene. Brain research 819: 120-131, 1999.

Waxman EA, Baconguis I, Lynch DR, and Robinson MB. N-methyl-D-aspartate receptor-dependent regulation of the glutamate transporter excitatory amino acid carrier 1. The Journal of biological chemistry 282: 17594-17607, 2007.

Weinstein RK, and Lee RH. Architectures for high-performance FPGA implementations of neural models. J Neural Eng 3: 21-34, 2006.

White RJ, and Reynolds IJ. Mitochondrial depolarization in glutamate-stimulated neurons: an early signal specific to excitotoxin exposure. J Neurosci 16: 5688-5697, 1996.

Wingrave JM, Schaecher KE, Sribnick EA, Wilford GG, Ray SK, Hazen-Martin DJ, Hogan EL, and Banik NL. Early induction of secondary injury factors causing activation of calpain and mitochondria-mediated neuronal apoptosis following spinal cord injury in rats. Journal of neuroscience research 73: 95-104, 2003.

Wood JD, Beaujeux TP, and Shaw PJ. Protein aggregation in motor neurone disorders. Neuropathol Appl Neurobiol 29: 529-545, 2003.

Wouters L, Gohlmann HW, Bijnens L, Kass SU, Molenberghs G, and Lewi PJ. Graphical exploration of gene expression data: a comparative study of three multivariate methods. Biometrics 59: 1131-1139, 2003.

Xiong Y, Rabchevsky AG, and Hall ED. Role of peroxynitrite in secondary oxidative damage after spinal cord injury. J Neurochem 100: 639-649, 2007.

Xu-Friedman MA, and Regehr WG. Ultrastructural contributions to desensitization at cerebellar mossy fiber to granule cell synapses. J Neurosci 23: 2182-2192, 2003.

Xu GY, Hughes MG, Ye Z, Hulsebosch CE, and McAdoo DJ. Concentrations of glutamate released following spinal cord injury kill oligodendrocytes in the spinal cord. Exp Neurol 187: 329-336, 2004.

Yanase M, Sakou T, and Fukuda T. Role of N-Methyl-D-Aspartate Receptor in Acute Spinal-Cord Injury. Journal of Neurosurgery 83: 884-888, 1995.

Yoo J, Kambara T, Gonda K, and Higuchi H. Intracellular imaging of targeted proteins labeled with quantum dots. Exp Cell Res 2008.

Yoshioka A, Bacskai B, and Pleasure D. Pathophysiology of oligodendroglial excitotoxicity. Journal of neuroscience research 46: 427-437, 1996.

Zhang B, Tu P, Abtahian F, Trojanowski JQ, and Lee VM. Neurofilaments and orthograde transport are reduced in ventral root axons of transgenic mice that express human SOD1 with a G93A mutation. J Cell Biol 139: 1307-1315, 1997.

Zhang F, Strom AL, Fukada K, Lee S, Hayward LJ, and Zhu H. Interaction between familial amyotrophic lateral sclerosis (ALS)-linked SOD1 mutants and the dynein complex. The Journal of biological chemistry 282: 16691-16699, 2007.

Zhang L, Rzigalinski BA, Ellis EF, and Satin LS. Reduction of voltage-dependent Mg2+ blockade of NMDA current in mechanically injured neurons. Science 274: 1921-1923, 1996.

Zhao W, Xie W, Le W, Beers DR, He Y, Henkel JS, Simpson EP, Yen AA, Xiao Q, and Appel SH. Activated microglia initiate motor neuron injury by a nitric oxide and glutamate-mediated mechanism. J Neuropathol Exp Neurol 63: 964-977, 2004.

VITA

CASSIE S. MITCHELL

Cassie Sue Mitchell was born in 1981 in Muskogee, Oklahoma. She graduated from Warner Public Schools in Warner, Oklahoma, in 1999 as the class valedictorian. She went on to attend Oklahoma State University (OSU) in Stillwater, Oklahoma, obtaining a B.S. in chemical engineering in 2004 with summa cum laude honors. During her four years at OSU, Cassie was a very active scholar and athlete. Her academic and research efforts were recognized as a recipient of the National Barry M. Goldwater Scholarship, selection as a member the 2004 *USA Today* All-USA College Academic First Team, recipient of the 2003 OSU Leadership Legacy Award, and selection as the High Impact Scholar for the Oklahoma Centennial celebration in 2007. Cassie was also a starting member of the Oklahoma State Wheelchair Basketball Team where she received All-American team honors. Cassie entered the joint Biomedical Engineering Ph.D. program at Georgia Institute of Technology and Emory University in Atlanta, Georgia, in the fall of 2004 to pursue a Ph.D. in Biomedical Engineering and a minor in Neuroscience. She was the recipient of both a 2004 National Science Foundation (NSF) Graduate Research Fellowship and a NSF Integrative Graduate Education Research Traineeship Fellowship in the Georgia Tech Laboratory for Neuroengineering's Hybrid Neural Microsystems program. While working on her Ph.D. Cassie fulfilled her passion to teach as a Gandy Teaching Fellow and as a five-time teaching assistant for the Georgia Tech biomedical engineering undergraduate program, namely BME 2210, Introduction to Biomedical Engineering. When not working on her research, one of Cassie's favorite pastimes is wheelchair sports. She is a member of a quadriplegic wheelchair rugby team, the Shepherd Smash, which competes nationally as part of the United States Quad Rugby Association. Finally, Cassie greatly enjoys serving others through a wide variety of academic, athletic, disability and mentoring and service programs.